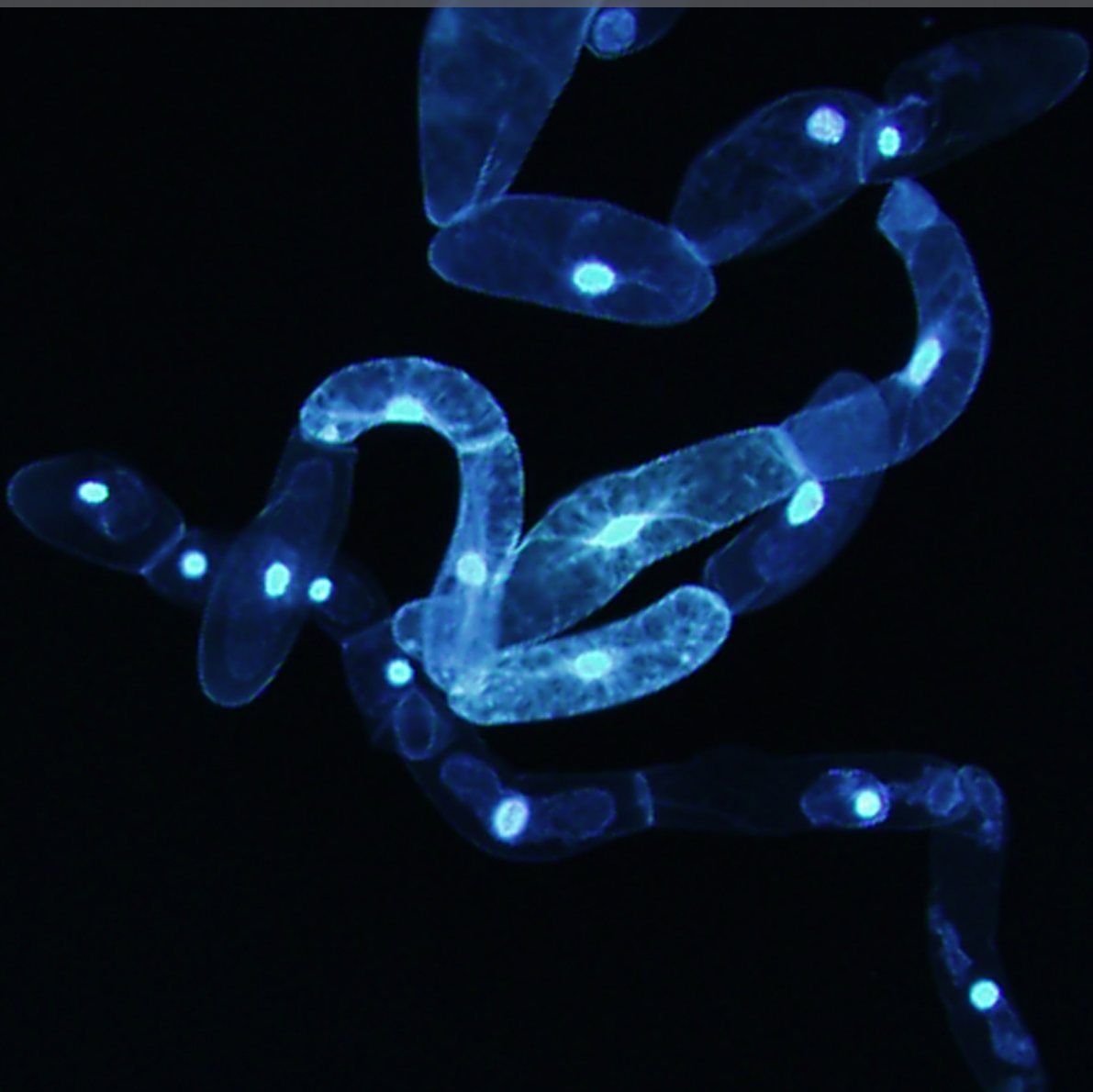
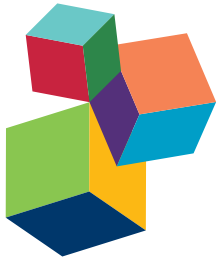


MAINTENANCE OF GENOME INTEGRITY: DNA DAMAGE SENSING, SIGNALING, REPAIR AND REPLICATION IN PLANTS

EDITED BY: Alma Balestrazzi, V. Mohan Murali Achary, Anca Macovei,
Kaoru Okamoto Yoshiyama and Ayako N. Sakamoto

PUBLISHED IN: Frontiers in Plant Science





frontiers

Frontiers Copyright Statement

© Copyright 2007-2016 Frontiers Media SA. All rights reserved.

All content included on this site, such as text, graphics, logos, button icons, images, video/audio clips, downloads, data compilations and software, is the property of or is licensed to Frontiers Media SA ("Frontiers") or its licensees and/or subcontractors. The copyright in the text of individual articles is the property of their respective authors, subject to a license granted to Frontiers.

The compilation of articles constituting this e-book, wherever published, as well as the compilation of all other content on this site, is the exclusive property of Frontiers. For the conditions for downloading and copying of e-books from Frontiers' website, please see the Terms for Website Use. If purchasing Frontiers e-books from other websites or sources, the conditions of the website concerned apply.

Images and graphics not forming part of user-contributed materials may not be downloaded or copied without permission.

Individual articles may be downloaded and reproduced in accordance with the principles of the CC-BY licence subject to any copyright or other notices. They may not be re-sold as an e-book.

As author or other contributor you grant a CC-BY licence to others to reproduce your articles, including any graphics and third-party materials supplied by you, in accordance with the Conditions for Website Use and subject to any copyright notices which you include in connection with your articles and materials.

All copyright, and all rights therein, are protected by national and international copyright laws.

The above represents a summary only. For the full conditions see the Conditions for Authors and the Conditions for Website Use.

ISSN 1664-8714

ISBN 978-2-88919-820-7

DOI 10.3389/978-2-88919-820-7

About Frontiers

Frontiers is more than just an open-access publisher of scholarly articles: it is a pioneering approach to the world of academia, radically improving the way scholarly research is managed. The grand vision of Frontiers is a world where all people have an equal opportunity to seek, share and generate knowledge. Frontiers provides immediate and permanent online open access to all its publications, but this alone is not enough to realize our grand goals.

Frontiers Journal Series

The Frontiers Journal Series is a multi-tier and interdisciplinary set of open-access, online journals, promising a paradigm shift from the current review, selection and dissemination processes in academic publishing. All Frontiers journals are driven by researchers for researchers; therefore, they constitute a service to the scholarly community. At the same time, the Frontiers Journal Series operates on a revolutionary invention, the tiered publishing system, initially addressing specific communities of scholars, and gradually climbing up to broader public understanding, thus serving the interests of the lay society, too.

Dedication to Quality

Each Frontiers article is a landmark of the highest quality, thanks to genuinely collaborative interactions between authors and review editors, who include some of the world's best academicians. Research must be certified by peers before entering a stream of knowledge that may eventually reach the public - and shape society; therefore, Frontiers only applies the most rigorous and unbiased reviews.

Frontiers revolutionizes research publishing by freely delivering the most outstanding research, evaluated with no bias from both the academic and social point of view.

By applying the most advanced information technologies, Frontiers is catapulting scholarly publishing into a new generation.

What are Frontiers Research Topics?

Frontiers Research Topics are very popular trademarks of the Frontiers Journals Series: they are collections of at least ten articles, all centered on a particular subject. With their unique mix of varied contributions from Original Research to Review Articles, Frontiers Research Topics unify the most influential researchers, the latest key findings and historical advances in a hot research area! Find out more on how to host your own Frontiers Research Topic or contribute to one as an author by contacting the Frontiers Editorial Office: researchtopics@frontiersin.org

MAINTENANCE OF GENOME INTEGRITY: DNA DAMAGE SENSING, SIGNALING, REPAIR AND REPLICATION IN PLANTS

Topic Editors:

Alma Balestrazzi, University of Pavia, Italy

V. Mohan Murali Achary, International Centre for Genetic Engineering and Biotechnology, India

Anca Macovei, International Rice Research Institute Los Banos, Philippines

Kaoru Okamoto Yoshiyama, Kyoto Sangyo University, Japan

Ayako N. Sakamoto, National Institutes for Quantum and Radiological Science and Technology, Japan



DAPI staining of nuclei of tobacco Bright Yellow-2 cells irradiated with high dose of Ultraviolet-B (UV-B). Here, round condensed nuclei seen in many cells are evidence for a large amount of DNA damage that leads to cell death. Also, some survival elongated cells are seen. One of the elongated cells containing elongated nuclei caused due to inhibition of cell proliferation. By contrast, low dose irradiation of UV-B induces only inhibition of cell proliferation.

Image taken from: Takahashi S, Kojo KH, Kutsuna N, Endo M, Toki S, Isoda H and Hasezawa S (2015) Differential responses to high- and low-dose ultraviolet-B stress in tobacco Bright Yellow-2 cells. *Front. Plant Sci.* 6:254. doi: 10.3389/fpls.2015.00254

Environmental stresses and metabolic by-products can severely affect the integrity of genetic information by inducing DNA damage and impairing genome stability. As a consequence, plant growth and productivity are irreversibly compromised. To overcome genotoxic injury, plants have evolved complex strategies relying on a highly efficient repair machinery that responds to sophisticated damage perception/signaling networks. The DNA damage signaling network contains several key components: DNA damage sensors, signal transducers, mediators, and effectors. Most of these components are common to other eukaryotes but some features are unique to the plant kingdom. ATM and ATR are well-conserved members of PIKK family, which amplify and transduce signals to downstream effectors. ATM primarily responds to DNA double strand breaks while ATR responds to various forms of DNA damage. The signals from the activated transducer kinases are transmitted to the downstream cell-cycle regulators, such as CHK1, CHK2, and p53 in many eukaryotes. However, plants have no homologue of CHK1, CHK2 nor p53. The finding of *Arabidopsis* transcription factor SOG1 that seems functionally but not structurally similar to p53 suggests that plants have developed unique cell cycle regulation mechanism.

The double strand break repair, recombination repair, postreplication repair, and lesion bypass, have been investigated in several plants. The DNA double strand break, a most critical damage for organisms are repaired non-homologous end joining (NHEJ) or homologous recombination (HR) pathway. Damage on template DNA makes replication stall, which is processed by translesion synthesis (TLS) or error-free postreplication repair (PPR) pathway. Deletion of the error-prone TLS polymerase reduces mutation frequencies, suggesting PPR maintains the stalled replication fork when TLS is not available. Unveiling the regulation networks among these multiple pathways would be the next challenge to be completed.

Some intriguing issues have been disclosed such as the cross-talk between DNA repair, senescence and pathogen response and the involvement of non-coding RNAs in global genome stability. Several studies have highlighted the essential contribution of chromatin remodeling in DNA repair DNA damage sensing, signaling and repair have been investigated in relation to environmental stresses, seed quality issues, mutation breeding in both model and crop plants and all these studies strengthen the idea that components of the plant response to genotoxic stress might represent tools to improve stress tolerance and field performance. This focus issue gives researchers the opportunity to gather and interact by providing Mini-Reviews, Commentaries, Opinions, Original Research and Method articles which describe the most recent advances and future perspectives in the field of DNA damage sensing, signaling and repair in plants. A comprehensive overview of the current progresses dealing with the genotoxic stress response in plants will be provided looking at cellular and molecular level with multidisciplinary approaches. This will hopefully bring together valuable information for both plant biotechnologists and breeders.

Citation: Balestrazzi, A., Achary, V. M. M., Macovei, A., Yoshiyama, K. O., Sakamoto, A. N., eds. (2016). Maintenance of Genome Integrity: DNA Damage Sensing, Signaling, Repair and Replication in Plants. Lausanne: Frontiers Media. doi: 10.3389/978-2-88919-820-7

Table of Contents

- 06 Editorial: Maintenance of Genome Integrity: DNA Damage Sensing, Signaling, Repair, and Replication in Plants**
Alma Balestrazzi, V. Mohan Murali Achary, Anca Macovei, Kaoru O. Yoshiyama and Ayako N. Sakamoto
- 08 Maintenance of genome stability in plants: repairing DNA double strand breaks and chromatin structure stability**
Sujit Roy
- 13 Signaling of double strand breaks and deprotected telomeres in Arabidopsis**
Simon Amiard, Maria E. Gallego and Charles I. White
- 19 DNA maintenance in plastids and mitochondria of plants**
Delene J. Oldenburg and Arnold J. Bendich
- 34 Arabidopsis DNA polymerase lambda mutant is mildly sensitive to DNA double strand breaks but defective in integration of a transgene**
Tomoyuki Furukawa, Karel J. Angelis and Anne B. Britt
- 48 Arabidopsis PCNA form complexes with selected D-type cyclins**
Wojciech K. Strzalka, Chhavi Aggarwal, Weronika Krzeszowiec, Agata Jakubowska, Olga Sztatelman and Agnieszka K. Banas
- 59 Differential responses to high- and low-dose ultraviolet-B stress in tobacco Bright Yellow-2 cells**
Shinya Takahashi, Kei H. Kojo, Natsumaro Kutsuna, Masaki Endo, Seiichi Toki, Hiroko Isoda and Seiichiro Hasezawa
- 69 DDM1 and ROS1 have a role in UV-B induced- and oxidative DNA damage in *A. thaliana***
Julia I. Qüesta, Julieta P. Fina and Paula Casati
- 81 Mitogen-activated protein kinase signal transduction and DNA repair network are involved in aluminum-induced DNA damage and adaptive response in root cells of Allium cepa L.**
Brahma B. Panda and V. Mohan M. Achary
- 91 Emerging Importance of Helicases in Plant Stress Tolerance: Characterization of *Oryza sativa* Repair Helicase XPB2 Promoter and Its Functional Validation in Tobacco under Multiple Stresses.**
Shailendra Raikwar, Vineet K. Srivastava, Sarvajeet S. Gill, Renu Tuteja and Narendra Tuteja
- 98 Genomic stability in response to high versus low linear energy transfer radiation in *Arabidopsis thaliana***
Neil D. Huefner, Kaoru Yoshiyama, Joanna D. Friesner, Phillip A. Conklin and Anne B. Britt

- 105 *High atomic weight, high-energy radiation (HZE) induces transcriptional responses shared with conventional stresses in addition to a core "DSB" response specific to clastogenic treatments***

Victor Missirian, Phillip A. Conklin, Kevin M. Culligan, Neil D. Huefner, and Anne B. Britt

- 122 *Identification of "safe harbor" loci in indica rice genome by harnessing the property of zinc-finger nucleases to induce DNA damage and repair***

Christian Cantos, Perigio Francisco, Kurniawan R. Trijatmiko, Inez Slamet-Loedin and Prabhjit K. Chadha-Mohanty



Editorial: Maintenance of Genome Integrity: DNA Damage Sensing, Signaling, Repair, and Replication in Plants

Alma Balestrazzi^{1*}, V. Mohan Murali Achary², Anca Macovei^{1,3}, Kaoru O. Yoshiyama⁴ and Ayako N. Sakamoto⁵

¹ Department of Biology and Biotechnology “L. Spallanzani”, University of Pavia, Pavia, Italy, ² Department of Plant Molecular Biology, International Centre for Genetic Engineering and Biotechnology, New Delhi, India, ³ Plant Breeding, Genetics and Biotechnology Division, International Rice Research Institute, Los Baños, Philippines, ⁴ Faculty of Life Sciences, Kyoto Sangyo University, Kyoto, Japan, ⁵ Biotechnology and Medical Application Division, Japan Atomic Energy Agency, Takasaki, Japan

Keywords: genome integrity, DNA damage, DNA repair, replication, double strand breaks

The Editorial on the Research Topic

Maintenance of Genome Integrity: DNA Damage Sensing, Signaling, Repair, and Replication in Plants

Because of their sessile lifestyles, plants are continuously exposed to DNA-damaging agents present in the environment. Although the basic mechanisms of genome maintenance are conserved between animal and plant kingdom, plants also have evolved specific mechanisms to cope with DNA damage. Indeed, studies in past decades have demonstrated the presence of elastic mechanisms in plants. For example, when exposed to DNA damaging agents, plants respond immediately to start repairing the damage, regulating cell proliferation, changing metabolic pathways. Here we are proud to have twelve outstanding articles focus on the maintenance of genome integrity: DNA damage sensing, signaling, repair and replication in plants.

The present e-book is opened by several comprehensive reviews dealing with genomic and extra-genomic DNA maintenance, as well as the role of double strand break (DSB) signaling in plants. In his minireview, Roy provides an upgraded view on the link connecting chromatin structure stability and DNA damage response at the genetic and epigenetic levels, while Amiard et al. present an overview on DSB repair pathways in *Arabidopsis thaliana*, with focus on the signaling of DNA breaks and deprotected telomeres. Stability of genomic DNA, not only in nuclei, but also in organelles is crucial for plant development. In contrast to nuclear genomes, the amount and structural integrity of organellar genomes changes during plant development. It is very interesting to consider why organellar genomes are less stable as the replication and repair machineries are encoded by the nuclear genome, yet the cause of the instability is poorly understood. Oldenburg and Bendich first explain the history of the studies into the size and structure of organellar DNA (orgDNA). They then address the copy number and integrity of orgDNA during plant development. The review continues with an overview of the proteins which are involved in the processes of orgDNA replication, repair, and recombination, and changes in the amount of these proteins during leaf development. It has been observed that plastid DNA (ptDNA) maintenance in grasses differs from that in dicots as it rapidly declines upon light exposure. From these observations, the authors propose the idea that instead of repairing damaged DNA, grasses use a cost-saving involving a loss of ptDNA.

DNA polymerases are crucial for maintenance of genome integrity in organisms. The family X DNA polymerases work in DNA repairs such as base excision repair (BER) and/or DSB repair. Plants are unique in having only one member of this family, polymerase lambda (Polλ). Furukawa et al. showed that the Polλ knockout *Arabidopsis* (*atpolλ-1*) is only mildly sensitive to DSB-inducing treatments, whereas the double-knockouts of AtPolλ and AtLig4 made the plants hypersensitive to DSB compared to each single knockout. These results suggest that the AtPolλ

OPEN ACCESS

Edited and reviewed by:

Steven Carl Huber,
United States Department of
Agriculture-Agricultural Research
Service, USA

*Correspondence:

Alma Balestrazzi
alma.balestrazzi@unipv.it

Specialty section:

This article was submitted to
Plant Physiology,
a section of the journal
Frontiers in Plant Science

Received: 16 December 2015

Accepted: 14 January 2016

Published: 15 February 2016

Citation:

Balestrazzi A, Achary VMM, Macovei A, Yoshiyama KO and Sakamoto AN (2016) Editorial: Maintenance of Genome Integrity: DNA Damage Sensing, Signaling, Repair, and Replication in Plants. *Front. Plant Sci.* 7:64.
doi: 10.3389/fpls.2016.00064

has a role in DSB repair, probably in an AtLig4-independent non-homologous end-joining (NHEJ) pathway. Proliferating cell nuclear antigen (PCNA) is a key component of eukaryotic DNA replication machinery. PCNA usually accompanies the DNA polymerase to gather a specific set of proteins onto the replication fork when replication is disturbed. Cyclin Ds are expressed in G2 and degraded during G2/M transition. When the checkpoint is activated, the degradation of cyclin D is inhibited to arrest cells at G2. Strzalka et al. demonstrated that *Arabidopsis* PCNAs directly interact with some members of the cyclin Ds in yeast and plant cells, suggesting that PCNAs link the signal of disturbed replication with cell cycle control. Ultraviolet (UV) light has been used to analyze cellular DNA-damage responses. UV induces cyclobutanate pyrimidine dimmers (CPDs) and other damage to DNA, which triggers various cellular responses: DNA repair, cell cycle delay or arrest, and cell death. Thus, UVB in sunlight can confer severe stress to plants, but plants have photorepair enzymes to correct the damage. Takahashi et al. investigated the responses of plant cells irradiated with low or high dose of UVB. UVB irradiated cells showed different reactions, depending on the dose, suggesting that accumulation of CPDs caused by high dose UVB induces formation of single or DSBs, which leads to cell death.

In their research article, Qüesta et al. discuss on the roles of the *DDM1* and *ROS1* genes in UVB-induced DNA repair by using *Arabidopsis* mutants and a set of analytical measurements. Disruption of these genes had an opposite impact of these two genes, with the *ddm1* mutants accumulating more DNA damage, while the *ros1* mutants showed less amount of DNA damage. Based on experimental work, they hypothesize that the DNA demethylation in the *ddm1* mutant can affect the accessibility of DNA repair systems in this region, while the better performance of *ros1* mutants can arise as a result of increased levels of photolyases. In their research on the MAPK signal transduction in response to aluminum (Al) treatments, Panda and Achary underline the biphasic mode of action of Al-induced DNA damage in *Allium cepa*. They observed that at high concentrations Al induces DNA damage, while at low concentration an adaptive response is present, and hypothesize that the MAPK-DNA repair network is responsible for both actions. The role played by DNA/RNA helicases against the genotoxic effects of abiotic stress is documented. XPB (xeroderma pigmentosum type B) helicases promote nucleotide excision repair (NER) by unwinding double strand DNA at the damaged sites. In the attempt to assess the potential of plant XPB helicases as tools in counteracting adverse environmental conditions, Raikwar et al. carried out an *in silico* and functional characterization of the rice *OsXPB2* gene promoter in response to abiotic stress and hormone-based treatments. Based on its multi-stress responsiveness, the *OsXPB2* promoter represents a promising tool for improving the response of crops to genotoxic stress.

Huefner et al. investigated the short- and long-term impact of high-LET (Linear Energy Transfer) HZE (high atomic weight, high energy) particles vs. low-LET gamma rays on genome stability, using *Arabidopsis* mutants defective in DNA repair and cell-cycle checkpoint. This study highlights the increased sensitivity of *Arabidopsis* plants to HZE radiation, revealing the predominant role played by ATR (ATM and Rad3-related)

protein kinase compared to ATM (ataxia-telangiectasia mutated) in the response to high-LET radiation. In the accompanying article, Missirian et al. compared the transcriptional response in *Arabidopsis* seedlings exposed to HZE radiation vs. DSB-inducing agents as gamma rays, bleomycin and mitomycin C. These treatments triggered an intense, short-term DSB-specific repair response which was not detected in plants challenged with conventional stresses. A distinctive feature of the HZE transcriptional response was the early activation of key genes involved in the catabolism of cellular components.

With genome editing being the cutting-edge topic of present days, the article by Cantos et al. deals with the implementation of such tool (zinc finger nucleases, ZFNs) for the identification of appropriate regions for safe gene insertion. By harnessing their ability to induce DSBs at the cutting site, ZFNs trigger the NHEJ or homologous recombination (HR) DNA repair pathways at the targeted site. This study used ZFNs with short DNA recognition domains, able to target multiple sites within the rice genome, and subsequently study the integration patterns of the GUS marker gene, allowing the identification of “safe harbors,” intergenic regions with potential high expression.

The present e-book provides an up-date overview of the ongoing research dealing with different aspects of the DNA damage response in plants, highlighting the complexity of molecular networks involved in genome maintenance. A better understanding of DNA damage accumulation/perception/signaling/repair mechanisms *in planta* is expected to speed up crop improvement through conventional breeding and gene-transfer based techniques.

AUTHOR CONTRIBUTIONS

AB commented the following articles: Huefner et al., Missirian et al., and Raikwar et al.; AM commented the following articles: Roy, Amiard et al., Qüesta et al., Panda and Achary, and Cantos et al.; KOY commented the following article: Oldenburg and Bendich; ANS commented the following articles: Furukawa et al., Strzalka et al., and Takahashi et al. All authors and read and revised the complete editorial.

FUNDING

This work was supported by research fellowship from the Japan Society for the Promotion of Science to KY (13J40017) and partially supported by Grant-in-Aid for Scientific Research to AS (No. 25440147) from the Japan Society for the Promotion of Science. Sponsorship from COST Action CM1201: “Biomimetic Radical Chemistry” is gratefully acknowledged.

Conflict of Interest Statement: The authors declare that the research was conducted in the absence of any commercial or financial relationships that could be construed as a potential conflict of interest.

Copyright © 2016 Balestrazzi, Achary, Macovei, Yoshiyama and Sakamoto. This is an open-access article distributed under the terms of the Creative Commons Attribution License (CC BY). The use, distribution or reproduction in other forums is permitted, provided the original author(s) or licensor are credited and that the original publication in this journal is cited, in accordance with accepted academic practice. No use, distribution or reproduction is permitted which does not comply with these terms.



Maintenance of genome stability in plants: repairing DNA double strand breaks and chromatin structure stability

Sujit Roy*

Protein Chemistry Laboratory, Department of Chemistry, Bose Institute, Kolkata, India

Edited by:

Alma Balestrazzi, University of Pavia, Italy

Reviewed by:

Paula Casati, Centro de Estudios Fotosintéticos – Consejo Nacional de Investigaciones Científicas y Técnicas, Argentina

Vasileios Fotopoulos, Cyprus University of Technology, Cyprus

***Correspondence:**

Sujit Roy, Protein Chemistry Laboratory, Department of Chemistry, Bose Institute, 93/1 Acharya Prafulla Chandra Road, Kolkata 700009, West Bengal, India
e-mail: sujitroy2006@gmail.com

Plant cells are subject to high levels of DNA damage resulting from plant's obligatory dependence on sunlight and the associated exposure to environmental stresses like solar UV radiation, high soil salinity, drought, chilling injury, and other air and soil pollutants including heavy metals and metabolic by-products from endogenous processes. The irreversible DNA damages, generated by the environmental and genotoxic stresses affect plant growth and development, reproduction, and crop productivity. Thus, for maintaining genome stability, plants have developed an extensive array of mechanisms for the detection and repair of DNA damages. This review will focus recent advances in our understanding of mechanisms regulating plant genome stability in the context of repairing of double stand breaks and chromatin structure maintenance.

Keywords: plant genome stability, environmental and genotoxic stress, DNA damage response, double strand breaks, chromatin remodeling

DNA DOUBLE STRAND BREAKS AND GENOME INSTABILITY

Plants, with their intrinsic immobility and obligatory exposure to sunlight for energy, are constantly facing the tremendous challenge of maintaining the genome integrity which is under continuous assault from environmental factors like solar UV and ionizing radiation, high soil salinity, drought and desiccation, chemical mutagens, and free radicals or alkylating agents generated by endogenous processes (Roy et al., 2009, 2013a; Tuteja et al., 2009; Waterworth et al., 2011; Yoshiyama et al., 2013). These agents cause variety of DNA damages including DNA base oxidation and alkylation, formation of pyrimidine dimers and abasic sites, single and double strand breaks (SSBs and DSBs), DNA inter-strand cross links and therefore seriously threat the integrity of plant genome. Lesions in the DNA, contributed by various damaging agents, may result in changes in both the chemical and physical structures of DNA and thus generate both cytotoxic and genotoxic effects, adversely affecting plant growth and development (Balestrazzi et al., 2011). Therefore, to survive under frequent and extreme environmental stress conditions, plant cells have evolved with highly efficient and wide-ranging mechanisms for the detection and repair of DNA damage to eliminate the chances of permanent genetic alterations and to maintain genome stability for faithful transfer of genetic information over generations (West et al., 2004; Kozak et al., 2009; Roy et al., 2011).

Among the various forms of DNA lesions, DSBs in DNA double helix are considered as one of the major form of DNA damage (West et al., 2004). In addition to genotoxic stress, which frequently induces DSBs, error prone DNA replication and defective repair of SSB or collapsed replication forks during trans lesion synthesis and steric stresses during DNA unwinding may also result in the formation of DSBs (Kuzminov, 2001). DSBs in the actively dividing plant tissues like shoot or root apical meristem (SAM and RAM) severely

affect plant growth since DNA synthesis events or progression through cell division with unrepaired DSBs often results in chromosomal aberrations at the structural levels leading into loss of chromosome fragments (deletions), insertions, and chromosome fusions. Such aberrant chromosomal structures eventually severely affect plant growth and development due to inhibition of DNA replication and transcription which in turn results in loss of cell viability (Fulcher and Sablowski, 2009; Waterworth et al., 2011).

Efficient detection, activation of cell-cycle checkpoint function and rapid repair of DSBs in the genome is crucial for the survival of all organisms including plants (Puchta, 2005). The DSBs are repaired by two fundamental mechanisms: the homologous recombination (HR) and the non-homologous end joining (NHEJ) pathway. The HR pathway is mediated by the proteins of RAD52 epistasis groups RAD51, RAD52, RAD54, RAD55, RAD57 and the MRN complex, comprising of MRE11, RAD50 and NBS1 (Symington, 2002). HR pathway requires an intact copy of the homologous DNA duplex for the formation of a heteroduplex for repairing the damaged strand using the non-damaged region as a template (Barzel and Kupiec, 2008). DSB repair via HR is commonly utilized in bacterial and yeast cells, depending on the availability of sequence homology. However, in eukaryotes, including mammals and plants, HR mediated DSB repair is crucial during the early stages of gamete formation in meiotic cells where a programmed induction of DSBs initiates homologous chromosome pairing and recombination (Edlinger and Schlogelhofer, 2011).

In mammals and plants with large and complex genomes, majority of DSBs in somatic cells are repaired via the NHEJ pathway (West et al., 2004; Puchta, 2005), in which the broken ends of double stranded DNA are directly joined irrespective of sequence homology. Thus, NHEJ repair is error-prone but represents the

predominant DSB repair pathway during G1 to early S-phase of cell cycle. However this pathway has also been found to be functional throughout the cell cycle (Abe et al., 2009). In NHEJ repair, the KU70/80 complex binds to the DNA ends at the site of DSBs in the double stranded DNA. Broken ends are then processed by the MRN complex for making the ends suitable substrate for joining by the activity of DNA ligase IV and XRCC4. The gap filling synthesis requires involvement of DNA polymerase λ (Pol λ), the sole member of family X DNA polymerase in plants (Roy et al., 2013b).

CELLULAR RESPONSE TO DNA DOUBLE STRAND BREAKS

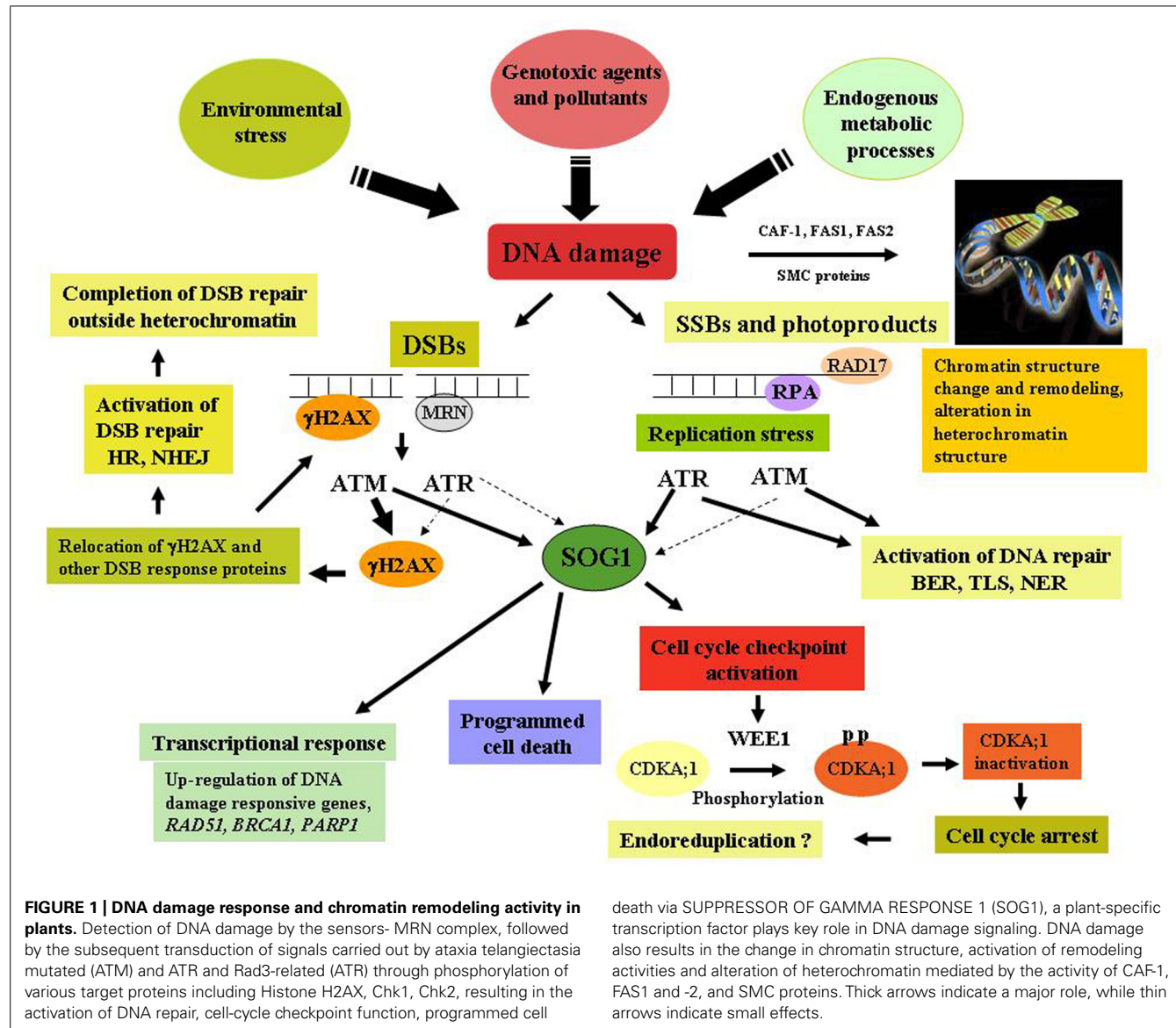
Cellular responses to DSBs in the DNA are initiated by activation of a complex damage response pathway which includes the detection of DSBs, followed by signaling to regulate the mechanisms governing cell cycle progression, programmed cell death, and direct activation of DNA repair pathways (Zhou and Elledge, 2000). The molecular components of the HR and NHEJ mediated DSB repair pathways are highly conserved among eukaryotes, and previous studies have revealed requirements of both these pathways for DSB repair in plants (Bray and West, 2005). The major components of DSB detection in plants include the KU70–KU80 complex, which has high affinity for broken DNA ends and also acts as a core component of the NHEJ pathway (West et al., 2004). In addition, the multiprotein MRN complex has also been implicated in DSB detection and shown to be involved in both NHEJ- and HR-mediated DSB repair (Amiard et al., 2010).

In eukaryotes, cellular response to DNA damage is governed by the two key regulators, ataxia telangiectasia mutated (ATM) and ATM and Rad3-related (ATR) kinases which are phosphoinositide-3-kinase-related protein kinases (PIKKs; Bradbury and Jackson, 2003), regulating cell cycle progression and activation of DNA repair pathways in response to DNA damage. ATM has been shown to be mainly activated by genotoxins which generate DSBs (Lee and Paull, 2004), resulting in the up-regulation of large number of genes encoding factors involved in DNA repair processes, DSB signaling and cell cycle regulation, while down regulating expression of G2 and M-phase specific genes, leading to cell cycle arrest in response to DNA damage (Culligan et al., 2006). Conversely, ATR is more strongly activated in response to replication stress, resulting in the activation of cell-cycle checkpoint function. Like other eukaryotes, the activation of ATM and ATR kinases are crucial in plants in regulating the DNA damage signaling directly or indirectly through phosphorylation of multiple target proteins, including the phosphorylation of histone 2A isoforms H2AX, NBS1 and the other checkpoint associated protein kinases, including Chk1 (check point kinase) and Chk2 (Matsuoka et al., 2007). In *Arabidopsis*, a unique plant-specific transcription factor SUPPRESSOR OF GAMMA RESPONSE 1 (SOG1) has been shown to act as the central regulator in DNA damage response pathway and suggested to perform analogous functions to mammalian p53 in plant genome, involved in majority of plant's response to DNA damage, such as transcriptional response, activation of cell cycle checkpoint and programmed death of stem cells (Yoshiyama et al., 2014; **Figure 1**).

UNDERSTANDING THE LINK BETWEEN CHROMATIN STRUCTURE STABILITY AND DNA DOUBLE STRAND BREAK REPAIR IN THE CONTEXT OF PLANT GENOME STABILITY MAINTENANCE

Like other eukaryotes, plant genome is organized into chromatin which is the functional template for variety of fundamental biological processes, like DNA replication, transcription, repair, and recombination. Chromatin structure is crucial for genome stability and is constituted by the association of histone complexes with DNA to form nucleosomes. This step is regulated by two major pathways (Polo and Almouzni, 2006), one of which is dependent on histone gene repressor (HIRA) whereas the other pathway requires chromatin assembly factor-1 (CAF-1), which is tightly linked with DNA replication (Ramirez-Parra and Gutierrez, 2007). The CAF-1 chaperone, a heterotrimeric complex, comprising of FASCIATA 1 (FAS1), FAS2, and MULTICOPY SUPPRESSOR OF IRA1 (MSI1) subunits in *Arabidopsis* (Hennig et al., 2003), targets acetylated histone H3/H4 onto nascent DNA strand, allowing *de novo* assembly of nucleosomes (Polo and Almouzni, 2006). In mammals including human, CAF-1 is essential for cell cycle progression, while in *Arabidopsis* CAF-1 mutants are fully viable but display defects in meristem organization, as found in *fas1* and *fas2* mutants (Ramirez-Parra and Gutierrez, 2007). The distorted meristem structure due to loss of CAF-1 function results in characteristic growth fasciation. Interestingly such phenotypes were also reported in DSB repair pathway mutants, like *mre11* and *brca2* and in wild-type *Arabidopsis* following high doses of irradiation (Abe et al., 2009).

Global transcriptomic analyses in *Arabidopsis* have revealed that despite pleiotropic developmental defects, <2% of genes are transcriptionally deregulated in *Arabidopsis* CAF-1 mutants and within this a fairly high proportion of the genes are associated with DNA damage repair (Schönrock et al., 2006), indicating functional link between CAF-1 and thus chromatin structure stability and DNA damage response (Ramirez-Parra and Gutierrez, 2007). In *fas1* mutant, up regulated expression of the DNA damage responsive genes, like *RAD51*, *PARP1*, and *BRCA1* and *CYCBL1* have been demonstrated as a result of selective epigenetic changes in histone H3 acetylation and methylation in the promoters of these genes, but not because of global changes in chromatin modeling. Similar responses were also detected when wild-type *Arabidopsis* were subjected to DNA damaging agents, indicating that defects in chromatin assembly during S-phase and DNA damage signaling probably share part of the similar pathway via changing the epigenetic status of the target genes (Ramirez-Parra and Gutierrez, 2007). In *fas1* and *fas2* mutants, defects in chromatin assembly has also been shown to cause hypersensitive response toward genotoxic agents along with the increased basal levels of DSBs and constitutive activation signal for DNA damage response pathway, resulting in significant increase in spontaneous intrachromosomal recombination (Takeda et al., 2004; Endo et al., 2006). The activation of DNA damage response and the associated decrease of cell number in *fas1* mutant were found to be dependent on ATM kinase, one of the master controllers in DDR pathway (Hisanaga et al., 2013). *Arabidopsis* mutants, deficient in DNA replication factors, including Replication Protein A1 (RPA1) and Topoisomerase VI, display phenotypes of chromatin assembly mutants,



such as constitutive activation of DNA damage response and in some cases loss of transcriptional gene silencing due to destabilization of heterochromatin (Elmayan et al., 2005; Breuer et al., 2007), as observed in mutants in CAF-1 complex (Ramirez-Parra and Gutierrez, 2007). In *Arabidopsis*, *BRU1* gene encodes a CAF. *Bru1* mutant plants showed hypersensitivity to genotoxic stress with constitutive activation of DNA damage response and loss of transcriptional gene silencing (Takeda et al., 2004), suggesting interesting cross talk points between chromatin assembly, DNA damage repair, and epigenetic inheritance. In addition, recent studies have revealed involvement of chromatin remodeling proteins in repair of DNA damages. In *Arabidopsis*, the histone acetyltransferases HAM1 and HAM2 participate in repair of UV-B induced DNA damage, suggesting importance of chromatin remodeling and histone acetylation during repair of UV-B induced DNA damage (Campi et al., 2012). In *Arabidopsis*, the key histone H3/H4 chaperone ANTI-SILENCING FUNCTION1

(ASF1) is involved in UV-B induced DNA damage repair (Lario et al., 2013). Together, these observations indicate that DNA repair in plants is regulated both at the genetic and epigenetic levels.

RAPID REPAIR OF DOUBLE STRAND BREAKS IN PLANTS: STRUCTURAL MAINTENANCE OF CHROMOSOME PROTEINS

Non-homologous-end joining has been considered as the preferred pathway involved in the repair of majority of DSBs in higher plants. Interestingly, *Arabidopsis* NHEJ knockout mutants *ku80* and *lig4* were found to repair DSBs very rapidly, with comparable rates to wild-type plants, indicating the involvement of “classic NHEJ” independent novel backup pathway which probably regulate rapid repair of the majority of DSBs in plant cells. Rapid repair of DSBs in plants has been shown to be mediated by the plant ortholog of structure maintenance of chromosome proteins, MIM (AtSMC6/AtRAD18) and kleisin (AtRAD21;

Kozak et al., 2009). The members of the STRUCTURAL MAINTENANCE OF CHROMOSOMES (SMC) family and the associated non-SMC factors play crucial role in the regulation of higher order chromatin structure in eukaryotes (Schubert, 2009). The SMC proteins contain characteristic ATPase activity and, along with the non-SMC proteins like kleisin subunits, form multiprotein complexes – cohesion, condensin, and the SMC5/6 complex (Watanabe et al., 2009). Cohesin, together with the SMC5/6 complex, is involved in DSB repair in G2 cells. In *Arabidopsis*, a subunit mutant of the cohesin complex, RAD21.1, displayed enhanced sensitivity to genotoxins with low DSB repair rates (Kozak et al., 2009). Homologs of additional cohesin establishment factors, including E2F target gene 1 (ETG) and CTF18, have been identified in *Arabidopsis* (Takahashi et al., 2010). The *etg* and *ctf18* mutants showed partial loss in chromatid cohesion, along with the constitutive activation of DNA damage response. The effect was more severe in the double mutant line (Takahashi et al., 2010). The involvement of cohesion establishment factor CHROMOSOME TRANSMISSION FIDELITY 7 (AtCTF7/ECO1) in DNA repair and cell division was established in *Arabidopsis*. The *ctf7-1* and *ctf7-2* mutants showed growth defects, poor anther development and sterility, deficiency in DNA repair and cell division with increased expression of DNA repair genes, such as *BRCA1* and *PARP2* (Bolanos-Villegas et al., 2013), demonstrating key role of cohesins for sister chromatid cohesion and DNA damage response in maintaining plant genome stability.

OUTLOOK

With the completion of *Arabidopsis* genome project, understanding the link between DSB repair and chromatin structure maintenance has become the subject of intense study over the past few years. The above discussion summarizes recent advancement in our understanding of the link connecting chromatin structure stability with DNA damage response for the genetic and epigenetic maintenance of genome stability in plants. Considering the impact of global change in climate on plant growth, development, and productivity, further research in this area in future will provide meaningful insight about how plants maintain genome stability under environmental and genotoxic stresses.

ACKNOWLEDGMENTS

Research from this laboratory cited in this article was partly supported by the CSIR Pool Scientist's scheme (Ref. No. 13(8611-A)/2013-Pool). I sincerely thank Prof. K. P. Das, Department of Chemistry, Bose Institute, Kolkata, India and Dr. Swarup Roy Choudhury, Donald Danforth Plant Science Center, St. Louis, Missouri, for the critical reading and corrections of the Manuscript. I apologize to all authors whose work was not cited due to the length limitations.

REFERENCES

- Abe, K., Osakabe, K., Ishikawa, Y., Tagiri, A., Yamanouchi, H., Takyuu, T., et al. (2009). Inefficient double-strand DNA break repair is associated with increased fasciation in *Arabidopsis* BRCA2 mutants. *J. Exp. Bot.* 60, 2751–2761. doi: 10.1093/jxb/erp135
- Amiard, S., Charbonnel, C., Allain, E., Depeiges, A., White, C. I., and Gallego, M. E. (2010). Distinct roles of the ATM kinase and the Mre11-Rad50-Nbs1 complex in the maintenance of chromosomal stability in *Arabidopsis*. *Plant Cell* 22, 3020–3033. doi: 10.1105/tpc.110.078527
- Balestrazzi, A., Confalonieri, M., Macovei, A., Dona, M., and Carbonera, D. (2011). Genotoxic stress and DNA repair in plants: emerging functions and tools for improving crop productivity. *Plant Cell Rep.* 30, 287–295. doi: 10.1007/s00299-010-0975-9
- Barzel, A., and Kupiec, M. (2008). Finding a match: how do homologous sequences get together for recombination? *Nat. Rev. Genet.* 9, 27–37. doi: 10.1038/nrg2224
- Bolanos-Villegas, P., Yang, X., Wang, H.-J., Juan, C.-T., Chuang, M.-H., Makaroff, C. A., et al. (2013). *Arabidopsis* CHROMOSOME TRANSMISSION FIDELITY 7 (AtCTF7/ECO1) is required for DNA repair, mitosis and meiosis. *Plant J.* 75, 927–940. doi: 10.1111/tpj.12261
- Bradbury, J. M., and Jackson, S. P. (2003). ATM and ATR. *Curr. Biol.* 13, R468. doi: 10.1016/S0960-9822(03)00403-2
- Bray, C. M., and West, C. E. (2005). DNA repair mechanisms in plants: crucial sensors and effectors for the maintenance of genome integrity. *New Phytol.* 168, 511–528. doi: 10.1111/j.1469-8137.2005.01548.x
- Breuer, C., Stacey, N. J., West, C. E., Zhao, Y., Chory, J., Tsukaya, H., et al. (2007). BIN4, a novel component of the plant DNA topoisomerase VI complex, is required for endoreduplication in *Arabidopsis*. *Plant Cell* 19, 3655–3668. doi: 10.1105/tpc.107.054833
- Campi, M., D'Andrea, L., Emiliani, J., and Casati, P. (2012). Participation of chromatin-remodeling proteins in the repair of ultraviolet-B-damaged DNA. *Plant Physiol.* 158, 981–995. doi: 10.1104/pp.111.191452
- Culligan, K. M., Robertson, C. E., Foreman, J., Doerner, P., and Britt, A. B. (2006). ATR and ATM play both distinct and additive roles in response to ionizing radiation. *Plant J.* 48, 947–961. doi: 10.1111/j.1365-313X.2006.02931.x
- Edlinger, B., and Schlogelhofer, P. (2011). Have a break: determinants of meiotic DNA double strand break (DSB) formation and processing in plants. *J. Exp. Bot.* 62, 1545–1563. doi: 10.1093/jxb/erq421
- Elmayan, T., Proux, F., and Vaucheret, H. (2005). *Arabidopsis* RPA2: a genetic link among transcriptional gene silencing, DNA repair, and DNA replication. *Curr. Biol.* 15, 1919–1925. doi: 10.1016/j.cub.2005.09.044
- Endo, M., Ishikawa, Y., Osakabe, K., Nakayama, S., Kaya, H., Araki, T., et al. (2006). Increased frequency of homologous recombination and T-DNA integration in *Arabidopsis* CAF-1 mutants. *EMBO J.* 25, 5579–5590. doi: 10.1038/sj.emboj.7601434
- Fulcher, N., and Sablowski, R. (2009). Hypersensitivity to DNA damage in plant stem cell niches. *Proc. Natl. Acad. Sci. U.S.A.* 106, 20984–20988. doi: 10.1073/pnas.0909218106
- Hennig, L., Taranto, P., Walter, M., Schonrock, N., and Grussem, W. (2003). *Arabidopsis* MS11 is required for epigenetic maintenance of reproductive development. *Development* 130, 2555–2565. doi: 10.1242/dev.00470
- Hisanaga, T., Ferjani, A., Horiguchi, G., Ishikawa, N., Fujikura, U., Kubo, M., et al. (2013). The ATM-dependent DNA damage response acts as an upstream trigger for compensation in the fas1 mutation during *Arabidopsis* leaf development. *Plant Physiol.* 162, 831–841. doi: 10.1104/pp.113.216796
- Kozak, J., West, C. E., White, C., da Costa-Nunes, J. A., and Angelis, K. J. (2009). Rapid repair of DNA double strand breaks in *Arabidopsis thaliana* is dependent on proteins involved in chromosome structure maintenance. *DNA Repair (Amst)* 8, 413–419. doi: 10.1016/j.dnarep.2008.11.012
- Kuzminov, A. (2001). Single-strand interruptions in replicating chromosomes cause double-strand breaks. *Proc. Natl. Acad. Sci. U.S.A.* 98, 8241–8246. doi: 10.1073/pnas.131009198
- Lario, L. D., Ramirez-Parra, E., Gutierrez, C., Spaminato, C. P., and Casati, P. (2013). ANTI-SILENCING FUNCTION1 proteins are involved in ultraviolet-induced DNA damage repair and are cell cycle regulated by E2F transcription factors in *Arabidopsis*. *Plant Physiol.* 162, 1164–1177. doi: 10.1104/pp.112.212837
- Lee, J. H., and Paull, T. T. (2004). Direct activation of the ATM protein kinase by the Mre11/Rad50/Nbs1 complex. *Science* 304, 93–96. doi: 10.1126/science.1091496
- Matsuoka, S., Ballif, B. A., Smogorzewska, A., McDonald, E. R. III, Hurov, K. E., Luo, J., et al. (2007). ATM and ATR substrate analysis reveals extensive protein networks responsive to DNA damage. *Science* 316, 1160–1166. doi: 10.1126/science.1140321
- Polo, S. E., and Almouzni, G. (2006). Chromatin assembly, a basic recipe with various flavours. *Curr. Opin. Genet. Dev.* 16, 104–111. doi: 10.1016/j.gde.2006.02.011
- Puchta, H. (2005). The repair of double-strand breaks in plants: mechanisms and consequences for genome evolution. *J. Exp. Bot.* 56, 1–14. doi: 10.1093/jxb/er025

- Ramirez-Parra, E., and Gutierrez, C. (2007). E2F regulates FASCIATA1, a chromatin assembly gene whose loss switches on the endocycle and activates gene expression by changing the epigenetic status. *Plant Physiol.* 144, 105–120. doi: 10.1104/pp.106.094979
- Roy, S., Roy Choudhury, S., and Das, K. P. (2013a). The interplay of DNA polymerase λ in diverse DNA damage repair pathways in higher plant genome in response to environmental and genotoxic stress factors. *Plant Signal. Behav.* 8:e22715. doi: 10.4161/psb.22715
- Roy, S., Roy Choudhury, S., Sengupta, D. N., and Das, K. P. (2013b). Involvement of AtPol λ in repair of high salt and DNA cross linking agent induced double strand breaks in *Arabidopsis thaliana*. *Plant Physiol.* 162, 1195–1210. doi: 10.1104/pp.113.219022
- Roy, S., Roy Choudhury, S., Singh, S. K., and Das, K. P. (2011). AtPol λ , a homolog of mammalian DNA polymerase λ in *Arabidopsis thaliana*, is involved in the repair of UV-B induced DNA damage through the dark repair pathway. *Plant Cell Physiol.* 52, 448–467. doi: 10.1093/pcp/pcr002
- Roy, S., Singh, S. K., Roy Choudhury, S., and Sengupta, D. N. (2009). An insight into the biological functions of family X-DNA polymerase in DNA replication and repair of plant genome. *Plant Signal. Behav.* 4, 678–681. doi: 10.4161/psb.4.7.9077
- Schönrock, N., Exner, V., Probst, A., Grussem, W., and Hennig, L. (2006). Functional genomic analysis of CAF-1 mutants in *Arabidopsis thaliana*. *J. Biol. Chem.* 281, 9560–9568. doi: 10.1074/jbc.M513426200
- Schubert, V. (2009). SMC proteins and their multiple functions in higher plants. *Cytogenet. Genome Res.* 124, 202–214. doi: 10.1159/000218126
- Symington, L. S. (2002). Role of RAD52 epistasis group genes in homologous recombination and double-strand break repair. *Microbiol. Mol. Biol. Rev.* 66, 630–670. doi: 10.1128/MMBR.66.4.630-670.2002
- Takahashi, N., Quimbaya, M., Schubert, V., Lammens, T., Vandepoele, K., Schubert, I., et al. (2010). The MCM-binding protein ETG1 aids sister chromatid cohesion required for postreplicative homologous recombination repair. *PLoS Genet.* 6:e1000817. doi: 10.1371/journal.pgen.1000817
- Takeda, S., Tadele, Z., Hofmann, I., Probst, A. V., Angelis, K. J., Kaya, H., et al. (2004). BRU1, a novel link between responses to DNA damage and epigenetic gene silencing in *Arabidopsis*. *Genes Dev.* 18, 782–793. doi: 10.1101/gad.295404
- Tuteja, N., Ahmad, P., Panda, B. B., and Tuteja, R. (2009). Genotoxic stress in plants: shedding light on DNA damage, repair and DNA repair helicases. *Mutat. Res.* 681, 134–149. doi: 10.1016/j.mrrev.2008.06.004
- Watanabe, K., Pacher, M., Dukowic, S., Schubert, V., Puchta, H., and Schubert, I. (2009). The STRUCTURAL MAINTENANCE OF CHROMOSOMES 5/6 complex promotes sister chromatid alignment and homologous recombination after DNA damage in *Arabidopsis thaliana*. *Plant Cell* 21, 2688–2699. doi: 10.1105/tpc.108.060525
- Waterworth, W. M., Drury, G. E., Bray, C. M., and West, C. E. (2011). Repairing breaks in the plant genome: the importance of keeping it together. *New Phytol.* 192, 805–822. doi: 10.1105/tpc.108.060525
- West, C. E., Waterworth, W. M., Sunderland, P. A., and Bray, C. M. (2004). *Arabidopsis* DNA double-strand break repair pathways. *Biochem. Soc. Trans.* 32, 964–966. doi: 10.1042/BST0320964
- Yoshiyama, K. O., Kimura, S., Maki, H., Britt, A. B., and Umeda, M. (2014). The role of SOGI1, a plant-specific transcriptional regulator, in the DNA damage response. *Plant Signal. Behav.* 9:e28889. doi: 10.4161/psb.28889
- Yoshiyama, K. O., Sakaguchi, K., and Kimura, S. (2013). DNA damage response in plants: conserved and variable response compared to animals. *Biology (Basel)* 2, 1338–1356. doi: 10.3390/biology2041338
- Zhou, B. B., and Elledge, S. J. (2000). The DNA damage response: putting checkpoints in perspective. *Nature* 408, 433–439. doi: 10.1038/35044005

Conflict of Interest Statement: The author declares that the research was conducted in the absence of any commercial or financial relationships that could be construed as a potential conflict of interest.

Received: 20 June 2014; accepted: 03 September 2014; published online: 23 September 2014.

Citation: Roy S (2014) Maintenance of genome stability in plants: repairing DNA double strand breaks and chromatin structure stability. *Front. Plant Sci.* 5:487. doi: 10.3389/fpls.2014.00487

This article was submitted to Plant Physiology, a section of the journal *Frontiers in Plant Science*.

Copyright © 2014 Roy. This is an open-access article distributed under the terms of the Creative Commons Attribution License (CC BY). The use, distribution or reproduction in other forums is permitted, provided the original author(s) or licensor are credited and that the original publication in this journal is cited, in accordance with accepted academic practice. No use, distribution or reproduction is permitted which does not comply with these terms.



Signaling of double strand breaks and deprotected telomeres in *Arabidopsis*

Simon Amiard, Maria E. Gallego and Charles I. White*

Génétique, Reproduction et Développement, UMR CNRS 6293/U1103 INSERM/Clermont Université, Université Blaise Pascal, Aubière cedex, France

Edited by:

Alma Balestrazzi, University of Pavia, Italy

Reviewed by:

Avraham Levy, Weizmann Institute of Science, Israel

Wanda Waaterworth, University of Leeds, UK

***Correspondence:**

Charles I. White, Génétique, Reproduction et Développement, UMR CNRS 6293/U1103 INSERM/Clermont Université, Université Blaise Pascal, BP80026, 63171 Aubière cedex, France

e-mail: chwhite@univ-bpclermont.fr

Failure to repair DNA double strand breaks (DSB) can lead to chromosomal rearrangements and eventually to cancer or cell death. Radiation and environmental pollutants induce DSB and this is of particular relevance to plants due to their sessile life style. DSB also occur naturally in cells during DNA replication and programmed induction of DSB initiates the meiotic recombination essential for gametogenesis in most eukaryotes. The linear nature of most eukaryotic chromosomes means that each chromosome has two "broken" ends. Chromosome ends, or telomeres, are protected by nucleoprotein caps which avoid their recognition as DSB by the cellular DNA repair machinery. Deprotected telomeres are recognized as DSB and become substrates for recombination leading to chromosome fusions, the "bridge-breakage-fusion" cycle, genome rearrangements and cell death. The importance of repair of DSB and the severity of the consequences of their misrepair have led to the presence of multiple, robust mechanisms for their detection and repair. After a brief overview of DSB repair pathways to set the context, we present here an update of current understanding of the detection and signaling of DSB in the plant, *Arabidopsis thaliana*.

Keywords: signaling, sensing, double strand breaks, telomere, DNA repair

DSBs REPAIR PATHWAYS IN ARABIDOPSIS THALIANA

Double strand breaks (DSB) repair pathways are classed as either homologous recombination (HR) or non-homologous end-joining (NHEJ), depending upon the dependence or not on DNA sequence homology between the recombining molecules. HR requires the presence of an intact homologous DNA template and is most active in S/G2 phase when the sister chromatid is present. The critical step during HR is the formation of RAD51 filament on the 3' ended single-stranded DNA (ssDNA) produced by resection of the breaks. The nucleofilament formed by RAD51 on the broken DNA molecule catalyzes the invasion of a homologous DNA template sequence by the 3' ended DNA strand(s), which are extended through DNA synthesis, and finally the joint recombination intermediate is resolved to complete the process (for review, Heyer and Liu, 2010). The major players in HR are very highly conserved and most have been identified and characterized in *Arabidopsis thaliana* (Mannuss et al., 2011).

The participation, or not, of the KU complex permits classification of NHEJ pathways into two categories: direct joining of breaks through the KU-dependent pathway and end-joining involving microhomologies by the KU-independent microhomology-mediated (MMEJ) and "alternative" or "back-up" end-joining (Alt-NHEJ or B-NHEJ; for review, Decottignies, 2013). In *Arabidopsis* the KU-dependent pathway has been the subject of a number of studies (Riha et al., 2002; Friesner and Britt, 2003; Gallego et al., 2003; Van Attikum et al., 2003). The distinction between KU-independent pathways is not clear because both imply the use of microhomology sequence to repair the break. In vertebrates, it is known that Alt-NHEJ is based on the action of proteins usually known for their role in single strand breaks repair

XRCC1, PARP1 and LIG3 (Decottignies, 2013). In *Arabidopsis*, the conservation of this pathway has been confirmed through studies of XRCC1 (Charbonnel et al., 2010) and PARP1/PARP2 (Jia et al., 2013). Concerning the MMEJ pathway, the first actors identified were the MRX (MRN) and the Rad1/Rad10 (ERCC1/XPF) complexes in yeast (Ma et al., 2003). Similarly in *Arabidopsis*, MRE11 has been implicated in the use of microhomologies in telomere fusions (Heacock et al., 2004) and XPF has been shown to be involved in a third NHEJ pathway of DSB repair independent of the KU complex and XRCC1 (Charbonnel et al., 2011).

The viability of the single and multiple mutants for each of these pathways in *Arabidopsis* permitted study of the kinetics of DSB repair *in planta*, establishing a hierarchy of DSB repair pathways in *Arabidopsis* (Charbonnel et al., 2011). A surprising result of this study was the ability of quadruple *ku80 xrcc1 xpf xrcc2* mutants (invalidated for all known HR and NHEJ pathways) to repair ionising radiation (IR)-induced DSB, but at a very reduced rate. Although this "repair" is accompanied by high levels of anaphase chromosome bridging, plants cells are thus able to repair DSB in the absence of all four major DSB repair pathways. This results points to another end-joining pathway that would be activated in case of extreme stress and could be one part of the explanation of the striking ability of plants to develop in presence of high levels of genome damage.

The choice of repair mechanisms is tightly regulated with respect to the cell cycle phase and the nature of the break (Chapman et al., 2012). DSB end resection has been shown to be an essential step for the choice of repair pathway, with recent reports showing the implication of 53BP1-RIF1 in blocking resection and thus stimulating NHEJ, and BRCA1-CtIP promoting DNA

resection and HR in mammals (Chapman et al., 2013; Escribano-Díaz et al., 2013; Zimmermann et al., 2013). CtIP (Uanschou et al., 2007) and BRCA1 (Lafarge and Montane, 2003; Trapp et al., 2011) orthologs, but not 53BP1 or RIF1, have been described in *Arabidopsis*, but no detail of their roles in these processes have been reported.

ncRNA (non-coding RNA) are clearly involved in multiple aspects of DNA repair. miRNA (microRNA) transcription is induced after DNA damage and these small RNA are believed to be involved in the regulation of DNA damage repair proteins (reviewed by Chowdhury et al., 2013). Recent work shows links directly to DSB repair in *Arabidopsis* as well as in mammalian cells. Small RNA (diRNA) are produced directly at break sites and are required for correct repair, probably through chromatin modifications or through the recruitment of repair proteins to facilitate repair (Wei et al., 2012).

SIGNALING OF DSBS

The first essential step of the repair process is the recognition and the signaling of the DNA break. This step is critical as it allows cell-cycle arrest, recruitment of DSB repair proteins, chromatin remodeling and eventually cell death or senescence (Goodarzi et al., 2010). In yeast as well as in mammals, the main factors involved in the sensing of the DSB are the MRX/N (Mre11, Rad50 and Xrs2/Nbs1) and the KU (Ku70/Ku80) complexes that compete for binding to unprocessed DSBs (Hiom, 2010). Together with DNA-PKcs, the human KU complex, forming the DNA-PK holoenzyme, functions as a DNA end-bridging factor leading to repair via NHEJ, essentially in G1 phase (Lieber, 2010). In G2 phase, the binding of KU is inhibited and the MRN complex initiates repair via HR (Heyer and Liu, 2010). In plants as well as in yeast, the DNA-PKcs enzyme is not conserved, hence the tethering of the DNA ends is presumably carried out by the MRN complex or by other proteins.

The signaling role is then assumed by specific kinases belonging to the PI3K-like protein kinase family (PIKK): Tel1/ATM and Mec1/ATR. The binding of the yeast MRX complex to the DSB promotes the recruitment of Tel1 leading to Tel1-dependent cell cycle checkpoint activation prior to DNA processing (Usui et al., 2001). Absence of Tel1 can be compensated for by Mec1 (Morrow et al., 1995), with the yeast *tel1* mutant being checkpoint sufficient and not hyper-sensitive to DNA damaging agents (Mantiero et al., 2007). In vertebrates, ATM is activated by DNA double-strand breaks, while ATR is activated by ssDNA, formed notably in processing blocked replication forks (Cimprich and Cortez, 2008). Once bound to DNA, MRN recruits and activates ATM via interaction with Nbs1 (Lavin, 2007) and Mre11 nuclease activity leads to the formation of single strand oligonucleotides that further promote ATM activation (Jazayeri et al., 2008). Further maturation of the DNA extremities can also lead to ssDNA formation and ATR activation (Jazayeri et al., 2006). Mutation of ATM in humans leads to Ataxia-telangiectasia (A-T), a genomic instability disorder characterized by neurodegeneration, immunodeficiency and sensibility to ionizing radiation. At the cellular level, the hallmarks of ATM deficiency are increased chromosomal breakage and premature senescence (Shiloh and Ziv, 2013). In the absence of ATM (in A-T cells), signaling of

DNA breaks can be accomplished by ATR helped by EXO1, however, the absence of both kinases results in the absence of cell cycle arrest due to defects in signaling of breaks (Tomimatsu et al., 2009).

Mec1/ATR is considered to be the specific sensor of DNA replication fork stalling and DNA replication damage, and is more generally activated by a variety of lesions that have in common the generation of ssDNA. Irrespective of the origin of the ssDNA, ATR is recruited by its cofactor ATRIP, which indirectly recognizes ssDNA through interaction with the ssDNA-binding protein, RPA. The 9-1-1 checkpoint clamp has also been implicated in activation of the ATR/Mec1 kinase (Majka et al., 2006). Mec1 is an essential gene in yeast (Weinert et al., 1994) and even in the absence of exogenous genotoxic stress, Mec1 mutants accumulate gross spontaneous chromosomal rearrangements (GCRs; Myung and Kolodner, 2002). ATR deficiency is lethal in mammalian cells but hypomorphic *atr* mutations have been described in a few patients with the rare Seckel syndrome, characterized by microcephaly and growth retardation (O'Driscoll et al., 2003).

The presence of ATM and ATR is well conserved while, as for yeast, no DNA-PK ortholog has been identified in plants. IR-induced gamma-H2AX foci are mediated essentially by ATM and less so by ATR, with no foci observed in irradiated *atm atr* mutant cells (Friesner et al., 2005), confirming that AtATM and AtATR are the only DSB signaling PIKK kinases in plants. The presence in *Arabidopsis* of the protein AtATRIP, necessary for AtATR activation as seen in mammals, further reinforces the idea that DNA damage signaling in plants is conserved (Sweeney et al., 2009). The role of the MRN complex in DNA damage detection and activation of kinase mediated signaling is conserved in *Arabidopsis* (Amiard et al., 2010) and plant homologs of the genes encoding the 9-1-1 (Rad9/Rad1/Hus1) sensor complex have been identified and are required for resistance to the DNA damaging agents Bleomycin and Mitomycin C (MMC; Heitzeberg et al., 2004).

Arabidopsis atm mutants are phenotypically wild type, except for a partial sterility (Culligan and Britt, 2008). These plants are however hypersensitive to ionizing irradiation and methyl methane sulphonate (MMS), but not to UV irradiation. *Arabidopsis atr* mutants are viable, fertile, and like *atm* mutants, phenotypically wild-type in the absence of exogenous DNA damaging agents. *atr* mutants are hypersensitive to hydroxyurea and aphidicolin, due to a defective G2 checkpoint response to blocked replication forks (Culligan et al., 2004). ATR can however partially compensate for the ATM response, as the double *atm atr* mutant is completely sterile due to meiotic prophase genome fragmentation (Culligan and Britt, 2008).

Neither ATR nor ATM signaling is thus essential during normal plant development – a surprising result given the conservation of the roles of these proteins in plants and the lethality of the corresponding mutants in mammals. A hint to a possible explanation for this could come from the ability of DSBs to be repaired in plants in the double *rad50 atr* mutant, which combines absence of ATM and ATR activities and absence of H2AX phosphorylation (see next section). Spontaneous DSBs appear in consequence of replication defects in these plants and result in high levels of anaphase bridging, showing that *Arabidopsis* can repair DSB in the absence of PIKK activation (Amiard et al., 2010).

Once activated, PIKK can activate many targets necessary to maintain genomic integrity (Culligan et al., 2006; Matsuoka et al., 2007). Phosphorylation of the histone variant H2A/H2AX around the break by PIKK is an early cellular response to the induction of DSBs and occurs over 50 kb in yeast to 2 Mb for H2AX in mammals. H2AX phosphorylation is easily detected using phospho-specific antisera and has emerged as a highly specific and sensitive molecular marker for monitoring DNA damage and its repair (Kinner et al., 2008). Although not required for the initial recruitment of signaling and repair factors, H2AX phosphorylation is essential for their accumulation at the breaks (Celeste et al., 2003; Fernandez-Capetillo et al., 2003; Fillingham et al., 2006). The importance of this is seen in the sensitivity to DSB damaging agents, impaired DSB repair and defects in G1 checkpoint activation of yeast mutants of the H2A gene (Downs et al., 2000; Redon et al., 2003; Hammet et al., 2007) and similar phenotypes of mammalian cells and mice deficient for H2AX (Celeste et al., 2002). Moreover H2AX deficient mice were radiation sensitive, growth retarded, immune deficient and males were infertile.

In contrast, *Arabidopsis* mutants for this histone develop normally and only a slight defect in DSB repair has been reported in RNAi knock-down lines (Lang et al., 2012). Moreover, the phosphorylation of this histone does not seem required for DSB repair in plants, as seen in the chromosome fusions observed in the *rad50 atr* double mutant (Amiard et al., 2010). This being so, how is DSB signaling mediated in the absence of H2AX phosphorylation in *Arabidopsis*? A possible answer comes from reports showing roles of modifications of other histones around DSB in mammals: ubiquitylation of H2A by RNF8 is required for proper 53BP1 recruitment (Marteijn et al., 2009; Rossetto et al., 2010) and a role for histone lysine methylation in DSB repair is supported by the observation that H3K36me2 enhances DNA repair by NHEJ (Fnu et al., 2011). H3K36me2, once formed at DSB site, may create docking sites for other repair proteins, recruiting them for transcription and DNA repair. It will be of great interest to see whether such modifications also play important roles in repair of DSBs in plants.

SIGNALING OF DEPROTECTED TELOMERES

Telomeres consist of an elaborate, higher-order assembly of specific DNA sequence and proteins that cooperatively provide protection against degradation and recombination of the ends of linear eukaryotic chromosomes. In vertebrates, telomere protection is provided mainly by Shelterin, a complex of six telomeric proteins (TRF1, TRF2, POT1, TIN2, TPP1 and RAP1) that prevents inappropriate recombination and fusion between telomeres, and also has complementary roles in telomere replication and length regulation (Palm and De Lange, 2008; Martínez and Blasco, 2011). TRF1 and TRF2 bind to the duplex region of the telomere and searches for TRF-like proteins in *Arabidopsis* have identified many proteins able to bind double-stranded telomeric DNA (Zellinger and Riha, 2007; Amiard et al., 2011b; Peška et al., 2011). None of these seems however to be essential for telomere protection, suggesting redundancy of double-stranded DNA binding telomeric proteins in plants. POT1 binds to the natural single-stranded (ss) extension of the G-rich strand of chromosome ends (G-overhang or 3'-overhang) and in both humans and

Saccharomyces pombe, POT1 plays a key role in telomere end protection (Baumann and Cech, 2001). *Arabidopsis* has two POT1 orthologs, POT1a and POT1b, both of which associate with the

Table 1 | Major factors involved in DNA double strand break signaling and repair and telomere protection in budding yeast, human and *Arabidopsis thaliana*.

	<i>Saccharomyces cerevisiae</i>	Human	<i>Arabidopsis thaliana</i>
Sensing	Mre11/Rad50/Xrs2	Mre11/Rad50/Nbs1	Mre11/Rad50/Nbs1
Signaling	Mec1	ATR	ATR
	Tel1	ATM	ATM
	H2A	H2AX	H2AX
Mediators			
ATM	Rad9	53BP1	n.i.
signaling	Rif1	RIF1	n.i.
	n.o.	BRCA1	BRCA1
	n.o.	BRCA2	BRCA2
	Sae2	CtIP	COM1
ATR	Ddc2	ATRIP	ATRIP
signaling	Ddc1/Rad17/Mec3	RAD9/RAD1/HUS1	RAD9/RAD1/HUS1
	Rfa	RPA	RPA
HR	Rad51	RAD51	RAD51
	Rad51 paralogs:	RAD51 paralogs:	RAD51 paralogs:
	(Rad55/Rad57/Shu1/	(RAD51B/C/D/	(RAD51B/C/D/
	Shu2/Csm2/Psy3)	XRCC2/XRCC3)	XRCC2/XRCC3)
	Rad52	RAD52	RAD52 (2 genes)
	Rad10	ERCC1	ERCC1
	Rad1	XPF	XPF
	Exo1	EXO1	EXO1
NHEJ	Ku70/Ku80	KU70/KU80	KU70/KU80
	Dnl4	LIG4	LIG4
	Lif1	XRCC4	XRCC4
	n.o.	XRCC1	XRCC1
	n.o.	PARP1	PARP1
	n.o.	PARP2	PARP2
	n.o.	LIG3	n.i.
	n.o.	DNA-PKcs	n.o.
Telomeric	n.o.	TRF1	n.i.
protection	n.o.	TRF2	n.i.
	n.o.	POT1	POT1A/POT1B
	n.o.	TIN2	n.i.
	n.o.	TPP1	n.i.
	Rap1	RAP1	n.i.
	Cdc13	CTC1	CTC1
	STN1	STN1	STN1
	TEN1	TEN1	TEN1

n.o., no ortholog; n.i., no identified orthologue reported.

telomerase ribonucleoprotein but do not bind telomeric ssDNA and are not essential for telomere capping (Surovtseva et al., 2007; Shakirov et al., 2009; Cifuentes-Rojas et al., 2011).

In *S. cerevisiae* there has been no shelterin-like complex identified to date and a somewhat simpler protection complex, consisting mainly of the CST complex (Cdc13, Stn1 and Ten1), is present (Garvik et al., 1995; Grandin et al., 2001; Shore and Bianchi, 2009). Yeast Cdc13, together with Stn1 and Ten1, plays a dual role in telomere end protection and regulation of telomere replication. Orthologs of the *S. cerevisiae* CST proteins have been found in humans and mouse, as well as in *Arabidopsis* (Miyake et al., 2009; Surovtseva et al., 2009). Recent studies in mammalian cells reveal that the CST complex seems to be implicated in facilitating telomere replication by rescuing replication after fork stalling (Stewart et al., 2012) and that this complex is involved in the regulation of the telomeric 3' overhang by C-strand fill-in by Polymerase alpha (Wang et al., 2012). Plants appear to represent an evolutionary intermediate between *S. cerevisiae*, which has only CST as a capping complex, and vertebrates which use both shelterin and CST complex for telomere capping and correct telomeric replication (Giraud-Panis et al., 2010; Price et al., 2010).

Deprotected telomeres are recognized by cells as DSB, and their “repair” results in chromosome fusions/rearrangements and genomic instability (De Lange, 2009). As for other DSB, deprotected telomeres are substrates for kinase activation and are characterized by the appearance of TIFs (telomere induced foci), DNA damage response factors that coincide with telomere signals. In mammals the absence of TRF2 or POT1 leads to the appearance of TIFs and this depends upon ATM and ATR, respectively (De Lange, 2009). In plants, we have shown that the appearance of TIFs in *ctc1* or *stn1* mutants are exclusively ATR-dependent and that in absence of the catalytic subunit of the telomerase (TERT), the short deprotected telomeres are recognized as DSBs through the activation of both ATM and ATR (Amiard et al., 2011a). Surprisingly, we have shown that in the *Arabidopsis* *ctc1*

atr mutant, which does not form TIFs, telomeres are still able to fuse. This result contrast clearly with the situation in vertebrates, where ATM and ATR are absolutely required for fusion of deprotected telomeres in absence of the TRF2 or POT1, respectively (Denchi and De Lange, 2007). Hence here again, plant repair pathways can still be activated in absence of the kinase activity.

CONCLUSION

This short review summarizes knowledge concerning DNA break signaling in *Arabidopsis thaliana*. A list of genes discussed here is presented in **Table 1** and we refer interested readers to a recent compilation of *Arabidopsis* DNA repair/recombination genes (http://www.plb.ucdavis.edu/labs/britt/Plant_DNA_Repair_Genes.html). Given the crucial importance of the signaling step in DNA repair it is not surprising to find strong conservation of these mechanisms in higher eukaryotes. Nevertheless, evidence points to a particular ability of plants to repair even in absence of signaling and the presence of an unknown plant specific repair pathway(s) is now suspected. Plants possess a not fully understood ability to resist and develop in presence of DNA damaging agents and the implication of plant specific recombination events could provide part of the explanation for this. The increased spontaneous recombination rates seen in plants subjected to biotic or abiotic stresses (review by Waterworth et al., 2011) has been proposed to be a programmed response increasing the plasticity of plant genome leading to acceleration of plant evolution (Molinier et al., 2006; Boyko and Kovalchuk, 2011).

ACKNOWLEDGMENTS

This work was supported by grants from European Union research grant (LSHG-CT-2005-018785), the Centre National de la Recherche Scientifique, the Université Blaise Pascal, the Université d'Auvergne, and the Institut National de la Santé et la Recherche Médicale.

REFERENCES

- Amiard, S., Charbonnel, C., Allain, E., Depeiges, A., White, C. I., and Gallego, M. E. (2010). Distinct roles of the ATR kinase and the Mre11-Rad50-Nbs1 complex in the maintenance of chromosomal stability in *Arabidopsis*. *Plant Cell* 22, 3020–3033. doi: 10.1105/tpc.110.078527
- Amiard, S., Depeiges, A., Allain, E., White, C. I., and Gallego, M. E. (2011a). *Arabidopsis* ATM and ATR kinases prevent propagation of genome damage caused by telomere dysfunction. *Plant Cell* 23, 4254–4265. doi: 10.1105/tpc.111.092387
- Amiard, S., White, C., and Gallego, M. E. (2011b). Recombination proteins and telomere stability in plants. *Curr. Protein Pept. Sci.* 12, 84–92. doi: 10.2174/138920311795684931
- Baumann, P., and Cech, T. R. (2001). Pot1, the putative telomere end-binding protein in fission yeast and humans. *Science* 292, 1171–1175. doi: 10.1126/science.1060036
- Boyko, A., and Kovalchuk, I. (2011). Genome instability and epigenetic modification – heritable responses to environmental stress? *Curr. Opin. Plant Biol.* 14, 260–266. doi: 10.1016/j.pbi.2011.03.003
- Celeste, A., Fernandez-Capetillo, O., Kruehlak, M. J., Pilch, D. R., Staudt, D. W., Lee, A., et al. (2003). Histone H2AX phosphorylation is dispensable for the initial recognition of DNA breaks. *Nat. Cell Biol.* 5, 675–679. doi: 10.1038/ncb1004
- Celeste, A., Petersen, S., Romanienko, P. J., Fernandez-Capetillo, O., Chen, H. T., Sedelnikova, O. A., et al. (2002). Genomic instability in mice lacking histone H2AX. *Science* 296, 922–927. doi: 10.1126/science.1069398
- Chapman, J. R., Barral, P., Vannier, J.-B., Borel, V., Steger, M., Tomas-Loba, A., et al. (2013). RIF1 is essential for 53BP1-dependent nonhomologous end joining and suppression of DNA double-strand break resection. *Mol. Cell* 49, 858–871. doi: 10.1016/j.molcel.2013.01.002
- Chapman, J. R., Taylor, M. R. G., and Boulton, S. J. (2012). Playing the end game: DNA double-strand break repair pathway choice. *Mol. Cell* 47, 497–510. doi: 10.1016/j.molcel.2012.07.029
- Charbonnel, C., Allain, E., Gallego, M. E., and White, C. I. (2011). Kinetic analysis of DNA double-strand break repair pathways in *Arabidopsis*. *DNA Repair* 10, 611–619. doi: 10.1016/j.dnarep.2011.04.002
- Charbonnel, C., Gallego, M. E., and White, C. I. (2010). Xrccl-dependent and Ku-dependent DNA double-strand break repair kinetics in *Arabidopsis* plants. *Plant J.* 64, 280–290. doi: 10.1111/j.1365-313X.2010.04331.x
- Chowdhury, D., Choi, Y. E., and Brault, M. E. (2013). Charity begins at home: non-coding RNA functions in DNA repair. *Nat. Rev. Mol. Cell Biol.* 14, 181–189. doi: 10.1038/nrm3523
- Cifuentes-Rojas, C., Kannan, K., Tseng, L., and Shippen, D. E. (2011). Two RNA subunits and POT1a are components of *Arabidopsis* telomerase. *Proc. Natl. Acad. Sci. U.S.A.* 108, 73–78. doi: 10.1073/pnas.1013021107
- Cimprich, K. A., and Cortez, D. (2008). ATR: an essential regulator of genome integrity. *Nat. Rev. Mol. Cell Biol.* 9, 616–627. doi: 10.1038/nrm2450
- Culligan, K., Tissier, A., and Britt, A. (2004). ATR regulates a G2-phase cell-cycle checkpoint in *Arabidopsis thaliana*. *Plant Cell* 16, 1091–1104. doi: 10.1105/tpc.018903
- Culligan, K. M., and Britt, A. B. (2008). Both ATM and ATR promote the efficient and accurate processing of programmed meiotic double-strand breaks. *Plant J.* 55, 629–638. doi: 10.1111/j.1365-313X.2008.03530.x

- Culligan, K. M., Robertson, C. E., Foreman, J., Doerner, P., and Britt, A. B. (2006). ATR and ATM play both distinct and additive roles in response to ionizing radiation. *Plant J.* 48, 947–961. doi: 10.1111/j.1365-313X.2006.02931.x
- Decottignies, A. (2013). Alternative end-joining mechanisms: a historical perspective. *Front. Genet.* 4:48–54. doi: 10.3389/fgene.2013.00048
- De Lange, T. (2009). How telomeres solve the end-protection problem. *Science* 326, 948–952. doi: 10.1126/science.1170633
- Denchi, E. L., and De Lange, T. (2007). Protection of telomeres through independent control of ATM and ATR by TRF2 and POT1. *Nature* 448, 1068–1071. doi: 10.1038/nature06065
- Downs, J. A., Lowndes, N. F., and Jackson, S. P. (2000). A role for *Saccharomyces cerevisiae* histone H2A in DNA repair. *Nature* 408, 1001–1004. doi: 10.1038/35050000
- Escribano-Díaz, C., Orthwein, A., Fradet-Turcotte, A., Xing, M., Young, J. T. F., Tkàč, J., et al. (2013). A cell cycle-dependent regulatory circuit composed of 53BP1-RIF1 and BRCA1-CHIP controls DNA repair pathway choice. *Mol. Cell* 49, 872–883. doi: 10.1016/j.molcel.2013.01.001
- Fernandez-Capetillo, O., Celeste, A., and Nussenzweig, A. (2003). Focusing on foci: H2AX and the recruitment of DNA-damage response factors. *Cell Cycle* 2, 426–427. doi: 10.4161/cc.2.5.509
- Fillingham, J., Keogh, M.-C., and Krogan, N. J. (2006). GammaH2AX and its role in DNA double-strand break repair. *Biochem. Cell Biol.* 84, 568–577. doi: 10.1139/o06-072
- Fnu, S., Williamson, E. A., De Haro, L. P., Brenneman, M., Wray, J., Shaheen, M., et al. (2011). Methylation of histone H3 lysine 36 enhances DNA repair by nonhomologous end-joining. *Proc. Natl. Acad. Sci. U.S.A.* 108, 540–545. doi: 10.1073/pnas.1013571108
- Friesner, J., and Britt, A. B. (2003). Ku80- and DNA ligase IV-deficient plants are sensitive to ionizing radiation and defective in T-DNA integration. *Plant J.* 34, 427–440. doi: 10.1046/j.1365-313X.2003.01738.x
- Friesner, J. D., Liu, B., Culligan, K., and Britt, A. B. (2005). Ionizing radiation-dependent gamma-H2AX focus formation requires ataxia telangiectasia mutated and ataxia telangiectasia mutated and Rad3-related. *Mol. Biol. Cell* 16, 2566–2576. doi: 10.1091/mbc.E04-10-0890
- Gallego, M. E., Bleuyard, J. Y., Daoudal-Cotterell, S., Jallut, N., and White, C. I. (2003). Ku80 plays a role in non-homologous recombination but is not required for T-DNA integration in *Arabidopsis*. *Plant J.* 35, 557–565. doi: 10.1046/j.1365-313X.2003.01827.x
- Garvik, B., Carson, M., and Hartwell, L. (1995). Single-stranded DNA arising at telomeres in cdc13 mutants may constitute a specific signal for the RAD9 checkpoint. *Mol. Cell. Biol.* 15, 6128–6138.
- Giraud-Panis, M.-J., Teixeira, M. T., Gély, V., and Gilson, E. (2010). CST meets shelterin to keep telomeres in check. *Mol. Cell* 39, 665–676. doi: 10.1016/j.molcel.2010.08.024
- Goodarzi, A. A., Jeggo, P., and Löbrich, M. (2010). The influence of heterochromatin on DNA double strand break repair: getting the strong, silent type to relax. *DNA Repair* 9, 1273–1282. doi: 10.1016/j.dnarep.2010.09.013
- Grandin, N., Damon, C., and Charbonneau, M. (2001). Ten1 functions in telomere end protection and length regulation in association with Stn1 and Cdc13. *EMBO J.* 20, 1173–1183. doi: 10.1093/emboj/20.5.1173
- Hammet, A., Magill, C., Heierhorst, J., and Jackson, S. P. (2007). Rad9 BRCT domain interaction with phosphorylated H2AX regulates the G1 checkpoint in budding yeast. *EMBO Rep.* 8, 851–857. doi: 10.1038/sj.embor.7401036
- Heacock, M., Spangler, E., Riha, K., Puizina, J., and Shippen, D. E. (2004). Molecular analysis of telomere fusions in *Arabidopsis*: multiple pathways for chromosome end-joining. *EMBO J.* 23, 2304–2313. doi: 10.1038/sj.emboj.7600236
- Heitzberg, F., Chen, I.-P., Hartung, F., Orel, N., Angelis, K. J., and Puchta, H. (2004). The Rad17 homologue of *Arabidopsis* is involved in the regulation of DNA damage repair and homologous recombination. *Plant J.* 38, 954–968. doi: 10.1111/j.1365-313X.2004.02097.x
- Heyer, W.-D., and Liu, J. (2010). Regulation of homologous recombination in eukaryotes. *Annu. Rev. Genet.* 44, 113–139. doi: 10.1146/annurev-genet-051710-150955
- Hiom, K. (2010). Coping with DNA double strand breaks. *DNA Repair* 9, 1256–1263. doi: 10.1016/j.dnarep.2010.09.018
- Jazayeri, A., Balestrini, A., Garner, E., Haber, J. E., and Costanzo, V. (2008). Mre11-Rad50-Nbs1-dependent processing of DNA breaks generates oligonucleotides that stimulate ATM activity. *EMBO J.* 27, 1953–1962. doi: 10.1038/emboj.2008.128
- Jazayeri, A., Falck, J., Lukas, C., Bartek, J., Smith, G. C. M., Lukas, J., et al. (2006). ATM- and cell cycle-dependent regulation of ATR in response to DNA double-strand breaks. *Nat. Cell Biol.* 8, 37–45. doi: 10.1038/ncb1337
- Jia, Q., Den Dulk-Ras, A., Shen, H., Hooykaas, P. J., and De Pater, S. (2013). Poly(ADP-ribose)polymerases are involved in microhomology mediated backup non-homologous end joining in *Arabidopsis thaliana*. *Plant Mol. Biol.* 82, 339–351. doi: 10.1007/s11103-013-0065-9
- Kinner, A., Wu, W., Staudt, C., and Iliakis, G. (2008). Gamma-H2AX in recognition and signaling of DNA double-strand breaks in the context of chromatin. *Nucleic Acids Res.* 36, 5678–5694. doi: 10.1093/nar/gkn550
- Lafarge, S., and Montane, M. H. (2003). Characterization of *Arabidopsis thaliana* ortholog of the human breast cancer susceptibility gene 1: AtBRCA1, strongly induced by gamma rays. *Nucleic Acids Res.* 31, 1148–1155. doi: 10.1093/nar/gkg202
- Lang, J., Smetana, O., Sanchez-Calderon, L., Lincker, F., Genestier, J., Schmitz, A.-C., et al. (2012). Plant γH2AX foci are required for proper DNA DSB repair responses and colocalize with E2F factors. *New Phytol.* 194, 353–363. doi: 10.1111/j.1469-8137.2012.04062.x
- Lavin, M. F. (2007). ATM and the Mre11 complex combine to recognize and signal DNA double-strand breaks. *Oncogene* 26, 7749–7758. doi: 10.1038/sj.onc.1210880
- Lieber, M. R. (2010). The mechanism of double-strand DNA break repair by the nonhomologous DNA end-joining pathway. *Annu. Rev. Biochem.* 79, 181–211. doi: 10.1146/annurev.biochem.052308.093131
- Ma, J.-L., Kim, E. M., Haber, J. E., and Lee, S. E. (2003). Yeast Mre11 and Rad1 proteins define a Ku-independent mechanism to repair double-strand breaks lacking overlapping end sequences. *Mol. Cell. Biol.* 23, 8820–8828. doi: 10.1128/MCB.23.23.8820-8828.2003
- Majka, J., Niedziela-Majka, A., and Burgers, P. M. J. (2006). The checkpoint clamp activates Mec1 kKinase during initiation of the DNA damage checkpoint. *Mol. Cell* 24, 891–901. doi: 10.1016/j.molcel.2006.11.027
- Mannuss, A., Trapp, O., and Puchta, H. (2011). Gene regulation in response to DNA damage. *Biochim. Biophys. Acta* 1819, 154–165. doi: 10.1016/j.bbagen.2011.08.003
- Mantiero, D., Clerici, M., Lucchini, G., and Longhese, M. P. (2007). Dual role for *Saccharomyces cerevisiae* Tel1 in the checkpoint response to double-strand breaks. *EMBO Rep.* 8, 380–387. doi: 10.1038/sj.embor.7400911
- Marteijn, J. A., Bekker-Jensen, S., Maijland, N., Lans, H., Schwertman, P., Gourdin, A. M., et al. (2009). Nucleotide excision repair-induced H2A ubiquitination is dependent on MDC1 and RNF8 and reveals a universal DNA damage response. *J. Cell Biol.* 186, 835–847. doi: 10.1083/jcb.200902150
- Martínez, P., and Blasco, M. A. (2011). Telomeric and extra-telomeric roles for telomerase and the telomere-binding proteins. *Nat. Rev. Cancer* 11, 161–176. doi: 10.1038/nrc3025
- Matsuoka, S., Ballif, B. A., Smogorzewska, A., McDonald, E. R., Hurw, K. E., Luo, J., et al. (2007). ATM and ATR substrate analysis reveals extensive protein networks responsive to DNA damage. *Science* 316, 1160–1166. doi: 10.1126/science.1140321
- Miyake, Y., Nakamura, M., Nabeta, A., Shimamura, S., Tamura, M., Yonehara, S., et al. (2009). RPA-like mammalian Ctc1-Stn1-Ten1 complex binds to single-stranded DNA and protects telomeres independently of the Pot1 pathway. *Mol. Cell* 36, 193–206. doi: 10.1016/j.molcel.2009.08.009
- Molinier, J., Ries, G., Zipfel, C., and Hohn, B. (2006). Trans-generation memory of stress in plants. *Nature* 442, 1046–1049. doi: 10.1038/nature05022
- Morrow, D. M., Tagle, D. A., Shiloh, Y., Collins, F. S., and Hieter, P. (1995). TEL1, an *S. cerevisiae* homolog of the human gene mutated in ataxia telangiectasia, is functionally related to the yeast checkpoint gene MEC1. *Cell* 82, 831–840. doi: 10.1016/0092-8674(95)90480-8
- Myung, K., and Kolodner, R. D. (2002). Suppression of genome instability by redundant S-phase checkpoint pathways in *Saccharomyces cerevisiae*. *Proc. Natl. Acad. Sci. U.S.A.* 99, 4500–4507. doi: 10.1073/pnas.062702199
- O'Driscoll, M., Ruiz-Perez, V. L., Woods, C. G., Jeggo, P. A., and Goodship, J. A. (2003). A splicing mutation affecting expression of ataxia-telangiectasia and Rad3-related protein (ATR) results in Seckel syndrome. *Nat. Genet.* 33, 497–501. doi: 10.1038/ng1129

- Palm, W., and De Lange, T. (2008). How shelterin protects mammalian telomeres. *Annu. Rev. Genet.* 42, 301–334. doi: 10.1146/annurev.genet.41.110306.130350
- Peška, V., Procházková Schrumpfová, P., and Fajkus, J. (2011). Using the telobox to search for plant telomere binding proteins. *Curr. Protein Pept. Sci.* 12, 75–83. doi: 10.2174/138920311795684968
- Price, C. M., Boltz, K. A., Chaiken, M. F., Stewart, J. A., Beilstein, M. A., and Shippenn, D. E. (2010). Evolution of CST function in telomere maintenance. *Cell Cycle* 9, 3157–3165. doi: 10.4161/cc.9.16.12547
- Redon, C., Pilch, D. R., Rogakou, E. P., Orr, A. H., Lowndes, N. F., and Bonner, W. M. (2003). Yeast histone 2A serine 129 is essential for the efficient repair of checkpoint-blind DNA damage. *EMBO Rep.* 4, 678–684. doi: 10.1038/sj.embo.embor871
- Riha, K., Matthew Watson, J., Parkey, J., and Shippenn, D. E. (2002). Telomere length deregulation and enhanced sensitivity to genotoxic stress in *Arabidopsis* mutants deficient in Ku70. *EMBO J.* 21, 2819–2826. doi: 10.1093/emboj/21.11.2819
- Rossetto, D., Truman, A. W., Kron, S. J., and Cote, J. (2010). Epigenetic modifications in double-strand break DNA damage signaling and repair. *Clin. Cancer Res.* 16, 4543–4552. doi: 10.1158/1078-0432.CCR-10-0513
- Shakirov, E. V., Song, X., Joseph, J. A., and Shippenn, D. E. (2009). POT1 proteins in green algae and land plants: DNA-binding properties and evidence of co-evolution with telomeric DNA. *Nucleic Acids Res.* 37, 7455–7467. doi: 10.1093/nar/gkp785
- Shiloh, Y., and Ziv, Y. (2013). The ATM protein kinase: regulating the cellular response to genotoxic stress, and more. *Nat. Rev. Mol. Cell Biol.* 14, 197–210. doi: 10.1038/nrm3546
- Shore, D., and Bianchi, A. (2009). Telomere length regulation: coupling DNA end processing to feedback regulation of telomerase. *28*, 2309–2322. doi: 10.1038/embj.2009.195
- Stewart, J. A., Wang, F., Chaiken, M. F., Kasbek, C., Chastain, P. D., Wright, W. E., et al. (2012). Human CST promotes telomere duplex replication and general replication restart after fork stalling. *EMBO J.* 31, 3537–3549. doi: 10.1038/embj.2012.215
- Surovtseva, Y. V., Churikov, D., Boltz, K. A., Song, X., Lamb, J. C., Warrington, R., et al. (2009). Conserved telomere maintenance component 1 interacts with STN1 and maintains chromosome ends in higher eukaryotes. *Mol. Cell* 36, 207–218. doi: 10.1016/j.molcel.2009.09.017
- Surovtseva, Y. V., Shakirov, E. V., Vespa, L., Osbun, N., Song, X., and Shippenn, D. E. (2007). *Arabidopsis* POT1 associates with the telomerase RNP and is required for telomere maintenance. *EMBO J.* 26, 3653–3661. doi: 10.1038/sj.emboj.7601792
- Sweeney, P. R., Britt, A. B., and Culigan, K. M. (2009). The *Arabidopsis* ATRIP ortholog is required for a programmed response to replication inhibitors. *Plant J.* 60, 518–526. doi: 10.1111/j.1365-313X.2009.03975.x
- Tomimatsu, N., Mukherjee, B., and Burma, S. (2009). Distinct roles of ATR and DNA-PKcs in triggering DNA damage responses in ATM-deficient cells. *EMBO Rep.* 10, 629–635. doi: 10.1038/embor.2009.60
- Trapp, O., Seeliger, K., and Puchta, H. (2011). Homologs of breast cancer genes in plants. *Front. Plant Sci.* 2:19. doi: 10.3389/fpls.2011.00019
- Uanschou, C., Siwiec, T., Pedrosa-Harand, A., Kerzendorfer, C., Sanchez-Moran, E., Novatchkova, M., et al. (2007). A novel plant gene essential for meiosis is related to the human CtIP and the yeast COM1/SAE2 gene. *EMBO J.* 26, 5061–5070. doi: 10.1038/sj.emboj.7601913
- Usui, T., Ogawa, H., and Petrini, J. H. (2001). A DNA damage response pathway controlled by Tel1 and the Mre11 complex. *Mol. Cell* 7, 1255–1266. doi: 10.1016/S1097-2765(01)00270-2
- Van Attikum, H., Bundock, P., Overmeer, R. M., Lee, L.-Y., Gelvin, S. B., and Hooykaas, P. J. J. (2003). The *Arabidopsis* AtLIG4 gene is required for the repair of DNA damage, but not for the integration of Agrobacterium T-DNA. *Nucleic Acids Res.* 31, 4247–4255. doi: 10.1093/nar/gkg458
- Wang, F., Stewart, J. A., Kasbek, C., Zhao, Y., Wright, W. E., and Price, C. M. (2012). Human CST has independent functions during telomere duplex replication and C-strand filling. *Cell Rep.* 2, 1096–1103. doi: 10.1016/j.celrep.2012.10.007
- Waterworth, W. M., Drury, G. E., Bray, C. M., and West, C. E. (2011). Repairing breaks in the plant genome: the importance of keeping it together. *New Phytol.* 192, 805–822. doi: 10.1111/j.1469-8137.2011.03926.x
- Wei, W., Ba, Z., Gao, M., Wu, Y., Ma, Y., Amiard, S., et al. (2012). A role for small RNAs in DNA double-strand break repair. *Cell* 149, 101–112. doi: 10.1016/j.cell.2012.03.002
- Weinert, T. A., Kiser, G. L., and Hartwell, L. H. (1994). Mitotic checkpoint genes in budding yeast and the dependence of mitosis on DNA replication and repair. *Genes Dev.* 8, 652–665. doi: 10.1101/gad.8.6.652
- Zellinger, B., and Riha, K. (2007). Composition of plant telomeres. *Biochim. Biophys. Acta* 1769, 399–409. doi: 10.1016/j.bbapex.2007.02.001
- Zimmermann, M., Lottersberger, F., Buonomo, S. B., Sfeir, A., and De Lange, T. (2013). 53BP1 regulates DSB repair using Rif1 to control 5' end resection. *Science* 339, 700–704. doi: 10.1126/science.1231573

Conflict of Interest Statement: The authors declare that the research was conducted in the absence of any commercial or financial relationships that could be construed as a potential conflict of interest.

Received: 23 August 2013; paper pending published: 09 September 2013; accepted: 24 September 2013; published online: 16 October 2013.

Citation: Amiard S, Gallego ME and White CI (2013) Signaling of double strand breaks and deprotected telomeres in *Arabidopsis*. *Front. Plant Sci.* 4:405. doi: 10.3389/fpls.2013.00405

This article was submitted to Plant Physiology, a section of the journal *Frontiers in Plant Science*.

Copyright © 2013 Amiard, Gallego and White. This is an open-access article distributed under the terms of the Creative Commons Attribution License (CC BY). The use, distribution or reproduction in other forums is permitted, provided the original author(s) or licensor are credited and that the original publication in this journal is cited, in accordance with accepted academic practice. No use, distribution or reproduction is permitted which does not comply with these terms.



DNA maintenance in plastids and mitochondria of plants

Delene J. Oldenburg and Arnold J. Bendich*

Department of Biology, University of Washington, Seattle, WA, USA

The DNA molecules in plastids and mitochondria of plants have been studied for over 40 years. Here, we review the data on the circular or linear form, replication, repair, and persistence of the organellar DNA (orgDNA) in plants. The bacterial origin of orgDNA appears to have profoundly influenced ideas about the properties of chromosomal DNA molecules in these organelles to the point of dismissing data inconsistent with ideas from the 1970s. When found at all, circular genome-sized molecules comprise a few percent of orgDNA. In cells active in orgDNA replication, most orgDNA is found as linear and branched-linear forms larger than the size of the genome, likely a consequence of a virus-like DNA replication mechanism. In contrast to the stable chromosomal DNA molecules in bacteria and the plant nucleus, the molecular integrity of orgDNA declines during leaf development at a rate that varies among plant species. This decline is attributed to degradation of damaged-but-not-repaired molecules, with a proposed repair cost-saving benefit most evident in grasses. All orgDNA maintenance activities are proposed to occur on the nucleoid tethered to organellar membranes by developmentally-regulated proteins.

OPEN ACCESS

Edited by:

Kaoru O. Yoshiyama,
Kyoto Sangyo University, Japan

Reviewed by:

Brent L. Nielsen,
Brigham Young University, USA
David Herrin,
University of Texas at Austin, USA

*Correspondence:

Arnold J. Bendich
bendich@uw.edu

Specialty section:

This article was submitted to
Plant Physiology,
a section of the journal
Frontiers in Plant Science

Received: 13 August 2015

Accepted: 05 October 2015

Published: 29 October 2015

Citation:

Oldenburg DJ and Bendich AJ (2015)
DNA maintenance in plastids
and mitochondria of plants.
Front. Plant Sci. 6:883.
doi: 10.3389/fpls.2015.00883

INTRODUCTION

In diploid plants and animals, the chromosomes of both parents are present in the nuclei of nearly all cells. Replication precisely duplicates the chromosomal DNA molecules, and checkpoint control ensures partition of the duplicated chromosomes to daughter cells only after all DNA damage is repaired, leading to constant properties of chromosomal DNA among tissues during development from embryo to adult. In contrast, the properties of chromosomal DNA molecules in the plastids and mitochondria change drastically during development. Why are organellar chromosomes not constant in cells containing constant nuclear chromosomes, despite the fact that the replication/repair apparatus for all cellular DNAs is encoded exclusively by the nuclear genome? The principal reason, we suspect, is that the level of DNA damage is far greater in the organelles than the nucleus. Furthermore, if an organellar DNA molecule is damaged but not repaired, the DNA molecule carrying the damage will be degraded in order to prevent mutagenesis—DNA abandonment (Bendich, 2010b, 2013). In this article, we describe the replication, repair, and persistence of chromosomal DNA molecules in plastids and mitochondria. We conclude that whereas DNA repair suffices for the nucleus, organellar DNA (orgDNA) turnover, copy number change, and abandonment are also needed to maintain cellular homeostasis during development.

THE SIZE AND STRUCTURE OF ORGANELLAR DNA MOLECULES IN PLANTS: A HISTORICAL PERSPECTIVE

In 1963, an autoradiographic image of an evidently intact DNA molecule from a lysed cell of *Escherichia coli* strain K12 was published at a time before the genome size of *E. coli* was known

(Cairns, 1963). This molecule had the form of the Greek letter “theta,” had no ends, and appeared to be undergoing replication. This single example reported of such a theta molecule gave rise to the notion that the bacterial genome was carried on one circular chromosome and profoundly influenced future research on the size and form of DNA molecules from chloroplasts and mitochondria. The measured length of each of the loops of the theta (the replicated portion of the molecule), when added to that of the unreplicated portion, gave a total of 1100 microns. Subsequent work with *E. coli* K12 revealed that the genome size was 4.6 Mb, equivalent to 1580 microns of B-form DNA, most circular molecules were much smaller than genome size (with a few at 2000–4000 microns), and circular molecules were extremely infrequent among all molecules (reviewed by Bendich, 2007). Nonetheless, the expectation was created that chromosomal DNA molecules in plastids and mitochondria would be found on genome-sized circular molecules, as in their bacterial ancestors, and this expectation is still widely held. For the mitochondrial genome of yeast, it took more than 30 years to realize that the nearly exclusively non-circular forms of mitochondrial DNA (mtDNA) should not have been dismissed as “broken circles,” but actually represented the wild-type chromosomes (Williamson, 2002; Bendich, 2007, 2010b).

For plants, contaminating nuclear DNA was successfully removed from mtDNA (Kolodner and Tewari, 1972a) and plastid DNA (ptDNA; Kolodner and Tewari, 1972b) in pea. Electron microscopy (EM) and DNA reassociation kinetics analysis (DRKA) led to the conclusion that the chromosomes in both organelles were present as genome-sized circles. For the chloroplasts, however, the DNA was fractionated before EM, which probably removed the very large and branched molecules subsequently revealed in total DNA obtained from plastids. In-gel procedures, pulsed-field gel electrophoresis (PFGE), and moving pictures of ethidium-stained molecules (DNA Movies) showed circular ptDNA as a minor component with most ptDNA in simple linear and branched forms (Figure 1C). For the mtDNA, some circular forms were of a size also obtained from DRKA, but this size is much smaller than the genome size of the pea mitochondrial genome subsequently obtained by DRKA and restriction fragment summation.

CHROMOSOMAL DNA MOLECULES IN THE MITOCHONDRIA AND CHLOROPLASTS OF PLANTS: CIRCULAR OR LINEAR?

In 1972 the chromosomes in plant mitochondria and chloroplasts were proposed to exist as genome-sized circular DNA molecules (Kolodner and Tewari, 1972a,b). Considering the profound influence of this conclusion on subsequent research, it is instructive to review the original evidence for circular chromosomes in plant mitochondria and chloroplasts.

Using EM with the contents released from osmotically-shocked mitochondria, 55% of the circular molecules that were measured were in circular form and ~30 microns (87 kb) in contour length, “10% of the circular molecules were present in dimer-length

circles” (63–64 microns), and the longest linear mtDNA reported was 51 microns (Kolodner and Tewari, 1972a). After treatment with protease and chloroform, 25% of the mtDNA was found as circles of about 30 microns. The authors concluded that molecules of DNA in pea mitochondria are circular with a molecular weight of about 70 Md (106 kb).

Kolodner and Tewari (1972a) also estimated the size of the pea mitochondrial genome from the rate with which denatured mtDNA strands reassociated relative to that for T4 phage DNA (size of 106 Md): $0.70 \times 106 = 74$ Md or 112 kb, using 662 d per base pair. This value becomes 190 kb when the apparent kinetic complexity of 180 Md (272 kb) for glucosylated T4 DNA is used (Ward et al., 1981). From DRKA, the size of the mitochondrial genome in pea was estimated by Ward et al. (1981) as ~215 Md (325 kb) when the genome size of the *Bacillus subtilis* standard was taken as 3500 kb. Using 4200 kb for the *B. subtilis* genome from sequencing data, Alverson et al. (2010) employed a 1.2-fold correction, which gives 390 kb for the pea mitochondrial genome. The size of the pea mitochondrial genome obtained by summing the lengths of restriction fragments was ~320 (Ward et al., 1981) and 430 kb (Stern and Palmer, 1984). To our knowledge, there are no genome size estimates from mitochondrial genome sequencing for pea. These data show that the 87-kb class of circular mtDNA molecules found by EM represents circles of subgenomic size, rather than circles of genome size as inferred by Kolodner and Tewari (1972a).

The size of DNA molecules from pea chloroplasts was measured by EM (Kolodner and Tewari, 1972a). The circular molecules, which accounted for as much as 37% of all measured DNA length, were tightly grouped near 39 microns (115 kb), and “none of the linear molecules...were...longer than the length of the circular molecules.” Using 106 Md for the T4 DNA standard, the kinetic complexity was reported as 94.6 Md (143 kb), which becomes 243 kb after correcting for T4 DNA glycosylation. The size of the pea plastid genome is 120 kb from restriction fragment summation (Palmer and Thompson, 1981) and 122 kb from genome sequencing (accession NC_014057).

These data show that the circular ptDNA molecules reported by Kolodner and Tewari (1972a,b) closely approximate the genome size as determined from restriction fragments and genome sequencing, whereas their DRKA data do not closely approximate the EM data or the genome size. How can we reconcile the EM data showing no linear molecules larger than the genome-sized circles with the data from PFGE and DNA Movies showing much or most of the ptDNA from pea and other plants in linear and branched-linear forms larger than the size of the genome (Bendich and Smith, 1990; Oldenburg and Bendich, 2004a; Shaver et al., 2006)? For PFGE and DNA Movies, the procedure starts with plastids embedded in agarose (in-gel), so that none of the DNA present in the organelles can be removed before analysis. Most of the in-liquid procedures described for both ptDNA and mtDNA, include centrifugation at $12,000 \times g$ for 30 min before the supernatant is sampled for analysis by EM (Kolodner and Tewari, 1972a,b). We suspect that the large, complex forms of orgDNA would be removed by this centrifugation, so that the orgDNA was fractionated prior to analysis. Furthermore, any complex, branched molecules seen by EM might have been

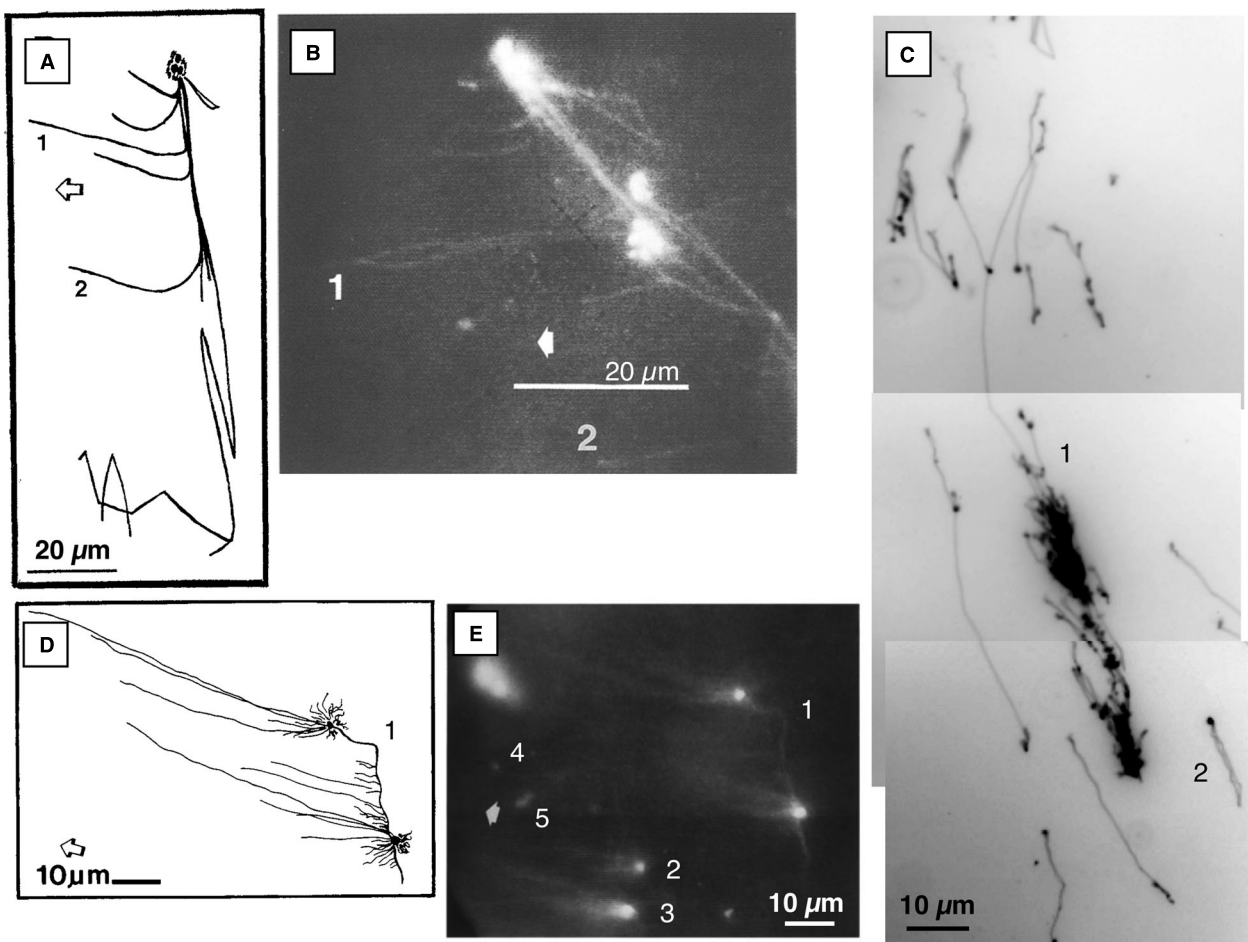


FIGURE 1 | Fluorescence microscopic images of ethidium-stained mtDNA and ptDNA molecules. (A) and (B) Images of DNA-protein structure from osmotically lysed tobacco BY-2 mitochondria. Complex branching DNA-protein structure with three bright nodes, long immobile fiber, and several fibers that extend leftward toward the anode (examples: 1 and 2) and rightward when the polarity of the electric field was reversed. (Adapted from Oldenburg and Bendich, 1998b). (C) Maize ptDNA molecules from the well-bound fraction following PFGE. Examples: (1) multigenomic complex structure with a Y-branch and (2) a genome-sized circular molecule. Approximately 84% of the DNA mass was in the large complex form, 11% in small branched molecules, and 4% in circular molecules. The in-gel ptDNA was prepared from 14-day maize seedlings. (Adapted from Oldenburg and Bendich, 2004a) (D) and (E) Images of liverwort mtDNA molecules from the well-bound fraction following PFGE. One large complex structure with two bright nodes of fluorescence that are connected by a bright fiber and several fibers extend from each node toward the anode (1). Two smaller “comet” structures with several “tail” fibers extending from the bright “head” (2, 3). A few small molecules were moving toward the anode (examples: 4, 5). (Adapted from Oldenburg and Bendich, 1998a) The molecules in (B) and (E) were recorded using an epifluorescence microscope equipped with a CCD camera, video monitor, and recorder. Photographs were then taken of ethidium-stained DNA on the monitor and the respective drawings, (A) and (D), were made by tracing the DNA on the monitor. The molecules in (C) were recorded using an epifluorescence microscope equipped with a digital camera and computer. Broad arrows point toward the anode in (A), (B), (D), and (E).

deemed uninterpretable and excluded from analysis. A hint that this may have occurred is that “lysed preparations...often resulted in tangled molecules” (Kolodner and Tewari, 1972b). In one of the procedures, osmotic shock was used to release the contents of isolated mitochondria, and EM was conducted without prior fractionation by centrifugation (Kolodner and Tewari, 1972a). When isolated mitochondria from tobacco and yeast were first embedded in agarose and then subjected to hypotonic medium to cause lysis within the gel, subsequent DNA Movies revealed apparently “naked” DNA molecules as well as enormous, complex, branched forms that migrated to the cathode during electrophoresis, indicating that they were bound to basic proteins (Figures 1A,B; Oldenburg and Bendich, 1998b). We suspect

that such complex forms would have been present in the lysed preparations produced by osmotic shock of pea mitochondria, but may have been dismissed as uninterpretable tangled molecules.

In conclusion, circular forms of orgDNA from plants appear to have exerted a profound influence on 40 years of research, despite the weakness of the data in support of the notion that most or all functions of organellar chromosomes are served by circular DNA molecules (Williamson, 2002; Bendich, 2010a). When in-gel methods are employed, chromosomal DNA molecules in the plastids and mitochondria of plants appear as linear and branched-linear forms of various sizes (Figure 1), are found in meristematic tissues, and are typically larger than the size of the genome. In maize, tobacco, and *Medicago truncatula*, restriction

digest analysis showed that the linear molecules have ends at defined regions of the plastid genome and isomers with three to six distinct ends (Oldenburg and Bendich, 2004a; Scharff and Koop, 2006, 2007; Shaver et al., 2008). For maize, the precise locations for two ends have been determined by sequencing, and both are near putative origins of replication (Oldenburg and Bendich, unpublished results). The circular forms account for a few percent or less of total orgDNA (Bendich, 1996; Oldenburg and Bendich, 1996, 1998a, 2004a) and are proposed to represent defective forms of orgDNA akin to the circular mtDNA molecules in *petite* mutants of yeast (Bendich, 2010a).

COPY NUMBER AND INTEGRITY OF ORGANELLAR GENOMES DURING PLANT DEVELOPMENT

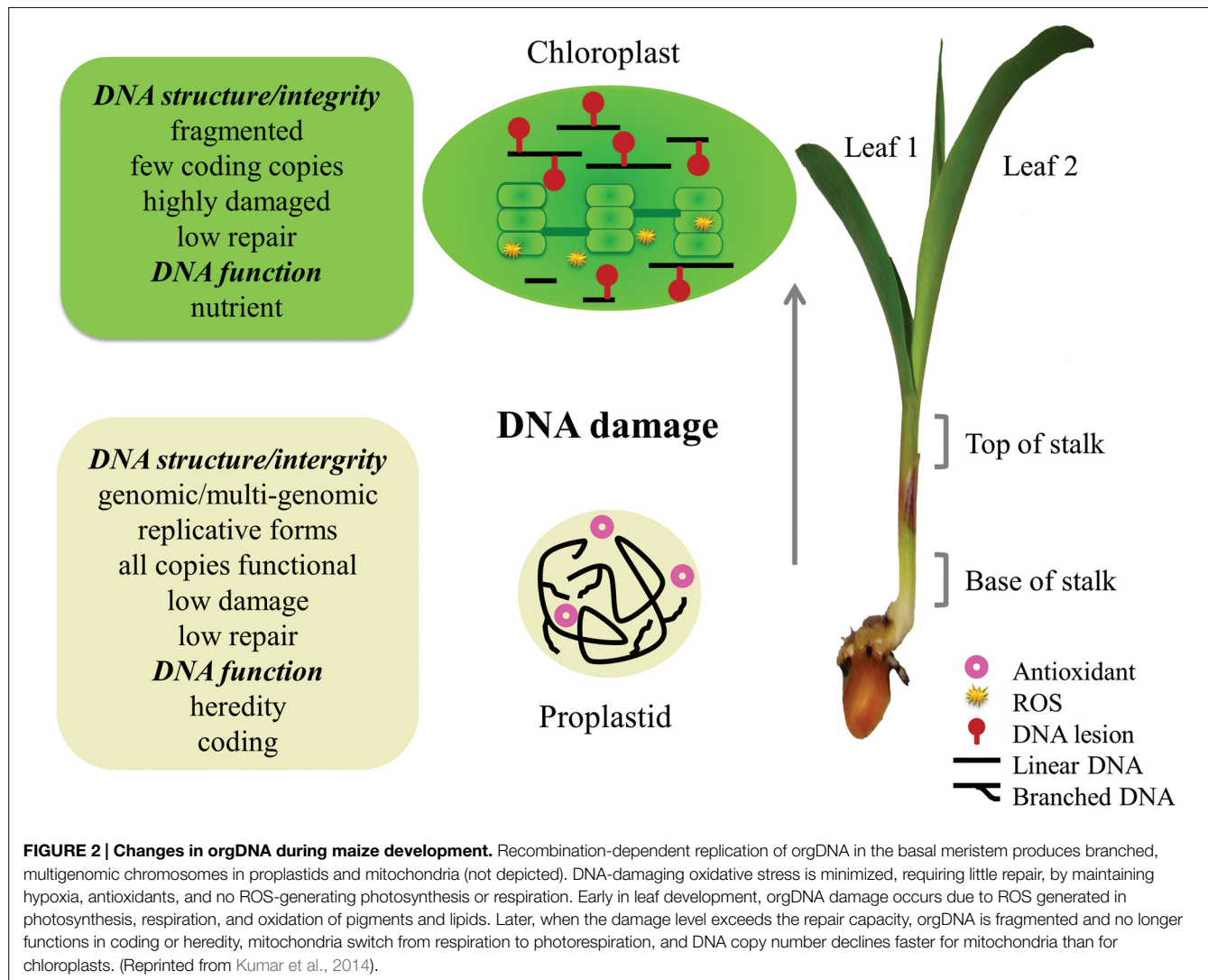
One of the curious facts about orgDNA in plants is that the number of genome equivalents (hereafter termed “copy number”) per diploid cell is large and highly variable during plant development, whereas the copy number in the nucleus of the diploid cell remains essentially constant throughout development. The curiosity of this fact increases when one considers that orgDNA-encoded proteins persist at fixed molar ratios with their nuclear DNA-encoded subunit partners in multi-subunit protein complexes, such as ribosomes, cytochrome oxidase, and RUBISCO. These facts alone indicate that the strategy for regulating gene expression differs greatly between the nuclear and organellar genomes. In an early proposal, high copy number of orgDNA reflects an increased demand for organellar ribosomes that can only be satisfied by increased rRNA gene number that results from genome amplification (Bendich, 1987). Recently, additional insight was obtained from the concept of DNA abandonment in which some or all of the copies of orgDNA, but not nuclear DNA, can be degraded during development because they have served their coding function and are damaged but not repaired (Bendich, 2010b, 2013).

Several methods have been used to estimate orgDNA copy number in plants: (i) measuring the increase in the rate of probe DNA strand reassociation caused by the addition of a large amount of DNA extracted from total tissue (Lamppa and Bendich, 1979a, 1984); (ii) blot hybridization of a probe to restriction-digested total tissue DNA (Li et al., 2006; Zheng et al., 2011; Udy et al., 2012; Oldenburg et al., 2013); (iii) fractionation of orgDNA by PFGE (Oldenburg et al., 2006; Shaver et al., 2006; Oldenburg et al., 2013); (iv) quantitative fluorescence using a DNA-specific fluorophore and either intact cells or organelles isolated from cells (Oldenburg and Bendich, 2004b; Rowan et al., 2004; Shaver et al., 2006; Oldenburg et al., 2013); and (v) real-time quantitative PCR (qPCR; Zoschke et al., 2007; Rowan et al., 2009; Preuten et al., 2010; Udy et al., 2012). These procedures should yield equivalent results providing that the molecular integrity of the DNA molecules is maintained, as is the case for chromosomal DNA in the nucleus.

Molecular integrity, however, changes drastically during development. The most sensitive assay we have to monitor molecular integrity is the analysis of DNA molecules using DNA Movies. Isolated organelles are first embedded in agarose gel (as

in preparation for PFGE), the gel is soaked in detergent, EDTA, and proteinase K to release intact DNA, and the movement of ethidium-stained molecules with and without an electric field in real time can be observed and recorded. Circular molecules up to several megabases in size are clearly distinguished from linear and branched forms, lengths of individual molecules can be measured, and a single double-strand break can be monitored (Bendich, 1991, 1996, 2001). PFGE (method iii) is also highly sensitive, and quantitative fluorescence (method iv) less so, to a decrease in molecular integrity, whereas methods i, ii, and v measure molecules fragmented either intentionally (by shearing or restriction digestion) or within the plant cell (by DNA damage response activities; see below). Recently, a method was developed for conducting quantitative PCR using primers spaced by 11 kb (long-PCR), rather than the typical spacing of about 0.1–0.15 kb used for qPCR: this is method (vi) molecular integrity PCR (miPCR), and orgDNA copy numbers were determined with both qPCR and miPCR during development of maize seedlings (Kumar et al., 2014, 2015). DNA copy number values using standard qPCR exceeded those using miPCR by 100- to 1000-fold, with the greatest disparity found for light-grown leaves. The drastic decrease in orgDNA molecular integrity from multigenomic structures in the meristem to less-than-genome-sized fragments in green leaf tissues revealed using DNA Movies and PFGE is paralleled in copy number assays using miPCR but not standard qPCR. Mechanistically, there is at least one single- or double-strand break or DNA polymerase-blocking lesion per 11 kb in nearly every molecule of orgDNA in green leaf, but such impediments to DNA amplification are infrequent at a length of 0.15 kb. In other words, orgDNA in green leaf tissue has been damaged, not repaired, and degraded to the small fragments detected in DNA Movies and the smear at the bottom of the gel in PFGE. Furthermore, about one-third of the ptDNA from green leaf is so small that it diffuses out of the gel plugs during the post-lysis plug washes and is lost before PGFE analysis begins (Kumar et al., 2014), whereas these fragments would still be scored as “copies” using standard qPCR and total tissue DNA. We conclude that the measurement of orgDNA copy number depends strongly on the assay method. Estimates provided by qPCR are probably accurate for meristematic cells containing the multigenomic molecules revealed by PFGE and DNA Movies, but greatly overestimate the level of functional DNA in mature leaves.

What causes intact orgDNA to become highly degraded when cells from the shoot meristem develop into green leaf cells? A damaged-but-unrepaired molecule is typically degraded in bacteria (Skarstad and Boye, 1993) and human mitochondria (Shokolenko et al., 2009), thus avoiding mutation, and we suggest the same applies to plant orgDNA (**Figure 2**). In consequence, almost none of the “copies” scored by standard qPCR for a green maize leaf serve a coding function. Since the rate of orgDNA decline during leaf development differs among plant species, with maize being the most extreme example among the five plants investigated (Shaver et al., 2006; Rowan and Bendich, 2009; Oldenburg et al., 2014), the transition from coding to nutrient function for orgDNA is expected to occur at different rates among plants. For example, the brightness of DAPI-stained plastid nucleoids decreased with age of the leaves over a 4-year period on a



single branch of an evergreen Rhododendron shrub; there were no 5-year-old leaves (Oldenburg and Bendich, unpublished results).

PROTEINS ASSOCIATED WITH ORGANELLAR DNA REPLICATION, RECOMBINATION, AND REPAIR

Proteins involved in orgDNA replication, recombination, and repair have been identified, the activities of a few have been investigated genetically, and changes in the levels of proteins found in plastids and mitochondria during leaf development have been revealed by proteomic analysis (Marechal and Brisson, 2010; Krupinska et al., 2013; Cupp and Nielsen, 2014; Moriyama and Sato, 2014; Powikrowska et al., 2014). These proteins are nuclear-encoded and can be categorized according to function and organelle localization. We now focus on the relationship between these proteins and orgDNA quantity/quality as the leaf develops.

Most orgDNA-associated proteins are largely confined to the meristem (proplastids) and young leaves (developing

chloroplasts). For example, the DNA polymerase, PolIA, was found in proplastids but not chloroplasts of maize (Majeran et al., 2012), and the plastid DNA polymerase genes of *Arabidopsis* and rice were expressed in meristematic tissues, not in mature green leaves (Kimura et al., 2002; Mori et al., 2005). Expression as determined by qRT-PCR of the *Arabidopsis* gene for the helicase/primase TWINKLE was greatest in young leaves and shoot apex tissues, and its protein level was shown to decrease with increasing age of rosette leaves (Diray-Arce et al., 2013).

Some DNA proteins are dual-targeted to both plastids and mitochondria, including PolIA, PolIB, Twinkle, and the recombination protein RecA2. Most proteins known to be dual-targeted are associated with DNA maintenance and mRNA translation (Carrie and Small, 2013). And yet, for some DNA-associated proteins there are plastid-specific and mitochondrial-specific homologs. For example, Why1, Why3, and RecA1 are plastid-targeted, whereas Why2 and RecA3 are mitochondria-targeted. Is there a functional explanation for the persistence of both dual-targeted and organelle-specific DNA maintenance proteins? We proposed that during development there is a

shift in a major mitochondrial function, from respiration to photorespiration, that is coordinated with the transition of non-green plastids to photosynthetically-active chloroplasts (Oldenburg et al., 2013; Kumar et al., 2014). Examples of tissue- or cell type-specific differences that would require such coordination are: roots compared with green leaves; and meristematic cells compared with mesophyll or epidermal cells. One way to achieve the coordination is to produce dual-targeted proteins such as those in the replisome, whereas the organelle-specific proteins would be useful for modulating the amount of functional (undegraded) orgDNA in a tissue-specific manner. Mitochondrial and plastid functions may thus coordinately respond to signals such as the redox state of the cell (Millar et al., 2011). For example, in meristematic cells conducting “quiet” metabolism [no respiration, no photosynthesis, low reactive oxygen species (ROS), Bendich, 2010b], dual-targeting of replisome proteins would maintain the copy number of both mtDNA and ptDNA at the pre-differentiation copy number. However, in roots where respiration is required, higher levels of mtDNA would be retained than in green mesophyll cells where the primary mitochondrial function is photorespiration. Thus the organelle-specific proteins may determine the selective retention or degradation of orgDNA among tissues. During development and upon receipt of the light-dependent phytochrome signal, cellular differentiation begins, the cellular redox state changes, and plastid-specific and mitochondrial-specific proteins would exert their effects on orgDNA levels and integrity in a tissue-specific manner (Zheng et al., 2011; Oldenburg et al., 2013; Kumar et al., 2014).

As the synthesis of proteins used during photosynthesis increases, the production of additional DNA to meet the increasing demand for gene products might be expected to increase, with the highly-labile D1 protein (the *psbA* gene product) as a critical example. Yet, as discussed above, the abundance of the proteins needed to produce and maintain ptDNA actually decreases. This observation is consistent with the declining copy number of ptDNA during leaf development and the high stability of *psbA* mRNA, but unexpected under the hypothesis that the fully functional gene for D1 must persist in mature maize leaves.

If orgDNA is to be maintained, replication/repair proteins should be present and active in these organelles, as in single-celled organisms like yeast, *Chlamydomonas*, and *Euglena*, and the cells leading to the germ cells of plants and animals. An alternative is to abandon orgDNA in somatic cells by not supplying those proteins. The proteomic analysis indicates that during leaf development in maize the level of replication/repair proteins targeted to chloroplasts decreases relative to proplastids. Although the activity of these proteins was not addressed, this decrease in the levels of orgDNA maintenance proteins is consistent with orgDNA abandonment in maize.

ORGANELLAR NUCLEOIDS: WHERE THE ACTION IS

After staining with a DNA fluorophore, brightly fluorescing regions within plastids and mitochondria identify regions that

contain high concentrations of DNA: the nucleoids. Nucleoids *in situ* appear in various forms, including dots that may or may not be connected by fibers and may be located at the periphery or toward the interior of the plastid (Coleman, 1979; Kuroiwa et al., 1981). The size and fluorescence intensity of the nucleoid reflect the DNA content, which can vary enormously among plant cells (Kuroiwa et al., 1981; Kuroiwa, 1991). When isolated from the organelles, nucleoids are found to contain DNA, RNA, and proteins, including the plastid-encoded RNA polymerase in the “transcriptionally active chromosome” (reviewed in Krupinska et al., 2013; Liere and Börner, 2013). It is believed that the functions of orgDNA (inheritance, replication, repair, and transcription) are served largely or exclusively from nucleoids bound to membranes (Gilkerson et al., 2013; Kindgren and Strand, 2015). We now combine morphological and biochemical data for nucleoids to elucidate the process of orgDNA maintenance during plant development.

An early study in tobacco showed that the composition of nucleoid-associated proteins differed between proplastids and chloroplasts (Nemoto et al., 1990). The nucleoids of maize plastids contain proteins associated not only with DNA, but also RNA metabolism including transcription, mRNA processing, and stability (Majeran et al., 2012). Changes in RNA-associated proteins indicated transcription as the primary function in developing plastids and mRNA translation and protein homeostasis in chloroplasts. Although many nucleoid-enriched proteins were assigned a function, function was not assigned to many others, including PPR proteins (likely associated with RNA processes). Of the DNA-associated nucleoid proteins (including those for replication/repair and ROS protection), most were more abundant in proplastids than chloroplasts, with the exception of three DNA repair proteins that were more abundant in the tip than the base of the leaf (Majeran et al., 2012). Two of these (FAD photolyase and a uvrB/uvrC-motif protein) likely function in repair of UV-induced damage and the third (MutS2) may function to suppress illegitimate recombination (Kang et al., 2005; Pinto et al., 2005; Fukui et al., 2007), so that none of these three is likely associated with repair of ROS-induced DNA damage. The primary repair pathway for ROS-induced oxidative lesions is base excision repair (BER), and in *Arabidopsis* BER enzymes were found in both mitochondrial and plastid nucleoids (Gutman and Niyogi, 2009; Boesch et al., 2011), although no information was given about the stage of plastid developmental or enzyme abundance.

A DNA-membrane anchoring function has been assigned to some nucleoid proteins, such as PEND specific for the plastid envelope and MFP1 for the thylakoids (Krupinska et al., 2013; Liere and Börner, 2013). In maize, six such anchoring proteins were identified, although only three were enriched in isolated nucleoids and one of these (pTAC16) was enriched in the leaf tip relative to the base (Majeran et al., 2012). Several proteins were classified as “DNA organization and quality control” (such as YlmG1 and Why1; Majeran et al., 2012) that may also mediate membrane attachment either directly or indirectly through protein-protein interactions. A function in nucleoid partitioning was reported for the YlmG1 family of proteins (Kabeya et al., 2010), and in maize YlmG1-1 was enriched in proplastids whereas

YlmG1-2 was enriched in chloroplasts (Majeran et al., 2012). The single-strand DNA-binding Whirly proteins are associated with nucleoids in plastids and mitochondria (Prikryl et al., 2008; Marechal and Brisson, 2010), and Why1 in maize is more abundant in proplastids than chloroplasts (Table 1 in Majeran et al., 2012). Thus during plastid development, changes in nucleoid protein composition likely reflect changes in DNA-membrane attachment.

Although the various forms (dots, rings, fibers) and plastid locations (peripheral, central, scattered) of plastid nucleoids were originally considered as characteristic for the plant or algal group, these morphological properties were found to change during proplastid-to-chloroplast development in wheat and *Arabidopsis* (Miyamura et al., 1986; Fujie et al., 1994). In proplastids and developing plastids, nucleoids are attached to the envelope membrane whereas in chloroplasts the nucleoids are attached to the thylakoid membrane (Krupinska et al., 2013; Powikowska et al., 2014). Combined with the changing protein composition during plastid development, it now seems likely that nucleoid appearance *in situ* reflects the biochemical activity of the cell. Attachment of orgDNA molecules to membranes *in vivo* would affect their maintenance, according to the following scenario. We suggest that (1) the three activities maintaining DNA integrity—replication, recombination, and repair—take place only on DNA firmly associated with membrane-attached nucleoids; (2) changes in nucleoid protein composition during development can result in release of damaged-but-unrepaired DNA from the membrane/nucleoid; (3) this unbound DNA is now susceptible to further degradation by nucleases; and (4) this process is indicated by the decrease in nucleoid size and DAPI-DNA intensity and ultimately the complete disappearance of nucleoids in many mature chloroplasts of maize.

If replication/repair requires that a DNA end be attached to the membrane, then once the DNA molecule leaves the membrane it can no longer replicate or be repaired and would be degraded by exonucleases. A supercoiled circular DNA has no end, cannot be replicated—and pulse-labeling shows it is not first-labeled—and leaves the membrane. But it would not be digested by exonucleases and could still be detected by EM, PFGE, and (in relaxed circular form) DNA Movies and be enriched in the supernatant after high-speed centrifugation (which would pellet the large complex forms), as performed by Kolodner and Tewari (1972a,b). The circular forms account for a few percent or less of total orgDNA, are proposed by-products of recombination used to replicate linear DNA (Bendich, 1996; Oldenburg and Bendich, 1996, 2004b), and are unlikely to serve as templates for DNA replication/repair or transcription within the organelles. Mung bean mtDNA was analyzed both from entire mitochondria and from nucleoids isolated from the mitochondria. For nucleoids, >50% of the mtDNA molecules were found in complex forms and ~30% were linear by EM; well-bound and 50–200-kb fractions were found by PFGE (Lo et al., 2011). For entire mitochondria, an additional prominent fraction was found at <50 kb (Dai et al., 2005), which we suggest was not associated with the nucleoid-on-membrane and resulted from nuclease digestion *in vivo*.

THE REPLICATION OF ORGANELLAR DNA IN PLANTS

The first model for the replication of plant orgDNA was proposed for ptDNA by Kolodner and Tewari (1975) and was based exclusively on EM images: circular products from a circular template involving a displacement loop and theta-type replication. Subsequently, ³H-labeled thymidine was used in pulse-chase experiments with cultured tobacco cells to quantify the forms of replicating mtDNA fractionated by PFGE (Oldenburg and Bendich, 1996). The first-labeled form was found in the well-bound fraction of the gel, with a zone of linear molecules at about 50–150 kb accumulating the tritium with time at the expense of the well-bound form. Genome-sized molecules (430 kb for tobacco; Sugiyama et al., 2005) in either linear or circular form were not detected by analysis of either radioactivity or ethidium staining. A well-bound precursor and a 50–200-kb product were also shown for mtDNA synthesis in mung bean seedlings (Dai et al., 2005). For cultured liverwort cells, the well-bound fraction, not the circular genome-sized band ($\leq 5\%$ of all mtDNA), contained the earliest form(s) of mtDNA produced during replication. The well-bound DNA is immobile during PFGE because of its large size and complex branching form (Figures 1D,E; Oldenburg and Bendich, 1998a).

Using a cytological approach and incorporation of bromodeoxyuridine (BrdU) to monitor DNA synthesis in roots of *Pelargonium* and *Arabidopsis* seedlings, most mtDNA synthesis was found in mitochondrial nucleoids of enormous size (several megabases of mtDNA) in the root tip meristem, with nucleoids containing ~90–140 kb of mtDNA in the root elongation zone (Kuroiwa et al., 1992; Fujie et al., 1993). Since the mitochondrial genome size is 367 kb for *Arabidopsis* (Unseld et al., 1997) and likely to be much larger than 140 kb for *Pelargonium*, the general conclusion is that replication of plant mtDNA occurs in meristematic cells with molecules of multigenomic size that are converted to simple linear forms of about 50 to 200 kb in non-dividing cells that no longer replicate their mtDNA. The same cytological/BrdU procedures were used to identify meristematic cells as the principal or only cell type in which ptDNA was replicated in roots of *Arabidopsis* and rice (Fujie et al., 1993; Suzuki et al., 1995). In maize, mtDNA replication was highest in the metabolically-active embryo and was also found in both roots and stalk, but not in the mature leaf blade (Oldenburg et al., 2013). As the first foliage leaf of *Arabidopsis* developed, the number of genomes per plastid increased from ~40 (3 days after seeds were sown) to 600 at day 7, when the leaf was <0.5 mm in length, whereas genome equivalents per mitochondrion decreased from 2 to <0.5 during this interval (Fujie et al., 1993, 1994). Similarly, in maize and other cereals, ptDNA replication was most intense in the stalk region above the basal meristem (Baumgartner et al., 1989; Hashimoto and Possingham, 1989; Oldenburg et al., 2006; Zheng et al., 2011). The replication of ptDNA in maize is stimulated by light, although it also occurs in dark-grown seedlings (Oldenburg et al., 2006; Zheng et al., 2011) and in the dark for *Chlamydomonas* growing on acetate (Kabeya and Miyagishima, 2013). *Chlamydomonas* ptDNA replication is regulated by the cellular redox state (Kabeya and Miyagishima, 2013).

Regions of the plastid genome that best supported DNA synthesis *in vitro* were designated as replication origins (*oris*), and led to the assignment of two major *oris* (known as oriA and oriB) in *Oenothera*, tobacco, and pea (Heinhorst and Cannon, 1993; Kunnumalaiyaan and Nielsen, 1997). Sequences similar to those of oriA and oriB have been identified in the plastid genomes of many plants (Oldenburg and Bendich, 2004a; Shaver et al., 2008; Krishnan and Rao, 2009). Plastid origin-binding proteins (OBP) have been identified for *Chlamydomonas* (Nie et al., 1987) and soybean (Lassen et al., 2011).

Three types of replication mechanism have been proposed for ptDNA: theta replication, rolling circle replication (RCR), and recombination-dependent replication (RDR; Kunnumalaiyaan and Nielsen, 1997; Marechal and Brisson, 2010). Although circular ptDNA molecules were reported for chloroplasts from entire light-grown shoots of several plants (Kolodner and Tewari, 1972b; Lampka and Bendich, 1979b; Bendich and Smith, 1990; Lilly et al., 2001), support for the theta and RCR mechanisms would seem to require the presence of circular ptDNA molecules in meristematic tissues. The base of the leaf in grasses is a rich source of meristematic cells. Using blot-hybridization and PFGE fractionation, a sharp band representing a supercoiled circular form of ptDNA (but only 3% of all ptDNA) was detected in dark-grown first and second leaf blade, but not stalk (meristem at the base of the leaf) tissue of maize seedlings. However, no circular ptDNA was detected in light-grown stalk, and in light-grown leaf blade most of the ptDNA was found as less than-genome-sized fragments and often barely detectable (Oldenburg and Bendich, 2004b; Oldenburg et al., 2006). Thus, support was not obtained for the theta or RCR models in maize. In fact, light triggered the rapid degradation of all forms of ptDNA (Oldenburg et al., 2006; Zheng et al., 2011). The circular ptDNA was found in a tissue no longer engaged in ptDNA replication. Support for RDR would seem to require the presence of multigenomic, branched molecules in the meristem. For stalk tissue, the well-bound fraction contained a large amount of ptDNA, and most ethidium-stained molecules imaged by fluorescence microscopy were in complex branched forms (Figure 1C; Oldenburg and Bendich, 2004b), in support of the RDR mechanism. These complex forms were also found in young leaf tissue of *Arabidopsis*, tobacco, and *Medicago truncatula* (Rowan et al., 2004; Shaver et al., 2006).

To summarize, we know rather little of the details of orgDNA replication in plants. The evidence indicates, however, that circular forms of the plastid genome, while detectable in some plant tissues, are not the principal template for ptDNA replication, and circular forms of the entire mitochondrial genome—the “master circle”—have been reported only for cultured liverwort cells. The data we do have are compatible with linear DNA molecules and an RDR mechanism for both mtDNA and ptDNA in which multiply-branched molecules larger than the size of the genome provide the orgDNA for progeny cells. Given the paucity of mutants with which to investigate orgDNA replication in plants, we may draw mechanistic inference from other DNA replication systems and data from organellar proteomics. For example, structural similarities between ptDNA and herpes simplex virus (HSV) DNA include a linear genome of ~150 kb, two single-copy regions separated by inverted repeats (IRs), and multigenomic

branched-linear replicative forms. Furthermore, although a theta-to-rolling-circle model was initially suggested, a RDR mechanism with linear molecules is now proposed for the replication of HSV DNA (Weller and Sawitzke, 2014).

Let us consider three processes associated with DNA replication: (1) initiation and opening of the double helix; (2) loading replication proteins and establishment of a replication fork; and (3) single-strand annealing (SSA) and recombination. In HSV DNA there are three *oris*, one in the long single copy region (U_L) and two in the IRs. Initiation occurs when UL9 (an OBP) binds to an *ori* leading to recruitment of the replisome (helicase/primase, DNA polymerase, etc.), followed by opening of an adjacent A/T-rich region and formation of a replication fork with both leading- and lagging-strand synthesis (Weller and Sawitzke, 2014). Similarly, a plastid OBP could bind at oriA/oriB (Lassen et al., 2011) recruiting the plastid replisome (Twinkle, PolIA, etc.; Moriyama and Sato, 2014). Although the OBP/*ori* system is widely used to initiate DNA replication, initiation could also occur by transcription, specifically in the rRNA genic region. Plastid *oris* are located near the rRNA genes in many organisms, leading to a transcription-coupled DNA replication process whereby transcription-mediated helix opening could allow subsequent access of the replisome (Chang and Wu, 2000).

A SSA mechanism has been described for HSV DNA that can generate concatemers, initiate DNA synthesis, and produce branched replicative forms (Weller and Sawitzke, 2014). We propose an analogous SSA mechanism for plant orgDNA (Figure 3): (1) 5'-to-3' exonuclease digestion of a double-stranded DNA (dsDNA) end to create a 3' single-strand overhang; (2) binding of a single-strand annealing protein (SSAP) to this single-stranded DNA (ssDNA) region; and (3) either annealing to a homologous DNA region of another 3'-overhang end to form a concatemer or annealing of the 3'-overhang to a ssDNA gap to form a branched structure that can prime DNA synthesis and create a replication fork. ICP8 has been identified as the SSAP in HSV and possesses helix-destabilizing activity (to unwind duplex DNA), binds non-specifically to ssDNA, promotes annealing of homologous ssDNA sequences, and forms thin helical filaments and oligomeric rings in the presence of ssDNA. Is there a plastid (and mitochondrial) protein with similar characteristics to function as a SSAP? Among the organellar DNA-binding proteins that have been identified thus far (Dickey et al., 2013; Moriyama and Sato, 2014), we suggest that the Whirly family of single-strand binding proteins are good candidates to fulfill this role. Although initially implicated in the regulation of nuclear transcription and maintenance of nuclear telomeres, localization to plastids has been demonstrated for Why1 and Why3 and to mitochondria for Why2 (Marechal and Brisson, 2010). The Whirlies are DNA-binding proteins that have a higher binding affinity for ssDNA (with no sequence specificity) than dsDNA, but do promote unwinding of the ends of dsDNA (Cappadocia et al., 2010). The Whirlies form tetramers on short stretches of ssDNA and filaments on long stretches of ssDNA by cooperative binding of hexamers-of-tetramers (24-mers; Cappadocia et al., 2012). Thus Whirlies share many characteristics with ICP8 of HSV. Studies of *whirly* mutants have shown rearrangements of orgDNA likely facilitated by microhomology-mediated recombination (MHMR;

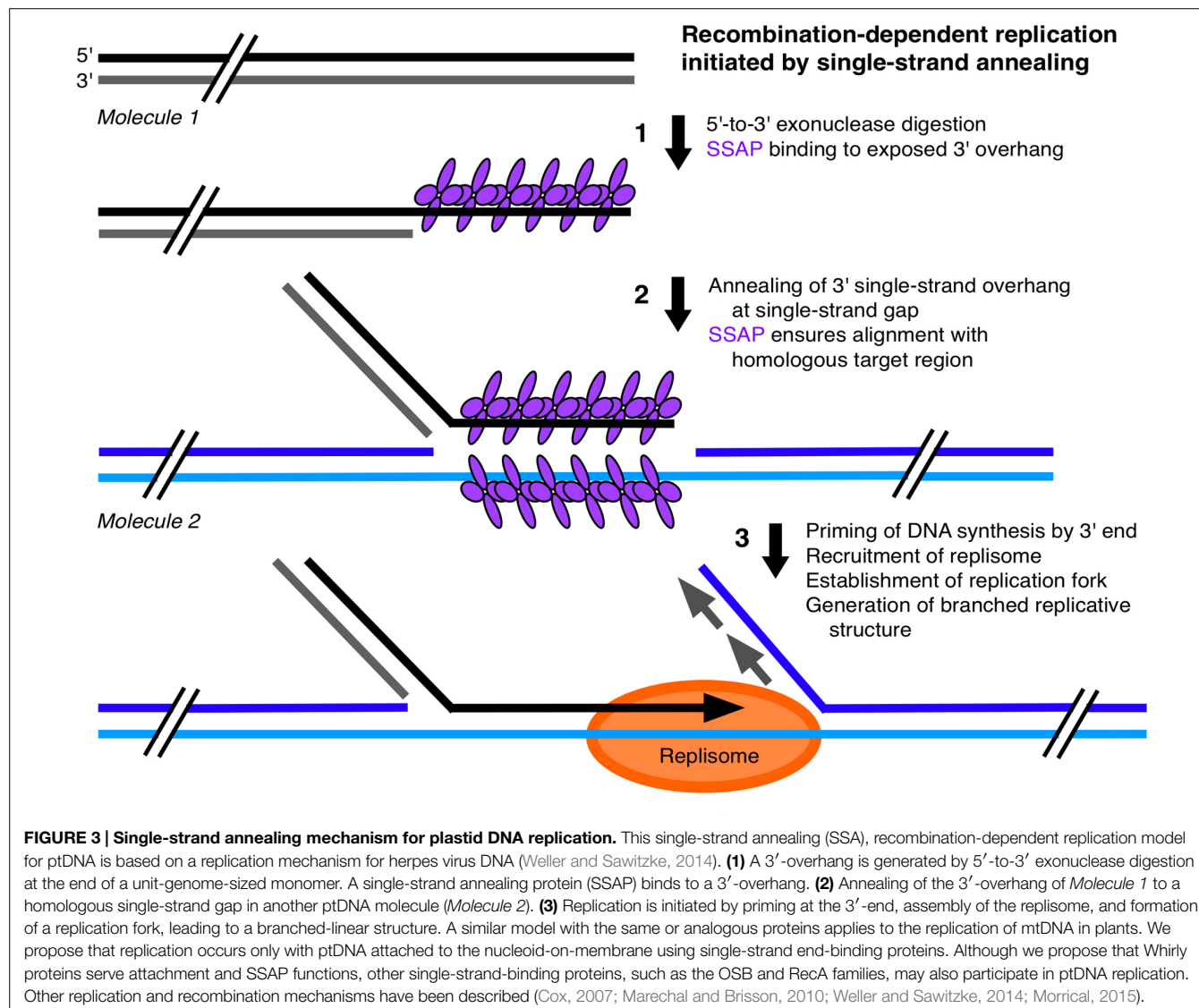


FIGURE 3 | Single-strand annealing mechanism for plastid DNA replication. This single-strand annealing (SSA), recombination-dependent replication model for ptDNA is based on a replication mechanism for herpes virus DNA (Weller and Sawitzke, 2014). (1) A 3'-overhang is generated by 5'-to-3' exonuclease digestion at the end of a unit-genome-sized monomer. A single-strand annealing protein (SSAP) binds to a 3'-overhang. (2) Annealing of the 3'-overhang of Molecule 1 to a homologous single-strand gap in another ptDNA molecule (Molecule 2). (3) Replication is initiated by priming at the 3'-end, assembly of the replisome, and formation of a replication fork, leading to a branched-linear structure. A similar model with the same or analogous proteins applies to the replication of mtDNA in plants. We propose that replication occurs only with ptDNA attached to the nucleoid-on-membrane using single-strand end-binding proteins. Although we propose that Whirly proteins serve attachment and SSAP functions, other single-strand-binding proteins, such as the OSB and RecA families, may also participate in ptDNA replication. Other replication and recombination mechanisms have been described (Cox, 2007; Marechal and Brisson, 2010; Weller and Sawitzke, 2014; Morrical, 2015).

Cappadocia et al., 2010; Zampini et al., 2015) and indicated that these proteins are important for maintaining organellar genome stability (Marechal and Brisson, 2010). We suggest that the filamentous Whirly-ssDNA structure ensures proper alignment of a strand-annealing end with its homologous target region and prevents MHMR as proposed for non-homologous end-joining whereby filament-forming proteins help align ends during double-strand break repair (Reid et al., 2015).

Additional functions proposed for the plant-specific Whirly protein family include attachment of plastid nucleoids to the thylakoid membrane and redox sensing in plastid-to-nucleus signaling (Foyer et al., 2014). We suggest that single-strand-binding proteins such as Whirlies also protect linear orgDNA molecules in a manner that changes during plant development. The ends of linear DNAs are susceptible to nuclease digestion unless protected by end structures including 5'-proteins, hairpin forms, and telomeric repeat sequences (Nosek et al., 2006; Chaconas and Kobryns, 2010; Smith and Keeling, 2013) and, as detailed above, the integrity of orgDNA declines sharply as

maize leaves green. In yeast mitochondria the nucleoid protein mtTBP has been shown to bind to single-stranded DNA at the telomeres and has been proposed to function in the replication, stabilization, and maintenance of linear mtDNA molecules (Tomaska et al., 2001). We propose that in plastids, Whirlies bind to and protect the ends of ptDNA, as well as mediating the attachment of nucleoids to membranes. If the Whirly interaction with the membrane is responsive to the plastid redox state, then dissociation of Whirlies from the membrane and from the ptDNA ends may be triggered in photosynthetically active chloroplasts, thus releasing DNA from the nucleoid and exposing the ends to nuclease activity.

REPAIR OF ORGANELLAR DNA DAMAGE

DNA damage and repair are typically studied by treating plants, animals, or their cultured cells with agents known to cause DNA damage (irradiation or peroxide, for example) and then comparing results from the treated and untreated samples (Yakes

and Van Houten, 1997; Parent et al., 2011). Whereas this approach provides information about the types of DNA damage and repair processes, it provides no information about the frequency of damage/repair during the normal process of development without the imposition of genotoxic agents. It also reports the net result of damage plus repair. Another approach is to quantify the amount of transcripts, protein, or enzymatic activity from DNA-repair genes, which provides information concerning the capacity to repair damage, rather than the act of repair itself. For plants, some types of orgDNA lesions and repair pathways have been identified (Marechal and Brisson, 2010; Balestrazzi et al., 2011; Boesch et al., 2011; Alexeyev et al., 2013), but quantification of damage and repair as the plant develops from meristem to mature organ is only beginning to be investigated.

A common approach to study replication in the absence of repair, and vice versa, is to obtain mutants in one or the other component of DNA maintenance. In *Arabidopsis*, mutation in the nucleus-encoded, plastid-targeted *recA1* (*cprecA*) gene led to no alteration in leaf morphology for three generations and only a rather subtle change in leaf variegation (yellow and white sectors) in the following 4 to 8 generations—a surprisingly mild defect considering that RecA is the most highly conserved recombination protein (Rowan et al., 2010). Similarly, *Arabidopsis* single mutants of *why1* and *why3* and the double mutant *recA1pol1b* resulted in no phenotypic alteration, and it was only in the *why1why3* double mutant and triple mutants *why1why3polb* and *why1why3recA1* that a defect in leaf morphology was evident (Marechal et al., 2009; Zampini et al., 2015). Thus, it appears that *Arabidopsis* employs several biochemical pathways to maintain sufficient levels of high-integrity ptDNA for chloroplast biogenesis. There was, however, a decrease in the amount of ptDNA in the *recA1*, *pol1a*, and *pol1b* single mutants compared to wild-type young seedlings (Rowan et al., 2010; Parent et al., 2011). Furthermore, these *recA*, *pol1*, and *why* mutants exhibited alterations in ptDNA structure, including a decrease in complex replicative forms as seen by DNA Movies, loss of the monomer and oligomer bands on PFGE, and an increase in microhomology-mediated DNA rearrangements as determined by PCR and next-generation sequencing (Rowan et al., 2010; Parent et al., 2011; Zampini et al., 2015). The general conclusion in these studies was that the wild-type proteins maintain genome stability/integrity by repair of orgDNA. These mutations may also have disrupted the normal replication process by inhibiting precise recombination at defined regions (adjacent to the *oris*) that leads to branched multigenomic molecules because these proteins likely function in both replication and repair.

Since both photosynthesis and respiration produce ROS as unavoidable by-products, it may be expected that damage to orgDNA would increase as maize leaves develop. The amount of damage (measured as impediments to DNA polymerase per 10 kb of orgDNA) was lowest at the base of the stalk and increased during leaf development in the dark as well as after transfer of dark-grown seedlings to light (Kumar et al., 2014). Treatment with a mixture of enzymes that can rectify most types of DNA lesions resulted in an increase in the amount of long-PCR product for both ptDNA and mtDNA, indicating that lesions were repaired *in vitro*. Repair was much greater for leaf than for stalk tissues in

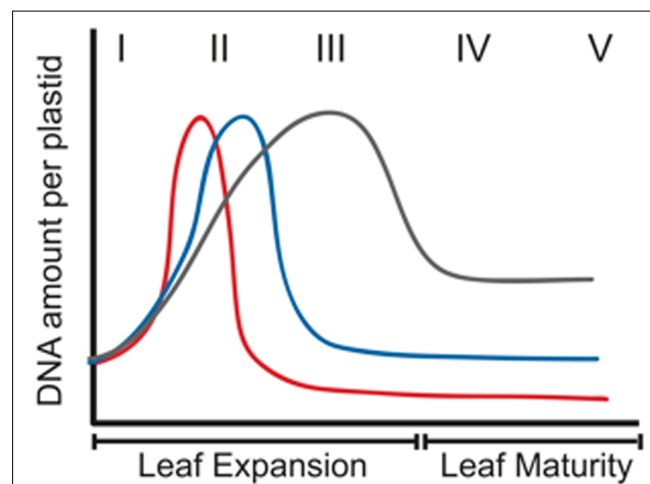


FIGURE 4 | Schematic representation of changes in the amount of ptDNA per plastid during development in three plant species. Increase in ptDNA amount due to ptDNA replication occurs very early in development in maize (red line), followed by a rapid decline. For *Arabidopsis* (blue line), the increase in ptDNA occurs slightly later and the decline in ptDNA amount is much later. For tobacco (gray line), ptDNA increases more gradually and the decline is less severe. The Roman numerals indicate stages of leaf development. I–III represent expanding leaves, and IV and V represent expanded leaves. (Reprinted from Rowan and Bendich, 2009).

both light and dark growth conditions, suggesting that orgDNA damage accumulates during “normal” growth conditions (without genotoxic treatment) without causing phenotypic change.

To summarize, although the capacity to repair damaged orgDNA has long been known for plants and animals, only recently—and for only one plant species—has repairable damage of orgDNA been quantified under normal development without the addition of stress or genotoxic agents. Light affects both damage and levels of functional DNA in both plastids and mitochondria, even though mitochondria have no known photoreceptors. Most “copies” of orgDNA from normal light-grown plants that are measured by standard qPCR are too highly degraded to serve a coding function, at least for maize. Although this conclusion likely applies to *Arabidopsis* (Rowan and Bendich, 2009), we currently lack long-PCR and *in vitro* repair assay data in order to evaluate the quantity and quality of orgDNA molecules as proplastids (and their mitochondrial counterparts) mature to the organelles found in the green leaf. New insight may be anticipated once the replication/repair mutants of *Arabidopsis* are identified in maize so as to complement the advantage of the linear gradient of staged cell development in maize leaves. One possibility is that repair in maize occurs only in the meristem, so that unrepaired orgDNA in the green chloroplasts is degraded: orgDNA abandonment.

DIFFERENCES IN LEAF GROWTH, PLASTID DEVELOPMENT, AND ORGANELLAR DNA MAINTENANCE AMONG PLANT SPECIES

During proplastid-to-chloroplast development, the DNA level per plastid first increases and then decreases, although the magnitude

of the decline varies among species. For example, ptDNA increases later and remains high longer for both *Arabidopsis* and tobacco than maize (**Figure 4**). In mature tobacco leaves, nearly all cells contain chloroplasts with DAPI-fluorescent nucleoids (Shaver et al., 2006), whereas nucleoids are not detectable in $\geq 40\%$ of maize cells (Oldenburg et al., 2014). Furthermore, the genomic monomer and oligomers are prominent in PFGE of ptDNA from mature leaves of many dicots, but in maize even the monomer is barely detectable (Lilly et al., 2001; Oldenburg et al., 2006; Shaver et al., 2006). These differences in ptDNA maintenance may result from differences in leaf growth and ptDNA-associated proteins.

Leaves of grasses, such as maize, exhibit a base-tip developmental gradient: dividing cells are restricted to the basal meristem; developing and elongating non-photosynthetic cells in the stalk are shielded from light by the coleoptile and/or outer sheath; and the mature leaf blade consists of fully-differentiated photosynthetic cells (Nelson and Langdale, 1989; Sylvester et al., 1990; Tardieu and Granier, 2000; Stern et al., 2004). In dicots, such as *Arabidopsis* and tobacco, cell division is not restricted to the apical meristem, but continues along a base-to-tip gradient in the expanding leaf (Donnelly et al., 1999; Tardieu and Granier, 2000; Rowan and Bendich, 2009). Except for the meristem, which is enclosed in the bud and shielded from light, cell development and elongation occur in the light. Thus in grasses, there is a prolonged etioplast-like developmental stage in the expanding leaf followed by an abrupt transition to a green chloroplast as the leaf tip emerges from the sheath, whereas photosynthetic chloroplasts are present throughout development of a dicot leaf. The ROS produced during photosynthesis would necessitate greater ptDNA-protective measures in the expanding dicot leaf, which could persist (at a reduced level) in mature leaves. In contrast, little ptDNA protection is evidently provided in green chloroplasts of maize, as indicated by the rapid ptDNA decline upon light exposure (Zheng et al., 2011). There are also differences in DNA maintenance proteins. For example, *Arabidopsis* has two DNA polymerases, PolIA and PolIB, with PolB implicated in ptDNA repair (Mori et al., 2005; Parent et al., 2011), whereas only PolIA has been reported for maize (Majeran et al., 2012; Udy et al., 2012). In maize only one Whirly protein, Why1, has been reported (Marechal et al., 2009; Majeran et al., 2012), whereas both Why1 and Why3 are present in *Arabidopsis* (Marechal et al., 2009; Cappadocia et al., 2010) where Why3 could provide protection against nucleases in chloroplasts by mediating DNA-nucleoid-membrane attachment. Therefore, greening during the etioplast-to-chloroplast transition in maize would lead to loss of ptDNA from ROS-mediated damage without repair. In *Arabidopsis* and other dicots, when the level of ptDNA damage exceeds the protective/repair capacity, ptDNA would also be degraded, although this would occur later in leaf development (**Figure 4**).

These dicot/grass differences in ptDNA maintenance may have ecological and evolutionary ramifications. The ptDNA in the dicot leaf must be kept in good repair—and at substantial cost—during the period of ptDNA replication, which is concurrent with photosynthesis and chloroplast expansion. In grasses, by contrast, etioplast expansion to a size equivalent to a green chloroplast,

ptDNA replication, and, critically, production of all the ptDNA-encoded mRNAs required for photosynthesis during the coming plant growth season, all proceed without the DNA-damaging ROS by-product of photosynthesis. The ptDNA may, therefore, be abandoned in green chloroplasts, avoiding the metabolic cost of ptDNA repair. Thus, leaf ptDNA maintenance is “low-cost” in the grass and “high-cost” in the dicot leaf.

This cost saving may have contributed to the rapid rise of grasses beginning in the Late Cretaceous-Paleocene (Strömberg, 2011; Christin et al., 2014). Replacement of the ancestral apical meristem proplastid-to-chloroplast progression in dicots with a basal meristem proplastid-to-etioplast-to-chloroplast transition in grasses may have been advantageous. In mid-latitudes 55–70 million years ago, selective pressures included seasonally dry climates, wildfires, and herbivory (Bond and Scott, 2010). A ground-level basal meristem may provide greater tolerance to drought-stress and defoliation by mammals. By abandoning ptDNA in mature leaves, grasses may realize a cost saving by not repairing DNA damaged by increased ROS from drought-stress and not investing in ptDNA maintenance in mature leaves that would be lost to fire or herbivory.

CAN ORGANELLAR DNA REALLY BE LOST IN HEALTHY LEAVES?

We have a relatively good understanding of the replication and repair apparatus that maintains nuclear DNA at a constant, diploid level throughout development. By comparison, there is disagreement concerning the maintenance of orgDNA in the same cells. Rather than infer the properties of orgDNA molecules from enzyme requirements and indirect methods like RNA analysis, the quality, quantity and stability of orgDNA molecules themselves should be investigated during development from meristem to green leaf.

The data showing the demise of orgDNA during leaf maturation have not been well received by some, and the controversy has been presented recently (Golczyk et al., 2014; Oldenburg et al., 2014). There are four main reasons for skepticism. First, some proteins, especially the product of the *psbA* gene (D1), turn over very rapidly and must be continuously replaced for photosynthesis to occur. Thus, either there must be a functional *psbA* gene in the green chloroplast to supply the mRNA for ongoing production of D1 protein during photosynthesis or the mRNA for D1 is extremely stable. In dismissing the latter alternative, the half-life of *psbA* mRNA (for barley) was mistakenly cited as “in the range of 40 h” (Golczyk et al., 2014), whereas the reported half-life was >40 h, the mRNA level did not change over a 30-h period, and mRNA stability increased during chloroplast development (Kim et al., 1993).

The second reason for skepticism is the fact that ptDNA copy number estimated from standard qPCR is ~ 800 to 1400 copies per haploid nuclear genome in mature green leaves of maize, with the assumption that each copy measured from a 0.15-kb PCR product represents a genome-sized molecule. Although the same approximate number was reported by both parties to the controversy, data from DNA Movies and PFGE and, more recently, from miPCR indicated that essentially all of those

"copies" were present as highly-fragmented or lesion-containing ptDNA molecules, as discussed above.

The third reason is that an *in vitro* run-on transcription assay shows that ptDNA is present in the chloroplasts isolated from green leaves of barley (Emanuel et al., 2004). In this assay, radiolabeled UTP is incorporated into the growing RNA chain that had been initiated before the leaves were harvested. However, the fraction of the millions of chloroplasts in the assay tube that are engaged in transcription is unknown—it could be <1 or 100%—and rare proplastids in the chloroplast preparation could be the source of the transcription activity. Furthermore, transcripts from highly-fragmented ptDNA might not benefit the cell from their coding potential, but instead represent the residuum from transcription-coupled repair, a proposed global surveyor of DNA damage (Epshteyn et al., 2014) and suggested to occur early in the development of plastids and mitochondria (Kumar et al., 2014).

The suggestion has also been made that the data indicating the demise of orgDNA are due to methodological artifacts (Golczyk et al., 2014; disputed by Oldenburg et al., 2014). Furthermore, for the artifact alternative to be correct, each of the types of data that document the decline of orgDNA—PFGE, DNA Movies, quantitative DAPI fluorescence, and miPCR—would have to be affected by an independent artifact, with none of these hypothetical artifacts occurring when we studied the orgDNA from the meristematic tissue. We conclude that during proplastid-to-chloroplast development, the ptDNA level initially increases to supply the gene products needed for photosynthesis. After chloroplast maturation, excess copies are no longer needed, degraded, and the nucleotides recycled. The net result is a decrease to a low constant ptDNA level in mature leaves with many molecules too damaged or fragmented to serve a coding function, even if they can be scored as "genome copies" by qPCR.

The fourth reason is that cytological images of DAPI-stained nucleoids indicate the persistence of some ptDNA in expanded green leaves of several plants (Golczyk et al., 2014). These data, however, are not quantitative, do not reflect the quality of the ptDNA molecules, and do not report the fraction of DAPI-positive chloroplasts among chloroplasts chosen at random for analysis. The genome copy number per individual chloroplast chosen at random before quantitative analysis of DAPI fluorescence varied

from 0 to 241 for the first green leaf of maize (Zheng et al., 2011; Oldenburg et al., 2014); 0 to 82 for the mature first rosette leaf of *Arabidopsis* (Rowan et al., 2009); 6 to 259 for the mature 16th leaf of tobacco; and 0 to 194 for the fully-expanded second leaf of *Medicago truncatula* (Shaver et al., 2006). In each case, DNA Movies showed that the ptDNA was highly fragmented. Thus the detection of DAPI-positive nucleoids does not necessarily indicate that the nucleoids contain ptDNA molecules of high quality.

CONCLUDING REMARKS

The amount and degree of molecular integrity of DNA present in a particular tissue are determined by replication, repair, and stability of the DNA. For the diploid nucleus, these processes are governed by checkpoint control in such a way as to result in a constant amount of stable, intact chromosomal DNA molecules throughout development, regardless of the physiological activities of the cells. For plastids and mitochondria, however, such tight control is not exercised, and the amount and quality of orgDNA can vary greatly among tissues, from pristine multigenomic chromosomes in meristematic cells to highly fragmented "copies" in mature leaves, without compromising the homeostasis of the wild-type plant. In other words, orgDNA—but usually not nuclear DNA—can be abandoned in somatic cells as part of the normal developmental process. In the single-celled alga *Euglena*, orgDNA cannot be abandoned but ptDNA and mtDNA are unstable (half-lives of 1.6 and 1.8 cell doublings, respectively), whereas nuclear DNA turnover could not be detected (Manning and Richards, 1972; Richards and Ryan, 1974). The advantage of DNA abandonment leading to DNA-repair cost savings and embryonic development in plants and animals has been discussed previously (Bendich, 2010b, 2013). Although DNA could not be abandoned in the bacterial ancestors of plastids and mitochondria, orgDNA abandonment in leaves has evidently been advantageous, especially for grasses.

ACKNOWLEDGMENTS

This work was funded by the Junat Fund (a private charitable fund). The authors thank Beth A. Rowan for critical reading of this manuscript.

REFERENCES

- Alexeyev, M., Shokolenko, I., Wilson, G., and LeDoux, S. (2013). The maintenance of mitochondrial DNA integrity—critical analysis and update. *Cold Spring Harb. Perspect. Biol.* 5, a012641. doi: 10.1101/cshperspect.a012641
- Alverson, A. J., Wei, X., Rice, D. W., Stern, D. B., Barry, K., and Palmer, J. D. (2010). Insights into the evolution of mitochondrial genome size from complete sequences of *Citrullus lanatus* and *Cucurbita pepo* (Cucurbitaceae). *Mol. Biol. Evol.* 27, 1436–1448. doi: 10.1093/molbev/msq029
- Balestrazzi, A., Confalonieri, M., Macovei, A., Dona, M., and Carbonera, D. (2011). Genotoxic stress and DNA repair in plants: emerging functions and tools for improving crop productivity. *Plant Cell Rep.* 30, 287–295. doi: 10.1007/s00299-010-0975-9
- Baumgartner, B. J., Rapp, J. C., and Mullet, J. E. (1989). Plastid transcription activity and DNA copy number increase early in barley chloroplast development. *Plant Physiol.* 89, 1011–1018. doi: 10.1104/pp.89.3.1011
- Bendich, A. J. (1987). Why do chloroplasts and mitochondria contain so many copies of their genome? *Bioessays* 6, 279–282. doi: 10.1002/bies.950060608
- Bendich, A. J. (1991). Moving pictures of DNA released upon lysis from bacteria, chloroplasts, and mitochondria. *Protoplasma* 160, 121–130. doi: 10.1007/BF01539964
- Bendich, A. J. (1996). Structural analysis of mitochondrial DNA molecules from fungi and plants using moving pictures and pulsed-field gel electrophoresis. *J. Mol. Biol.* 255, 564–588. doi: 10.1006/jmbi.1996.0048
- Bendich, A. J. (2001). The form of chromosomal DNA molecules in bacterial cells. *Biochimie* 83, 177–186. doi: 10.1016/S0300-9084(00)01209-8
- Bendich, A. J. (2007). The size and form of chromosomes are constant in the nucleus, but highly variable in bacteria, mitochondria and chloroplasts. *Bioessays* 29, 474–483. doi: 10.1002/bies.20576
- Bendich, A. J. (2010a). The end of the circle for yeast mitochondrial DNA. *Mol. Cell.* 39, 831–832. doi: 10.1016/j.molcel.2010.09.005
- Bendich, A. J. (2010b). Mitochondrial DNA, chloroplast DNA and the origins of development in eukaryotic organisms. *Biol. Direct.* 5, 42. doi: 10.1186/1745-6150-5-42

- Bendich, A. J. (2013). DNA abandonment and the mechanisms of uniparental inheritance of mitochondria and chloroplasts. *Chromosome Res.* 21, 287–296. doi: 10.1007/s10577-013-9349-9
- Bendich, A. J., and Smith, S. B. (1990). Moving pictures and pulsed-field gel electrophoresis show linear DNA molecules from chloroplasts and mitochondria. *Curr. Genet.* 17, 421–425. doi: 10.1007/BF00334522
- Boesch, P., Weber-Lotfi, F., Ibrahim, N., Tarasenko, V., Cosset, A., Paulus, F., et al. (2011). DNA repair in organelles: pathways, organization, regulation, relevance in disease and aging. *Biochim. Biophys. Acta* 1813, 186–200. doi: 10.1016/j.bbamcr.2010.10.002
- Bond, W. J., and Scott, A. C. (2010). Fire and the spread of flowering plants in the Cretaceous. *New Phytol.* 188, 1137–1150. doi: 10.1111/j.1469-8137.2010.03418.x
- Cairns, J. P. (1963). The chromosome of *Escherichia coli*. *Proc. Cold Spring Harb. Symp. Quant. Biol.* 28, 43–46. doi: 10.1101/sqb.1963.028.01.011
- Cappadocia, L., Marechal, A., Parent, J. S., Lepage, E., Sygusch, J., and Brisson, N. (2010). Crystal structures of DNA-Whirly complexes and their role in *Arabidopsis* organelle genome repair. *Plant Cell* 22, 1849–1867. doi: 10.1105/tpc.109.071399
- Cappadocia, L., Parent, J. S., Zampini, E., Lepage, E., Sygusch, J., and Brisson, N. (2012). A conserved lysine residue of plant Whirly proteins is necessary for higher order protein assembly and protection against DNA damage. *Nucleic Acids Res.* 40, 258–269. doi: 10.1093/nar/gkr740
- Carrie, C., and Small, I. (2013). A reevaluation of dual-targeting of proteins to mitochondria and chloroplasts. *Biochim. Biophys. Acta* 1833, 253–259. doi: 10.1016/j.bbamcr.2012.05.029
- Chaconas, G., and Kobryn, K. (2010). Structure, function, and evolution of linear replicons in *Borrelia*. *Annu. Rev. Microbiol.* 64, 185–202. doi: 10.1146/annurev.micro.112408.134037
- Chang, C. H., and Wu, M. (2000). The effects of transcription and RNA processing on the initiation of chloroplast DNA replication in *Chlamydomonas reinhardtii*. *Mol. Gen. Genet.* 263, 320–327. doi: 10.1007/s004380051174
- Christin, P. A., Spriggs, E., Osborne, C. P., Stromberg, C. A., Salamin, N., and Edwards, E. J. (2014). Molecular dating, evolutionary rates, and the age of the grasses. *Syst. Biol.* 63, 153–165. doi: 10.1093/sysbio/syt072
- Coleman, A. W. (1979). Use of the fluorochrome 4'-6-diamidino-2-phenylindole in genetic and developmental studies of chloroplast DNA. *J. Cell Biol.* 82, 299–305. doi: 10.1083/jcb.82.1.299
- Cox, M. M. (2007). Motoring along with the bacterial RecA protein. *Nat. Rev. Mol. Cell Biol.* 8, 127–138. doi: 10.1038/nrm2099
- Cupp, J. D., and Nielsen, B. L. (2014). Minireview: DNA replication in plant mitochondria. *Mitochondrion* 19 Pt B, 231–237. doi: 10.1016/j.mito.2014.03.008
- Dai, H., Lo, Y. S., Litvinchuk, A., Wang, Y. T., Jane, W. N., Hsiao, L. J., et al. (2005). Structural and functional characterizations of mung bean mitochondrial nucleoids. *Nucleic Acids Res.* 33, 4725–4739. doi: 10.1093/nar/gki783
- Dickey, T. H., Altschuler, S. E., and Wuttke, D. S. (2013). Single-stranded DNA-binding proteins: multiple domains for multiple functions. *Structure* 21, 1074–1084. doi: 10.1016/j.str.2013.05.013
- Diray-Arce, J., Liu, B., Cupp, J. D., Hunt, T., and Nielsen, B. L. (2013). The *Arabidopsis* At1g30680 gene encodes a homologue to the phage T7 gp4 protein that has both DNA primase and DNA helicase activities. *BMC Plant Biol.* 13:36. doi: 10.1186/1471-2229-13-36
- Donnelly, P. M., Bonetta, D., Tsukaya, H., Dengler, R. E., and Dengler, N. G. (1999). Cell cycling and cell enlargement in developing leaves of *Arabidopsis*. *Dev. Biol.* 215, 407–419. doi: 10.1006/dbio.1999.9443
- Emanuel, C., Weihe, A., Graner, A., Hess, W. R., and Börner, T. (2004). Chloroplast development affects expression of phage-type RNA polymerases in barley leaves. *Plant J.* 38, 460–472. doi: 10.1111/j.0960-7412.2004.02060.x
- Epshtain, V., Kamarthapu, V., McGary, K., Svetlov, V., Ueberheide, B., Proshkin, S., et al. (2014). UvrD facilitates DNA repair by pulling RNA polymerase backwards. *Nature* 505, 372–377. doi: 10.1038/nature12928
- Foyer, C. H., Karpinska, B., and Krupinska, K. (2014). The functions of WHIRLY1 and REDOX-RESPONSIVE TRANSCRIPTION FACTOR 1 in cross tolerance responses in plants: a hypothesis. *Philos. Trans. R. Soc. Lond. B. Biol. Sci.* 369, 20130226. doi: 10.1098/rstb.2013.0226
- Fujie, M., Kuroiwa, H., Kawano, S., and Kuroiwa, T. (1993). Studies on the behavior of organelles and their nucleoids in the root apical meristem of *Arabidopsis thaliana* (L.) Col. *Planta* 189, 443–452. doi: 10.1007/BF00194444
- Fujie, M., Kuroiwa, H., Kawano, S., Mutoh, S., and Kuroiwa, T. (1994). Behavior of organelles and their nucleoids in the shoot apical meristem during leaf development in *Arabidopsis thaliana* L. *Planta* 194, 395–405. doi: 10.1007/BF00197541
- Fukui, K., Kosaka, H., Kuramitsu, S., and Masui, R. (2007). Nuclease activity of the MutS homologue MutS2 from *Thermus thermophilus* is confined to the Smr domain. *Nucleic Acids Res.* 35, 850–860. doi: 10.1093/nar/gkl735
- Gilkerson, R., Bravo, L., Garcia, I., Gaytan, N., Herrera, A., Maldonado, A., et al. (2013). The mitochondrial nucleoid: integrating mitochondrial DNA into cellular homeostasis. *Cold Spring Harb. Perspect. Biol.* 5, a011080. doi: 10.1101/cshperspect.a011080
- Golczyk, H., Greiner, S., Wanner, G., Weihe, A., Bock, R., Börner, T., et al. (2014). Chloroplast DNA in mature and senescing leaves: a reappraisal. *Plant Cell* 26, 847–854. doi: 10.1105/tpc.113.117465
- Gutman, B. L., and Niygaki, K. K. (2009). Evidence for base excision repair of oxidative DNA damage in chloroplasts of *Arabidopsis thaliana*. *J. Biol. Chem.* 284, 17006–17012. doi: 10.1074/jbc.M109.008342
- Hashimoto, H., and Possingham, J. V. (1989). DNA levels in dividing and developing plastids in expanding primary leaves of *Avena sativa*. *J. Exp. Bot.* 40, 257–262. doi: 10.1093/jxb/40.2.257
- Heinhorst, S., and Cannon, G. C. (1993). DNA replication in chloroplasts. *J. Cell Sci.* 104, 1–9.
- Kabeya, Y., Nakanishi, H., Suzuki, K., Ichikawa, T., Kondou, Y., Matsui, M., et al. (2010). The YlmG protein has a conserved function related to the distribution of nucleoids in chloroplasts and cyanobacteria. *BMC Plant Biol.* 10:57. doi: 10.1186/1471-2229-10-57
- Kabeya, Y., and Miyagishima, S. Y. (2013). Chloroplast DNA replication is regulated by the redox state independently of chloroplast division in *Chlamydomonas reinhardtii*. *Plant Physiol.* 161, 2102–2112. doi: 10.1104/pp.113.216291
- Kang, J., Huang, S., and Blaser, M. J. (2005). Structural and functional divergence of MutS2 from bacterial MutS1 and eukaryotic MSH4-MSH5 homologs. *J. Bacteriol.* 187, 3528–3537. doi: 10.1128/JB.187.10.3528-3537.2005
- Kim, M., Christopher, D. A., and Mullet, J. E. (1993). Direct evidence for selective modulation of psbA, rpoA, rbcL, and 16S RNA stability during barley chloroplast development. *Plant Mol. Biol.* 22, 447–463. doi: 10.1007/BF00015975
- Kimura, S., Uchiyama, Y., Kasai, N., Namekawa, S., Saotome, A., Ueda, T., et al. (2002). A novel DNA polymerase homologous to *Escherichia coli* DNA polymerase I from a higher plant, rice (*Oryza sativa* L.). *Nucleic Acids Res.* 30, 1585–1592. doi: 10.1093/nar/30.7.1585
- Kindgren, P., and Strand, A. (2015). Chloroplast transcription, untangling the Gordian Knot. *New Phytol.* 206, 889–891. doi: 10.1111/nph.13388
- Kolodner, R., and Tewari, K. K. (1972a). Physicochemical characterization of mitochondrial DNA from pea leaves. *Proc. Natl. Acad. Sci. U.S.A.* 69, 1830–1834.
- Kolodner, R., and Tewari, K. K. (1972b). Molecular size and conformation of chloroplast deoxyribonucleic acid from pea leaves. *J. Biol. Chem.* 247, 6355–6364.
- Kolodner, R., and Tewari, K. K. (1975). Presence of displacement loops in the covalently closed circular chloroplast deoxyribonucleic acid from higher plants. *J. Biol. Chem.* 250, 8840–8847.
- Krishnan, N. M., and Rao, B. J. (2009). A comparative approach to elucidate chloroplast genome replication. *BMC Genomics* 10:237. doi: 10.1186/1471-2164-10-237
- Krupinska, K., Melonek, J., and Krause, K. (2013). New insights into plastid nucleoid structure and functionality. *Planta* 237, 653–664. doi: 10.1007/s00425-012-1817-5
- Kumar, R. A., Oldenburg, D. J., and Bendich, A. J. (2014). Changes in DNA damage, molecular integrity, and copy number for plastid DNA and mitochondrial DNA during maize development. *J. Exp. Bot.* 65, 6425–6439. doi: 10.1093/jxb/eru359
- Kumar, R. A., Oldenburg, D. J., and Bendich, A. J. (2015). Molecular integrity of chloroplast DNA and mitochondrial DNA in mesophyll and bundle sheath cells of maize. *Planta* 241, 1221–1230. doi: 10.1007/s00425-015-2253-0
- Kunnimalaiyaan, M., and Nielsen, B. L. (1997). Chloroplast DNA replication: mechanism, enzymes and replication origins. *J. Plant Biochem. Biotechnol.* 6, 1–7. doi: 10.1007/BF03263000
- Kuroiwa, T. (1991). The replication, differentiation, and inheritance of plastids with emphasis on the concept of organelle nuclei. *Internal. Rev. Cytol.* 128, 1–62. doi: 10.1016/S0074-7696(08)60496-9
- Kuroiwa, T., Fujie, M., and Kuroiwa, H. (1992). Studies on the behavior of mitochondrial DNA: synthesis of mitochondrial DNA occurs actively in a specific region just above the quiescent center in the root meristem of *Pelargonium zonale*. *J. Cell Sci.* 101, 483–493.

- Kuroiwa, T., Suzuki, T., Ogawa, K., and Kawano, S. (1981). The chloroplast nucleus: distribution, number, size, and shape, and a model for multiplication of the chloroplast genome during chloroplast development. *Plant Cell Physiol.* 22, 381–396.
- Lamppa, G. K., and Bendich, A. J. (1979a). Changes in chloroplast DNA levels during development of pea (*Pisum sativum*). *Plant Physiol.* 64, 126–130.
- Lamppa, G. K., and Bendich, A. J. (1979b). Chloroplast DNA sequence homologies among vascular plants. *Plant Physiol.* 63, 660–668.
- Lamppa, G. K., and Bendich, A. J. (1984). Changes in mitochondrial DNA levels during development of pea (*Pisum sativum L.*). *Planta* 162, 463–468. doi: 10.1007/BF00393460
- Lassen, M. G., Kochhar, S., and Nielsen, B. L. (2011). Identification of a soybean chloroplast DNA replication origin-binding protein. *Plant Mol. Biol.* 76, 463–471. doi: 10.1007/s11103-011-9736-6
- Liere, K., and Börner, T. (2013). “Development-dependent changes in the amount and structural organization of plastid DNA,” in *Plastid Development in Leaves During Growth and Senescence, Advances in Photosynthesis and Respiration*, eds B. Biswal, K. Krupinska, and U. C. Biswal (Dordrecht: Springer Science+Business Media), 215–237. doi: 10.1007/978-94-007-5724-0_11
- Lilly, J. W., Havey, M. J., Jackson, S. A., and Jiang, J. (2001). Cytogenomic analyses reveal the structural plasticity of the chloroplast genome in higher plants. *Plant Cell* 13, 245–254. doi: 10.1105/tpc.13.2.245
- Li, W., Ruf, S., and Bock, R. (2006). Constancy of organellar genome copy numbers during leaf development and senescence in higher plants. *Mol. Genet. Genomics.* 275, 185–192. doi: 10.1007/s00438-005-0075-7
- Lo, Y. S., Hsiao, L. J., Cheng, N., Litvinchuk, A., and Dai, H. (2011). Characterization of the structure and DNA complexity of mung bean mitochondrial nucleoids. *Mol. Cells* 31, 217–224. doi: 10.1007/s10059-011-0036-4
- Majeran, W., Friso, G., Asakura, Y., Qu, X., Huang, M., Ponnala, L., et al. (2012). Nucleoid-enriched proteomes in developing plastids and chloroplasts from maize leaves: a new conceptual framework for nucleoid functions. *Plant Physiol.* 158, 156–189. doi: 10.1104/pp.111.188474
- Manning, J. E., and Richards, O. C. (1972). Synthesis and turnover of *Euglena gracilis* nuclear and chloroplast deoxyribonucleic acid. *Biochemistry* 11, 2036–2043. doi: 10.1021/bi00761a007
- Marechal, A., Parent, J. S., Veronneau-Lafortune, F., Joyeux, A., Lang, B. F., and Brisson, N. (2009). Whirly proteins maintain plastid genome stability in *Arabidopsis*. *Proc. Natl. Acad. Sci. U.S.A.* 106, 14693–14698. doi: 10.1073/pnas.0901710106
- Marechal, A., and Brisson, N. (2010). Recombination and the maintenance of plant organelle genome stability. *New Phytol.* 186, 299–317. doi: 10.1111/j.1469-8137.2010.03195.x
- Miller, A. H., Whelan, J., Soole, K. L., and Day, D. A. (2011). Organization and regulation of mitochondrial respiration in plants. *Annu. Rev. Plant Biol.* 62, 79–104. doi: 10.1146/annurev-arplant-042110-103857
- Miyamura, S., Nagata, T., and Kuroiwa, T. (1986). Quantitative fluorescence microscopy on dynamic changes of plastid nucleoids during wheat development. *Protoplasma* 133, 66–72. doi: 10.1007/BF01293188
- Moriyama, T., and Sato, N. (2014). Enzymes involved in organellar DNA replication in photosynthetic eukaryotes. *Front. Plant Sci.* 5:480. doi: 10.3389/fpls.2014.00480
- Mori, Y., Kimura, S., Saotome, A., Kasai, N., Sakaguchi, N., Uchiyama, Y., et al. (2005). Plastid DNA polymerases from higher plants, *Arabidopsis thaliana*. *Biochem. Biophys. Res. Commun.* 334, 43–50. doi: 10.1016/j.bbrc.2005.06.052
- Morrical, S. W. (2015). DNA-pairing and annealing processes in homologous recombination and homology-directed repair. *Cold Spring Harb. Perspect. Biol.* 7, a016444. doi: 10.1101/cshperspect.a016444
- Nelson, T., and Langdale, J. A. (1989). Patterns of leaf development in C4 plants. *Plant Cell* 1, 3–13. doi: 10.1105/tpc.1.1.3
- Nemoto, Y., Nagata, T., and Kuroiwa, T. (1990). Studies on plastid-nuclei (nucleoids) in *Nicotiana tabacum* L. III. Disassembly and reassembly of proplastid-nuclei isolated from cultured cells. *Plant Cell Physiol.* 31, 767–776.
- Nie, Z. Q., Chang, D. Y., and Wu, M. (1987). Protein-DNA interaction within one cloned chloroplast DNA replication origin of *Chlamydomonas*. *Mol. Gen. Genet.* 209, 265–269. doi: 10.1007/BF00329652
- Nosek, J., Kosa, P., and Tomaska, L. (2006). On the origin of telomeres: a glimpse at the pre-telomerase world. *Bioessays* 28, 182–190. doi: 10.1002/bies.20355
- Oldenburg, D. J., and Bendich, A. J. (1996). Size and structure of replicating mitochondrial DNA in cultured tobacco cells. *Plant Cell* 8, 447–461. doi: 10.1105/tpc.8.3.447
- Oldenburg, D. J., and Bendich, A. J. (1998a). The structure of mitochondrial DNA from the liverwort, *Marchantia polymorpha*. *J. Mol. Biol.* 276, 745–758. doi: 10.1006/jmbi.1997.1581
- Oldenburg, D. J., and Bendich, A. J. (1998b). Fluorescence microscopy of DNA-protein structures from osmotically lysed mitochondria of yeast and tobacco. *Protoplasma* 201, 53–63. doi: 10.1007/BF01280711
- Oldenburg, D. J., and Bendich, A. J. (2004a). Most chloroplast DNA of maize seedlings in linear molecules with defined ends and branched forms. *J. Mol. Biol.* 335, 953–970. doi: 10.1016/j.jmb.2003.11.020
- Oldenburg, D. J., and Bendich, A. J. (2004b). Changes in the structure of DNA molecules and the amount of DNA per plastid during chloroplast development in maize. *J. Mol. Biol.* 344, 1311–1330. doi: 10.1016/j.jmb.2004.10.001
- Oldenburg, D. J., Kumar, R. A., and Bendich, A. J. (2013). The amount and integrity of mtDNA in maize decline with development. *Planta* 237, 603–617. doi: 10.1007/s00425-012-1802-z
- Oldenburg, D. J., Rowan, B. A., Kumar, R. A., and Bendich, A. J. (2014). On the fate of plastid DNA molecules during leaf development: response to the Golczyk et al. Commentary. *Plant Cell* 26, 855–861. doi: 10.1105/tpc.113.121772
- Oldenburg, D. J., Rowan, B. A., Zhao, L., Walcher, C. L., Schleh, M., and Bendich, A. J. (2006). Loss or retention of chloroplast DNA in maize seedlings is affected by both light and genotype. *Planta* 225, 41–55. doi: 10.1007/s00425-006-0329-6
- Palmer, J. D., and Thompson, W. F. (1981). Rearrangements in the chloroplast genomes of mung bean and pea. *Proc. Natl. Acad. Sci. U.S.A.* 78, 5533–5537. doi: 10.1073/pnas.78.9.5533
- Parent, J. S., Lepage, E., and Brisson, N. (2011). Divergent roles for the two PolI-like organelle DNA polymerases of *Arabidopsis*. *Plant Physiol.* 156, 254–262. doi: 10.1104/pp.111.173849
- Pinto, A. V., Mathieu, A., Marsin, S., Veautre, X., Ielpi, L., Labigne, A., et al. (2005). Suppression of homologous and homeologous recombination by the bacterial MutS2 protein. *Mol. Cell.* 17, 113–120. doi: 10.1016/j.molcel.2004.11.035
- Powikrowska, M., Oetke, S., Jensen, P. E., and Krupinska, K. (2014). Dynamic composition, shaping and organization of plastid nucleoids. *Front. Plant Sci.* 5:424. doi: 10.3389/fpls.2014.00424
- Preuten, T., Cincu, E., Fuchs, J., Zoschke, R., Liere, K., and Börner, T. (2010). Fewer genes than organelles: extremely low and variable gene copy numbers in mitochondria of somatic plant cells. *Plant J.* 64, 948–959. doi: 10.1111/j.1365-313X.2010.04389.x
- Prikryl, J., Watkins, K. P., Friso, G., van Wijk, K. J., and Barkan, A. (2008). A member of the Whirly family is a multifunctional RNA- and DNA-binding protein that is essential for chloroplast biogenesis. *Nucleic Acids Res.* 36, 5152–5165. doi: 10.1093/nar/gkn492
- Reid, D. A., Keegan, S., Leo-Macias, A., Watanabe, G., Strande, N. T., Chang, H. H., et al. (2015). Organization and dynamics of the nonhomologous end-joining machinery during DNA double-strand break repair. *Proc. Natl. Acad. Sci. U.S.A.* 112, E2575–E2584. doi: 10.1073/pnas.1420115112
- Richards, O. C., and Ryan, R. S. (1974). Synthesis and turnover of *Euglena gracilis* mitochondrial DNA. *J. Mol. Biol.* 82, 57–75. doi: 10.1016/0022-2836(74)90574-9
- Rowan, B. A., and Bendich, A. J. (2009). The loss of DNA from chloroplasts as leaves mature: fact or artefact? *J. Exp. Bot.* 60, 3005–3010. doi: 10.1093/jxb/erp158
- Rowan, B. A., Oldenburg, D. J., and Bendich, A. J. (2004). The demise of chloroplast DNA in *Arabidopsis*. *Curr. Genet.* 46, 176–181. doi: 10.1007/s00294-004-0515-7
- Rowan, B. A., Oldenburg, D. J., and Bendich, A. J. (2009). A multiple-method approach reveals a declining amount of chloroplast DNA during development in *Arabidopsis*. *BMC Plant Biol.* 9:3. doi: 10.1186/1471-2229-9-3
- Rowan, B. A., Oldenburg, D. J., and Bendich, A. J. (2010). RecA maintains the integrity of chloroplast DNA molecules in *Arabidopsis*. *J. Exp. Bot.* 61, 2575–2588. doi: 10.1093/jxb/erq088
- Scharff, L. B., and Koop, H. U. (2006). Linear molecules of tobacco ptDNA end at known replication origins and additional loci. *Plant Mol. Biol.* 62, 611–621. doi: 10.1007/s11103-006-9042-x
- Scharff, L. B., and Koop, H. U. (2007). Targeted inactivation of the tobacco plastome origins of replication A and B. *Plant J.* 50, 782–794. doi: 10.1111/j.1365-313X.2007.03087.x
- Shaver, J. M., Oldenburg, D. J., and Bendich, A. J. (2006). Changes in chloroplast DNA during development in tobacco, *Medicago truncatula*, pea, and maize. *Planta* 224, 72–82. doi: 10.1007/s00425-005-0195-7

- Shaver, J. M., Oldenburg, D. J., and Bendich, A. J. (2008). The structure of chloroplast DNA molecules and the effects of light on the amount of chloroplast DNA during development in *Medicago truncatula*. *Plant Physiol.* 146, 1064–1074. doi: 10.1104/pp.107.112946
- Shokolenko, I., Venediktova, N., Bochkareva, A., Wilson, G. L., and Alexeyev, M. F. (2009). Oxidative stress induces degradation of mitochondrial DNA. *Nucleic Acids Res.* 37, 2539–2548. doi: 10.1093/nar/gkp100
- Skarstad, K., and Boye, E. (1993). Degradation of individual chromosomes in recA mutants of *Escherichia coli*. *J. Bacteriol.* 175, 5505–5509.
- Smith, D. R., and Keeling, P. J. (2013). Gene conversion shapes linear mitochondrial genome architecture. *Genome Biol. Evol.* 5, 905–912. doi: 10.1093/gbe/evt059
- Stern, D. B., Hanson, M. R., and Barkan, A. (2004). Genetics and genomics of chloroplast biogenesis: maize as a model system. *Trends Plant Sci.* 9, 293–301. doi: 10.1016/j.tplants.2004.04.001
- Stern, D. B., and Palmer, J. D. (1984). Recombination sequences in plant mitochondrial genomes: diversity and homologies to known mitochondrial genes. *Nucleic Acids Res.* 12, 6141–6157. doi: 10.1093/nar/12.15.6141
- Strömberg, C. A. E. (2011). Evolution of grasses and grassland ecosystems. *Annu. Rev. Earth Planet. Sci.* 39, 517–544. doi: 10.1146/annurev-earth-040809-152402
- Sugiyama, Y., Watase, Y., Nagase, M., Makita, N., Yagura, S., Hirai, A., et al. (2005). The complete nucleotide sequence and multipartite organization of the tobacco mitochondrial genome: comparative analysis of mitochondrial genomes in higher plants. *Mol. Genet. Genomics.* 272, 603–615. doi: 10.1007/s00438-004-1075-8
- Suzuki, T., Sasaki, N., Sakai, A., Kawano, S., and Kuroiwa, T. (1995). Localization of organelle DNA synthesis within the root apical meristem of rice. *J. Exp. Bot.* 46, 19–25. doi: 10.1093/jxb/46.1.19
- Sylvester, A. W., Cande, W. Z., and Freeling, M. (1990). Division and differentiation during normal and liguleless-1 maize leaf development. *Development* 110, 985–1000.
- Tardieu, F., and Granier, C. (2000). Quantitative analysis of cell division in leaves: methods, developmental patterns and effects of environmental conditions. *Plant Mol. Biol.* 43, 555–567. doi: 10.1023/A:1006438321386
- Tomaska, L., Makhov, A. M., Nosek, J., Kucejova, B., and Griffith, J. D. (2001). Electron microscopic analysis supports a dual role for the mitochondrial telomere-binding protein of *Candida parapsilosis*. *J. Mol. Biol.* 305, 61–69. doi: 10.1006/jmbi.2000.4254
- Udy, D. B., Belcher, S., Williams-Carrier, R., Gualberto, J. M., and Barkan, A. (2012). Effects of reduced chloroplast gene copy number on chloroplast gene expression in maize. *Plant Physiol.* 160, 1420–1431. doi: 10.1104/pp.112.204198
- Unsel, M., Marienfeld, J. R., Brandt, P., and Brennicke, A. (1997). The mitochondrial genome of *Arabidopsis thaliana* contains 57 genes in 366,924 nucleotides. *Nat. Genet.* 15, 57–61. doi: 10.1038/ng0197-57
- Ward, B. L., Anderson, R. S., and Bendich, A. J. (1981). The mitochondrial genome is large and variable in a family of plants (Cucurbitaceae). *Cell* 25, 793–803. doi: 10.1016/0092-8674(81)90187-2
- Weller, S. K., and Sawitzke, J. A. (2014). Recombination promoted by DNA viruses: phage lambda to herpes simplex virus. *Annu. Rev. Microbiol.* 68, 237–258. doi: 10.1146/annurev-micro-091313-103424
- Williamson, D. (2002). The curious history of yeast mitochondrial DNA. *Nat. Rev. Genet.* 3, 475–481. doi: 10.1038/nrg814
- Yakes, F. M., and Van Houten, B. (1997). Mitochondrial DNA damage is more extensive and persists longer than nuclear DNA damage in human cells following oxidative stress. *Proc. Natl. Acad. Sci. U.S.A.* 94, 514–519. doi: 10.1073/pnas.94.2.514
- Zampini, E., Lepage, E., Tremblay-Belzile, S., Truche, S., and Brisson, N. (2015). Organelle DNA rearrangement mapping reveals U-turn-like inversions as a major source of genomic instability in *Arabidopsis* and humans. *Genome Res.* 25, 645–654. doi: 10.1101/gr.188573.114
- Zheng, Q., Oldenburg, D. J., and Bendich, A. J. (2011). Independent effects of leaf growth and light on the development of the plastid and its DNA content in *Zea species*. *J. Exp. Bot.* 62, 2715–2730. doi: 10.1093/jxb/erq441
- Zoschke, R., Liere, K., and Börner, T. (2007). From seedling to mature plant: *Arabidopsis* plastidial genome copy number, RNA accumulation and transcription are differentially regulated during leaf development. *Plant J.* 50, 710–722. doi: 10.1111/j.1365-313X.2007.03084.x

Conflict of Interest Statement: The authors declare that the research was conducted in the absence of any commercial or financial relationships that could be construed as a potential conflict of interest.

Copyright © 2015 Oldenburg and Bendich. This is an open-access article distributed under the terms of the Creative Commons Attribution License (CC BY). The use, distribution or reproduction in other forums is permitted, provided the original author(s) or licensor are credited and that the original publication in this journal is cited, in accordance with accepted academic practice. No use, distribution or reproduction is permitted which does not comply with these terms.

***Arabidopsis* DNA polymerase lambda mutant is mildly sensitive to DNA double strand breaks but defective in integration of a transgene**

OPEN ACCESS

Edited by:

Ayako N. Sakamoto,
Japan Atomic Energy Agency, Japan

Reviewed by:

Charles I. White,
Centre National de la Recherche

Scientifique, France

Katarzyna Bebenek,

National Institute of Environmental
Health Sciences/National Institutes of
Health, USA

Yuichiro Yokota,
Japan Atomic Energy Agency, Japan

***Correspondence:**

Anne B. Britt,

Department of Plant Biology,
University of California at Davis, One

Shields Avenue, Davis,
CA 95616, USA

abritt@ucdavis.edu

†Present Address:

Tomoyuki Furukawa,
Breeding Research Department,
Mikado Kyowa Seed Co Ltd., Otaki,
Japan

Specialty section:

This article was submitted to
Plant Physiology,
a section of the journal
Frontiers in Plant Science

Received: 01 March 2015

Accepted: 05 May 2015

Published: 27 May 2015

Citation:

Furukawa T, Angelis KJ and Britt AB
(2015) *Arabidopsis* DNA polymerase
lambda mutant is mildly sensitive to
DNA double strand breaks but
defective in integration of a transgene.
Front. Plant Sci. 6:357.

doi: 10.3389/fpls.2015.00357

Tomoyuki Furukawa^{1†}, Karel J. Angelis² and Anne B. Britt^{1*}

¹ Department of Plant Biology, University of California at Davis, Davis, CA, USA, ² DNA Repair Lab, Institute of Experimental Botany of the Academy of Sciences of the Czech Republic, Praha, Czech Republic

The DNA double-strand break (DSB) is a critical type of damage, and can be induced by both endogenous sources (e.g., errors of oxidative metabolism, transposable elements, programmed meiotic breaks, or perturbation of the DNA replication fork) and exogenous sources (e.g., ionizing radiation or radiomimetic chemicals). Although higher plants, like mammals, are thought to preferentially repair DSBs via nonhomologous end joining (NHEJ), much remains unclear about plant DSB repair pathways. Our reverse genetic approach suggests that DNA polymerase λ is involved in DSB repair in *Arabidopsis*. The *Arabidopsis* T-DNA insertion mutant (*atpol*/ λ -1) displayed sensitivity to both gamma-irradiation and treatment with radiomimetic reagents, but not to other DNA damaging treatments. The *atpol*/ λ -1 mutant showed a moderate sensitivity to DSBs, while *Arabidopsis* Ku70 and DNA ligase 4 mutants (*atku70*-3 and *atlig4*-2), both of which play critical roles in NHEJ, exhibited a hypersensitivity to these treatments. The *atpol*/ λ -1/*atlig4*-2 double mutant exhibited a higher sensitivity to DSBs than each single mutant, but the *atku70*/*atpol*/ λ -1 showed similar sensitivity to the *atku70*-3 mutant. We showed that transcription of the *DNA ligase 1*, *DNA ligase 6*, and *Wee1* genes was quickly induced by BLM in several NHEJ deficient mutants in contrast to wild-type. Finally, the T-DNA transformation efficiency dropped in NHEJ deficient mutants and the lowest transformation efficiency was scored in the *atpol*/ λ -1/*atlig4*-2 double mutant. These results imply that AtPol λ is involved in both DSB repair and DNA damage response pathway.

Keywords: DNA polymerase, DNA repair, Non homologous end joining, DNA damage response, double strand breaks

Introduction

The 3R mechanisms (DNA replication, repair, and recombination) are key machineries for all living organisms. DNA-dependent DNA polymerases play critical roles in 3R mechanisms. To date, at least 13 types of DNA polymerases (Pol α , β , γ , δ , ε , ζ , η , θ , ι , κ , λ , μ , and ν) and two polymerase homologs, terminal deoxyribonucleotidyl transferases (TdT), and REV1, have been found in the human genome. Based on amino acid sequence homology, DNA polymerases are classified into four different polymerase families (A, B, X, and Y). DNA polymerase λ belongs to the Pol X-family

along with three other non-replicative mammalian DNA polymerases (Pol β , Pol μ , and TdT). The structure of the Pol λ protein consists of three functional domains: a BRCT (BRCA1 C-terminus) domain at the N-terminus, a DNA binding domain in the central region, and a DNA polymerization domain at the C-terminus, respectively. Biochemical studies have revealed that the human Pol λ protein has three enzymatic activities: DNA polymerase activity, TdT activity, and 5'-Deoxyribose-5-phosphate (dRP lyase) activity. Although the human Pol λ protein is able to incorporate multiple nucleotides during the *in vitro* reaction, its processivity is low compared to replicative-type DNA polymerases (Pol α , δ , ϵ). These enzymatic activities suggest that Pol λ participates in two DNA repair pathways; base excision repair and NHEJ (Braithwaite et al., 2005a,b, 2010; Garcia-Diaz et al., 2005; Nick McElhinny et al., 2005). Both DNA polymerase and dRP lyase activities are required for short-patch base excision repair (spBER). Physical interaction of Pol λ with the XRCC4/Lig4 complex implies that Pol λ also participates in alignment-based gap filling during NHEJ (Fan and Wu, 2004; Lee et al., 2004; Capp et al., 2006).

In contrast to a long history of study of mammalian and yeast DNA polymerases, much remains unclear regarding the plant DNA polymerases. A recent advance of plant genome projects has revealed that plant genomes encode homologs for 10 DNA polymerases (Pol α , δ , ϵ , ζ , η , θ , κ , λ , σ , and ν) (Yokoi et al., 1997; Uchiyama et al., 2002, 2004; Sakamoto et al., 2003; Garcia-Ortiz et al., 2004; Takahashi et al., 2005; Inagaki et al., 2006; Anderson et al., 2008) and two plastid-specific Pol I-like DNA polymerases (Kimura et al., 2002; Mori et al., 2005; Ono et al., 2007). Despite the fact that Pol λ is widely conserved in the genome regardless of higher (*Oryza sativa* as monocots and *Arabidopsis* as dicots) and lower (*Chlamydomonas reinhardtii*, Uchiyama et al., 2009) plants, no other Pol X-family homolog genes have been identified in plant genomes. These observations strongly indicate that plants have only Pol λ among Pol X-family members.

The function of plant Pol λ has been studied using rice and *Arabidopsis* as model plants (Garcia-Diaz et al., 2000; Uchiyama et al., 2004; Amoroso et al., 2011; Roy et al., 2011). Like human Pol λ , rice Pol λ protein (OsPol λ) possesses DNA polymerase activity, weak TdT activity, and dRP lyase activity and this polymerase activity is activated by rice PCNA (proliferating cell nuclear antigen) protein. Expression analysis of OsPol λ transcripts suggests that it functions in DNA replication and/or repair in both meristematic and meiotic tissues (Uchiyama et al., 2004). The physical partner of plant Pol λ protein has been identified by yeast two-hybrid or pull-down assay. OsPol λ is able to bind with rice exonuclease-1, but not with rice XRCC1 (Furukawa et al., 2008; Uchiyama et al., 2008). Physical interaction of AtPol λ with AtPCNA2 stimulates its fidelity and efficiency in translesion synthesis (Amoroso et al., 2011). The role of *Arabidopsis* Pol λ (AtPol λ) in DNA repair has been recently reported. UV-B radiation induces the expression of AtPol λ , and three AtPol λ mutants (*atpol λ -1*, *atpol λ -2*, and *atpol λ -3*) exhibit sensitivity to UV-B and MMC (Roy et al., 2011, 2013). The AtPol λ mutants show increased sensitivity when exposed to high salinity and MMC treatment. AtPol λ is able to interact with AtLig4 and AtXRCC4 through its BRCT domain

and *atpol λ -2/atxrc4* and *atpol λ -2/atlig4* double mutants show delayed repair of salinity-induced DSBs (Roy et al., 2013). These findings suggest that plant Pol λ plays a role in various DNA repair pathways. Recent studies have indicated a role for Pol λ in the repair of transposable element excision sites, suggesting involvement in the repair of DSBs (Huefner et al., 2011).

We report here that *Arabidopsis* DNA polymerase λ (AtPol λ) is employed in DSB repair in response to clastogenic agents and is involved in T-DNA integration. In addition, our results imply that AtPol λ , in concert with AtLig1 and AtLig6, may participate in the Lig4-independent alternative NHEJ pathway.

Materials and Methods

Isolation of Mutants

We used the *Arabidopsis thaliana* parental strain ecotype Col (Columbia) in this study. The *atpol λ -1* (SALK_75391C) and *atku70-3* (SALK_123114C) mutants were identified using the Salk SIGnAL Web site (<http://signal.salk.edu/>), and their seeds were obtained from the ABRC. The *atlig4-2* line has been previously described (Friesner and Britt, 2003). The *atpol λ -1* and *atku70* homozygous mutants were identified by genotyping PCR with gene-specific primer sets. To analyze the *atpol λ -1* transcript, PCR with three different primer sets (pol λ -1AF + pol λ -1AR, pol λ -1BF + pol λ -1BR, and pol λ -1CF + pol λ -1CR) were performed with cDNA synthesized from *atpol λ -1* total RNA. The upstream region of the *atpol λ -1* transcript containing a RB border region was amplified by PCR with the pol λ -1BF + RBc1 primer set and the amplified PCR product was sequenced using the RBb1 primer. The downstream region containing a LB border was amplified with the LBb1 + pol λ -1CR primer set and the amplified product was sequenced using the LBb1 primer. The *atpol λ -1* line was crossed with either *atku70-3* or *atlig4-2* line to make double mutants. Homozygous F2 offsprings were screened by genotyping PCR with gene specific primer sets; pol λ -1BF, pol λ -1BR, ku70F, ku70R and T-DNA specific primer LBb1 for *atku70-3/atpol λ -1* double mutants and pol λ -1BF, pol λ -1BR, lig4-2B, lig4-2C, and LBb1 for *atpol λ -1/atlig4-2* double mutants. Primers sequences were shown in Supplemental Table S1.

Growth of *Arabidopsis*

Seeds in microcentrifuge tubes were surface-sterilized in an airtight container filled with chlorine gas for 2 h. Chlorine gas was produced by mixing 30 ml of bleach and 5 ml of hydrochloric acid. Following degassing of chlorine gas in a fume hood, sterilized seeds were imbibed in water for 2 days at 4°C. The sterilized seeds were then sown on solid 1 × Murashige and Skoog (MS, Sigma-Aldrich, St. Louis, MO, USA) with pH adjusted to 5.8 using 1N KOH containing 0.8% phytoagar (PlantMedia, Dublin, OH, USA) plates or on soil, and grown in a climate chamber under cool-white lamps at an intensity of 100–150 $\mu\text{mol m}^{-2} \text{s}^{-1}$ with a cycle of 16 h day/8 h night at 20°C.

DNA Damaging Treatments

For sensitivity tests to DNA damaging reagents such as methyl methanesulfonate (MMS, Fisher Scientific, Pittsburgh, PA, USA),

mitomycin C (MMC, Fisher), methyl viologen (MV, Fisher), and bleomycin (BLM, Bleocin inj., Euro Nippon Kayaku GmbH, Germany), chlorine gas-sterilized seeds were sown on solid MS-agar plates supplemented with each chemical. Seeds were grown for 7 days in a growth chamber under the normal growth condition as shown above. For the root-swollen assay, the 3 day-old seedlings were transferred to MS-agar plates containing 0.1 or 0.25 $\mu\text{g mL}^{-1}$ bleomycin and grown in a growth chamber under the normal condition. Ultraviolet B (UV-B) irradiation was performed according to Jiang et al. (1997). Sterilized seeds were planted on solid 1 x MS medium and grown with the plate oriented vertically for 3 days as described above. Seedlings were irradiated with UV-B in the absence of visible light using a UV-transilluminator (Fisher) filtered with 0.005 ml cellulose acetate membrane, with a flux rate of 5.5 mW cm^{-2} . The UV-B irradiated plates were rotated by 90°, then were cultivated for two more days under orange light to prevent photoreactivation. To investigate sensitivity of mutants to γ -irradiation, chlorine gas-sterilized seeds in water were γ -irradiated at 0, 40, 60, 80, and 100 Gy (6.43 Gy min $^{-1}$) from a ^{137}Cs source (Institute of Toxicology and Environmental Health, University of California, Davis). Gamma-irradiated seeds were sown on soil or MS-agar plates and grown in a growth chamber as described above.

Gamma-Irradiation and Detection of Cell Death in Irradiated *Arabidopsis* Plants

Observation of cell death in gamma-irradiated *Arabidopsis* roots were performed as described in Furukawa et al. (2010). Briefly, 5 day-old seedlings on MS-agar plates were γ -irradiated to a final dose of 20 Gy (6.43 Gy min $^{-1}$). Dead cells were visualized by staining of roots with 5 $\mu\text{g mL}^{-1}$ propidium iodide (PI, Sigma-Aldrich) and were observed using a Leica TSC SP2 confocal microscope.

Quantitative RT-PCR

Prior to treatment, 5 day-old seedlings were gently transferred from agar to MS liquid medium ($\pm 30 \mu\text{g mL}^{-1}$ bleomycin in 5 cm petri plates. The bleomycin treatment time for the expression analysis of DDR genes was 1.5 h, while that of DNA repair genes was 1 h. Treated seedlings were thoroughly rinsed in sterilized water and placed on solid MS plates. Seedlings were collected at each time point after wash. Mock seedlings were treated with liquid MS medium.

Total RNA was extracted from 100 mg of untreated, treated and recovered *Arabidopsis* seedlings collected using the RNeasy kit (Qiagen, Hilden, Germany) according to the manufacturer's protocol. The cDNAs from 1 μg of total RNA were synthesized using iScript cDNA Synthesis kit (Bio-Rad, Hercules, USA) with the help of oligo (dT) blend and random hexamer primers in a 20 μl reaction according to supplied protocol. One microliter of heat denatured cDNA reaction mixture was used for quantitative RT-PCR assay in 20 μl reaction volume using iTaq SYBR Green Supermix with ROX master mix (Bio-Rad) with the following primers at final concentration of 500 nM.

PCR amplification was carried with LightCycler 480 (Roche, Basel, Switzerland) or MX 3005P cycler (Stratagene, La Jolla, USA). For the reaction with LightCycler 480, an initial

denaturation step was for 95°C, 5 min and subsequent 45 cycles of PCR amplification proceeded as follows: denaturation 20 s at 95°C; annealing 20 s at 59°C; extension 30 s at 72°C. For the reaction with MX3005P cycler, an initial denaturation step was for 95°C, 3 min and subsequent 40 cycles of PCR amplification proceeded as follows: denaturation 15 s at 95°C; annealing 40 s at 55°C; extension 40 s at 72°C. After amplification, all fluorescence data were analyzed by the supplied software and normalized against *AtUBQ10* and *AtActin2*, or *AtROC3* reference gene transcripts. Sequences of primers used for qRT-PCR were listed in Supplemental Table S1.

Plant Transformation and Observation of Fluorescent Seeds

The pFLUAR101 fluorescent binary vector (Stuitje et al., 2003) was used to calculate transformation efficiency and transformation of *Arabidopsis* plants was performed by the *Agrobacterium*-mediated floral dip method. All siliques, flowers, and buds whose stage was later than stage 12 were trimmed from plants 1 day before transformation. The pFLAR101 vector was transformed into *Agrobacterium tumefaciens* strain GV3101 by electroporation. *Agrobacterium* transformant cells were cultured in liquid LB medium supplemented with kanamycin overnight at 30°C to reach stationary phase. Following centrifugation, the *Agrobacterium* cells were diluted to an OD600 of 1.8 with 5% sucrose solution. Silwet L-77 was added to a final concentration of 0.02% immediately before dipping. Second trimming was carried out 10 days after dipping to hold 12 siliques seeded from young buds that escaped from first trimming per brunch, and thereafter trimmed bolts were bagged in a glassine paper. Seeds were harvested 3 weeks after second trimming by collecting them in each glassine paper. Transformant seeds expressing fluorescence were screened by the Zeiss SteREO Discovery V12 microscope with a fluorescent filter for DsRED. The number of T_0 plants, harvested T_1 seeds, T_1 seeds expressing DsRED fluorescence, and each plant's transformation efficiency over three trials are described in Supplementary Table S3.

Statistical Analysis

Experimental results were examined using either *t*-test or One-Way ANOVA (analysis of variance) depending the number of samples. The *post-hoc* test (Tukey's HSD) was also used to find which means were significantly different. A *P*-value less than 0.05 (**P* < 0.05) and 0.01 (***P* < 0.01) was considered significant.

Results

Identification of the *Arabidopsis Pol λ* Mutant

We took a reverse genetic approach in order to examine the *in vivo* function of *AtPol λ* . The Salk T-DNA insertion collection was searched using the amino acid sequence of the rice Pol λ protein (GenBank Accession: BAD18976) as a template and the SALK_075391C line was found as a homozygous mutant carrying the T-DNA insertion in the *AtPol λ* gene (gene ID: At1g10520). Sequence analysis of the flanking regions of T-DNA revealed that the T-DNA was inserted in ninth intron of the *AtPol λ* gene

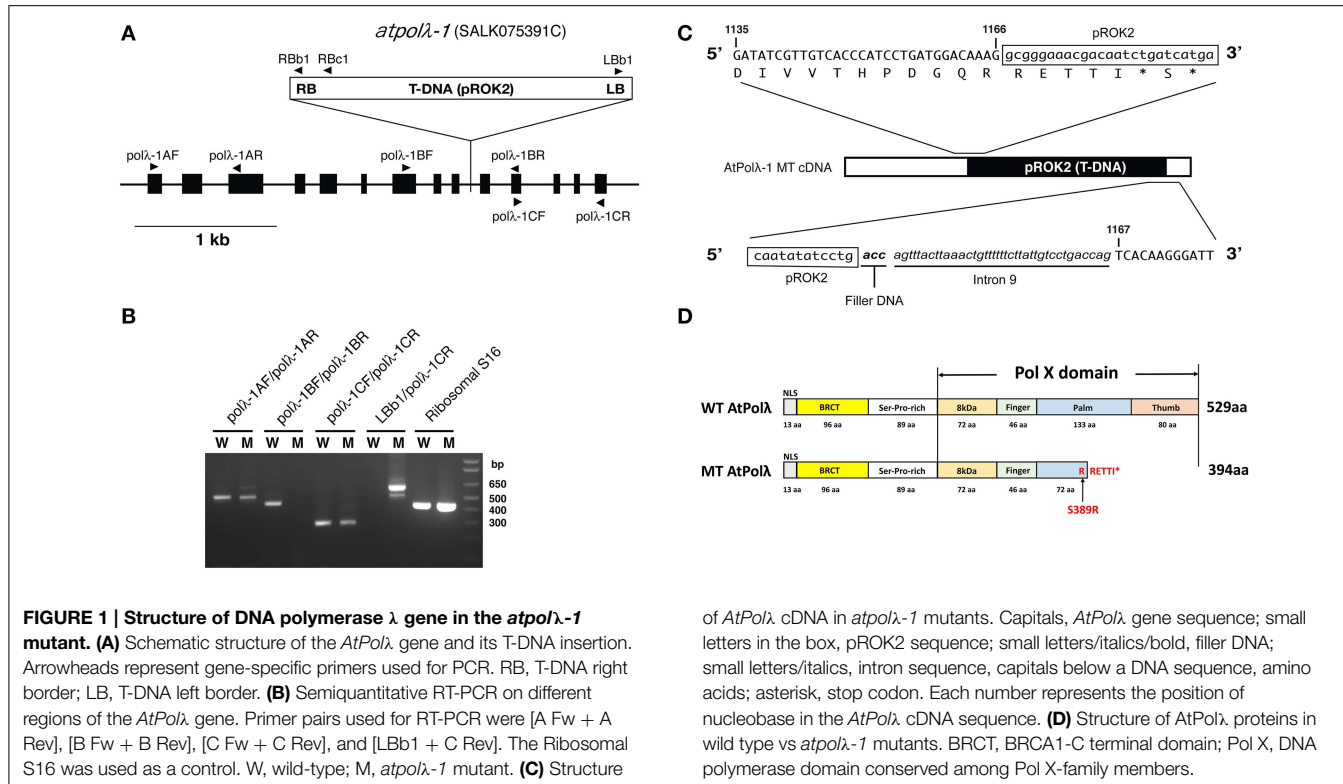


(Figure 1A). To date, three *Arabidopsis* *pol\lambda* mutants (*atpol\lambda-1*, *atpol\lambda-2*, and *atpol\lambda-3*) have been isolated from the SALK T-DNA insertion line (Roy et al., 2011). Because both the SALK_075391C mutant and the *atpol\lambda-1* mutant reported by Roy have the same allele, we designate this mutant as *atpol\lambda-1*. The effect of T-DNA insertion on transcription of *AtPol\lambda* in *atpol\lambda-1* mutants was investigated by RT-PCR. No amplification was obtained by RT-PCR with the *pol\lambda-1BF/pol\lambda-1BR* primer combination, while other two primer combinations aiming to amplify either upstream or downstream region of the T-DNA insertion site produced RT-PCR products, suggesting that the homozygous mutant does not express a wild-type transcript (Figure 1B), as previously observed (Roy et al., 2011). Sequencing of the *AtPol\lambda* transcript in the mutant revealed that this transcript contains partial sequences of T-DNA and intron 9 and that the joint between the T-DNA's right border and intron 9 includes filler DNA (Figure 1C). Thus, this insertion event generates a new stop codon inside of the pol X domain of the AtPol λ protein, which, if translated, would result in the C-terminal truncation (Figure 1D). This predicted mutant AtPol λ protein would contain a BRCT domain in the N-terminal region. The pol X domain plays a critical role in DNA synthesis, while the BRCT domain interacts with other DNA repair proteins (Leung and Glover, 2011). Thus, we regarded *atpol\lambda-1* as a loss-of-function mutant lacking in a DNA synthesis capability but still retaining an ability to interact with other proteins. The *atpol\lambda-1* mutants are fertile and develop normally, and did not show any obvious phenotypic differences compared to with wild-type Col plants (data not shown).

Sensitivity of the *atpol\lambda-1* mutant to Various DNA Damages

Previous studies have reported that mammalian *Pol\lambda* is involved in NHEJ and short-patch BER (Fan and Wu, 2004; Lee et al., 2004; Braithwaite et al., 2005a,b, 2010; Garcia-Diaz et al., 2005; Nick McElhinny et al., 2005). However, mice *Pol\lambda* deficient cells showed hypersensitivity to oxidative DNA damages but not to ionizing radiation (IR) (Kobayashi et al., 2002; Braithwaite et al., 2005b). This paradox might arise from the fact that mammals have four pol X family polymerases whose functions are partly overlapped. Higher plants are ideal organisms to study functions of *Pol\lambda* gene because *Pol\lambda* is the only member of the pol X-family in higher plants. In order to investigate its role in plant DNA repair, we first examined sensitivity of *atpol\lambda-1* mutants to various types of DNA damage by comparing root growth with or without DNA damaging treatments. The *atpol\lambda-1* mutants showed wild-type levels of sensitivity to methylmethane sulfonate (DNA alkylation), mitomycin C (cross-links), and methyl viologen (oxidative damage) when compared to wild-type plants (Figures 2A–C). UV radiation induces both cyclobutane pyrimidine dimers (CPDs) and 6-4 photoproducts (6-4 PPs) in DNA. These UV-B induced damages are repaired via blue-light-dependent photorepair catalyzed by photolyases and through light-independent nucleotide excision repair (NER). Growth of the light-treated *atpol\lambda-1* mutants after UV-B irradiation was similar to wild type, while the mutant grown under orange light showed a slightly increased, but not statistically significant, resistance at the dose of 6 kJ m^{-2} (Figures 2D,E). The *atpol\lambda-1* mutants exhibited a mild but statistically significant sensitivity to

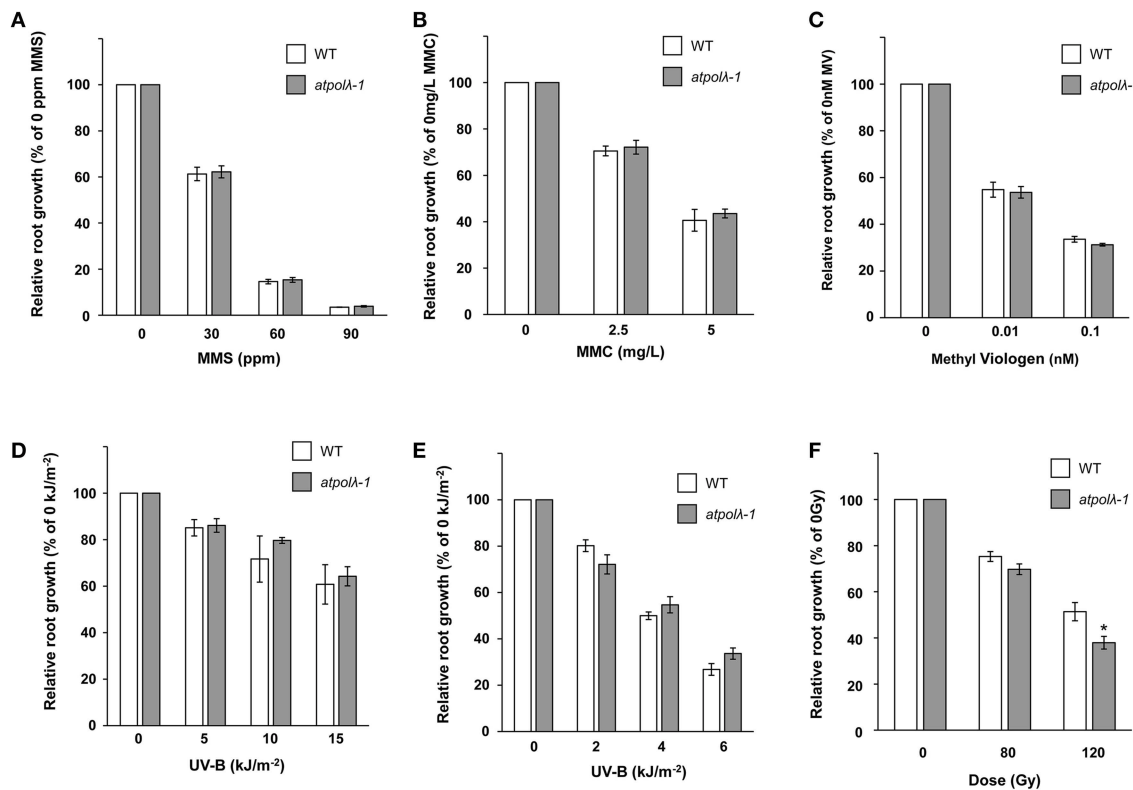


FIGURE 2 | Sensitivity of the *atpolλ-1* mutant to various DNA damages. Sterilized wild-type and *atpolλ-1* seeds were sown on solid MS agar containing methylmethane sulfate (**A**) mitomycin C (**B**), or methyl viologen (**C**), and root length was measured after 7 days. The 3 day-old wild-type and *atpolλ-1* seedlings grown on MS plates were exposed to UV-B, and then grown for two more days under normal light (**D**) or orange light (**E**). Sterilized wild-type and *atpolλ-1* seeds were γ -irradiated and sown on MS-agar plates. Root length was measured after 7 days (**F**).

Error bars represent the standard error of the mean of three independent experiments with 24–32 seedlings (average $n = 30$) for 2A, with 23–36 seedlings (average $n = 28$) for 2B, with 15–32 seedlings (average $n = 25$) for 2C, with 13–23 seedlings (average $n = 20$) for 2D, with 12–19 seedlings (average $n = 15$) for 2E, and with 18–48 seedlings (average $n = 28$) for 2F per line, per concentration, per replicate plates. The difference in relative root growth between wild type and *atpolλ-1* mutants was significant at 120 Gy in Panel (F) (* $p < 0.05$, t-test).

IR. Irradiation of γ -ray at a dose of 120 Gy inhibited root growth of *atpolλ-1* mutants more effectively than that of wild-type plants ($P < 0.05$, Figure 2F). Next, we tested the effects of γ -irradiation on formation of true leaves. The size of γ -irradiated seedlings was similar between wild-type and the *atpolλ-1* mutants (Figure 3), however the number of true leaves was decreased in the 100 Gy-irradiated *atpolλ-1* mutants ($P < 0.05$, Table 1). Gamma irradiation induces both DNA double strand breaks (DSBs) and oxidative damage. Given that we had not observed sensitivity to methyl viologen, this result suggests that AtPol λ may be involved in DSB repair.

Genetic Analysis of AtPol λ Function in DSB Repair

DSBs are repaired through both NHEJ and HR (homologous recombination) pathways. Ku heterodimer (Ku70 and Ku80) and Lig4 play a critical role in NHEJ in all eukaryotes, their homologs have been identified in *Arabidopsis* (Bundock et al., 2002; Riha et al., 2002; Tamura et al., 2002; Friesner and Britt, 2003), and *Arabidopsis* mutants defective in these genes are hypersensitive to IR. Our observations that the *atpolλ-1* mutants

showed sensitivity to IR imply that Pol λ may be involved in the repair of IR-induced breaks in *Arabidopsis*. To elucidate the relation between AtPol λ and these NHEJ core genes in DSB repair, we made double knockout mutants by crossing *atpolλ-1* with either *atku70-3*, a newly isolated T-DNA mutant from the SALK T-DNA insertion collection in the Col background (Figure S1), or the *atlig4-2* mutant (Friesner and Britt, 2003). IR did not influence true leaf formation of wild-type plants, while the number of true leaves was decreased in the 80 Gy- and 100 Gy-irradiated *atpolλ-1* mutants (Table 1). Inhibition of true leaf formation clearly appeared in four mutants except the *atpolλ-1* mutants irradiated as seeds at 40 Gy radiation (Table 1). At this dose, the *atlig4-2* mutant was able to produce at least one true leaf on average while irradiated *atpolλ-1/atlig4-2*, *atku70-3*, and *atku70-3/atpolλ-1* mutants produced less than one true leaf. Seven days after 60 Gy or higher dose γ -irradiation, formation of true leaves was severely inhibited in *atlig4-2* and *atku70-3*, as previously observed. The double *atpolλ-1/atlig4-2* and *atku70-3/atpolλ-1* mutants were not significantly more sensitive to IR than the *atku70-3* and *atlig4-2* mutants, although they tended to show slightly higher sensitivity than each single mutant (Table 1).

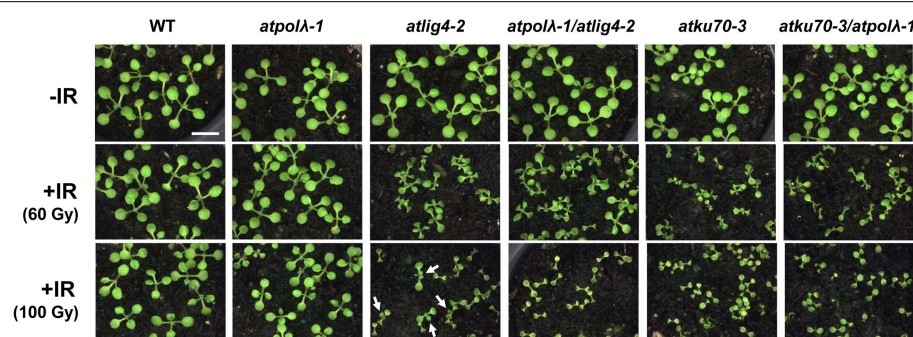


FIGURE 3 | Effects of γ -irradiation on true leaf formation in wild-type and mutant plants. Wild-type and mutant seeds were exposed to gamma-radiation at 0 (mock-irradiation) or 100 Gy, and sown on soil.

These images were captured 10 days after γ -irradiation. Bar = 1 mm. All pictures were taken at the same magnification. Arrows show true leaves with abnormal shapes produced after γ -irradiation.

TABLE 1 | The number of true leaves among DSB repair-deficient mutants 7 days after irradiation.

Genotype	The number of true leaves 7 days after irradiation (Average \pm SD)				
	Dose (Gy)				
	0	40	60	80	100
WT Col	2.00 \pm 0.00 (55)	1.98 \pm 0.03 (48)	2.00 \pm 0.00 (46)	2.00 \pm 0.00 (54)	1.97 \pm 0.04 (43)
atpolλ-1	2.00 \pm 0.00 (47)	1.96 \pm 0.06 (55)	1.98 \pm 0.02 (60)	1.79 \pm 0.05 (65)	1.46 \pm 0.08 (53)*
atlig4-2	2.00 \pm 0.00 (40)	1.31 \pm 0.14 (66)	0.29 \pm 0.06 (58)*	0.05 \pm 0.07 (70)*	0.02 \pm 0.03 (70)*
atpolλ-1/atlig4-2	2.00 \pm 0.00 (42)	0.83 \pm 0.08 (61)*	0.23 \pm 0.32 (73)	0.00 \pm 0.00 (65)**	0.08 \pm 0.11 (54)*
atku70-3	1.92 \pm 0.03 (49)	0.75 \pm 0.28 (55)	0.11 \pm 0.15 (47)*	0.00 \pm 0.00 (57)**	0.00 \pm 0.00 (67)*
atku70-3/atpolλ-1	2.00 \pm 0.00 (55)	0.57 \pm 0.17 (70)*	0.03 \pm 0.01 (63)**	0.03 \pm 0.04 (62)**	0.00 \pm 0.00 (58)*

Seeds were imbedded in cold water for 2 days before irradiation. The γ -ray irradiated seeds from a ^{137}Cs source were sown on soil and grown for 7 days in a growth chamber under cool-white lamps at an intensity of $100\text{--}150 \mu\text{mol m}^{-2} \text{s}^{-1}$ with a cycle of 16 h day/8 h night at 20°C . Values are mean \pm standard deviation (SD). Numbers in parenthesis indicate the total number of plants scored across all two replicates. *Significant at $P < 0.05$; **significant at $P < 0.01$.

Phenotypic difference in true leaf formation among mutants appeared 10 days after 100 Gy dose irradiation. The wild-type and *atpolλ-1* mutants produced normal true leaves and some *atlig4-2* mutants were able to produce one or two true leaves with abnormal shapes. However, other three mutants had only cotyledons (Figure 3).

Sensitivity of these mutants to DSBs was also analyzed by investigating the effects of bleomycin (BLM), a radiomimetic reagent that generates DSBs, on root growth (Figures 4A–D). Roots of mutants exposed to BLM exhibited morphological changes such as short root length, swollen root tips, and disorganized layers (Figures 4A,B). Root length of treated plants was similar to those of untreated control plants at $0.35 \mu\text{g mL}^{-1}$ of BLM. Inhibition of root growth became obvious at $0.7 \mu\text{g mL}^{-1}$ BLM. The *atpolλ-1* mutants were more sensitive than wild-type plants, but exhibited mild sensitivity when compared to other four mutants. Sensitivity of the *atpolλ-1/atlig4-2* double mutants was higher than each *atpolλ-1* and *atlig4-2* single mutant ($P < 0.05$). On the other hand, no significant difference was observed between *atku70-3* vs. *atku70-3/atpolλ-1* mutants. The $1.0 \mu\text{g mL}^{-1}$ BLM-treated wild type and mutant roots showed a similar inhibition tendency as seen in the $0.7 \mu\text{g mL}^{-1}$ BLM-treated plants although root length became shorter than

that of $0.7 \mu\text{g mL}^{-1}$ BLM treated-plants (Figure 4C). Next, we examined the timing when swollen root tips appeared after BLM treatment. At $0.1 \mu\text{g mL}^{-1}$ of BLM, swelling of root tips occurred 2 days after transplant in *atlig4-2*, *atpolλ-1/atlig4-2*, *atku70-3*, *atku70-3/atpolλ-1* mutants although the ratio of abnormal root tip shape differed among four mutants. The *atku70-3* mutants were more sensitive than *atlig4-2* mutants despite the fact that both genes play critical roles in the canonical NHEJ pathway. Both the *atpolλ-1* mutants and wild type root tips shape appeared to be normal until 3 days after transplant, but became abnormal in the *atpolλ-1* mutants 4 days and in the wild-type plants 7 days after transplant, respectively (Figure 4D). A similar sensitivity pattern among wild-type and mutants was observed even at $0.25 \mu\text{g mL}^{-1}$ BLM although the ratio of abnormal root tip in wild-type and the *atpolλ-1* mutants was higher (Table S2).

Taken together, the IR- and BLM-sensitivity indicate that AtPol λ has a function in DSB repair in plants. Ku complex and DNA ligase 4 have already been implicated in the canonical NHEJ pathway. It is entirely possible that AtPol λ also participates in this Ku/Lig4 pathway of NHEJ, but if so, it is not essential for every repair event catalyzed by these enzymes, as the *atpolλ-1* mutant clearly does not share the hypersensitivity of *atku70-3* and *atlig4-2* to higher doses of BLM and IR.

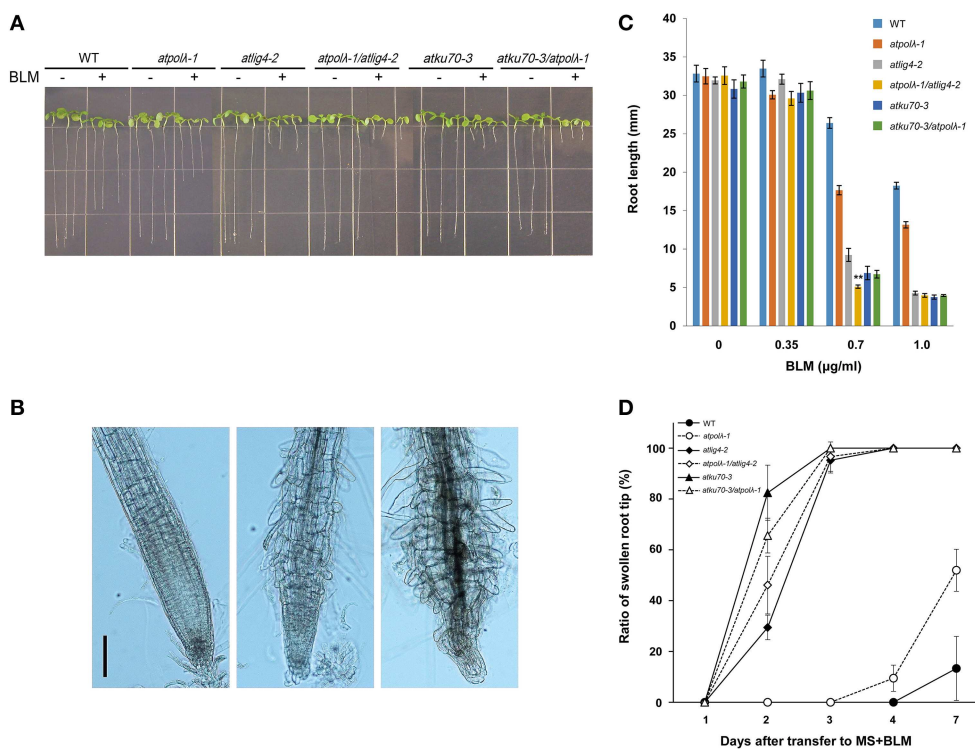


FIGURE 4 | Effects of bleomycin-induced DSBs on root growth. (A)

Root length of 1 week-old wild-type and mutant seedlings grown on MS agar containing $0.7 \mu\text{g mL}^{-1}$ bleomycin (BLM). **(B)** Morphology of BLM-treated mutant primary root tips. The 3 day-old seedlings were transferred to MS agar plates supplemented without (left panel, mock treatment) or with $0.1 \mu\text{g mL}^{-1}$ bleomycin (center and right panels). Images were captured 1 day after transfer. Abnormal root tips displayed disorganized root tip structure; randomly swelling cells and emerging of rounded root hairs above the meristem. Bar = $100 \mu\text{m}$. **(C)** Root length of 1 week-old wild-type and

mutant seedlings grown on MS plates containing 0, 0.35, 0.7, and $1.0 \mu\text{g mL}^{-1}$ BLM. Error bar represents the standard error of the mean of three independent experiments with 17–36 seedlings (average $n = 29$) per line, per concentration, per replicate plates. **Significantly different from the value of the *atpol λ -1* and *atlig4-2* mutants ($**P < 0.01$). **(D)** Ratio of abnormal root tips after transplant to MS agar plates containing $0.1 \mu\text{g mL}^{-1}$ BLM. Error bar represents the standard error of the mean of three independent experiments with 20–23 seedlings (average $n = 21$) per line, per concentration, per replicate plates.

DNA Damage Response in Mutants

Previous studies demonstrate that DSBs trigger two robust responses in plants: programmed cell death (PCD) and the ATM/ATR/SOG1-dependent expression of an enormous number of genes (Culligan et al., 2004, 2006; Fulcher and Sablowski, 2009; Yoshiyama et al., 2009; Furukawa et al., 2010). This PCD requires ATM or ATR, and the SOG1 transcription factor and is largely restricted to a specific subset of the cells of the root tip meristem—the precursors of the stele. It is possible that PCD occurs with higher frequency in γ -irradiated mutant root tips that are deficient in DNA repair. To test this hypothesis, we examined post-irradiation (20 Gy and 80 Gy) PCD events in 5 day-old seedlings of mutant and wild-type plants (Figure 5 and Figure S2). In 20 Gy-irradiated wild-type plants, PCD first occurred sometime between 8 and 24 h after radiation and the frequency of dead cells was decreasing by 72 h after radiation (Figure S2). The 20 Gy-irradiated *atpol λ -1* mutants showed a similar cell death pattern to wild-type plants, with perhaps a slight enhancement in the frequency and persistence of dead cells. In contrast, in the other four mutants dead cells were observed by 8 h after 20 Gy radiation, the PI-staining was more persistent.

Moreover, initiation of swelling of root tips was observed in the *atku70-3* mutants at 72 h after radiation (Figure S2). Gamma-irradiation at 80 Gy induced more PCD events in both wild-type and mutants at 8 h after radiation (Figure 5). Enlargement of root tip cells occurred in four mutants (*atlig4-2*, *atpol λ -1/atlig4-2*, *atku70-3*, and *atku70-3/atpol λ -1*), while wild-type and the *atpol λ -1* root tips displayed slightly swollen but still kept normal root tip shape. These results suggest that AtPol λ is involved in resistance to IR-induced meristematic death, but is not as critical to this process as AtKu70 or AtLig4.

Next, we performed quantitative RT-PCR (qRT-PCR) to investigate whether lack of NHEJ influences transcriptional responses to IR (Figures 6A–E). Expression of three cell cycle marker genes and two cell cycle checkpoint genes was measured up to 24 h after $30 \mu\text{g mL}^{-1}$ BLM treatment. *AtCDKB2;1* (Figure 6A, G2 phase marker), *AtKNOLLE* (Figure 6B, M phase marker), and *AtHistone4* (Figure 6C, S phase marker) were selected as each phase-specific marker gene. Our qRT-PCR analysis showed that expressions of all marker genes were significantly downregulated at 1.5 h after BLM treatment and had not recovered by 24 h after treatment ($P < 0.05$ or $P <$

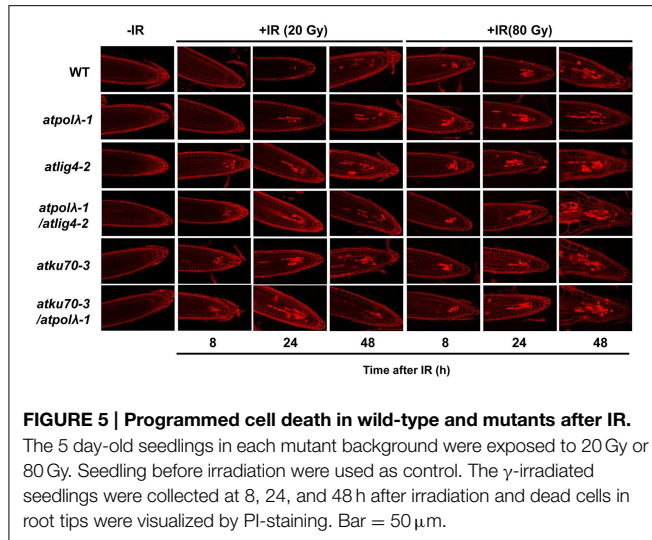


FIGURE 5 | Programmed cell death in wild-type and mutants after IR.

The 5 day-old seedlings in each mutant background were exposed to 20 Gy or 80 Gy. Seedling before irradiation were used as control. The γ -irradiated seedlings were collected at 8, 24, and 48 h after irradiation and dead cells in root tips were visualized by PI-staining. Bar = 50 μ m.

0.01). We used *AtCYCB1;1* and *AtWee1* as a marker of cell cycle checkpoint genes (Figures 6D,E). *AtCYCB1;1* is a plant-specific B-type cyclin playing an unique role in DDR pathway, and DSB-inducible accumulation of *AtCYCB1;1* transcripts reflects G2/M cell cycle arrest (Culligan et al., 2006). *AtWee1* is a protein kinase controlling the progression of plant cell cycle in an ATM/ATR-dependent manner; lack of *AtWee1* causes extension of S-phase as well as more PCD events in response to replication stresses (Sorrell et al., 2002; De Schutter et al., 2007; Cools et al., 2011). Rapid upregulation of *AtCYCB1;1* occurred in all genotypes at 1.5 h after BLM treatment although the degree of expression level varied among mutants. The induction of *AtCYCB1;1* expression continued at 8 h after treatment, and DSB-inducible upregulation of *AtCYCB1;1* observed at 1.5 and 8 h after treatment in wild-type and all mutants was significant ($P < 0.05$ or $P < 0.01$). At 24 h after treatment the expression of *AtCYCB1;1* in wild-type and *atpolλ-1* mutants was recovered to the untreated level, whereas it still remained significantly high level in other five mutants ($P < 0.05$ in *atku70-3* and *atku70-3/atpolλ-1* mutants and $P < 0.01$ in *atlig4-2*, *atpolλ-1/atlig4-2*, and *atku70-3/atpolλ-1/atlig4-2* mutants). As shown in Figure 6E, an induced expression of *AtWee1* occurred in wild-type and the *atpolλ-1/atlig4-2/atku70* triple mutant at 1.5 h after treatment ($P < 0.01$). At later time point *AtWee1* expression gradually decreased. The *AtWee1* expression in wild-type recovered to the untreated level, but high expression of *AtWee1* continued in the triple mutant at 8 h after treatment ($P < 0.05$). Except the triple mutant, the *AtWee1* expression was significantly decreased in BLM treated plants at 24 h after treatment ($P < 0.05$ or $P < 0.01$). Taken together, these expression data suggest that DSB-inducible G2/M cell cycle arrest equally occurs in both wild-type and six mutants and that DSBs may prolong the duration of S-phase of the *atku70-3/atpolλ-1/atlig4-2* triple mutant.

It is possible that lack of *AtPol λ* and other NHEJ-involved genes may induce expression of substitute DNA repair genes to compensate for lost functions. To test this hypothesis, expressions of *Arabidopsis BRCA1* (as a positive control for induction), *Ku80*, and three DNA ligases (*Lig1*, *Lig4*, and *Lig6*) were measured by qRT-PCR immediately after BLM

treatment ($t = 0$) and after 20 and 60 min of repair recovery (Figures 7A–C). *BRCA1*, breast cancer susceptibility gene 1, is a signal transducer largely linked to the ATM pathway required for the efficient repair of DSBs by homologous recombination in somatic cells of *A. thaliana* with strongly induced transcription by IR (Lafarge and Montane, 2003). DSBs generated by BLM treatment strongly upregulated *AtBRCA1* expression in wild-type and mutants (Figure 7A). *AtBRCA1* expression in the *atpolλ-1* mutant was dramatically enhanced from 10- at $t = 0$ to 33-fold after 60 min of repair, and even higher induction from 10- to 40-fold was observed in the *atpolλ-1/atlig4-2* double mutants. In all other lines, the expression of *AtBRCA1* during repair period was only slightly higher than that of wild-type and ranged from 10- to 20-fold. In contrast to *AtBRCA1*, the expression of *AtKu80* was not significantly induced after BLM treatment. *AtKu80* expression resulted in 2- to 6-fold increase compared to untreated controls during the recovery period (Figure 7B). Except the *atku70-3/atpolλ-1/atlig4-2* mutant *AtKu80* expression tended to increase as the recovery time went. *AtKu80* expression was significantly induced in wild-type and the *atku70-3/atpolλ-1* mutants at 20 min after treatment ($P < 0.05$ or $P < 0.01$, Figure 7B). Figure 7C showed DSB-induced upregulation of three DNA ligase genes in wild-type and mutants. In wild-type, all assayed ligases were slightly induced (2- to 3-fold) compared to untreated control, and they showed a similar expression pattern during repair period. At 20 and 60 min after BLM treatment *AtLig1* and *AtLig4* expressions were different from expressions at 0 min after treatment ($P < 0.05$). An induction pattern of ligase genes among all mutant lines differed from wild-type. In the *atpolλ-1* mutant *AtLig1* and *AtLig6* expressions were induced during the repair period, but no induction of *AtLig4* occurred. The expression of *AtLIG1* increased from 2.2- to 5.1-fold during the repair period, and *AtLig6* expression showed 2.5-fold increase at 60 min after treatment. Compared to wild-type, *AtLig1* expression was strongly induced in mutants whose genetic background was *atlig4-2* (*atlig4-2*, *atpolλ-1/atlig4-2*, and *atku70-3/atpolλ-1/atlig4-2*). The strong induction of *AtLig1* expression was also observed in the *atpolλ-1/atku70-3* mutants. It reached up to 15-fold increase at 0 min after treatment and then constantly kept a high level of expression even 60 min after treatment. Interestingly, the expression of *AtLig6* was gradually increased 3- to 10-fold in all *AtLig4* mutated lines during recovery period ($P < 0.05$ or $P < 0.01$), while *AtLig6* expression was not significantly induced in the *atku70-3/atpolλ-1* mutant. In the *atku70-3* mutants, only *AtLig1* expression was slightly induced after treatment although its expression level was lower than wild-type.

Lack of AtPol λ and Other NHEJ-Involved Genes Affects Transformation Efficiency

It has been reported that DSB repair plays a critical role in integration of transgenes in plants (Friesner and Britt, 2003; Li et al., 2005; Mestiri et al., 2014). In order to uncover functions of these DSB repair genes in this process, we investigated their transformation efficiency using the pFLUAR101 reporter construct. This pFLUAR101 reporter construct contains both the promoter for the seed storage protein napin driving the DsRED gene. Transformed embryos display red fluorescence due

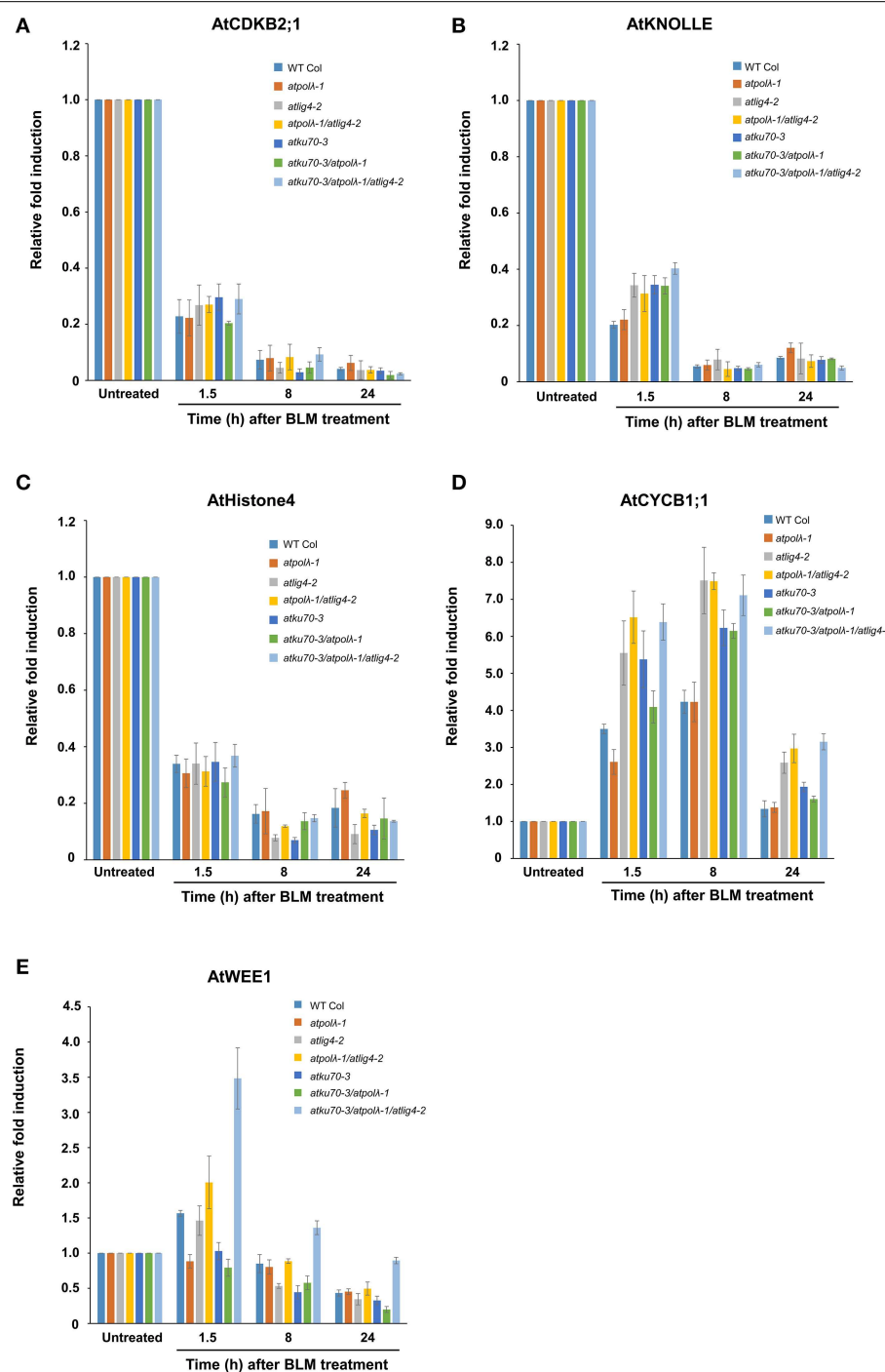


FIGURE 6 | Transcriptional responses of cell cycle-related genes in wild-type and mutants in response to DSBs. Expression levels of (A) *AtCDKB2;1*, (B) *AtKNOLLE*, (C) *AtHistone H4*, (D) *AtCYCB1;1*, and (E) *AtWEE1* after BLM treatment. Five day-old wild-type and mutant seedlings grown on MS agar plates were embedded in water

to accumulation of the DsRED protein. This enables us to identify transformed seeds using a fluorescent microscope (Stuitje et al., 2003). The pFLUAR101 construct was transformed into wild-type and five mutants (*atpolλ-1*, *atlig4-2*, *atpolλ-1/atlig4-2*,

containing 30 μ g mL $^{-1}$ BLM for 1.5 h. Followed by rinse with sterilized water, BLM-treated seedlings were transferred onto MS agar plates before collection at each time point after treatment. All values were normalized to the expression level of control genes. Error bars indicate the standard error of the mean.

atku70-3, and *atku70-3/atpolλ-1*) by *Agrobacterium*-mediated floral dip, and then the transformation efficiency of each plant line was calculated based on the number of T₁ DsRED seeds (Figure 8 and Table S3). All DSB-deficient mutants tended to

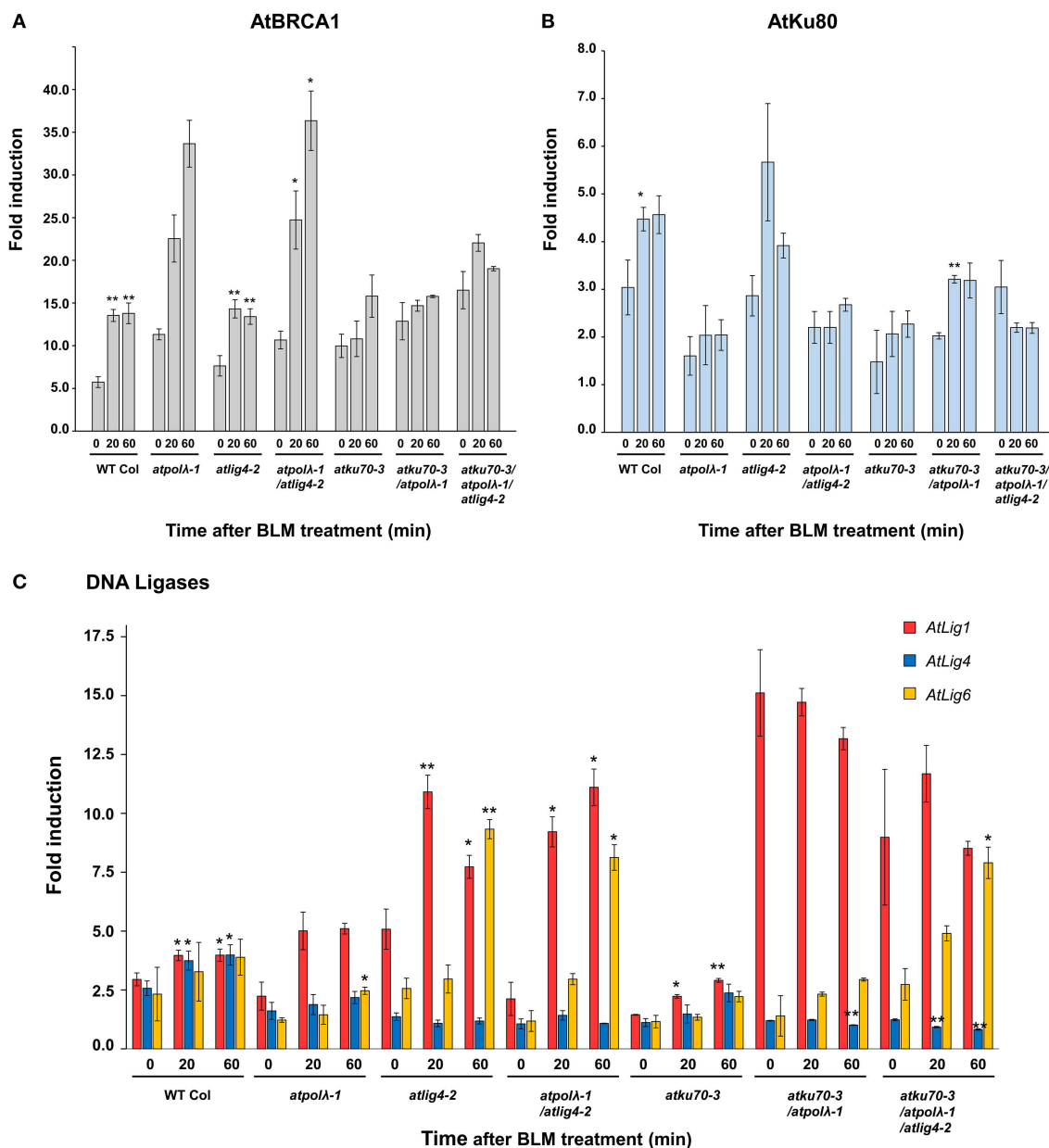


FIGURE 7 | Transcriptional responses of DSB repair genes in wild-type and mutants in response to DSBs. Expression levels of (A) *AtBRCA1*, (B) *AtKu80*, and (C) DNA ligases (*AtLig1*, *AtLig4*, and *AtLig6*) after BLM treatment. Five day-old wild-type and mutant seedlings grown on MS agar plates were embedded in water containing 30 μ g mL $^{-1}$ BLM for 1 h. Followed by rinse with sterilized

water, BLM-treated seedlings were transferred onto MS agar plates before collection at each time point after treatment. All values were normalized to the expression level of control genes, and then relative expressions compared to untreated controls were calculated. Error bars indicate the standard error of the mean. *Significant at $P < 0.05$; **significant at $P < 0.01$.

show a lower transformation efficiency than wild-type plants in each trial despite the fact that it was not statistically significant due to a wide range of transformation efficiencies over three trials (Figure 8). As shown in Table S3, the *atpolλ-1* mutants showed a lower transformation efficiency than wild-type, and tended to exhibit lower efficiency than *atlig4-2* and *atku70-3* mutants. The reduction of transformation efficiency of the *atpolλ-1* was 1.5- to 8-fold compared to wild-type, 1.7- to 3.0-fold for *atlig4-2*, and

1.3- to 3.0-fold for *atku70-3*, respectively. The *atpolλ-1/atlig4-2* double mutants showed a lower transformation efficiency than *atpolλ-1* or *atlig4-2* single mutant and its transformation efficiency in each trial was the lowest among five mutants (Table S3). In contrast, no significant difference was observed among *atku70-3*, *atpolλ-1*, and *atku70-3/atpolλ-1* mutants (Figure 8). These results suggest that *AtPol λ* may play a more important role in transgene integration than either *AtLig4* or *AtKu70*.

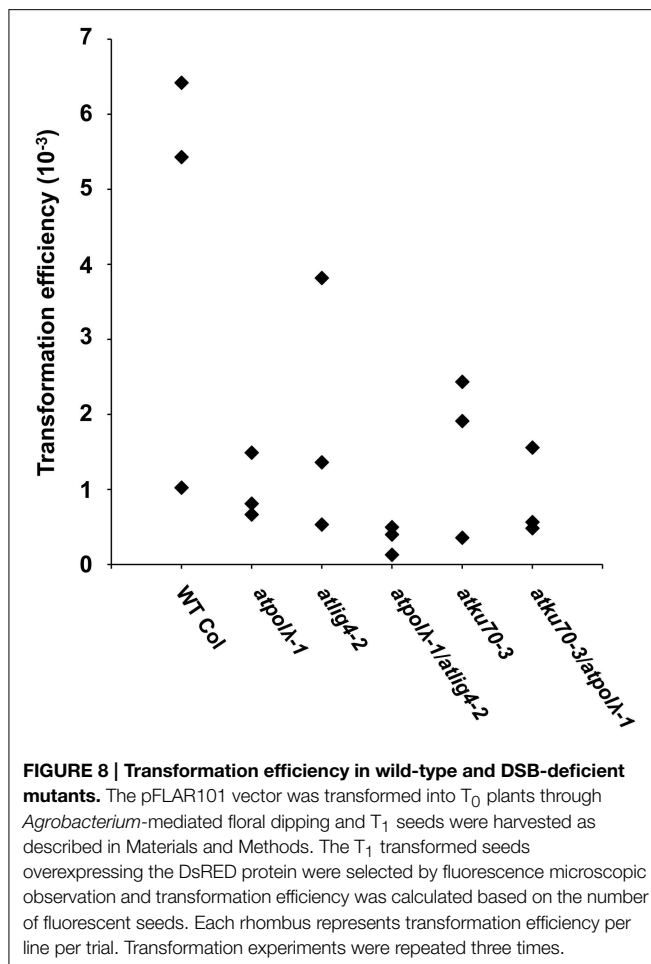


FIGURE 8 | Transformation efficiency in wild-type and DSB-deficient mutants.

The pFLAR101 vector was transformed into T₀ plants through *Agrobacterium*-mediated floral dipping and T₁ seeds were harvested as described in Materials and Methods. The T₁ transformed seeds overexpressing the DsRED protein were selected by fluorescence microscopic observation and transformation efficiency was calculated based on the number of fluorescent seeds. Each rhombus represents transformation efficiency per line per trial. Transformation experiments were repeated three times.

Discussion

Despite the fact that only Pol λ is encoded in plant genomes among Pol-X family members, its biological function is poorly understood. In this paper, we took a reverse genetic approach to study Pol λ functions in various plant DNA repair pathways. The expression of Pol λ is induced by MMS treatment, MMC treatment, and UV-B radiation, suggesting that plant Pol λ may participate in repair of alkylated DNA, DNA crosslink, and UV-damaged DNA (Uchiyama et al., 2004; Roy et al., 2011, 2013). However, the *atpolλ-1* mutant exhibits sensitivity to DSBs caused by IR or bleomycin treatment, but does not display hypersensitivity to other DNA damages such as DNA alkylation (MMS), crosslink (MMC), oxidative damages (MV), and UV damages such as CPDs and 6-4 PPs (UV-B). Analysis of the *AtPol λ* transcript in the *atpolλ-1* mutant reveals that the transcriptional error occurs in this mutant, which results in producing the truncated Pol λ protein (Figure 1D). The intact AtPol λ protein consists of two major domains; N-terminus and Pol β -like C-terminus (Roy et al., 2011). The N-terminus, which is comprised of 198 amino acid residues (aa), includes a nuclear localization signal (13 aa), a BRCT domain (96 aa), and a Ser-Pro-rich domain (91 aa). The C-terminus domain is occupied by the Pol X domain (329 aa) consisting of 8 kDa domain as

well as fingers, palm and the thumb subdomains. Insertion of T-DNA of the *atpolλ-1* occurs in an intron within the palm subdomain of the Pol X domain. The loss of half of the palm, the entire thumb, and several catalytic residues (the equivalent of the human Pol λ amino acids R488 and E529, as described in Cisneros et al. (2008) and aligned in Roy et al., 2013) indicates that this truncated protein lacks any significant DNA polymerase activity. In contrast, the mutant protein still contains the intact 8 kDa and BRCT domains and might possess dRP lyase activity if the mutant protein is stable. In an earlier study (Roy et al., 2013), Roy et al. analyzed three different alleles (including *atpolλ-1*), and found no sensitivity to MMS. The *atpolλ-2* and *atpolλ-3* mutants carry insertions in the 5' UTR and the last exon, respectively, and thus might conceivably express a functional protein, however, the authors were unable to detect Pol λ via Western blot and therefore the level of this protein of wild-type size in these two mutants, must be quite low. Thus, we propose two possibilities to explain the lack of sensitivity of the *atpolλ-1* mutants to MMS treatment; (1) the truncated Pol λ protein may play a role in repair of alkylated and oxidative DNA damages via preserved dRP lyase activity (though this would require that *atpolλ-2* and *atpolλ-3* are also expressing a functional protein, though none was detected via Western blot). (2) Plants prefer to use a *Pol λ*-independent repair pathway such as long-patch BER to repair AP sites generated by base repair glycosylases (we regard this as the simpler and more likely hypothesis).

In our hands the *atpolλ-1* mutant did not display UV-B sensitivity when irradiated as a seedling and then cultivated under non-photoreactivating light. We used the *Arabidopsis XPF* (*atxpf-2*) mutant as a control in our root-bending assay under dark condition because it was hypersensitive to UV-B radiation due to lack of NER (Jiang et al., 1997; Fidantsef et al., 2000). The relative root growth of UV-B irradiated *atxpf-2* mutants was decreased to 24% at a dose of 2 kJ m⁻² and to 6% at 4 kJ m⁻² compared to unirradiated control plants (unpublished data), which indicates that our UV-B treatment produces UV damages that sufficiently inhibit root growth of NER-deficient mutants. In contrast to our observation, the *atpolλ-1* mutant showed hypersensitivity when seeds were exposed to UV-B and seedlings germinated from UV-B radiated seeds had slower repair rates for both CPDs and DSBs (Roy et al., 2011). The 5 day-old *atpolλ-1* mutant seedlings were radiated with UV-B for a short period (ex. 18 s radiation for 1 kJ m⁻²) in our experiment, whereas mutant seeds are irradiated for 60 min at the dose of 5.4 kJ m⁻² before sowing in Roy's experiment. About sensitivity to MMC, the sensitive phenotype of the *atpolλ-1* mutants is observed only when mutant plants are grown on MS agar plates supplemented with 10 μ g ml⁻¹ MMC, and the phenotypic difference between wild-type plants and the *atpolλ-1* mutants is not statistically significant at 3 and 5 μ g ml⁻¹ MMC (Roy et al., 2013). Taken these findings together, it is possible that the effect of Pol λ on repair of UV-B induced damage or DNA crosslink is too subtle to detect in our growth assay and that bombardment of high-dose UV radiation for a long period or MMC treatment of mutant plants at higher concentration may be necessary to cause hypersensitive phenotype. Besides CPDs and 6-4 PPs, it is also known that UV-B radiation often

induces reactive oxygen species that cause oxidative damages to DNA. Accumulation of unrepaired single strand breaks is often converted to DSBs if positions of breaks in the genome are very close. Interstrand crosslinks (ICLs) generated by MMC at replication forks stall the process of DNA replication, and then the collapse of ICL-stalled replication forks provokes DSBs. In this paper we have demonstrated by IR and radiomimetic chemical treatment that the *atpol λ -1* mutants display mild sensitivity to DSBs. Therefore, it could be also possible that hypersensitivity of *atpol λ -1* mutants to UV-B and MMC may reflect sensitivity to DSBs as well as direct UV damages (CPDs and 6-4 PPs) or ICLs.

As in animals, DSBs are thought to be mainly repaired by Ku- and Lig4-dependent NHEJ in plants (West et al., 2000, 2002; Bundock et al., 2002; Riha et al., 2002; Friesner and Britt, 2003; Gallego et al., 2003). Both *atku70* and *atlig4-2* mutants show hypersensitivity to DSBs generated by gamma-irradiation or BLM treatment. Unlike these NHEJ-deficient mutants, the sensitivity of the *atpol λ -1* mutants is only observed when mutants are gamma-irradiated at high dose (100 Gy and 120 Gy) or treated with a high concentration of BLM (0.7 μ g mL $^{-1}$ and 1.0 μ g mL $^{-1}$). Moreover, the fraction of root tips with disorganized structure in the *atpol λ -1* mutants is lower than that of *atku70* or *atlig4-2* mutant. The observation that the *atpol λ -1* mutant exhibits a mild sensitivity to IR suggests that AtPol λ participates in DSB repair, just as it participates in DSB repair in mammals. Results using double mutants provide additional hints to consider Pol λ functions in NHEJ. The *atpol λ -1/atlig4-2* double mutant always shows higher sensitivity than each single mutant, while the sensitivity of the *atku70/atpol λ -1* double displays similar sensitivity to the *atku70* mutant. In canonical NHEJ, broken ends of DNA strands are first shielded by the Ku70/Ku80 heterodimer and then the Lig4/XRCC4 complex ligates guarded DNA ends. Although AtKu70 and AtLig4 functions in the same NHEJ pathway, we found that the *atku70* mutant is more sensitive to DSBs than the *atlig4-2* mutant. Taken together, these results suggest that plants may have two pathways for DSB repair, AtLig4-dependent canonical (C-NHEJ) and AtLig4-independent alternative (A-NHEJ), pathways downstream of the DNA protection process catalyzed by AtKu70/AtKu80. Our results also suggest that AtPol λ is employed in A-NHEJ. Recent studies on mammalian DSB repair have shown that microhomology-mediated end joining (MMEJ) is one of backup NHEJ pathways in which Ku80 and poly(ADP-ribose) polymerases (PARP) play essential roles. *In vitro* studies show that human DNA polymerase λ and Lig1, but not Lig4, are required for sufficient MMEJ reaction (Liang et al., 2008; Crespan et al., 2012). Similar to mammals, a study using RNAi-silenced *AtLig1* demonstrates that *AtLig1* plays an important role in DSB repair as well as single strand break repair (Waterworth et al., 2009). In addition, our qRT-PCR analysis reveals that DSBs induce expression of *AtLig1* and *AtLig6* in mutants lacking *AtLig4*. Given that Ku80 and PARP-dependent MMEJ is conserved in plants (Jia et al., 2013), our data are consistent with a model in which AtPol λ functions in some A-NHEJ pathway, (possibly MMEJ), in concert with *AtLig1* and/or *AtLig6*.

Recent studies have demonstrated that plants have a robust DNA damage response to DSBs (Culligan et al., 2006; Ricaud et al., 2007; Yoshiyama et al., 2009; Furukawa et al., 2010; Missrian et al., 2014). To investigate the role of AtPol λ in DDR, we investigated both the frequency of PCD and the transcriptional response after BLM treatment. Although the number of dead cells is slightly increased in the *atpol λ -1* mutant compared to wild-type, its influence on frequency of PCD is smaller than NHEJ-defective mutants. The DSB-inducible transcriptional response appears to be similar between wild-type and mutants. BLM treatment causes upregulation of *AtCYCB1;1* expression, while it downregulates expressions of other cell cycle specific marker genes, *AtCDKB2;1*, *AtKNOLLE*, and *AtHistone H4*. These results suggest that cell cycle is arrested at G2/M in BLM-treated root tip cells although there is no direct evidence. The expression of *AtCYCB1;1* remains high level in *atlig4-2* mutants at 24 h after treatment. Given that the high expression of *AtCYCB1;1* is associated with the existence of unrepaired DSBs, this result may reflect that A-NHEJ requires more time to repair DSBs than the AtLig4-dependent pathway does. Moreover, *AtWee1* expression is highly induced only in the *atku70/atpol λ -1/atlig4-2* triple mutant and this high expression continues at 24 h after treatment. It has been reported that *AtWee1* controls many aspects of response to replication blocks (Cools et al., 2011). This result raises the possibility that response to DNA damage of the triple mutant is enhanced because its DSB repair activity via both C-NHEJ and A-NHEJ is completely lost.

It has been reported that NHEJ plays an important role in the integration of a transgene. The efficiency of T-DNA insertion to the plant genome is decreased in *atku80* and *atlig4* mutants though this effect is not consistently observed (Friesner and Britt, 2003; Li et al., 2005). Given that AtPol λ functions in A-NHEJ, the efficiency of T-DNA insertion in the *atpol λ -1* mutant is expected to be decreased as in NHEJ-defective mutants. Decreased T-DNA insertion efficiency is observed in the *atpol λ -1* mutant as anticipated. However, its frequency tends to be lower than that of *atku70* or *atlig4-2* single mutant. The *atpol λ -1/atlig4-2* double mutant shows the lowest transformation efficiency among six tested plant lines. These results suggest that T-DNAs may insert via either C-NHEJ or A-NHEJ.

In summary, the results and discussion presented here provide new insights into functions of AtPol λ in plant DSB repair. Although AtPol λ is suggested to participate in A-NHEJ, much remains unclear about its molecular machinery. Further studies would be required to clarify the role of AtPol λ in A-NHEJ.

Acknowledgments

Experimental design and analysis by TF and AB, preparation of *Arabidopsis* T-DNA insertion mutants, and microscopic observations by TF, DNA damaging treatments and irradiations performed by TF and Phillip A. Conklin, qRT-PCR analysis performed by TF and KA, text and figures prepared by TF, KA, and AB. Work in the Britt lab was funded by DOE Office of Basic Energy Sciences grant no. DE-FG02-05ER15668 and by the National Research Initiative of the USDA Cooperative State Research, Education and Extension Service, grant no.

2004-35301-14740. Dr. Furukawa was also supported by a Postdoctoral Fellowship for Research Abroad from the Japan Society for the Promotion of Science (JSPS). Work in Angelis Lab was supported by Czech Science Foundation grant no. 13-06595S.

Supplementary Material

The Supplementary Material for this article can be found online at: <http://journal.frontiersin.org/article/10.3389/fpls.2015.00357/abstract>

References

- Amoroso, A., Concia, L., Maggio, C., Raynaud, C., Bergounioux, C., Crespan, E., et al. (2011). Oxidative DNA damage bypass in *Arabidopsis thaliana* requires DNA polymerase λ and proliferating cell nuclear antigen 2. *Plant Cell* 23, 806–822. doi: 10.1105/tpc.110.081455
- Anderson, H. J., Vonarx, E. J., Pastushok, L., Nakagawa, M., Katafuchi, A., Gruz, P., et al. (2008). *Arabidopsis thaliana* Y-family DNA polymerase eta catalyses translesion synthesis and interacts functionally with PCNA2. *Plant J.* 55, 895–908. doi: 10.1111/j.1365-313X.2008.03562.x
- Braithwaite, E. K., Kedar, P. S., Lan, L., Polosina, Y. Y., Asagoshi, K., Poltoratsky, V. P., et al. (2005b). DNA polymerase lambda protects mouse fibroblasts against oxidative DNA damage and is recruited to sites of DNA damage/repair. *J. Biol. Chem.* 280, 31641–31647. doi: 10.1074/jbc.C500256200
- Braithwaite, E. K., Kedar, P. S., Stumpo, D. J., Bertocci, B., Freedman, J. H., Samson, L. D., et al. (2010). DNA polymerases beta and lambda mediate overlapping and independent roles in base excision repair in mouse embryonic fibroblasts. *PLoS ONE* 5:e12229. doi: 10.1371/journal.pone.0012229
- Braithwaite, E. K., Prasad, R., Shock, D. D., Hou, E. W., Beard, W. A., and Wilson, S. H. (2005a). DNA polymerase lambda mediates a back-up base excision repair activity in extracts of mouse embryonic fibroblasts. *J. Biol. Chem.* 280, 18469–18475. doi: 10.1074/jbc.M411864200
- Bundock, P., van Attikum, H., and Hooykaas, P. (2002). Increased telomere length and hypersensitivity to DNA damaging agents in an *Arabidopsis* KU70 mutant. *Nucleic Acids Res.* 30, 3395–3400. doi: 10.1093/nar/gkf445
- Capp, J. P., Boudsocq, F., Bertrand, P., Laroche-Clary, A., Pourquier, P., Lopez, B. S., et al. (2006). The DNA polymerase lambda is required for the repair of non-compatible DNA double strand breaks by NHEJ in mammalian cells. *Nucleic Acids Res.* 34, 2998–3007. doi: 10.1093/nar/gkl380
- Cisneros, G. A., Perera, L., Garcia-Diaz, M., Bebenek, K., Kunkel, T. A., and Pedersen, L. G. (2008). Catalytic mechanisms of human DNA polymerase λ with Mg²⁺ and Mn²⁺ from ab initio quantum mechanical/molecular mechanical studies. *DNA Repair (Amst)* 7, 1824–1834. doi: 10.1016/j.dnarep.2008.07.007
- Cools, T., Iantcheva, A., Weimer, A. K., Boens, S., Takahashi, N., Maes, S., et al. (2011). The *Arabidopsis thaliana* checkpoint kinase WEE1 protects against premature vascular differentiation during replication stress. *Plant Cell* 23, 1435–1448. doi: 10.1105/tpc.110.082768
- Crespan, E., Czabany, T., Maga, G., and Hubscher, U. (2012). Microhomology-mediated DNA strand annealing and elongation by human DNA polymerases λ and β on normal and repetitive DNA sequences. *Nucleic Acids Res.* 40, 5577–5590. doi: 10.1093/nar/gks186
- Colligan, K., Tissier, A., and Britt, A. (2004). ATR regulates a G2-phase cell-cycle checkpoint in *Arabidopsis thaliana*. *Plant Cell* 16, 1091–1104. doi: 10.1105/tpc.018903
- Colligan, K. M., Robertson, C. E., Foreman, J., Doerner, P., and Britt, A. B. (2006). ATR and ATM play both distinct and additive roles in response to ionizing radiation. *Plant J.* 48, 947–961. doi: 10.1111/j.1365-313X.2006.02931.x
- De Schutter, K., Joubes, J., Cools, T., Verkest, A., Corellou, F., Babiyuchuk, E., et al. (2007). *Arabidopsis* WEE1 kinase controls cell cycle arrest in response to activation of the DNA integrity checkpoint. *Plant Cell* 19, 211–225. doi: 10.1105/tpc.106.045047
- Fan, W., and Wu, X. (2004). DNA polymerase lambda can elongate on DNA substrates mimicking non-homologous end joining and interact with XRCC4-ligase IV complex. *Biochem. Biophys. Res. Commun.* 323, 1328–1333. doi: 10.1016/j.bbrc.2004.09.002
- Fidantsef, A. L., Mitchell, D. L., and Britt, A. B. (2000). The *Arabidopsis* UVH1 gene is a homolog of the yeast repair endonuclease RAD1. *Plant Physiol.* 124, 579–586. doi: 10.1104/pp.124.2.579
- Friesner, J., and Britt, A. B. (2003). Ku80- and DNA ligase IV-deficient plants are sensitive to ionizing radiation and defective in T-DNA integration. *Plant J.* 34, 427–440. doi: 10.1046/j.1365-313X.2003.01738.x
- Fulcher, N., and Sablowski, R. (2009). Hypersensitivity to DNA damage in plant stem cell niches. *Proc. Natl. Acad. Sci. U.S.A.* 106, 20984–20988. doi: 10.1073/pnas.0909218106
- Furukawa, T., Curtis, M. J., Tominey, C. M., Duong, Y. H., Wilcox, B. W., Aggoune, D., et al. (2010). A shared DNA-damage-response pathway for induction of stem-cell death by UVB and by gamma irradiation. *DNA Repair (Amst)* 9, 940–948. doi: 10.1016/j.dnarep.2010.06.006
- Furukawa, T., Imamura, T., Kitamoto, H. K., and Shimada, H. (2008). Rice exonuclease-1 homologue, OsEXO1, that interacts with DNA polymerase lambda and RPA subunit proteins, is involved in cell proliferation. *Plant Mol. Biol.* 66, 519–531. doi: 10.1007/s11103-008-9288-6
- Gallego, M. E., Bleuyard, J. Y., Daoudal-Cotterell, S., Jallut, N., and White, C. I. (2003). Ku80 plays a role in non-homologous recombination but is not required for T-DNA integration in *Arabidopsis*. *Plant J.* 35, 557–565. doi: 10.1046/j.1365-313X.2003.01827.x
- Garcia-Diaz, M., Bebenek, K., Gao, G., Pederson, L. C., London, R. E., and Kunkel, T. A. (2005). Structure-function studies of DNA polymerase lambda. *DNA Repair (Amst)* 4, 1358–1367. doi: 10.1016/j.dnarep.2005.09.001
- Garcia-Diaz, M., Dominguez, O., Lopez-Fernandez, L. A., de Lera, L. T., Saniger, M. L., Ruiz, J. F., et al. (2000). DNA polymerase lambda (Pol lambda), a novel eukaryotic DNA polymerase with a potential role in meiosis. *J. Mol. Biol.* 301, 851–867. doi: 10.1006/jmbi.2000.4005
- Garcia-Ortiz, M. V., Ariza, R. R., Hoffman, P. D., Hays, J. B., and Roldán-Arjona, T. (2004). *Arabidopsis thaliana* AtPOLK encodes a DinB-like DNA polymerase that extends mispaired primer termini and is highly expressed in a variety of tissues. *Plant J.* 39, 84–97. doi: 10.1111/j.1365-313X.2004.0112.x
- Huefner, N. D., Mizuno, Y., Weil, C. F., Korf, I., and Britt, A. B. (2011). Breadth by depth: expanding our understanding of the repair of transposon-induced DNA double strand breaks via deep sequencing. *DNA Repair (Amst)* 10, 1023–1033. doi: 10.1016/j.dnarep.2011.07.011
- Inagaki, S., Suzuki, T., Ohto, M. A., Urawa, H., Horiuchi, T., Nakamura, K., et al. (2006). *Arabidopsis* TEBICHI, with helicase and DNA polymerase domains, is required for regulated cell division and differentiation in meristems. *Plant Cell* 18, 879–892. doi: 10.1105/tpc.105.036798
- Jia, Q., den Dulk-Ras, A., Shen, H., Hooykaas, P. J., and de Pater, S. (2013). Poly(ADP-ribose) polymerases are involved in microhomology mediated back-up non-homologous end joining in *Arabidopsis thaliana*. *Plant Mol. Biol.* 82, 339–351. doi: 10.1007/s11103-013-0065-9
- Jiang, C. Z., Yen, C. N., Cronin, K., Mitchell, D., and Britt, A. B. (1997). UV- and gamma-radiation sensitive mutants of *Arabidopsis thaliana*. *Genetics* 147, 1401–1409.

Supplementary Figure 1 | Structure of *Ku70* gene in the *atk70-3* mutant.

(A) Schematic structure of the *AtKu70* gene and its T-DNA insertion. Arrowheads represent gene-specific primers used for PCR. RB, T-DNA right border; LB, T-DNA left border. **(B)** Semiquantitative RT-PCR on different regions of the *AtKu70* gene. Primer pairs used for RT-PCR were LBb1 + Ku70R (left panel) and Ku70F + Ku70R (right panel). W, wild type; M, *atk70* mutant. **(C)** Sequence data for T-DNA: DNA junctions in the *atk70* mutant. Capitals, *AtKu70* gene sequence; Capitals/bold in the box, pROK2 sequence.

Supplementary Figure 2 | PCD and phenotypical differences of WT and mutants after γ -irradiation.

The 5-day-old seedlings in each mutant background were exposed to 20 Gy or mock-irradiated (0 h). The γ -irradiated seedlings were collected at 72 h after irradiation and dead cells in root tips were visualized by PI-staining. Bar = 50 μ m.

- Kimura, S., Uchiyama, Y., Kasai, N., Namekawa, S., Saotome, A., Ueda, T., et al. (2002). A novel DNA polymerase homologous to *Escherichia coli* DNA polymerase I from a higher plant, rice (*Oryza sativa L.*). *Nucleic Acids Res.* 30, 1585–1592. doi: 10.1093/nar/30.7.1585
- Kobayashi, Y., Watanabe, M., Okada, Y., Sawa, H., Takai, H., Nakanishi, M., et al. (2002). Hydrocephalus, situs inversus, chronic sinusitis, and male infertility in DNA polymerase lambda-deficient mice: possible implication for the pathogenesis of immotile cilia syndrome. *Mol. Cell. Biol.* 22, 2769–2776. doi: 10.1128/MCB.22.8.2769-2776.2002
- Lafarge, S., and Montane, M. H. (2003). Characterization of *Arabidopsis thaliana* ortholog of the human breast cancer susceptibility gene 1: AtBRCA1, strongly induced by gamma rays. *Nucleic Acids Res.* 31, 1148–1155. doi: 10.1093/nar/gkg202
- Lee, J. W., Blanco, L., Zhou, T., Garcia-Diaz, M., Bebenek, K., Kunkel, T. A., et al. (2004). Implication of DNA polymerase lambda in alignment-based gap filling for nonhomologous DNA end joining in human nuclear extracts. *J. Biol. Chem.* 279, 805–811. doi: 10.1074/jbc.M307913200
- Leung, C. C., and Glover, J. N. (2011). BRCT domains: easy as one, two, three. *Cell Cycle* 10, 2461–2470. doi: 10.4161/cc.10.15.16312
- Li, J., Vaidya, M., White, C., Vainstein, A., Citovsky, V., and Tzfira, T. (2005). Involvement of KU80 in T-DNA integration in plant cells. *Proc. Natl. Acad. Sci. U.S.A.* 102, 19231–19236. doi: 10.1073/pnas.0506437103
- Liang, L., Deng, L., Nguyen, S. C., Zhao, X., Maulion, C. D., Shao, C., et al. (2008). Human DNA ligases I and III, but not ligase IV, are required for microhomology-mediated end joining of DNA double-strand breaks. *Nucleic Acids Res.* 36, 3297–3310. doi: 10.1093/nar/gkn184
- Mestiri, I., Norre, F., Gallego, M. E., and White, C. I. (2014). Multiple host-cell recombination pathways act in *Agrobacterium*-mediated transformation of plant cells. *Plant J.* 77, 511–520. doi: 10.1111/tpj.12398
- Missirian, V., Conklin, P. A., Culligan, K. M., Huefner, N. D., and Britt, A. B. (2014). High atomic weight, high-energy radiation (HZE) induces transcriptional responses shared with conventional stresses in addition to a core “DSB” response specific to clastogenic treatments. *Front. Plant Sci.* 5:364. doi: 10.3389/fpls.2014.00364
- Mori, Y., Kimura, S., Saotome, A., Kasai, N., Sakaguchi, N., Uchiyama, Y., et al. (2005). Plastid DNA polymerases from higher plants, *Arabidopsis thaliana*. *Biochem. Biophys. Res. Commun.* 334, 43–50. doi: 10.1016/j.bbrc.2005.06.052
- Nick McElhinny, S. A., Havener, J. M., Garcia-Diaz, M., Juarez, R., Bebenek, K., Kee, B. L., et al. (2005). A gradient of template dependence defines distinct biological roles for family X polymerases in nonhomologous end joining. *Mol. Cell* 19, 357–366. doi: 10.1016/j.molcel.2005.06.012
- Ono, Y., Sakai, A., Takechi, K., Takio, S., Takusagawa, M., and Takano, H. (2007). NtPoli-like1 and NtPoli-like2, bacterial DNA polymerase I homologs isolated from BY-2 cultured tobacco cells, encode DNA polymerases engaged in DNA replication in both plastids and mitochondria. *Plant Cell Physiol.* 48, 1679–1692. doi: 10.1093/pcp/pcm140
- Ricaud, L., Proux, C., Renou, J. P., Pichon, O., Fochesato, S., Ortet, P., et al. (2007). ATM-mediated transcriptional and developmental responses to gamma-rays in *Arabidopsis*. *PLoS ONE* 2:e430. doi: 10.1371/journal.pone.0000430
- Riha, K., Watson, J. M., Parkey, J., and Shippen, D. E. (2002). Telomere length deregulation and enhanced sensitivity to genotoxic stress in *Arabidopsis* mutants deficient in Ku70. *EMBO J.* 21, 2819–2826. doi: 10.1093/emboj/21.11.2819
- Roy, S., Choudhury, S. R., Sengupta, D. N., and Das, K. P. (2013). Involvement of *AtPolλ* in the repair of high salt- and DNA cross-linking agent-induced double strand breaks in *Arabidopsis*. *Plant Physiol.* 162, 1195–1210. doi: 10.1104/pp.113.219022
- Roy, S., Choudhury, S. R., Singh, S. K., and Das, K. P. (2011). *AtPolλ*, a homolog of mammalian DNA polymerase λ in *Arabidopsis thaliana*, is involved in the repair of UV-B induced DNA damage through the dark repair pathway. *Plant Cell Physiol.* 52, 448–467. doi: 10.1093/pcp/pcr002
- Sakamoto, A., Lan, V. T., Hase, Y., Shikazono, N., Matsunaga, T., and Tanaka, A. (2003). Disruption of the AtREV3 gene causes hypersensitivity to ultraviolet light and gamma-rays in *Arabidopsis*: implication of the presence of a translesion synthesis mechanism in plants. *Plant Cell* 15, 2042–2057. doi: 10.1105/tpc.012369
- Sorrell, D. A., Marchbank, A., McMahon, K., Dickinson, J. R., Rogers, H. J., and Francis, D. A. (2002). wee1 homologue from *Arabidopsis thaliana*. *Planta* 215, 518–522. doi: 10.1007/s00425-002-0815-4
- Stuitje, A. R., Verbree, E. C., van der Linden, K. H., Mietkiewska, E. M., Nap, J. P., and Kneppers, T. J. (2003). Seed-expressed fluorescent proteins as versatile tools for easy (co)transformation and high-throughput functional genomics in *Arabidopsis*. *Plant Biotechnol. J.* 1, 301–309. doi: 10.1046/j.1467-7652.2003.00028.x
- Takahashi, S., Sakamoto, A., Sato, S., Kato, T., Tabata, S., and Tanaka, A. (2005). Roles of *Arabidopsis* AtREV1 and AtREV7 in translesion synthesis. *Plant Physiol.* 138, 870–881. doi: 10.1104/pp.105.060236
- Tamura, K., Adachi, Y., Chiba, K., Oguchi, K., and Takahashi, H. (2002). Identification of Ku70 and Ku80 homologues in *Arabidopsis thaliana*: evidence for a role in the repair of DNA double-strand breaks. *Plant J.* 29, 771–781. doi: 10.1046/j.1365-313X.2002.01258.x
- Uchiyama, Y., Hatanaka, M., Kimura, S., Ishibashi, T., Ueda, T., Sakakibara, Y., et al. (2002). Characterization of DNA polymerase δ from a higher plant, rice (*Oryza sativa L.*). *Gene* 295, 19–26. doi: 10.1016/S0378-1119(02)00822-3
- Uchiyama, Y., Kimura, S., Yamamoto, T., Ishibashi, T., and Sakaguchi, K. (2004). Plant DNA polymerase λ, a DNA repair enzyme that functions in plant meristematic and meiotic tissues. *Eur. J. Biochem.* 271, 2799–2807. doi: 10.1111/j.1432-1033.2004.04214.x
- Uchiyama, Y., Suzuki, Y., and Sakaguchi, K. (2008). Characterization of plant XRCC1 and its interaction with proliferating cell nuclear antigen. *Planta* 227, 1233–1241. doi: 10.1007/s00425-008-0695-3
- Uchiyama, Y., Takeuchi, R., Kodera, H., and Sakaguchi, K. (2009). Distribution and roles of X-family DNA polymerases in eukaryotes. *Biochimie* 91, 165–170. doi: 10.1016/j.biochi.2008.07.005
- Waterworth, W. M., Kozak, J., Provost, C. M., Bray, C. M., Angelis, K. J., and West, C. E. (2009). DNA ligase 1 deficient plants display severe growth defects and delayed repair of both DNA single and double strand breaks. *BMC Plant Biol.* 9:79. doi: 10.1186/1471-2229-9-79
- West, C. E., Waterworth, W. M., Jiang, Q., and Bray, C. M. (2000). *Arabidopsis* DNA ligase IV is induced by gamma-irradiation and interacts with an *Arabidopsis* homologue of the double strand break repair protein XRCC4. *Plant J.* 24, 67–78. doi: 10.1046/j.1365-313x.2000.00856.x
- West, C. E., Waterworth, W. M., Story, G. W., Sunderland, P. A., Jiang, Q., and Bray, C. M. (2002). Disruption of the *Arabidopsis* AtKu80 gene demonstrates an essential role for AtKu80 protein in efficient repair of DNA double-strand breaks *in vivo*. *Plant J.* 31, 517–528. doi: 10.1046/j.1365-313X.2002.01370.x
- Yokoi, M., Ito, M., Izumi, M., Miyazawa, H., Nakai, H., and Hanaoka, F. (1997). Molecular cloning of the cDNA for the catalytic subunit of plant DNA polymerase alpha and its cell-cycle dependent expression. *Genes Cells* 2, 695–709. doi: 10.1046/j.1365-2443.1997.1560354.x
- Yoshiyama, K., Conklin, P. A., Huefner, N. D., and Britt, A. B. (2009). Suppressor of gamma response 1 (SOG1) encodes a putative transcription factor governing multiple responses to DNA damage. *Proc. Natl. Acad. Sci. U.S.A.* 106, 12843–12848. doi: 10.1073/pnas.0810304106

Conflict of Interest Statement: The authors declare that the research was conducted in the absence of any commercial or financial relationships that could be construed as a potential conflict of interest.

Copyright © 2015 Furukawa, Angelis and Britt. This is an open-access article distributed under the terms of the Creative Commons Attribution License (CC BY). The use, distribution or reproduction in other forums is permitted, provided the original author(s) or licensor are credited and that the original publication in this journal is cited, in accordance with accepted academic practice. No use, distribution or reproduction is permitted which does not comply with these terms.

Arabidopsis PCNAs form complexes with selected D-type cyclins

Wojciech K. Strzalka^{1,2*}, Chhavi Aggarwal³, Weronika Krzeszowiec¹,
Agata Jakubowska¹, Olga Sztatelman^{1†} and Agnieszka K. Banas¹

¹ Department of Plant Biotechnology, Faculty of Biochemistry, Biophysics and Biotechnology, Jagiellonian University, Krakow, Poland, ² The Bioremediation Department, Małopolska Centre of Biotechnology, Jagiellonian University, Krakow, Poland,

³ Department of Gene Expression, Faculty of Biology, Adam Mickiewicz University, Poznań, Poland

OPEN ACCESS

Edited by:

Ayako N. Sakamoto,
Japan Atomic Energy Agency, Japan

Reviewed by:

Naoki Takahashi,
Nara Institute of Science and
Technology, Japan

María de la Paz Sánchez,
Universidad Nacional Autónoma de
México, Mexico

*Correspondence:

Wojciech K. Strzalka,
Department of Plant Biotechnology,
Faculty of Biochemistry, Biophysics
and Biotechnology, Jagiellonian
University, Gronostajowa 7,
Krakow 30-387, Poland
wojciech.strzalka@uj.edu.pl

†Present Address:

Olga Sztatelman,
Institute of Biochemistry and
Biophysics, Polish Academy of
Sciences, Warsaw, Poland

Specialty section:

This article was submitted to
Plant Physiology,
a section of the journal
Frontiers in Plant Science

Received: 27 March 2015

Accepted: 26 June 2015

Published: 17 July 2015

Citation:

Strzalka WK, Aggarwal C,
Krzeszowiec W, Jakubowska A,
Sztatelman O and Banas AK (2015)
Arabidopsis PCNAs form complexes
with selected D-type cyclins.
Front. Plant Sci. 6:516.
doi: 10.3389/fpls.2015.00516

Proliferating Cell Nuclear Antigen (PCNA) is a key nuclear protein of eukaryotic cells. It has been shown to form complexes with cyclin dependent kinases, cyclin dependent kinase inhibitors and the D-type cyclins which are involved in the cell cycle control. In Arabidopsis two genes coding for PCNA1 and PCNA2 proteins have been identified. In this study by analyzing Arabidopsis PCNA/CycD complexes we tested the possible functional differentiation of PCNA1/2 proteins in cell cycle control. Most out of the 10 cyclins investigated showed only nuclear localization except CycD2;1, CycD4;1, and CycD4;2 which were observed both in the nucleus and cytoplasm. Using the Y2H, BiFC and FLIM-FRET techniques we identified D-type cyclins which formed complexes with either PCNA1 or PCNA2. Among the candidates tested only CycD1;1, CycD3;1, and CycD3;3 were not detected in a complex with the PCNA proteins. Moreover, our results indicate that the formation of CycD3;2/PCNA and CycD4;1/PCNA complexes can be regulated by other as yet unidentified factor(s). Additionally, FLIM-FRET analyses suggested that *in planta* the distance between PCNA1/CycD4;1, PCNA1/CycD6;1, PCNA1/CycD7;1, and PCNA2/CycD4;2 proteins was shorter than that between PCNA2/CycD4;1, PCNA2/CycD6;1, PCNA2/CycD7;1, and PCNA1/CycD4;2 pairs. These data indicate that the nine amino acid differences between PCNA1 and PCNA2 have an impact on the architecture of Arabidopsis CycD/PCNA complexes.

Keywords: **Arabidopsis, PCNA, D-type cyclins, DNA replication, DNA repair, cell cycle**

Introduction

Proliferating Cell Nuclear Antigen (PCNA) is the fundamental eukaryotic protein which is present mainly in the nuclei of dividing cells. Its elevated synthesis is observed in the early S phase of the cell cycle (Morris and Mathews, 1989). Molecular studies on plant organisms have demonstrated that the genomes of some species, e.g., carrot (Hata et al., 1992), maize (Lopez et al., 1997) and Arabidopsis (Arabidopsis Genome Initiative, 2000) have two genes coding for PCNA1 and PCNA2 proteins. An analysis of PCNA amino acid sequences from different plant species, including rice (Suzuka et al., 1991), maize (Lopez et al., 1997), common bean (Strzalka and Ziemiennowicz, 2007), and runner bean (Strzalka et al., 2010) showed that the identity between these proteins is over 85%. Interestingly, although the amino acid sequence identity between Arabidopsis/yeast and Arabidopsis/human PCNA is 40 and 65% respectively, crystallographic data demonstrated that these proteins have a very similar and conserved three dimensional architecture (Gulbis et al., 1996; Strzalka et al., 2009). A PCNA monomer, a 29 kDa polypeptide composed of two structural domains

linked by an inter-domain connecting loop, naturally forms a homotrimer, ring-like in structure (Strzalka and Ziemiencowicz, 2011). This trimer plays a crucial function during DNA replication. After the initiation of DNA synthesis to provide the undisturbed continuation of this process, PCNA must be recruited to the replication fork. With the help of Replication Factor C, PCNA is loaded onto the DNA duplex where it acts as a sliding platform which coordinates and affects the activity of the proteins involved in DNA replication (Wu et al., 1996; Tom et al., 2001; Strzalka and Ziemiencowicz, 2011). PCNA is involved not only in DNA replication but also in DNA repair and cell cycle control (Strzalka and Ziemiencowicz, 2011). In yeasts, animals and plants, cell cycle proteins, cyclin dependent kinases (CDK), cyclin dependent kinase inhibitors (CDKI) and D-type cyclins were found in complexes with PCNA (Paz Sanchez et al., 2002; Vivona and Kelman, 2003). Detailed studies on mouse cyclin D1, D3, and PCNA revealed that both the N- and C-terminal regions of PCNA are involved in interactions with these cyclins (Matsuoka et al., 1994).

Comparative analysis of mammalian and higher plant genomes has demonstrated that the latter have a much higher number of genes coding for D-type cyclins. For example, in contrast to the human genome which encodes only cyclin D1, D2, and D3 (Sherr and Roberts, 2004), the genome of Arabidopsis, rice and maize has 10, 14, and 17 genes respectively coding for D-type cyclins. These are grouped into seven different classes (Arabidopsis Genome Initiative, 2000; Buendia-Monreal et al., 2011). In the sequence of plant D-type cyclins, typical motifs and domains which are also characteristic of other cyclin types can be distinguished. These include, (i) a cyclin core composed of either a conserved N-terminal domain or both an N- and less conserved C-terminal domain, and (ii) a cyclin box located within the N-terminal domain which is a binding site for CDKs. (Wang et al., 2004; Buendia-Monreal et al., 2011). Additionally, in some of the D-type cyclins there is, (i) a PEST domain, rich in proline, glutamate, serine and threonine residues which is a marker for unstable proteins (Wang et al., 2004; Buendia-Monreal et al., 2011), and (ii) a conserved retinoblastoma protein (pRB) binding motif located at the N-terminus (Buendia-Monreal et al., 2011). The consensus sequence of the pRB binding motif is LXCXE where L, E, C represent leucin, cysteine and glutamic acid respectively, while X represents any amino acid residue.

D-type cyclins interact with CDKs regulating their activity. They can be found in complexes not only with CDKs but also other proteins. For example, the human CycD1 was found to be a component of a larger complex containing CDK2, CDK4, CDK5, p21, and PCNA (Xiong et al., 1992). Moreover, the results from studies on mammalian cell cycle proteins showed that the excess of CycD1 repressed cell proliferation by inhibiting DNA synthesis and CDK2 activity, possibly through the binding of CycD1 to PCNA and CDK2 (Fukami-Kobayashi and Mitsui, 1999). The mammalian cyclins D1, D2, D3 and their partners CDK4 and CDK6 have been shown to act early in G1 phase (Sherr and Roberts, 2004). It is assumed that CycD/CDK complexes bind and phosphorylate pRB in the early G1 phase. This results in the release of the E2F transcription factor and allows cells to progress from the G1 to the S phase (Harbour and Dean, 2000). Studies on plant cyclins have revealed

that, as with yeast and mammalian proteins they can form complexes with CDKs. Co-immunoprecipitation experiments demonstrated that Arabidopsis CycD4;2 can be observed in complex with CDKA;1, CDKB1;1, or CDKB2;1 (Kono et al., 2006). A constructed Arabidopsis protein interaction network revealed the presence of D-type cyclins/CDK complexes (Boruc et al., 2010). Another study showed the formation of CycD2;2/CDKA, CycD2;2/CDKB1;1, CycD4;2/CDKA, CycD4;1/CDKB1;1, CycD5;3/CDKA, or CycD5;2/CDKB1;1 complexes in germinating maize. Additionally, changes in the total level of the tested (i) D-type cyclins, (ii) CDKs and (iii) both D-type cyclins and CDKs present in the CycD/CDK complexes were also demonstrated (Godinez-Palma et al., 2013). The analysis of the tobacco retinoblastoma-related (RBR) protein and CycD3;1 using Y2H and pull down/immunoprecipitation experiments revealed that these proteins are parts of the same complex (Nakagami et al., 1999). Moreover, in this study the tobacco Cdc2/CycD3;1 complex, produced and purified from the insect cells, has been shown to phosphorylate RBR protein. Similarly, Arabidopsis CycD2;1 and CDKA;1 were shown to form complex with maize RBR protein (Bonatti and Gutierrez, 2001). Concluding, the presence of CycD/CDK as well as pRB/E2F complexes in plant cells suggests that the mitogenic signal transmission pathway is conserved in higher eukaryotes (Meijer and Murray, 2000).

Despite significant progress in plant D-type cyclin studies over recent years, the role of these proteins in Arabidopsis cells in the context of interaction with PCNA is still unknown. To shed more light on the interplay between Arabidopsis PCNA1/2 proteins and D-type cyclins we employed the following techniques: a split ubiquitin yeast two hybrid system (Y2H), a bimolecular fluorescence complementation (BiFC) and fluorescence-lifetime imaging microscopy-Froster resonance energy transfer (FLIM-FRET). In this study we present the results from the analysis of Arabidopsis CycD/PCNA complexes.

Materials and Methods

Computational Analysis

The nucleotide and protein sequences of Arabidopsis D-type cyclins were identified using the NCBI database. The N- and C-terminal cyclin domains were detected with the help of the Pfam database (<http://pfam.xfam.org/>). The putative PEST motif analysis was performed using pestfind software (<http://emboss.bioinformatics.nl/cgi-bin/emboss/pestfind>) with *E*-value 0.01 as the cutoff. The theoretical PI and MW values were calculated through the ExPASy bioinformatics resource portal. The exon-intron gene structure was built with the help of exon-intron graphic maker (<http://wormweb.org/exonintron>). The presence of the putative importin α -dependent nuclear localization signal in Arabidopsis D-type cyclins was analyzed using cNLS mapper (http://nls-mapper.iab.keio.ac.jp/cgi-bin/NLS_Mapper_form.cgi) with the cut off 6.0.

Construction of Vectors Used for Y2H Analysis

The pDHB1 bait and pPR3-N prey plasmids used in the split-ubiquitin Y2H system transactivating starter kit (MoBiTec) were

reconstructed into Gateway-compatible vectors. The gateway cassette containing the *ccdB* gene was amplified using a RAPID PCR mix (A&A Biotechnology, Poland), containing an appropriate set of primers (**Supplementary Table 1**), with pDONR221 as a template. The PCR product, pDHB1 and pPR3-N vectors were digested with the SfiI restriction enzyme (FastDigest, Thermo Scientific). The digested PCR product was ligated into both plasmids and transformed into the *E. coli* DB3.1 strain. The bacterial colonies selected on an LB plate supplemented with 25 mg/L of chloramphenicol were used for the isolation of the pDHB1Gateway and pPR3-NGateway vectors. Then, the kanamycin resistance coding gene (*KanR*) of the pDHB1Gateway vector was replaced with a spectinomycin resistance coding gene (*SpmR*). The *SpmR* gene was amplified from the pK7WGF2 vector using Easy-A polymerase (Stratagene) and an appropriate set of primers (**Supplementary Table 1**). For gene exchange, yeast homologous recombination was employed. The NMY51 strain cells were transformed with a mixture containing pDHB1Gateway vector digested with HindIII and XhoI and the PCR product followed by selection on an SD-Leu solid medium. The plasmids isolated from growing yeast colonies were transformed into the DB3.1 cells. Transformed bacterial cells were plated on an LB solid medium supplemented with spectinomycin (100 mg/L) and the plasmid from growing colonies was isolated.

To construct the entry vectors coding for Arabidopsis D-type cyclins, PCNA1 and PCNA2 with stop codon appropriate open reading frames (ORFs) were amplified with the help of Pfu polymerase (Fermentas) using specific primers (**Supplementary Table 1**). The PCR products were purified and cloned into the pDONR221 vector using a Gateway BP Clonase II Enzyme mix (Life Technologies) followed by sequencing. The other entry pDONR221 plasmids containing ORFs without stop codon were either purchased from the Arabidopsis Biological Stock Centre (ABRC) or constructed as previously described (Strzalka et al., 2012). To prepare the destination vectors appropriate ORFs were transferred from pDONR221 either into the pDHB1Gateway (bait) or pPR3-NGateway (prey) vector (**Supplementary Table 2**) with the help of a Gateway LR Clonase enzyme mix (Life Technologies).

Construction of Vectors Used for Plant Transformation

To prepare final binary vectors, pDONR221 plasmids containing appropriate ORFs were either (i) purchased from the ABRC, or (ii) obtained in a previous study (Strzalka et al., 2012), or (iii) constructed in this study (Section Construction of Vectors Used for Y2H Analysis). The ORFs were transferred to destination vectors (**Supplementary Table 2**) as described in the Section Construction of Vectors Used for Y2H Analysis. The final destination plasmids were transformed into *Agrobacterium tumefaciens* strain C58. The binary vectors containing Arabidopsis PCNA1_GFP, PCNA1_NtermGFP, PCNA1_CtermGFP, PCNA2_GFP, PCNA2_NtermGFP, PCNA2_CtermGFP ORFs were constructed during previous studies (Strzalka et al., 2012, 2013) (**Supplementary Table 2**).

Yeast Two-hybrid Analysis

A split-ubiquitin Y2H system transactivating starter kit was used to test interactions between Arabidopsis D-type cyclins and PCNA1 or PCNA2. Yeast strain NMY51 was transformed with appropriate combinations of bait (pDHB1Gateway) and prey (pPR3-NGateway) plasmids (**Supplementary Table 2**) along with positive and negative control vectors according to the supplied protocol. After transformation, the yeast cells were transferred onto SC-Leu-Trp selection plates followed by a 3-day incubation at 30°C. The transformed cells were inoculated in a liquid SC-Leu-Trp medium and grown with vigorous shaking overnight at 30°C. The overnight cultures were plated on an SC-Leu-Trp solid medium, an SC-Leu-Trp-His selection solid medium supplemented with 10 mM 3-aminotriazol (3-AT) or a nitrocellulose filter placed on the surface of a YPAD solid medium. The SC plates were incubated for 4 days at 30°C before analysis. The yeast cells plated on nitrocellulose filter/YPAD medium were incubated for 24 h at 30°C. The filter was then immersed in liquid nitrogen for 60 s and placed on Whatman filter paper saturated with buffer A (60 mM Na₂HPO₄, 40 mM Na₂HPO₄, 10 mM KCl, 1 mM MgSO₄, 85 mM 2-mercaptoethanol, 1 mg/ml of 5-bromo-4-chloro-3-indolyl-D-galactopyranoside (X-gal), pH 7.0) and kept at 37°C for 18 h.

Bimolecular Fluorescence Complementation Analysis

Wild type *Nicotiana benthamiana* plants were grown in the greenhouse under natural light supplemented with artificial light (High Pressure Sodium Lamp 600 Watt, Phytolit™) to maintain a 16 h L/8 h D photoperiod at 23°C and relative humidity 40%. For the experiments the leaves of an 8-week old plant were used. The BiFC analysis was performed as described previously (Strzalka et al., 2012, 2013). The interactions were tested using: NtermGFP_PCNA/CycD_CtermGFP/p19 (viral-encoded suppressor of gene silencing), PCNA_NtermGFP/CycD_CtermGFP/p19, CtermGFP_PCNA/CycD_NtermGFP/p19, or PCNA_CtermGFP/CycD_NtermGFP/p19 binary vectors (**Supplementary Figure 1**). Before imaging the leaves were syringe-infiltrated with water and evaluated with the help of a BioRad MRC 1024 confocal microscope (BioRad Hercules, CA, U.S.A.). Images were collected using a 60x (NA 1.4) PlanApo oil-immersion objective mounted on the microscope. The excitation wavelength was 488 nm emitted by a 100 mW argon-ion laser (ITL, U.S.A.). GFP fluorescence was collected with a 540 DF30 filter and chloroplast autofluorescence with a 585LP filter.

FLIM-FRET Analysis

The leaves of *N. benthamiana* plants were transiently transformed as described in Section Bimolecular Fluorescence Complementation Analysis using appropriate RFP_PCNA/CycD_GFP and PCNA_RFP/CycD_GFP combinations. Prior to FLIM data collection, the GFP and RFP fluorescence levels in the plant samples within the region of interest were confirmed using a Nikon A1R confocal microscope with excitation at 488 and 543 nm, respectively. FLIM was performed using the Picoquant PicoHarp TCSPC Module. As control of donor-acceptor pairs, GFP (from pK7WGF2) and RFP

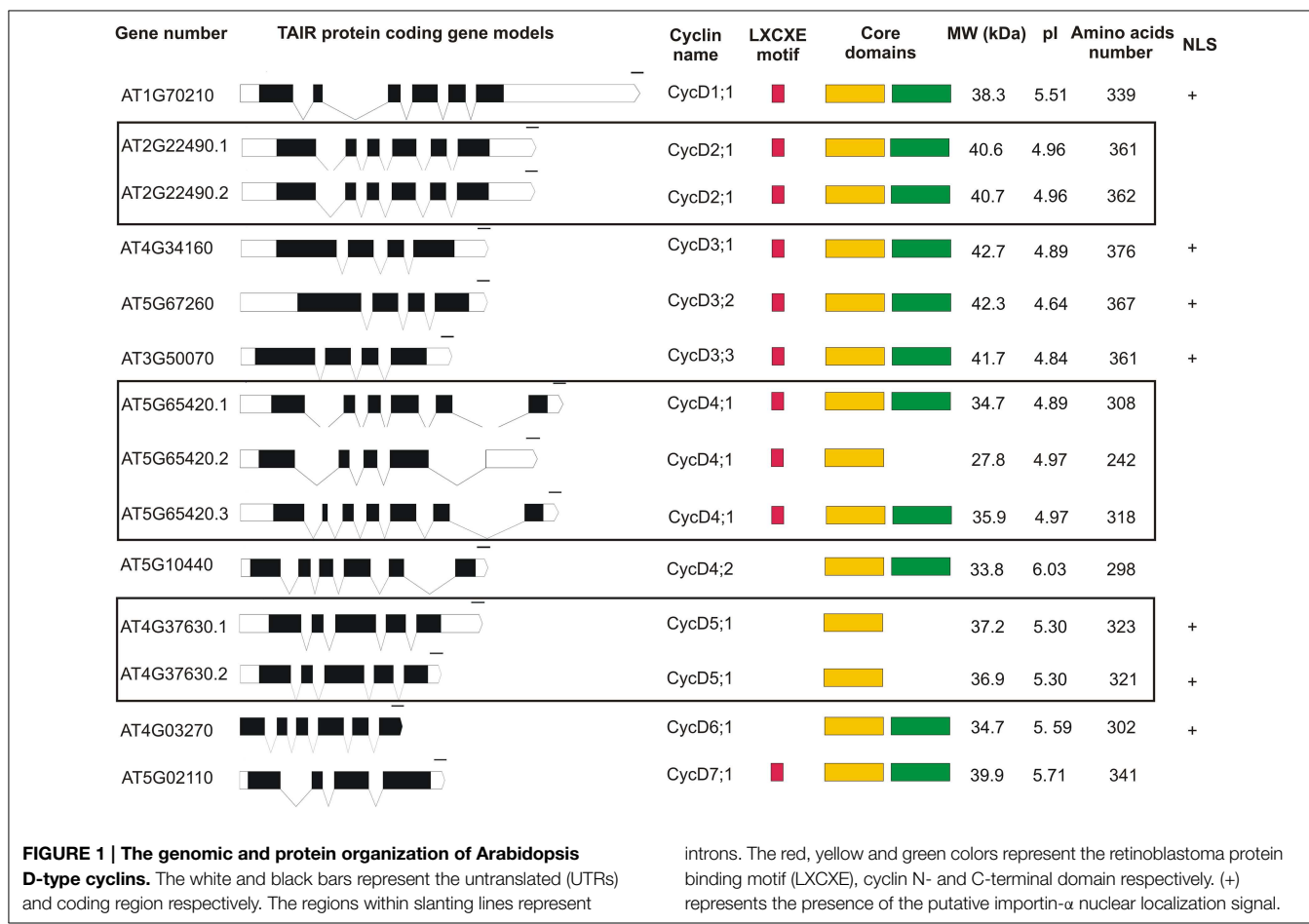
(from pSITE4CA) were chosen. The GFP (donor) was excited with a 485 nm pulsed diode laser (PDL 800-D, 40 mHz). The excitation light was directly coupled with the microscope and focused on the sample using a CFI Apo 40X water immersion objective lens. GFP emission was selected using a 520/535 nm filter. Photons were detected using a SPAD detector module. Images were acquired with a frame size of 256×256 pixels. Data analysis was performed with Picoquant's Symphotime software. From the obtained images, complete fluorescence lifetime decays were calculated per pixel for nuclei and fitted using a double exponential decay model. χ^2 of 1 was considered as a perfect fit. For FRET analysis the fluorescence lifetime of the donor/acceptor pair (τ_{DA}) was compared with that of donor alone (τ_D). The FRET efficiency (E) was calculated as $E = (1 - \tau_{DA}/\tau_D) \times 100\%$, where τ_D is the fluorescence lifetime of a donor in the absence of an acceptor and τ_{DA} that of a donor in the presence of an acceptor. At least six to eight nuclei per combination were analyzed and the average of the values was taken for analysis.

Results

In Silico Analysis of Arabidopsis D-type Cyclins

Analysis of the *Arabidopsis thaliana* genome database revealed that 10 D-type cyclins are encoded by the nuclear DNA of this

plant (**Figure 1**). The data deposited in TAIR (The Arabidopsis Information Resource <http://www.arabidopsis.org>) show only one type of gene model for CycD1;1, CycD3;1, CycD3;2, CycD3;3, CycD4;2, CycD6;1, CycD7;1, two for CycD2;1, CycD5;1 and three for CycD4;1. Transcript coding for CycD1;1, CycD2;1 (AT2G22490.1 and AT2G22490.2 splicing variants), CycD4;1 (splicing variant AT5G65420.1), CycD4;2 and CycD6;1 consist of six exons. In the structure of gene coding for CycD3;1, CycD3;2, CycD3;3 and CycD7;1 four exons are found. The CycD4;1 (transcript variant AT5G65420.2) and CycD5;1 (AT4G37630.1 and AT4G37630.2 transcript variants) are products of five exons. Finally, transcript variant AT5G65420.3 coding for CycD4;1 is a product of seven exons. The gene coding for CycD1;1, CycD2;1, CycD3;1/CycD5;1/CycD6;1, CycD3;2/CycD4;1/CyD4;2/CycD7;1, CycD3;3 are located on chromosomes 1, 2, 4, 5 and 3 respectively. Arabidopsis D-type cyclins are acidic proteins with an isoelectric point ranging from 4.64 to 6.03 and a molecular weight (MW) between 27.8 and 42.7 kDa. Within the first thirty amino acids of CycD1;1, CycD2;1, CycD3;1, CycD3;2, CycD3;3, CycD4;1, and CycD7;1, a consensus pRB binding sequence (LXCXE motif) is found (**Figure 1**). The analysis of the investigated D-type cyclin amino acid sequences using the Pfam database revealed that the cyclin core of CycD1;1, CycD2;1 (both splicing variants), CycD3;1, CycD3;2, CycD3;3, CycD4;1 (AT5G65420.1 and AT5G65420.3



gene models), CycD4;2, CycD6;1 and CycD7;1 is composed of a conserved N- and less conserved C-terminal domain. On the other hand for CycD4;1 (AT5G65420.2 splicing variant) and CycD5;1 (AT4G37630.1 and AT4G37630.2 transcript variants) only an N-terminal domain fold was detected (**Figure 1**). The putative PEST motif was identified in all of the analyzed Arabidopsis D-type cyclins. Finally, using cNLS mapper tool the presence of putative importin α -dependent nuclear localization signal was predicted for CycD1;1, CycD3;1, CycD3;2, CycD3;3, CycD5;1 (both splicing variants) and CycD6;1 (**Figure 1**).

Analysis of Subcellular Localization of Arabidopsis D-type Cyclins

A subcellular localization analysis of Arabidopsis D-type cyclins_GFP fusions in *N. benthamiana* cells revealed that all of the tested proteins were present in the nucleus (**Figure 2**). Furthermore, investigation of CycD2;1, Cyc4;1, and CycD4;2 showed that these proteins could be detected not only in the nucleus but also in the cytoplasm (**Figure 2**), similar to previously tested PCNA1 and PCNA2 (Strzalka et al., 2012).

Identification of Those Arabidopsis D-type Cyclin Candidates Which Form Complexes with PCNA1/2

At the first stage of this study the Y2H technique was employed to identify which Arabidopsis D-type cyclin candidates may form complexes with PCNA1 and/or PCNA2. The interactions between PCNA1/2 and D-type cyclins were tested in two different combinations. In the first combination PCNA1/2 proteins were used as bait. The result of this analysis demonstrated that PCNA1 formed a complex with CycD3;2, CycD4;1, and CycD4;2 (**Figure 3A**) while PCNA2 showed interaction only with CycD4;1 and CycD4;2 but not CycD3;2 (**Figure 3B**). Testing the opposite combination, where D-type cyclins were expressed as bait, interactions between CycD2;1/PCNA1, CycD3;2/PCNA1, CycD4;2/PCNA1, CycD2;1/PCNA2, CycD3;2/PCNA2, and CycD4;2/PCNA2 were observed (**Figure 3C**). Moreover, complex formation was also observed for CycD5;1/PCNA2 and CycD6;1/PCNA2 (**Figure 3C**).

Following the Y2H analysis, an *N. benthamiana* transient transformation assay was employed. Complex formation between Arabidopsis PCNA1/2 and D-type cyclins was analyzed *in planta* using BiFC and FLIM-FRET techniques. In BiFC studies, four different combinations including CycD_NtermGFP/PCNA_CtermGFP (**Figure 2**) were analyzed. When CycD1;1, CycD3;1, CycD3;2, and CycD3;3 were investigated, no complexes with PCNA1/2 were observed. On the other hand, presence of GFP fluorescence was observed only in the nucleus when the formation of complexes between PCNA1/2 and CycD4;1, CycD5;1, CycD6;1, or CycD7;1 was tested. Moreover, in the case of CycD2;1/PCNA and CycD4;2/PCNA, complexes were observed both in the nucleus and cytoplasm. Simultaneously to BiFC experiments, FLIM-FRET analysis was performed. First, either GFP alone or GFP together with RFP was transiently expressed in *N. benthamiana* leaf cells using the agroinfiltration method. The lifetime of GFP

(donor protein) was determined in the absence (τ_D) and in the presence (τ_{DA}) of RFP (potential acceptor), to calculate the value of FRET efficiency for non-interacting GFP/RFP partners (negative control). In the presence of RFP the average lifetime of GFP decreased from 2.51 to 2.48 ns and the calculated FRET efficiency was 1.19% (**Table 1**) which was used as a threshold. In subsequent experiments the values of FRET efficiency above the threshold were considered as putative PCNA/D-type cyclin complexes. Additionally, a similar experiment was performed for PCNA2_GFP/RFP_PCNA2 pair (positive control) based on the previous studies where the formation of complexes between PCNA2 monomers was shown (Strzalka and Aggarwal, 2013). The calculated FRET efficiency for this pair of proteins was 4.78%. Finally, complex formation between D-type cyclins_GFP and RFP_PCNA1/2 fusions was tested. The FLIM analysis showed a decrease in donor fluorescence lifetime for cyclin D4;1, D4;2, D6;1, and D7;1 when expressed with PCNA1/2 suggesting complex formation between these protein pairs (**Table 1**). During FLIM measurement, co-localization studies of PCNA1/2 and D-type cyclins (Pearson's correlation coefficient, **Table 1**) were performed. Despite good co-localization between PCNA1/2 and CycD1;1, CycD2;1, CycD3;1, CycD3;2, CycD3;3, or CycD5;1 the calculated FRET efficiency values were similar or lower than the threshold value, indicating that these protein pairs were not a part of the same complex (**Table 1**). Interestingly, the value of FRET efficiency obtained for PCNA1/CycD4;1, PCNA1/CycD6;1, PCNA1/CycD7;1, and PCNA2/CycD4;2 pairs was higher than that of PCNA2/CycD4;1, PCNA2/CycD6;1, PCNA2/CycD7;1, and PCNA1/CycD4;2 complexes (**Table 1**). FLIM-FRET analysis of D-type cyclins_GFP and PCNA1/2_RFP did not demonstrate formation of complexes between tested proteins (**Table 1**).

Discussion

Arabidopsis PCNA1 and PCNA2 genes are spatially separated and located on chromosome 1 and 2 respectively (Arabidopsis Genome Initiative, 2000). The high level of identity between Arabidopsis PCNA1 and PCNA2 proteins (97%) results from there being only nine differences in amino acid residues. Although studies on eukaryotic PCNA have been carried out over the last decades, the question of the functional relevance of PCNA1/2 proteins in plants is still a matter for debate. Crystal structure analysis of Arabidopsis PCNA (Strzalka et al., 2009) does not indicate any functional differentiation between PCNA1 and PCNA2. However, results presented by others suggest a peculiar role for just PCNA2 in DNA repair (Anderson et al., 2008; Amoroso et al., 2011).

The *in silico* study of Arabidopsis D-type cyclins revealed that the motif/domain organization of individual proteins is not identical to corresponding maize cyclins. In Arabidopsis the pRB binding motif (LXCXE) was not detected in CycD4;2, CycD5;1, and CycD6;1 (**Figure 1**) while in case of maize proteins it is absent only in the CycD6;1 (Buendia-Monreal et al., 2011). Testing Arabidopsis proteins using Pfam database we could not detect the C-terminal domain in the CycD4;1 (splicing variant AT5G65420.2) and CycD5;1 (both splicing variants).

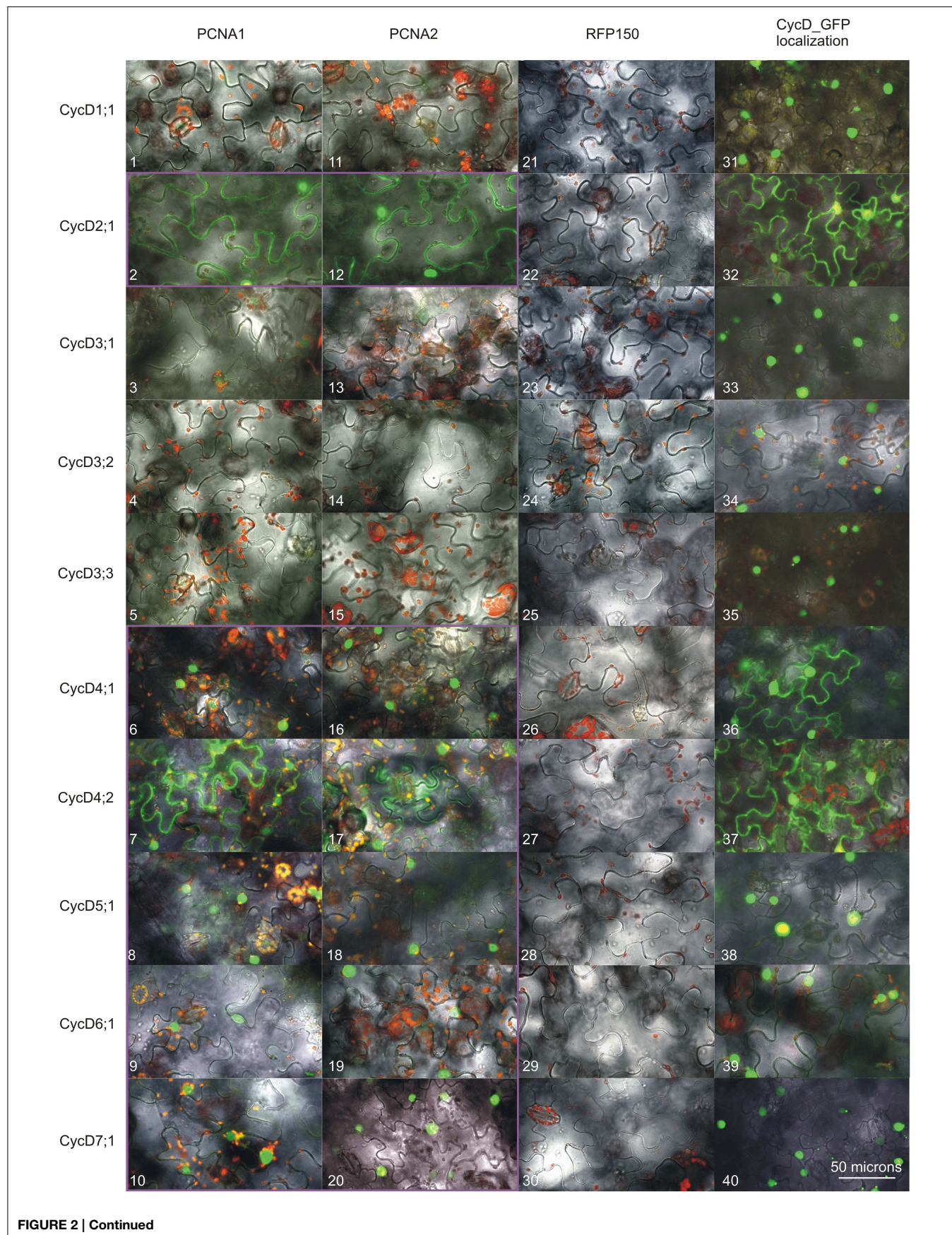


FIGURE 2 | Continued

Analysis of D-type cyclins subcellular localization and the formation of complexes with either PCNA1 or PCNA2. Confocal images of *N. benthamiana* leaf cells expressing transiently analyzed open reading frames. Split GFP complex formed between PCNA1_CtermGFP and (1) CycD1;1_NtermGFP, (2) CycD2;1_NtermGFP, (3) CycD3;1_NtermGFP, (4) CycD3;2_NtermGFP, (5) CycD3;3_NtermGFP, (6) CycD4;1_NtermGFP, (7) CycD4;2_NtermGFP, (8) CycD5;1_NtermGFP, (9) CycD6;1_NtermGFP, (10) CycD7;1_NtermGFP. Split GFP complex formed between PCNA2_CtermGFP and (11) CycD1;1_NtermGFP, (12) CycD2;1_NtermGFP, (13) CycD3;1_NtermGFP, (14) CycD3;2_NtermGFP, (15) CycD3;3_NtermGFP, (16) CycD4;1_NtermGFP, (17) CycD4;2_NtermGFP,

(18) CycD5;1_NtermGFP, (19) CycD6;1_NtermGFP, (20) CycD7;1_NtermGFP. Split GFP complex formed between RFP150_CtermGFP and (21) CycD1;1_NtermGFP, (22) CycD2;1_NtermGFP, (23) CycD3;1_NtermGFP, (24) CycD3;2_NtermGFP, (25) CycD3;3_NtermGFP, (26) CycD4;1_NtermGFP, (27) CycD4;2_NtermGFP, (28) CycD5;1_NtermGFP, (29) CycD6;1_NtermGFP, (30) CycD7;1_NtermGFP. (31) CycD1;1_GFP, (32) CycD2;1_GFP, (33) CycD3;1_GFP, (34) CycD3;2_GFP, (35) CycD3;3_GFP, (36) CycD4;1_GFP, (37) CycD4;2_GFP, (38) CycD5;1_GFP, (39) CycD6;1_GFP, (40) CycD7;1_GFP. All the images are overlays of the bright field, autofluorescence of chlorophyll (red) and GFP fluorescence (green). The PCNA/CycD complexes are in the magenta frame. This result is representative of three independently repeated experiments.

Similar analysis for maize D-type cyclins showed that C-terminal domain was not found in the CycD3;1a, CycD3;1b, CycD5;3a, CycD5;3b, and also CycD7;1 (Buendia-Monreal et al., 2011). Investigation of genes structure demonstrated that Arabidopsis CycD1;1/CycD2;1 (both splicing variants)/CycD4;1 (splicing variant AT5G65420.1)/CycD4;2/CycD6;1 and CycD5;1 are products of six and five exons respectively (Figure 1) similarly to the corresponding maize transcripts (Buendia-Monreal et al., 2011). On the other hand the number of exons identified for the other corresponding Arabidopsis/maize D-type cyclin transcripts differed. The *in silico* investigation, where the presence of the putative nuclear localization signal in D-type cyclins was analyzed, suggests that the mechanism of CycD2;1, CycD4;1, CycD4;2, and CycD7;1 (Figure 1) import into the nucleus might be not dependent on importin α .

To investigate whether Arabidopsis PCNA1/2 can play different functions in cell cycle control we tested the formation of complexes between PCNA1/2 and D-type cyclins. This group of proteins was selected based on previous data from maize and animal studies where PCNA was demonstrated to interact/co-precipitate with D-type cyclins (Matsuoka et al., 1994; Shimizu and Mori, 1998; Gutierrez et al., 2005; Lara-Nunez et al., 2008; Becerril et al., 2012). Firstly, we tested the subcellular localization of Arabidopsis D-type cyclins to confirm that they are present in the same compartment as PCNA1 and PCNA2 (Strzalka et al., 2012, 2013). All of the tested cyclins could be observed in the nucleus, although not all of them were detected in the cytoplasm (Figure 2). Most of our results were in accordance with previous reports with a few exceptions (Kono et al., 2007; Boruc et al., 2010). In our experimental conditions CycD2;1 was observed in the nucleus and cytoplasm which is in opposition to the results of others who showed exclusively nuclear localization of this protein (Boruc et al., 2010; Sanz et al., 2011). In contrast to data published by Boruc and co-workers our studies showed only nuclear localization of CycD3;1 (Boruc et al., 2010). The analysis of CycD3;3 (this study) revealed that this protein was observed only in the nucleus. This is in contrast to data presented for tobacco CycD3;3 which was detected primarily in the nucleus although it was also visible in the cytoplasm (Nakagami et al., 2002). Previous studies of CycD6;1 subcellular localization in the root cells revealed that in some cells it could be detected in the nucleus, as in our studies, and in other cells in the cytoplasm (Cruz-Ramirez et al., 2012). To conclude, in this study we found some discrepancies in the subcellular localization of

the tested cyclins when compared to data presented previously in other reports. This may results from, e.g., (i) different tissue type, (ii) type of expression system (transient/stable, Arabidopsis/tobacco), and (iii) promotor type (35S/natural) used during subcellular localization analysis of these proteins. Taking into account the fact that in the nucleus we could detect all of the analyzed Arabidopsis D-type cyclins, we tested their ability to form complexes with either PCNA1 or PCNA2. Our experiments revealed that among all the cyclins tested only CycD1;1, CycD3;1, and CycD3;3 could not be detected in complexes with PCNA1/2 by any of used experimental technique. This might be due to several reasons: (i) these cyclins are not involved in PCNA-dependent cell cycle control, (ii) there are other factor(s), absent under our experimental conditions, which are necessary for complex formation, and (iii) steric hindrance may prevent complex formation.

The experimental results from the Y2H system and BiFC showed the presence of complex composed of CycD2;1 and PCNA1/2. This is in agreement with data from studies, conducted on maize embryo axes, where PCNA was shown to co-precipitate with CycD2 (Gutierrez et al., 2005). The results from our FLIM-FRET analysis did not indicated that CycD2;1 and PCNA1 are parts of the same complex. The calculated FRET efficiency was less than 2% which is close to the value calculated for the non-interacting GFP/RFP pair. Moreover, neither did our FLIM-FRET analyzes demonstrate the presence of CycD2;1/PCNA2 complexes in tobacco leaf cells. This could be a result of GFP/RFP steric hindrance. The results of the CycD3;2 study in the Y2H system, which are opposite to the data from the BiFC and FLIM-FRET analyzes, suggested that Arabidopsis D3-type cyclins can form complexes with PCNA1/2. This is consistent with other data presented by Shimizu and Mori, who showed presence of the pea CycD3;1/PCNA complex (Shimizu and Mori, 1998). Moreover, the authors using anti-CycD3;1 immunoaffinity column chromatography demonstrated that PCNA could be co-precipitated only when extracts were prepared from dormant buds, but not growing buds. This finding indicates that the formation of D-type cyclin/PCNA complexes in plant cells might be dependent on cell status/developmental stage which could explain our results from the CycD3;2/PCNA analyzes. Studying CycD4;1 and CycD4;2, using Y2H, BiFC and FLIM-FRET technique, we discovered that both proteins were able to form complexes with PCNA1 and PCNA2. This result is consistent with experiments performed on maize embryos

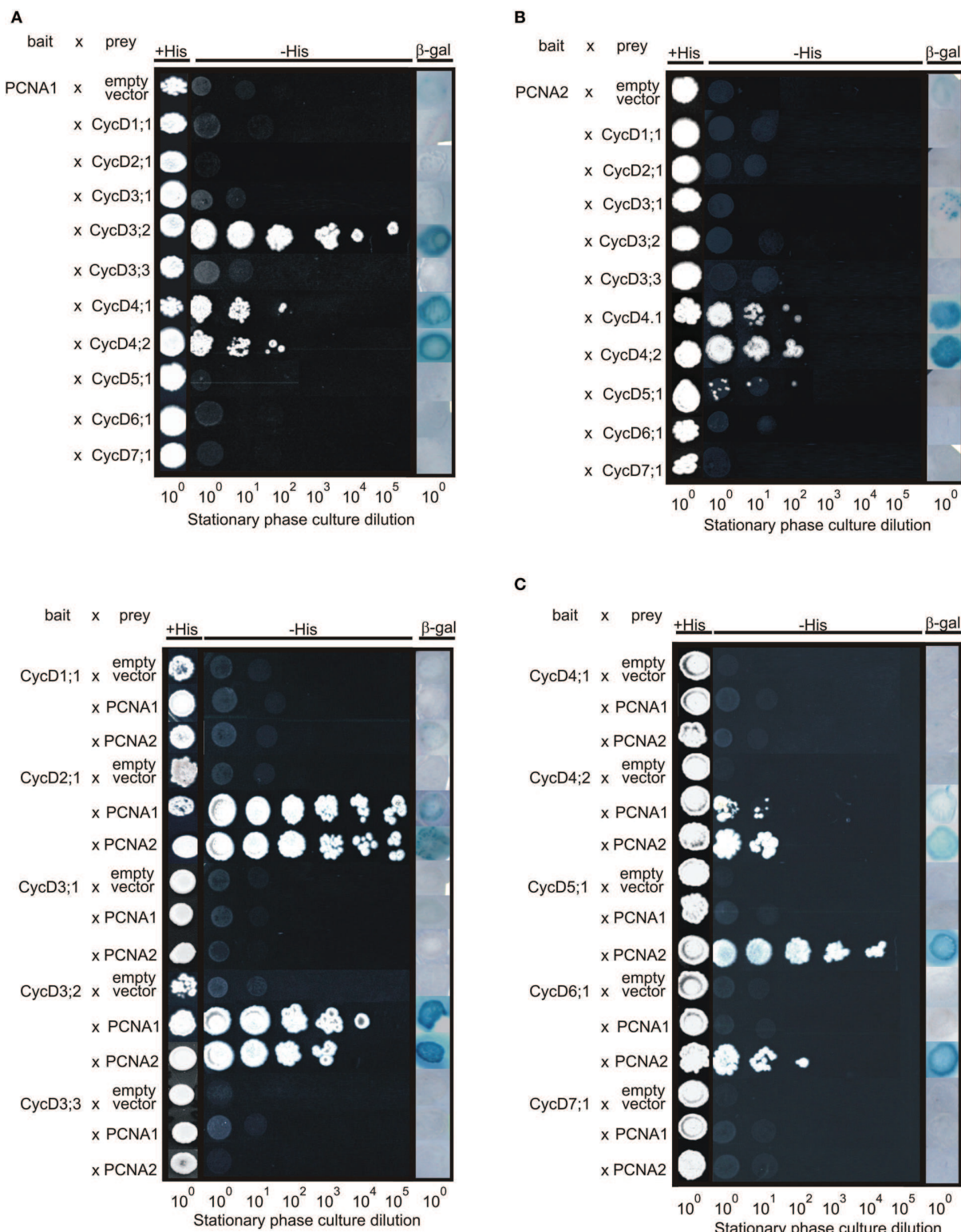


FIGURE 3 | Analysis of interactions between *Arabidopsis* PCNA1/2 and D-type cyclins using the split-uiquitin Y2H system. The interactions were tested in the following combinations. **(A)** PCNA1 (bait)/D-type cyclins (prey), **(B)** PCNA2 (bait)/D-type cyclins (prey), and **(C)** D-type cyclins (bait)/PCNA1/2 (prey). The transformed yeast cells were plated on either an SC-Leu-Trp control solid medium or an

SC-Leu-Trp-His selection solid medium supplemented with 10 mM 3-aminotriazol (3-AT). For the beta-galactosidase assay, the yeast transformants were grown on a nitrocellulose filter placed on the surface of a YPAD solid medium followed by incubation with X-gal. The results are representative of three independently repeated experiments.

TABLE 1 | Results of FLIM-FRET analysis and co-localization measurement (Pearson's correlation coefficient).

Donor protein	Acceptor protein	Pearson's correlation coefficient ± SD	Donor lifetime [τ_D (ns) ± SD]	Donor lifetime in the presence of potential acceptor [τ_{DA} (ns) ± SD]	FRET efficiency (%)
GFP	RFP	0.78 ± 0.03	2.51 ± 0.01	2.48 ± 0.01	1.19
PCNA2_GFP	RFP_PCNA2	0.77 ± 0.01	2.51 ± 0.01	2.39 ± 0.01	4.78
CycD1;1_GFP	RFP_PCNA1	0.83 ± 0.01	2.38 ± 0.02	2.37 ± 0.02	0.42
CycD1;1_GFP	RFP_PCNA2	0.84 ± 0.01	2.38 ± 0.02	2.36 ± 0.01	0.84
CycD2;1_GFP	RFP_PCNA1	0.71 ± 0.09	2.45 ± 0.01	2.41 ± 0.01	1.63
CycD2;1_GFP	RFP_PCNA2	0.70 ± 0.04	2.45 ± 0.01	2.43 ± 0.02	0.82
CycD3;1_GFP	RFP_PCNA1	0.92 ± 0.02	2.45 ± 0.02	2.44 ± 0.02	0.41
CycD3;1_GFP	RFP_PCNA2	0.92 ± 0.01	2.45 ± 0.02	2.44 ± 0.03	0.41
CycD3;2_GFP	RFP_PCNA1	0.86 ± 0.01	2.49 ± 0.01	2.48 ± 0.00	0.40
CycD3;2_GFP	RFP_PCNA2	0.84 ± 0.05	2.49 ± 0.01	2.48 ± 0.01	0.40
CycD3;3_GFP	RFP_PCNA1	0.80 ± 0.02	2.43 ± 0.04	2.42 ± 0.02	0.41
CycD3;3_GFP	RFP_PCNA2	0.90 ± 0.02	2.43 ± 0.04	2.40 ± 0.02	1.23
CycD4;1_GFP	RFP_PCNA1	0.80 ± 0.01	2.53 ± 0.01	2.43 ± 0.02	3.95
CycD4;1_GFP	RFP_PCNA2	0.71 ± 0.02	2.53 ± 0.01	2.48 ± 0.02	1.98
CycD4;2_GFP	RFP_PCNA1	0.70 ± 0.00	2.53 ± 0.01	2.44 ± 0.02	3.56
CycD4;2_GFP	RFP_PCNA2	0.74 ± 0.01	2.53 ± 0.01	2.40 ± 0.01	5.14
CycD5;1_GFP	RFP_PCNA1	0.83 ± 0.01	2.32 ± 0.02	2.31 ± 0.01	0.43
CycD5;1_GFP	RFP_PCNA2	0.85 ± 0.02	2.32 ± 0.02	2.30 ± 0.03	0.86
CycD6;1_GFP	RFP_PCNA1	0.85 ± 0.03	2.44 ± 0.01	2.34 ± 0.02	4.10
CycD6;1_GFP	RFP_PCNA2	0.82 ± 0.04	2.44 ± 0.01	2.37 ± 0.02	2.87
CycD7;1_GFP	RFP_PCNA1	0.93 ± 0.00	2.40 ± 0.01	2.25 ± 0.02	6.25
CycD7;1_GFP	RFP_PCNA2	0.86 ± 0.01	2.40 ± 0.01	2.31 ± 0.02	3.75
CycD1;1_GFP	PCNA1_RFP	0.87 ± 0.02	2.48 ± 0.01	2.45 ± 0.02	1.13
CycD1;1_GFP	PCNA2_RFP	0.87 ± 0.01	2.48 ± 0.01	2.49 ± 0.02	0.08
CycD2;1_GFP	PCNA1_RFP	0.79 ± 0.05	2.57 ± 0.01	2.54 ± 0.02	1.17
CycD2;1_GFP	PCNA2_RFP	0.77 ± 0.04	2.57 ± 0.01	2.54 ± 0.01	0.94
CycD3;1_GFP	PCNA1_RFP	0.90 ± 0.00	2.52 ± 0.01	2.48 ± 0.01	1.75
CycD3;1_GFP	PCNA2_RFP	0.89 ± 0.01	2.52 ± 0.01	2.50 ± 0.01	0.87
CycD3;2_GFP	PCNA1_RFP	0.82 ± 0.03	2.51 ± 0.01	2.49 ± 0.01	0.72
CycD3;2_GFP	PCNA2_RFP	0.83 ± 0.02	2.51 ± 0.01	2.48 ± 0.01	1.04
CycD3;3_GFP	PCNA1_RFP	0.84 ± 0.01	2.53 ± 0.01	2.49 ± 0.01	1.50
CycD3;3_GFP	PCNA2_RFP	0.86 ± 0.03	2.53 ± 0.01	2.49 ± 0.01	1.42
CycD4;1_GFP	PCNA1_RFP	0.93 ± 0.01	2.54 ± 0.03	2.49 ± 0.01	2.13
CycD4;1_GFP	PCNA2_RFP	0.91 ± 0.01	2.54 ± 0.03	2.50 ± 0.02	1.50
CycD4;2_GFP	PCNA1_RFP	0.86 ± 0.02	2.52 ± 0.02	2.50 ± 0.01	0.48
CycD4;2_GFP	PCNA2_RFP	0.80 ± 0.03	2.52 ± 0.02	2.50 ± 0.02	0.48
CycD5;1_GFP	PCNA1_RFP	0.85 ± 0.01	2.40 ± 0.03	2.39 ± 0.03	0.50
CycD5;1_GFP	PCNA2_RFP	0.86 ± 0.01	2.40 ± 0.03	2.40 ± 0.04	0.08
CycD6;1_GFP	PCNA1_RFP	0.87 ± 0.01	2.49 ± 0.01	2.46 ± 0.02	0.57
CycD6;1_GFP	PCNA2_RFP	0.87 ± 0.02	2.49 ± 0.01	2.48 ± 0.01	0.08
CycD7;1_GFP	PCNA1_RFP	0.92 ± 0.01	2.49 ± 0.02	2.43 ± 0.01	1.94
CycD7;1_GFP	PCNA2_RFP	0.90 ± 0.01	2.49 ± 0.02	2.44 ± 0.02	1.53

(τ_D) and (τ_{DA}) represent the average fluorescence lifetimes of donor proteins and donor proteins in the presence of a potential acceptor respectively. SD, standard deviation. The results are an average of three independent experiments.

where in immunoprecipitation studies PCNA was shown to be associated with CycD4;1 and CycD4;2 (Lara-Nunez et al., 2008; Becerril et al., 2012). Unexpectedly, the BiFC findings demonstrated that the complex of CycD4;1 and PCNA1/2 was not localized in the nucleus and cytoplasm, as observed for these proteins when analyzed separately, but was exclusively in the nuclear compartment (Figure 2; Strzalka et al., 2012). This

suggests that the formation of the CycD4;1/PCNA complex *in planta* is dependent on nuclear factor(s) or post-translational modification(s) which have not yet been identified. CycD5;1 studies in the yeast system revealed that this protein could be observed only in complex with PCNA2. This may suggest functional differentiation between PCNA1 and PCNA2 in the context of interaction with D-type cyclins. Nevertheless, BiFC

analysis did not confirm this finding but revealed that CycD5;1 formed complexes with both PCNA1 and PCNA2. In contrast to the BiFC experiments, the FLIM-FRET analysis did not show the formation of complexes between CycD5;1 and PCNA1/2 which is most probably the result of steric hindrance caused by GFP/RFP proteins. The results of the CycD6;1 analysis were identical to data from the CycD4;2 studies. Finally, in contrast to the results from Y2H analysis of CycD7;1, a very poorly characterized Arabidopsis D-type cyclin, the data from BiFC and FLIM-FRET studies showed formation of putative CycD7;1/PCNA1 or CycD7;1/PCNA2 complexes exclusively in the nucleus. Comparative analysis of the results from the FLIM-FRET analysis undoubtedly showed that the site of RFP fusion to PCNA affected the possibility of PCNA/D-type cyclin complexes formation.

The differences in the FRET efficiency detected for individual CycD and PCNA1/2 complexes were unexpected and possibly result from differences between PCNA1 and PCNA2 amino acid sequences. Unfortunately, the biochemical data which could help to characterize and compare the properties of Arabidopsis CycD and PCNA1/2 complexes are still not available mainly due to the lack of an efficient system which could provide large quantities of biologically active D-type cyclins. These data are necessary to verify and understand in detail the impact of PCNA1/2 amino acid differences on the formation of complexes with individual D-type cyclines, in the absence of other nuclear proteins.

In conclusion, we showed that most of the tested Arabidopsis D-type cyclins formed complexes with PCNA1/2 under the experimental conditions applied. The data from the Y2H and BiFC experiments did not provide convincing evidence for functional differentiation between PCNA1 and PCNA2 proteins in the context of their interaction with Arabidopsis D-type cyclins. However, FLIM-FRET analysis revealed a significant difference in the distance between PCNA1/2 and the CycD4;1, CycD4;2, CycD6;1, or CycD7;1 proteins (**Table 1**). The nine amino acid differences between PCNA1 and PCNA2 seems to have an impact on the architecture of CycD/PCNA complexes, which is reflected in the different spatial proximity between PCNA1/CycD4;1, PCNA1/CycD6;1, PCNA1/CycD7;1, and PCNA2/CycD4;2 proteins in comparison to PCNA2/CycD4;1, PCNA2/CycD6;1, PCNA2/CycD7;1, and PCNA1/CycD4;2 respectively. The key question is how far these differences are functionally relevant? It should be verified in the future whether the difference in the distance between PCNA1/2 and CycDs is related to the difference in the affinity between individual CycDs and PCNA1/PCNA2. If so, this could suggest that the formation of, e.g., CycD4;1/PCNA1 complex, which is characterized by

a shorter distance between this protein pair and possibly a lower value of the dissociation constant when compared to CycD4;1/PCNA2, could be preferred. If this is true then the complex characterized by a higher association constant could be functionally relevant. However, to verify this hypothesis additional new data are needed. The presented study does not yet provide the evidence for functional differentiation between PCNA1/CycD and PCNA2/CycD complexes in Arabidopsis. On the other hand the fact that not all of the 10 tested D-type cyclins were observed in complexes with PCNA shows that their roles are not equal in the context of interactions with Arabidopsis PCNA1/2. To conclude, the presented data are one of the significant milestones before the functional relevance of identified Arabidopsis CycDs/PCNA complexes will be the finally uncovered, especially in DNA replication and cell cycle control.

Acknowledgments

This project was supported by the National Science Center Poland (project no. Sonata-Bis3/UMO-2013/10/E/NZ1/00749 to WS). The Faculty of Biochemistry, Biophysics and Biotechnology is a partner of the Leading National Research Center (KNOW) supported by the Ministry of Science and Higher Education. We would like to thank Antonina Naskalska, Katarzyna Pels, Filip Bartnicki, and Carolina Borghetti for technical assistance.

Supplementary Material

The Supplementary Material for this article can be found online at: <http://journal.frontiersin.org/article/10.3389/fpls.2015.00516>

Supplementary Figure 1 | (A,B) Analysis of split GFP complexes formed between PCNA1 or PCNA2 and D-type cyclins. Confocal images of *N. benthamiana* leaf cells transiently expressing the analyzed open reading frames. All the images are overlays of bright field, autofluorescence of chlorophyll (red) and GFP fluorescence (green). This result is representative of three independently repeated experiments. **(C)** Analysis of D-type cyclin subcellular localization and the formation of complexes with either PCNA1 or PCNA2—bright-field confocal images of *N. benthamiana* leaf cells transiently expressing open reading frames presented at **Figure 2**. **(D)** Analysis of Arabidopsis PCNA1_GFP and PCNA2_GFP subcellular localization. The upper panel represents images that are overlays of bright field, autofluorescence of chlorophyll (red) and GFP fluorescence (green). The lower panel represents bright field confocal images of *N. benthamiana* leaf cells transiently expressing PCNA1_GFP or PCNA2_GFP.

Supplementary Table 1 | List of primers used in this study.

Supplementary Table 2 | The list of plasmids used in this study.

References

- Amoroso, A., Concia, L., Maggio, C., Raynaud, C., Bergounioux, C., Crespan, E., et al. (2011). Oxidative DNA damage bypass in *Arabidopsis thaliana* requires DNA polymerase λ and proliferating cell nuclear antigen 2. *Plant Cell* 23, 806–822. doi: 10.1105/tpc.110.081455

- Anderson, H. J., Vonarx, E. J., Pastushok, L., Nakagawa, M., Katafuchi, A., Gruz, P., et al. (2008). *Arabidopsis thaliana* Y-family DNA polymerase η catalyses translesion synthesis and interacts functionally with PCNA2. *Plant J.* 55, 895–908. doi: 10.1111/j.1365-313X.2008.03562.x
- Arabidopsis Genome Initiative. (2000). Analysis of the genome sequence of the flowering plant *Arabidopsis thaliana*. *Nature* 408, 796–815. doi: 10.1038/35048692

- Becerril, N., Martínez, M. A., García, E., and Vazquez-Ramos, J. M. (2012). Chromatin bound PCNA is complexed with cell cycle protein regulators as determined by chromatin immunoprecipitation. *J. Mex. Chem. Soc.* 56, 10–14.
- Boniotti, M. B., and Gutierrez, C. (2001). A cell-cycle-regulated kinase activity phosphorylates plant retinoblastoma protein and contains, in Arabidopsis, a CDKA/cyclin D complex. *Plant J.* 28, 341–350. doi: 10.1046/j.1365-313X.2001.01160.x
- Boruc, J., den Daele, H. V., Hollunder, J., Rombauts, S., Mylle, E., Hilson, P., et al. (2010). Functional modules in the *Arabidopsis* core cell cycle binary protein-protein interaction network. *Plant Cell* 22, 1264–1280. doi: 10.1105/tpc.109.073635
- Buendia-Monreal, M., Renteria-Canett, I., Guerrero-Andrade, O., Bravo-Alberto, C. E., Martinez-Castilla, L. P., Garcia, E., et al. (2011). The family of maize D-type cyclins: genomic organization, phylogeny and expression patterns. *Physiol. Plantarum.* 143, 297–308. doi: 10.1111/j.1399-3054.2011.01498.x
- Cruz-Ramirez, A., Diaz-Trivino, S., Blilou, I., Grieneisen, V. A., Sozzani, R., Zamioudis, C., et al. (2012). A bistable circuit involving SCARECROWRETINOBLASTOMA integrates cues to inform asymmetric stem cell division. *Cell* 150, 1002–1015. doi: 10.1016/j.cell.2012.07.017
- Fukami-Kobayashi, J., and Mitsui, J. (1999). Cyclin D1 inhibits cell proliferation through binding to PCNA and cdk2. *Exp. Cell Res.* 246, 338–347. doi: 10.1006/excr.1998.4306
- Godinez-Palma, S. K., García, E., de la Paz Sánchez, M., Rosas, F., and Vazquez-Ramos, J. M. (2013). Complexes of D-type cyclins with CDKs during maize germination. *J. Exp. Bot.* 64, 5661–5671. doi: 10.1093/jxb/ert340
- Gulbis, J. M., Kelman, Z., Hurwitz, J., O'Donnell, M., and Kuriyan, J. (1996). Structure of the C-terminal region of p21(WAF1/CIP1) complexed with human PCNA. *Cell* 87, 297–306.
- Gutierrez, R., Quiroz-Figueroa, F., and Vazquez-Ramos, J. M. (2005). Maize cyclin D2 expression, associated kinase activity and effect of phytohormones during germination. *Plant Cell Physiol.* 46, 166–173. doi: 10.1093/pcp/pcp007
- Harbour, J. W., and Dean, D. C. (2000). The Rb/E2F pathway: expanding roles and emerging paradigms. *Genes Dev.* 14, 2393–2409. doi: 10.1101/gad.813200
- Hata, S., Kouchi, H., Tanaka, Y., Minami, E., Matsumoto, T., Suzuka, I., et al. (1992). Identification of carrot cDNA clones encoding a second putative proliferating cell-nuclear antigen, DNA polymerase δ auxiliary protein. *Eur. J. Biochem.* 203, 367–371. doi: 10.1111/j.1432-1033.1992.tb16559.x
- Kono, A., Ohno, R., Umeda-Hara, C., Uchimiya, H., and Umeda, M. (2006). A distinct type of cyclin D, CYCD4;2, involved in the activation of cell division in *Arabidopsis*. *Plant Cell Rep.* 25, 540–545. doi: 10.1007/s00299-005-0075-4
- Kono, A., Umeda-Hara, C., Adachi, S., Nagata, N., Konomi, M., Nakagawa, T., et al. (2007). The *Arabidopsis* D-type cyclin CYCD4 controls cell division in the stomatal lineage of the hypocotyl epidermis. *Plant Cell* 19, 1265–1277. doi: 10.1105/tpc.106.046763
- Lara-Nunez A., de Jesus N., and Vazquez-Ramos, J. M. (2008). Maize D4;1 and D5 cyclin proteins in germinating maize. Associated kinase activity and regulation by phytohormones. *Physiol. Plant.* 132, 79–88. doi: 10.1111/j.1399-3054.2007.00995.x
- Lopez, I., Kahn, S., Vazquez, J., and Hussey, P. (1997). The proliferating cell nuclear antigen (PCNA) gene family in *Zea mays* is composed of two members that have similar expression programmes. *Biochim. Biophys. Acta* 1353, 1–6. doi: 10.1016/S0167-4781(97)00072-9
- Matsuoka, S., Yamaguchi, M., and Matsukage, A. (1994). D-type cyclin-binding regions of proliferating cell nuclear antigen. *J. Biol. Chem.* 269, 11030–11036.
- Meijer, M., and Murray, J. A. H. (2000). The role and regulation of D-type cyclins in the plant cell cycle. *Plant Mol. Biol.* 43, 621–633. doi: 10.1023/A:1006482115915
- Morris, G. F., and Mathews, M. B. (1989). Regulation of proliferating cell nuclear antigen during the cell cycle. *J. Biol. Chem.* 264, 13856–23864.
- Nakagami, H., Kawamura, K., Sugisaka, K., Sekine, M., and Shinmyo, A. (2002). Phosphorylation of Retinoblastoma-Related Protein by the cyclin D/cyclin-dependent kinase complex is activated at the G1/S-phase transition in Tobacco. *Plant Cell* 14, 1847–1857. doi: 10.1105/tpc.002550
- Nakagami, H., Sekine, M., Murakami, H., and Shinmyo, A. (1999). Tobacco retinoblastoma-related protein phosphorylated by a distinct cyclin- dependent kinase complex with Cdc2/cyclin D *in vitro*. *Plant J.* 18, 243–225. doi: 10.1046/j.1365-313X.1999.00449.x
- Paz Sanchez, M., Torres, A., Boniotti, M. B., Gutierrez, C., and Vazquez-Ramo, J. M. (2002). PCNA protein associates to Cdk-A type protein kinases in germinating maize. *Plant Mol. Biol.* 50, 167–175. doi: 10.1023/A:1016029001537
- Sanz, L., Dewitte, W., Forzani, C., Patell, F., Nieuwland, J., Wen, B., et al. (2011). The *Arabidopsis* D-Type cyclin CYCD2;1 and the inhibitor ICK2/KRP2 modulate auxin-induced lateral root formation. *Plant Cell* 23, 641–660. doi: 10.1105/tpc.110.080002
- Sherr, C. J., and Roberts, J. M. (2004). Living with or without cyclins and cyclin-dependent kinases. *Genes Dev.* 18, 2699–2711. doi: 10.1101/gad.1256504
- Shimizu, S., and Mori, H. (1998). Changes in protein interactions of cell cycle-related genes during the dormancy-to-growth transition in pea axillary buds. *Plant Cell Physiol.* 39, 1073–1079. doi: 10.1093/oxfordjournals.pcp.a029304
- Strzalka, W., and Aggarwal, C. (2013). *Arabidopsis thaliana* proliferating cell nuclear antigen 1 and 2 possibly form homo- and hetero-trimeric complexes in the plant cell. *Plant Signal. Behav.* 8:e24837. doi: 10.4161/psb.24837
- Strzalka, W., Bartnicki, F., Pels, K., Jakubowska, A., Tsurimoto, T., and Tanaka, K. (2013). RAD5a ubiquitin ligase is involved in ubiquitination of *Arabidopsis thaliana* proliferating cell nuclear antigen. *J. Exp. Bot.* 64, 859–869. doi: 10.1093/jxb/ers368
- Strzalka, W., Kaczmarek, A., Naganowska, B., and Ziemiowicz, A. (2010). Identification and functional analysis of PCNA1 and PCNA-like1 genes of *Phaseolus coccineus*. *J. Exp. Bot.* 61, 873–888. doi: 10.1093/jxb/erp354
- Strzalka, W., Labecki, P., Bartnicki, F., Aggarwal, C., Rapala-Kozik, M., Tani, C., et al. (2012). *Arabidopsis thaliana* proliferating cell nuclear antigen has several potential sumoylation sites. *J. Exp. Bot.* 63, 2971–2983. doi: 10.1093/jxb/ers002
- Strzalka, W., Oyama, T., Tori, K., and Morikawa, K. (2009). Crystal structure of the *Arabidopsis thaliana* proliferating cell nuclear antigen 1 and 2 proteins complexed with the human p21 C-terminal segment. *Prot. Sci.* 18, 1072–1080. doi: 10.1002/pro.117
- Strzalka, W., and Ziemiowicz, A. (2007). Molecular cloning of *Phaseolus vulgaris* cDNA encoding proliferating cell nuclear antigen. *J. Plant Physiol.* 164, 209–213. doi: 10.1016/j.jplph.2006.04.009
- Strzalka, W., and Ziemiowicz, A. (2011). Proliferating cell nuclear antigen (PCNA): a key factor in DNA replication and cell cycle regulation. *Ann. Bot.* 107, 1127–1140. doi: 10.1093/aob/mcq43
- Suzuka, I., Hata, S., Matsuoka, M., Kosugi, S., and Hashimoto, J. (1991). Highly conserved structure of proliferating cell nuclear antigen (DNA polymerase delta auxiliary protein) gene in plants. *Eur. J. Biochem.* 195, 571–575. doi: 10.1111/j.1432-1033.1991.tb15739.x
- Tom, S., Henricksen, L. A., Park, M. S., and Bambara, R. A. (2001). DNA Ligase I and proliferating cell nuclear antigen form a functional complex. *J. Biol. Chem.* 276, 24817–24825. doi: 10.1074/jbc.M101673200
- Vivona, J. B., and Kelman, Z. (2003). The diverse spectrum of sliding clamp interacting proteins. *FEBS Lett.* 546, 167–172. doi: 10.1016/S0014-5793(03)00622-7
- Wang, G., Kong, H., Sun, Y., Zhang, X., Zhang, W., Altman, N., et al. (2004). Genome-wide analysis of the cyclin family in *Arabidopsis* and comparative phylogenetic analysis of plant cyclin-like proteins. *Plant Physiol.* 135, 1084–1099. doi: 10.1104/pp.104.040436
- Wu, X., Li, J., Li, X., Hsieh, C.-L., Burgers, P. M. J., and Lieber, M. R. (1996). Processing of branched DNA intermediates by a complex of human FEN-1 and PCNA. *Nucleic Acids Res.* 24, 2036–2043. doi: 10.1093/nar/24.11.2036
- Xiong, Y., Zhang, H., and Beach, D. (1992). D type cyclins associate with multiple protein kinases and the DNA replication and repair factor PCNA. *Cell* 30, 505–514. doi: 10.1016/0092-8674(92)90518-H
- Conflict of Interest Statement:** The authors declare that the research was conducted in the absence of any commercial or financial relationships that could be construed as a potential conflict of interest.
- Copyright © 2015 Strzalka, Aggarwal, Krzeszowiec, Jakubowska, Sztatelman and Banas. This is an open-access article distributed under the terms of the Creative Commons Attribution License (CC BY). The use, distribution or reproduction in other forums is permitted, provided the original author(s) or licensor are credited and that the original publication in this journal is cited, in accordance with accepted academic practice. No use, distribution or reproduction is permitted which does not comply with these terms.**

Differential responses to high- and low-dose ultraviolet-B stress in tobacco Bright Yellow-2 cells

Shinya Takahashi^{1,2,3*}, **Kei H. Kojo**^{1,4}, **Natsumaro Kutsuna**^{1,4}, **Masaki Endo**⁵,
Seiichi Toki⁵, **Hiroko Isoda**^{2,3} and **Seiichiro Hazezawa**¹

¹ Department of Integrated Biosciences, Graduate School of Frontier Sciences, The University of Tokyo, Kashiwa, Japan,

² Alliance for Research on North Africa, University of Tsukuba, Tsukuba, Japan, ³ Ph. D. Program in Life Science Innovation, University of Tsukuba, Tsukuba, Japan, ⁴ LPixel Inc., Bunkyo-ku, Japan, ⁵ Plant Genome Engineering Research Unit, Agrogenomics Research Center, National Institute of Agrobiological Sciences, Tsukuba, Japan

OPEN ACCESS

Edited by:

Kaoru Okamoto Yoshiyama,
Kyoto Sangyo University, Japan

Reviewed by:

Jun Hidema,
Tohoku University, Japan
Gary Gardner,
University of Minnesota, USA

*Correspondence:

Shinya Takahashi,
Alliance for Research on North Africa,
University of Tsukuba, Tennodai 1-1-1,
Tsukuba, Ibaraki 305-8577, Japan
takahashi.shinya.fp@u.tsukuba.ac.jp

Specialty section:

This article was submitted to
Plant Physiology,
a section of the journal
Frontiers in Plant Science

Received: 29 January 2015
Paper pending published:
17 February 2015

Accepted: 31 March 2015
Published: 21 April 2015

Citation:

Takahashi S, Kojo KH, Kutsuna N,
Endo M, Toki S, Isoda H and
Hazezawa S (2015) Differential
responses to high- and low-dose
ultraviolet-B stress in tobacco Bright
Yellow-2 cells. *Front. Plant Sci.* 6:254.
doi: 10.3389/fpls.2015.00254

Ultraviolet (UV)-B irradiation leads to DNA damage, cell cycle arrest, growth inhibition, and cell death. To evaluate the UV-B stress-induced changes in plant cells, we developed a model system based on tobacco Bright Yellow-2 (BY-2) cells. Both low-dose UV-B (low UV-B: 740 J m⁻²) and high-dose UV-B (high UV-B: 2960 J m⁻²) inhibited cell proliferation and induced cell death; these effects were more pronounced at high UV-B. Flow cytometry showed cell cycle arrest within 1 day after UV-B irradiation; neither low- nor high-UV-B-irradiated cells entered mitosis within 12 h. Cell cycle progression was gradually restored in low-UV-B-irradiated cells but not in high-UV-B-irradiated cells. UV-A irradiation, which activates cyclobutane pyrimidine dimer (CPD) photolyase, reduced inhibition of cell proliferation by low but not high UV-B and suppressed high-UV-B-induced cell death. UV-B induced CPD formation in a dose-dependent manner. The amounts of CPDs decreased gradually within 3 days in low-UV-B-irradiated cells, but remained elevated after 3 days in high-UV-B-irradiated cells. Low UV-B slightly increased the number of DNA single-strand breaks detected by the comet assay at 1 day after irradiation, and then decreased at 2 and 3 days after irradiation. High UV-B increased DNA fragmentation detected by the terminal deoxynucleotidyl transferase dUTP nick end labeling assay 1 and 3 days after irradiation. Caffeine, an inhibitor of ataxia telangiectasia mutated (ATM) and ataxia telangiectasia and Rad3-related (ATR) checkpoint kinases, reduced the rate of cell death in high-UV-B-irradiated cells. Our data suggest that low-UV-B-induced CPDs and/or DNA strand-breaks inhibit DNA replication and proliferation of BY-2 cells, whereas larger contents of high-UV-B-induced CPDs and/or DNA strand-breaks lead to cell death.

Keywords: BY-2, cell cycle, cell death, checkpoint, DNA damage, ultraviolet-B

Introduction

Ultraviolet (UV)-B radiation (280–320 nm), a component of sunlight, is unavoidable for plants because of their sessile life. This radiation may lead to growth inhibition or even cell death. UV-B induces formation of pyrimidine photodimers, such as cyclobutane pyrimidine dimers (CPDs) and pyrimidine (6-4) pyrimidone photoproducts, and thus inhibits DNA replication and

transcription, increases the number of mutations, and induces cell cycle arrest and cell death (Lo et al., 2005; de Lima-Bessa et al., 2008). Higher plants have multiple DNA repair mechanisms (Mannuss et al., 2012). For example, under light, the UV-B-induced photodimers are repaired by photolyases specific to each photodimer; mammals have no homologous genes (Ahmad et al., 1997; Nakajima et al., 1998; Hidema et al., 2000; Takeuchi et al., 2007). Photolyases are activated by UV-A/blue light (Hada et al., 2000; Teranishi et al., 2008). The dark repair involves nucleotide excision repair and base excision repair mechanisms (Mannuss et al., 2012). Severe damage by ionizing radiation and UV-B radiation may also result in generation of DNA strand breaks, which are repaired by the homologous recombination, non-homologous end joining, and microhomology-mediated end joining systems (Ries et al., 2000; Amiard et al., 2013). Endoreduplication in response to UV-B irradiation has been reported; whether it may play a protective role in UV-B tolerance is unknown (Radziejewski et al., 2011).

In mammals, UV-B radiation interferes with cell cycle progression (Garinis et al., 2005; Ortolan and Menck, 2013). In Arabidopsis, photodimer formation causes cell cycle arrest and inhibits hypocotyl elongation (Biever et al., 2014). Arabidopsis shares several DNA damage checkpoint mechanisms with mammals and yeast (Yoshiyama et al., 2013b). The phosphatidyl-3-kinase family members, ataxia telangiectasia mutated (ATM) and ataxia telangiectasia and Rad3-related (ATR) kinases, are required for initiation of DNA damage responses (DDRs) (Roy, 2014). ATM mainly responds to DNA double-strand break (DSB) induced by ionizing radiation and chemical mutagens (Garcia et al., 2003). ATR mainly responds to single-stranded DNA (ssDNA) and replication stressors, such as hydroxyurea, aphidicolin, and UV stress (Culligan et al., 2004). In Arabidopsis, ATR, and its partner protein ATRIP are involved in tolerance to UV-B stress (Culligan et al., 2004; Sakamoto et al., 2009). Mammalian ATR and ATM phosphorylate checkpoint kinases 1 and 2 (CHK1 and CHK2) and activate the p53 transcription factor (Cimprich and Cortez, 2008; Shiloh and Ziv, 2013). However, plants have no homologs of p53, CHK1, or CHK2. In Arabidopsis, suppressor of gamma 1 (SOG1) functions in genotoxic stress-induced cell death and checkpoint mechanisms (Yoshiyama et al., 2009, 2013a; Adachi et al., 2011), and in UV-B-induced programmed cell death and growth retardation (Furukawa et al., 2010; Biever et al., 2014).

Although inhibition of cell cycle progression by UV-B in Arabidopsis root cells synchronized with hydroxyurea has been reported (Jiang et al., 2011), the details of UV-B-induced production of photodimers and their role in growth inhibition, cell cycle arrest, and cell death in higher plants remain unclear, in part because of the lack of appropriate experimental models.

Tobacco bright yellow-2 (BY-2) cells are non-green because they lack developed chloroplasts. They are larger than Arabidopsis cells, have high proliferation rates (80–100-fold per week) and are easy to synchronize for cell cycle progression studies (Nagata et al., 1992; Kumagai-Sano et al., 2006). BY-2 cells have also been used to study responses to pathogens, oxidative stress, and genotoxic stress, including UV stress (Perennes et al., 1999; Kadota et al., 2005; Sano et al., 2006; Lytvyn et al., 2010; Smetana et al.,

2012). They are highly suitable for observations of cell death and organelle alterations in response to stresses (Higaki et al., 2007).

In this study, to investigate cellular responses to UV-B irradiation, we developed a model using BY-2 cells. Low-dose UV-B irradiation inhibited cell proliferation and induced cell death with low frequency, whereas high doses induced cell death. This difference may have been caused by differences in the amounts of UV-B-induced photodimers, DNA strand breaks, or both. We also found that ATM, ATR, or both kinases mediated UV-B stress-induced cell death.

Materials and Methods

Plant Material and Culture Conditions

Tobacco BY-2 (*Nicotiana tabacum* L. cv. Bright Yellow 2) suspension-cultured cells were maintained by weekly dilution (1:95) with modified Linsmaier and Skoog (LS) medium as described by Kumagai-Sano et al. (2006). Cell suspensions were agitated on a rotary shaker at 130 rpm at 27°C in the dark.

UV Treatments

A UV-B fluorescent lamp (FL20SE; Kyokko Denki, Japan, **Supplemental Figure 1**) was used. Seven day-old BY-2 cells were diluted (1:40) with LS medium (Perennes et al., 1999) and incubated as above for 1 h; 10 mL of cell suspension was transferred into a plastic Petri dish, covered with a UV29 quartz glass filter (cut-off of <290 nm; Hoya Glass, Japan) (Ioki et al., 2008), and exposed to 1.6 W m^{-2} of UV-B for up to 31 min. In some experiments, immediately after UV-B irradiation, UV-A (18.3 W m^{-2}) was supplied by a UV-A fluorescent lamp (FL20S-BL; Toshiba, Japan, **Supplemental Figure 1**) through the UV29 quartz glass filter for 30 min. After irradiation, BY-2 cells were transferred to a flask and cultured with agitation under standard conditions. The intensities of UV-B and UV-A irradiation were measured by a MS-211-I UV photometer with a sensor specific to the UV-B and UV-A lamp spectrum (EKO Instruments, Japan).

Fresh Weight Determination

A 1-mL aliquot of cell suspension were transferred to microtubes and centrifuged for 30 s at 5000 rpm. Supernatants were removed by aspiration and pellets were weighed in at least three independent experiments.

Dead Cell Counting

Dead cells were detected by the Evans blue method as described by Ohno et al. (2011). In brief, cells from a 1-mL aliquot of suspension were collected by centrifugation, incubated with 0.05% Evans blue (Wako, Japan) for 10 min and then washed with water. Dead cells (stained blue) were counted under a microscope (BX51; Olympus, Japan). At least 500 cells were counted in each experiment.

Flow Cytometry

Flow cytometry was performed as described by Ohno et al. (2011). Frozen BY-2 cell pellets were chopped in extraction buffer with a sharp razor blade to extract the nuclei, filtered through 30- μm filters; isolated nuclei were stained with a CyStain UV Precise

P kit (Partec, Germany). DNA content was determined with a Ploidy Analyzer (Partec).

Synchronization of BY-2 Cells and Determination of Mitotic Index

BY-2 cells were synchronized as described by Kumagai-Sano et al. (2006). Mitotic index was determined by counting 4', 6-Diamidino-2-phenylindole, dihydrochloride (DAPI) stained nuclei using a fluorescence microscope (BX51). At least 300 cells were counted in each experiment.

DNA Extraction and Detection of UV-Induced CPD Formation by ELISA

Total genomic DNA was extracted from frozen BY-2 cell pellets using DNeasy Plant Mini Kit (QIAGEN, CA) and samples were diluted to $0.5 \mu\text{g mL}^{-1}$ with phosphate buffered saline (PBS) buffer. CPD formation was measured by enzyme-linked immuno-sorbent assay (ELISA) as previously described (Takeuchi et al., 1996; Takahashi et al., 2002) with slight modifications. Commercial monoclonal antibody BM12 (1:5000; Kyowa Medex Co., Japan) and ECL Anti-mouse IgG, Horseradish Peroxidase-linked Whole antibody (from sheep) (GE Healthcare, UK) were used and absorbance was measured at 492 nm by using a microplate reader (Viento nano; DS Pharma Biomedical, Japan).

Detection of DNA Strand Breaks by Comet Assay

Comet assay was performed as described by Menke et al. (2001) with modifications. In brief, frozen BY-2 cell pellets were chopped in PBS buffer with a razor blade to release the nuclei. The nuclei were filtered through the 30- μm filters, mixed with Comet LM agarose, applied to CometSlide (CometAssay kit; Trevigen Inc., Germany) on a heating block at 42°C; slides were incubated for 15 min at 4°C in the dark. The number of single-strand breaks was measured according to the alkaline/neutral (A/N) protocol (Menke et al., 2001). Slides were incubated in 0.3 M NaOH, 5 mM EDTA (pH 13.5) for 10 min at room temperature, equilibrated with 1× TBE buffer (3 × 5 min) at 4°C in the dark. Electrophoresis (25 V, 6 mA) was performed at room temperature in 1× TBE for 20 min. Then the slides were soaked in 1% Triton X-100 for 10 min, 70% EtOH (2 × 5 min), 99.5% EtOH (2 × 5 min), dried at 37°C for 30 min and stained with SYBR Green Gold Nucleic Acid cell stain (Invitrogen-Life Technologies, CA). Images were captured using a fluorescence microscope (BX51). Comet tails were quantified using the KBI plug-in “Cometassay” for ImageJ software (<http://hasezawa.ib.k.u-tokyo.ac.jp/zp/Kbi/ImageJKbiPlugins>).

Detection of DNA Fragmentation by TUNEL Assay

Terminal deoxynucleotidyl transferase dUTP nick-end labeling (TUNEL) assay was performed according to the manufacturer's protocol (*In Situ* Cell Death Detection Kit, Fluorescein; Roche Diagnostics GmbH, Germany) with modifications. Samples were fixed in 4% paraformaldehyde buffered with PBS for 20 min at 4°C, and labeled with fluorescein. Fluorescein signals and DAPI-stained cells were detected by using a fluorescence microscope.

Caffeine Treatment

Cells were treated with caffeine as described by Smetana et al. (2012). In brief, BY-2 cells were pretreated with 5 mM caffeine for 1 h, irradiated with high UV-B, cultured for 24 h, and the dead cells were counted as described above.

Statistical Analysis

Student's *t*-test in Microsoft Excel 2007 software was used for statistical analysis.

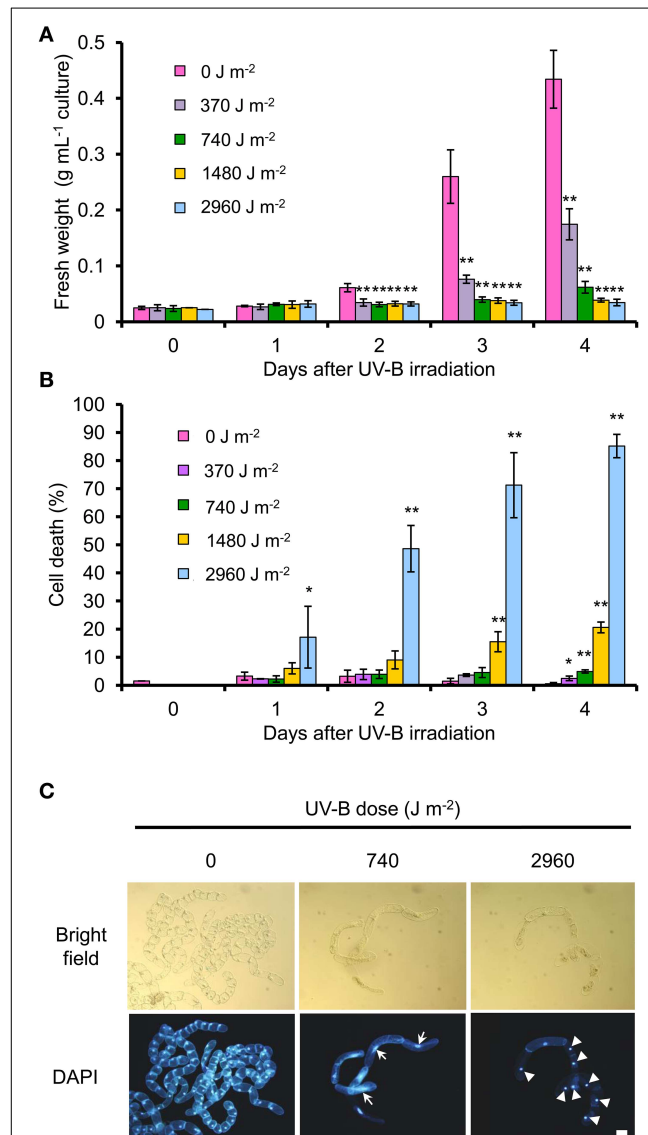


FIGURE 1 | Effect of UV-B radiation on cell proliferation and cell death. BY-2 cells were irradiated with UV-B (0–2960 J m^{-2}) and cultured for 4 days. The cells (1 mL) were centrifuged and the supernatant discarded. **(A)** Fresh weight of the collected cells was measured. **(B)** Evans blue staining was used to quantify dead cells. Results from at least two independent experiments are shown. Error bars show SD. Asterisks indicate significant differences from control (no UV-B) (* $P < 0.05$, ** $P < 0.01$). **(C)** Bright-field images and DAPI staining of control cells (no UV-B), or cells irradiated with low UV-B (740 J m^{-2}) or high UV-B (2960 J m^{-2}). Arrows indicate enlarged cells with elongated nuclei. Arrowheads indicate putative condensed nuclei. Bar = 50 μm .

Results

Effect of UV-B Irradiation on BY-2 Cell

Proliferation and Death

We determined how four different UV-B doses affect BY-2 cell proliferation and cell death. As an indicator of cell proliferation, we used fresh weight of centrifuged cell pellets. Cell proliferation was inhibited at 2 days after irradiation at all UV-B doses tested (**Figure 1A**). At 4 days after irradiation, the fresh weight of cells irradiated at 2960, 1480, and 740 J m^{-2} was <15% of that of non-irradiated cells, whereas the fresh weight of cells irradiated at 370 J m^{-2} was 41% of that of the control cells (**Figure 1A**). The number of dead cells reached 17% after UV-B irradiation at 2960 J m^{-2} at 1 day. At 4 days, it was 85% at 2960 J m^{-2} , 20.6% at 1480 J m^{-2} , and <10% at 740 J m^{-2} and 370 J m^{-2} (**Figure 1B**).

Thus, we set two UV-B conditions, low UV-B (740 J m^{-2}) to inhibit cell proliferation, and high UV-B (2960 J m^{-2}) to inhibit cell proliferation and induce cell death. Low UV-B resulted in only a small number of dead cells but led to the enlargement of the cells and nuclei (**Figure 1C**). Cell enlargement and nuclear elongation may be caused by increasing the nuclear DNA content above 4C (Yasuhara and Kitamoto, 2014). Low UV-B-irradiated cells did not reach the nuclear DNA content of 8C (data not shown). High UV-B irradiation led to cytoplasm shrinkage and nuclear condensation in dead cells (**Figure 1C**).

UV-B Irradiation Induces Cell Cycle Arrest in BY-2 Cells

The DNA content of most BY-2 cells in the stationary phase was 2C, indicating that most cells were at G1 phase before UV-B irradiation. At 1 day after low UV-B irradiation, the cell cycle was arrested at the 2C–4C transition (G1/S transition). At 3–4 days after UV-B irradiation, the number of cells at 4C (G2/M phase) increased but transition from S to G2/M phase and from G2/M to G1 was slower than that of non-irradiated cells (**Figure 2A**). After high UV-B irradiation, almost all cells were arrested at 2C at 1 or 2 days, and only a small number of cells reached 4C (**Figure 2A**).

Next, we synchronized the cells at the S phase by adding aphidicolin. In control cells, the mitotic index peaked at 7–9 h after aphidicolin release (**Figure 2B**). In low and high UV-B-irradiated cells, no clear peak of mitotic index was detected within 12 h after aphidicolin release (**Figure 2B**). Thus, we concluded that low and high UV-B irradiation induced cell cycle arrest at G1 or S phase; cell cycle arrest at G2/M may be also induced at 3–4 days after low UV-B irradiation.

UV-A Irradiation Suppresses Changes Induced by Low UV-B and Cell Death Induced by High UV-B Irradiation

To examine the possibility of repair of UV-B-induced damage by activating a photolyase, we checked the effects of UV-A irradiation. A 30-min exposure to UV-A radiation immediately after UV-B irradiation partially prevented inhibition of cell proliferation induced by low UV-B (**Figure 3A**) and cell death induced by low and high UV-B (**Figure 3B**). The number of low UV-B-irradiated cells with enlarged nuclei and increased cell volume decreased at 4 days after UV-A irradiation (**Figure 3C**).

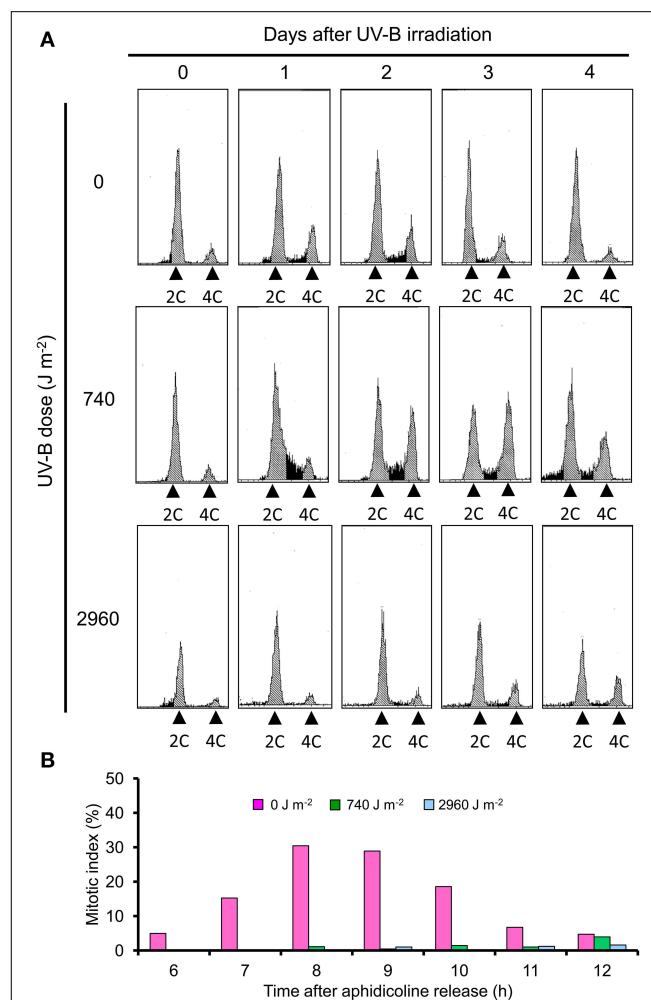


FIGURE 2 | Analysis of cell cycle progression in UV-B-irradiated BY-2 cells. (A) Cells irradiated with UV-B (0, 740, or 2960 J m^{-2}) were analyzed by flow cytometry. DNA ploidy distribution was measured with a ploidy analyzer (Partec, Germany). Typical data from at least two independent experiments are shown. **(B)** BY-2 cells were synchronized at S phase by aphidicolin and irradiated with UV-B (0, 740, or 2960 J m^{-2}) after release. Mitotic index was determined at indicated time points. Typical data from at least two independent experiments are shown.

UV-B Irradiation Induces CPD Formation, Which May Be Reduced by UV-A Irradiation

Immediately after irradiation, the CPD amounts in high UV-B-irradiated cells were approximately twice those in low UV-B-irradiated cells. In low UV-B-irradiated cells, the CPD content decreased by approximately 66% at 4 days after irradiation. In high UV-B-irradiated cells, the CPD content decreased by 52% at 4 days after irradiation (**Figure 4A, Supplemental Figure 2**).

The CPD content in cells exposed to UV-A following low UV-B irradiation was decreased by half in comparison with control cells. In high UV-B-irradiated cells, the CPD content was also significantly reduced by UV-A irradiation and reached the level observed in low UV-B-irradiated cells without UV-A irradiation (**Figure 4B**).

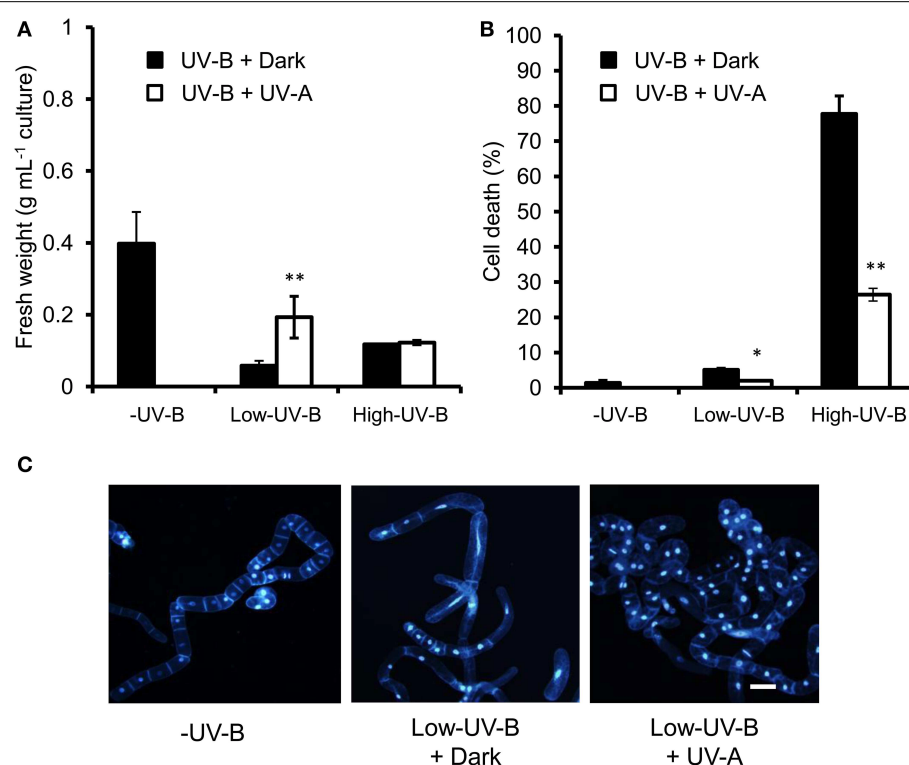


FIGURE 3 | Effects of UV-A radiation on UV-B-induced changes in cell proliferation and cell death. BY-2 cells were irradiated with UV-B (0, 740, or 2960 J m^{-2}), followed by 30-min incubation in the dark (UV-B + Dark) or 30 min UV-A irradiation (UVB + UVA). **(A)** Fresh

weight; **(B)** the percentage of dead cells. Error bars in **(A,B)** show SD ($n = 3$). Asterisks indicate significant differences from the UV-B + Dark treatment ($P < 0.05$, $^{**}P < 0.01$). **(C)** DAPI-stained cells at 4 d after irradiation. Bar = $50 \mu\text{m}$.

UV-B Irradiation Induces DNA Strand Breaks in BY-2 Cells

Immediately after irradiation with low or high UV-B, the number of single-strand breaks increased significantly. Single-strand breaks transiently increased at 1 day after low UV-B irradiation, and then gradually decreased at 2–3 days, whereas they continued to increase over 3 days after high UV-B irradiation (Figure 5). TUNEL assay detects fluorescent labeling of DNA strand breaks by using terminal deoxynucleotidyl transferase (TdT), which catalyzes the polymerization of labeled nucleotides to free 3'-OH DNA ends in a template-independent manner (Gavrieli et al., 1992). The TUNEL assay is often used to detect DNA fragmentation, including single-strand breaks and DSBs (Kwon et al., 2013). At 1 and 3 days after irradiation, TUNEL signals were detected in both low and high UV-B irradiated cells; the signals were observed more frequently in high UV-B-irradiated cells than in low UV-B-irradiated cells (Figure 6). These results suggest that low and high UV-B irradiation induces the single-strand breaks, and may cause DSB formation.

High UV-B Irradiation Induces ATM and ATR Kinase-Mediated Cell Cycle Arrest and/or Cell Death in BY-2 Cells

To confirm the roles of ATM and ATR kinases in the UV-B-induced cell death, we used their inhibitor, caffeine.

Pretreatment with caffeine for 1 h followed by high UV-B irradiation reduced cell death at 24 h (Figure 7). This result indicates that checkpoint signaling mediated by ATM, ATR, or both kinases is involved in high UV-B-induced cell death.

Discussion

UV-B radiation induces cell cycle arrest and cell death, yet how DNA damage triggers cell cycle arrest and cell death in plant cells remains unclear. In this study, we investigated the dose-dependence of inhibition of cell proliferation and induction of cell death by UV-B in BY-2 cells.

BY-2 Cells Irradiated with Low and High UV-B Show Different Damage Responses

Low UV-B inhibited cell proliferation and induced cell death with low frequency. The low UV-B-induced CPDs were formed but declined within several days. The UV-A exposure immediately after low UV-B irradiation prevented inhibition of cell proliferation and reduced the CPD content. High UV-B induced inhibition of cell proliferation and cell death. High UV-B induced larger amounts of CPDs than low UV-B, and they declined although somewhat slower. The UV-A exposure immediately after high UV-B irradiation prevented cell death but did not

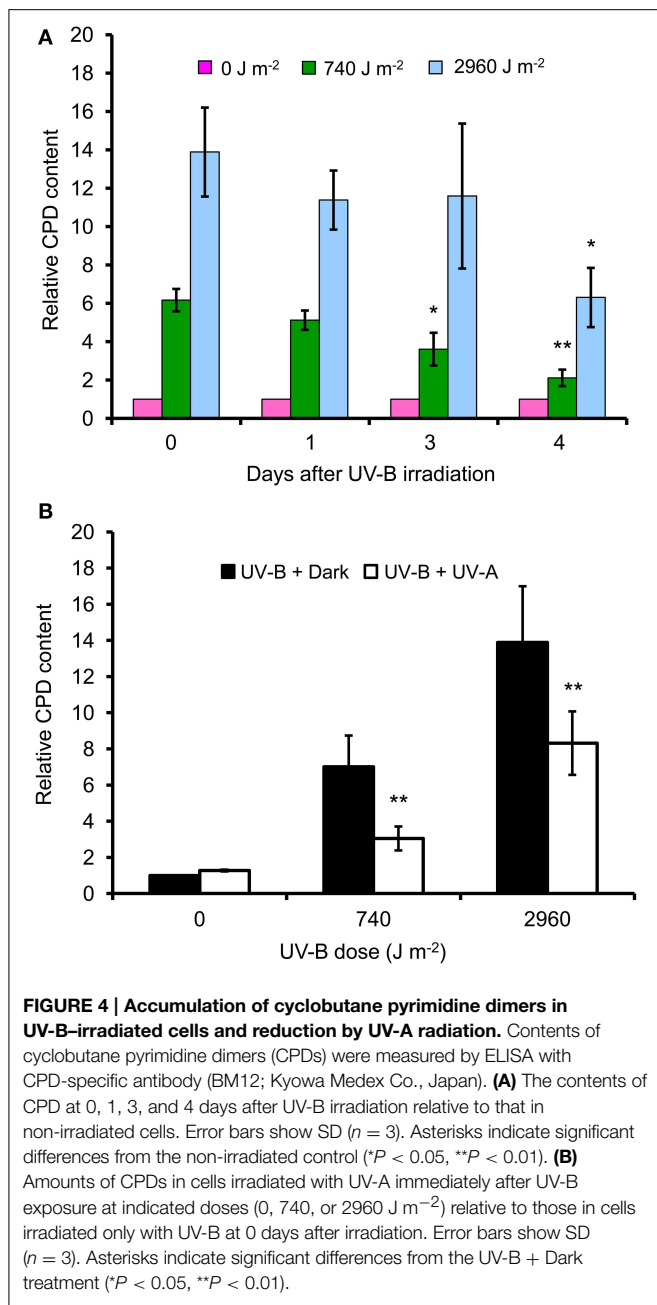


FIGURE 4 | Accumulation of cyclobutane pyrimidine dimers in UV-B-irradiated cells and reduction by UV-A radiation. Contents of cyclobutane pyrimidine dimers (CPDs) were measured by ELISA with CPD-specific antibody (BM12; Kyowa Medex Co., Japan). **(A)** The contents of CPD at 0, 1, 3, and 4 days after UV-B irradiation relative to that in non-irradiated cells. Error bars show SD ($n = 3$). Asterisks indicate significant differences from the non-irradiated control ($*P < 0.05$, $**P < 0.01$). **(B)** Amounts of CPDs in cells irradiated with UV-A immediately after UV-B exposure at indicated doses (0, 740, or 2960 J m⁻²) relative to those in cells irradiated only with UV-B at 0 days after irradiation. Error bars show SD ($n = 3$). Asterisks indicate significant differences from the UV-B + Dark treatment ($*P < 0.05$, $**P < 0.01$).

prevent inhibition of cell proliferation. These results suggest a strong relationship between CPD formation and dose-dependent inhibition of cell proliferation and induction of cell death by UV-B.

In low UV-B-irradiated cells, CPDs were detected until 3–4 days, but cell proliferation and cell cycle progression were observed. In plants, translesion DNA synthesis is involved in UV-B tolerance (Sakamoto et al., 2003; Takahashi et al., 2005; Anderson et al., 2008). Translesion DNA synthesis-type DNA polymerases bypass DNA lesions and allow DNA synthesis to progress with DNA lesions. This mechanism might be functional in BY-2 cells.

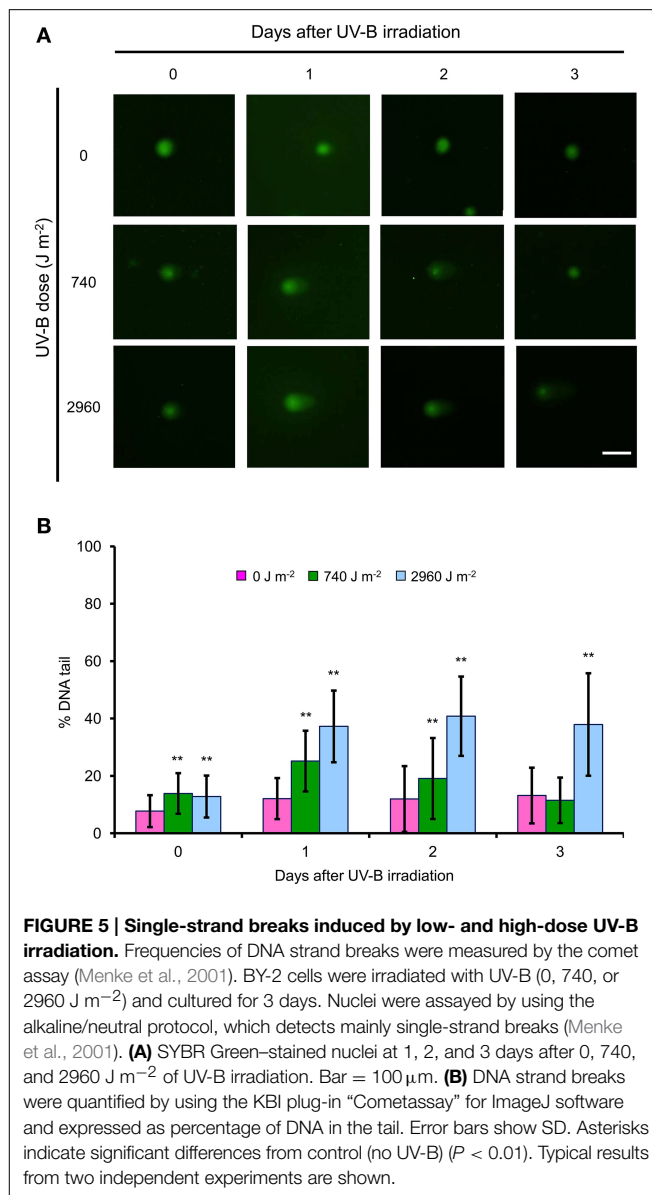
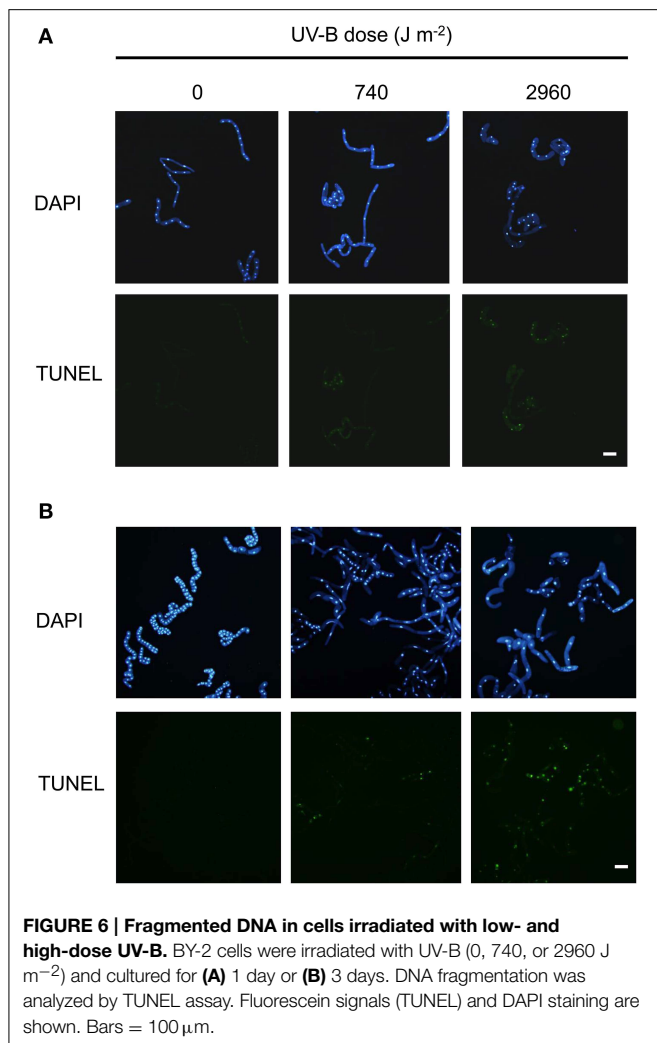


FIGURE 5 | Single-strand breaks induced by low- and high-dose UV-B irradiation. Frequencies of DNA strand breaks were measured by the comet assay (Menke et al., 2001). BY-2 cells were irradiated with UV-B (0, 740, or 2960 J m⁻²) and cultured for 3 days. Nuclei were assayed by using the alkaline/neutral protocol, which detects mainly single-strand breaks (Menke et al., 2001). **(A)** SYBR Green-stained nuclei at 1, 2, and 3 days after 0, 740, and 2960 J m⁻² of UV-B irradiation. Bar = 100 μm. **(B)** DNA strand breaks were quantified by using the KBI plug-in “Cometassay” for ImageJ software and expressed as percentage of DNA in the tail. Error bars show SD. Asterisks indicate significant differences from control (no UV-B) ($P < 0.01$). Typical results from two independent experiments are shown.

Low UV-B-Induced CPDs May Generate Transient single-Strand Breaks and Induce Cell Cycle Arrest

Low UV-B irradiation led to transient single-strand breaks and cell cycle arrest during the G1 and S phases at 1–2 days. The amounts of CPDs and single-strand breaks were reduced and cell cycle progression restarted at 3–4 days after UV-B irradiation. In *Arabidopsis*, the ATR-mediated pathway provides tolerance to UV-B stress (Culligan et al., 2004; Sakamoto et al., 2009). DNA integrity may be restored by ATR recruitment and DNA lesion bypass activity (Furukawa et al., 2010; Curtis and Hays, 2011). The ATR-mediated pathway might be activated by the presence of single-strand breaks and trigger cell cycle arrest in our system.

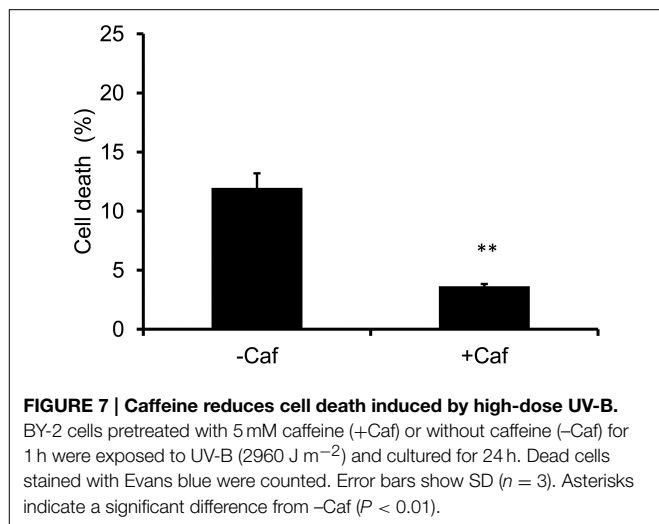
In addition to cell cycle arrest during the G1 and S phases at 1–2 days after UV-B irradiation, many cells were arrested at the G2/M checkpoint at 2–3 days after UV-B irradiation. In



Arabidopsis roots, UV-B downregulates the expression of *Histone H4* and *E2Fa* (cell cycle progression markers), delays *CYCD3;1* (a positive factor in G1-to-S transition) expression, and upregulates the expression of *KRP2* (a negative regulator of the G1-to-S transition), suggesting that UV-B irradiation induces the G1-to-S arrest (Jiang et al., 2011). Molecular mechanisms of UV-B-induced cell cycle arrest are still mostly unknown. It is interesting to analyze the temporal expression of G1/S or G2/M-specific marker genes after UV-B irradiation.

High UV-B Induces Large CPD Amounts, Persistent Single-strand Breaks, Permanent Cell Cycle Arrest, and High Rate of Cell Death

High UV-B irradiation induced CPDs (twice as many as low UV-B did), single-strand breaks, and permanent cell cycle arrest at the G1/S transition. CPD accumulation may induce single-strand breaks (and eventually DSBs), and prolonged presence of CPDs or single-strand breaks may accelerate cell death (Garinis et al., 2005; Lopes et al., 2006). In Arabidopsis root tip stem-cell niches, programmed cell death induced by roughly 30,000 unrepaired photoadducts generated by UV-B irradiation was



similar to that caused by 24 DSBs generated by gamma radiation (Furukawa et al., 2010). In Arabidopsis, the entry into S phase in the presence of ssDNA may generate DSBs due to collapse of DNA replication forks (Curtis and Hays, 2011). Thus, high UV-B may induce not only CPDs and single-strand breaks but DSB formation, and trigger cell death.

Among high UV-B-irradiated cells, TUNEL-positive cells were observed from the next day after irradiation; fewer TUNEL-positive cells were observed upon low UV-B irradiation. Bleomycin-treated BY-2 cells show paraptosis-type cell death without DNA fragmentation (Smetana et al., 2012), whereas BY-2 cells exposed to very high UV-B (283 kJ m^{-2}) show apoptosis-type programmed cell death that involves DNA fragmentation (Lytvyn et al., 2010). High UV-B-induced cell death observed in this study is likely apoptosis-like programmed cell death.

Checkpoint Kinases, ATM and ATR, May Regulate UV-B-Induced Cell Death

In our study, caffeine treatment reduced high UV-B-induced cell death. UV-B may activate both ATR-mediated and ATM-mediated pathways (Furukawa et al., 2010). Because caffeine inhibits both ATR and ATM pathways, their relative contributions are unclear. In mammals, caffeine inhibits UV-B mediated ATR/Chk1 pathways and decreases the levels and phosphorylation of Cyclin B1, which mediates entry to mitosis (Conney et al., 2013). Whether this also takes place in plants is unclear. In the future, we will need to investigate which pathway contributes most to UV-B-induced cell death in BY-2 cells.

ATM and ATR kinase-mediated DDRs regulate programmed cell death (Fulcher and Sablowski, 2009). In Arabidopsis DDR mutants, UV-B-induced DNA strand breaks trigger ATM/ATR/SOG1-mediated cell death (Furukawa et al., 2010; Curtis and Hays, 2011). In this study, we directly observed the formation of UV-B-induced CPDs and transient formation of single-strand breaks. Their content may affect the survival vs. cell death choice in UV-B-irradiated BY-2 cells; at least, our data show that the ATM/ATR pathways mediate

high UV-B-induced cell death and thus provide evidence for DDR-mediated UV-B-induced cell death in BY-2 cells.

Advantages and Disadvantages of the BY-2 Cell Model for Studying UV-B Responses

In green tissues, it may often be difficult to interpret the effects of UV-B on growth retardation because UV-B also affects photosynthesis (Allen et al., 1997; Takeuchi et al., 2002). Thus, the potential effects of UV-B on the cell cycle or signal transduction are difficult to distinguish from its direct effects on photosynthesis. As BY-2 cells are non-green, they do not pose these problems in studies of UV-B responses.

Non-green tissues, such as those of etiolated seedlings, might offer an advantage for investigations of photoregulation of light-responsive genes (Gardner et al., 2009). UV-B activates the phenylpropanoid pathway, which includes phenylalanine ammonia-lyase and chalcone synthase (CHS), and it serves to synthesize UV-B-absorbing compounds such as flavonoids (Kusano et al., 2011). This mechanism is mediated by the UV-B-specific receptor UV-resistance 8 (UVR8) (Brown and Jenkins, 2008; Biever et al., 2014). It would be interesting to investigate the physiological roles of the UV-B-inducible flavonoid biosynthesis pathway in regulation of the cell cycle by using the BY-2 model system if the CHS and UVR8 genes are expressed in these cells.

Few studies of UV-B effects on plant cellular components are available (Lytvyn et al., 2010). In mammalian cells, UV-B induces apoptosis by a mechanism that involves caspase-8 activation and mitochondrial dysfunction (Takasawa et al., 2005). BY-2 cells are also good experimental tools for studying organelles, including mitochondria (Arimura et al., 2004; Sano et al., 2005; Higaki et al., 2007); it would be interesting to investigate UV-B-induced changes in subcellular compartments to clarify the mechanisms leading to cell death in these cells.

References

- Adachi, S., Minamisawa, K., Okushima, Y., Inagaki, S., Yoshiyama, K., Kondou, Y., et al. (2011). Programmed induction of endoreduplication by DNA double-strand breaks in *Arabidopsis*. *Proc. Natl. Acad. Sci. U.S.A.* 108, 10004–10009. doi: 10.1073/pnas.1103584108
- Ahmad, M., Jarillo, J. A., Klimczak, L. J., Landry, L. G., Peng, T., Last, R. L., et al. (1997). An enzyme similar to animal type II photolyases mediates photoreactivation in *Arabidopsis*. *Plant Cell*. 9, 199–207. doi: 10.1105/tpc.9.2.199
- Allen, D. J., McKee, I. F., Farage, P. K., and Baker, N. R. (1997). Analysis of limitations to CO₂ assimilation on exposure of leaves of two *Brassica napus* cultivars to UV-B. *Plant Cell Environ.* 20, 633–640 doi: 10.1111/j.1365-3040.1997.00093.x
- Amiard, S., Gallego, M. E., and White, C. I. (2013). Signaling of double strand breaks and deprotected telomeres in *Arabidopsis*. *Front. Plant Sci.* 4:405. doi: 10.3389/fpls.2013.00405
- Anderson, H. J., Vonarx, E. J., Pastushok, L., Nakagawa, M., Katafuchi, A., Gruz, P., et al. (2008). *Arabidopsis thaliana* Y-family DNA polymerase eta catalyzes translesion synthesis and interacts functionally with PCNA2. *Plant J.* 55, 895–908. doi: 10.1111/j.1365-313X.2008.03562.x
- Arimura, S., Yamamoto, J., Aida, G. P., Nakazono, M., and Tsutsumi, N. (2004). Frequent fusion and fission of plant mitochondria with unequal nucleoid disruption. *Proc. Natl. Acad. Sci. U.S.A.* 101, 7805–7808. doi: 10.1073/pnas.0401077101
- Biever, J. J., Brinkman, D., and Gardner, G. (2014). UV-B inhibition of hypocotyl growth in etiolated *Arabidopsis thaliana* seedlings is a consequence of cell cycle arrest initiated by photodimer accumulation. *J. Exp. Bot.* 65, 2949–2961. doi: 10.1093/jxb/eru035
- Brown, B. A., and Jenkins, G. I. (2008). UV-B signaling pathways with different fluence-rate response profiles are distinguished in mature arabidopsis leaf tissue by requirement for UVR8, HY5, and HYH. *Plant Physiol.* 146, 576–588 doi: 10.1104/pp.107.108456
- Cimprich, K. A., and Cortez, D. (2008). ATR: an essential regulator of genome integrity. *Nat. Rev. Mol. Cell. Biol.* 9, 616–627. doi: 10.1038/nrm2450
- Conney, A. H., Lu, Y. P., Lou, Y. R., Kawasumi, M., and Nghiem, P. (2013). Mechanisms of caffeine-induced inhibition of UVB carcinogenesis. *Front. Oncol.* 3:144. doi: 10.3389/fonc.2013.00144
- Culligan, K., Tissier, A., and Britt, A. (2004). ATR regulates a G2-phase cell-cycle checkpoint in *Arabidopsis thaliana*. *Plant Cell* 16, 1091–1104. doi: 10.1105/tpc.018903
- Curtis, M. J., and Hays, J. B. (2011). Cooperative responses of DNA-damage-activated protein kinases ATR and ATM and DNA translesion polymerases to replication-blocking DNA damage in a stem-cell niche. *DNA Repair* 10, 1272–1281. doi: 10.1016/j.dnarep.2011.10.001
- de Lima-Bessa, K. M., Armelin, M. G., Chigancas, V., Jacysyn, J. F., Amarante-Mendes, G. P., Sarasin, A., et al. (2008). CPDs and 6-4PPs play different roles in UV-induced cell death in normal and NER-deficient human cells. *DNA Repair* 7, 303–312. doi: 10.1016/j.dnarep.2007.11.003

Although an expressed sequence tag clone library of BY-2 cells has been established (Matsuoka et al., 2004; Gális et al., 2006), the complete tobacco genome sequence (unlike the Arabidopsis genome sequence) has not been available until recently, and this has limited molecular analysis in BY-2 cells. In 2014, the draft genome sequence of *Nicotiana tabacum*, which is the source of the BY-2 line, was published (Siervo et al., 2014). In future, this information, coupled with use of the BY-2 cell model, may help to clarify in detail how UV-B affects plant cells, from the initial signaling events to cellular responses to UV-B irradiation.

In this study, we used an experimental model to investigate temporal changes in UV-B-induced damage responses in BY-2 cells. Our results suggest that DNA damage mediates UV-B dose-dependent responses that affect cell cycle regulation and cell death.

Acknowledgments

The authors thank Dr. Nobuyoshi Nakajima (National Institute for Environmental Studies), Dr. Kazuhito Matsuo (National Institute for Agro-Environmental Sciences), Dr. Yuichi Takeuchi (Tokai University), Dr. Shigeyuki Kawano (The University of Tokyo), Dr. Yasuhiro Kadota (RIKEN) and Dr. Takumi Higaki (The University of Tokyo) for their technical support and valuable suggestions. This work was supported by Japan Society for the Promotion of Science KAKENHI Grant No. 26340044 (to ST) and No. 24770038 (to NK).

Supplementary Material

The Supplementary Material for this article can be found online at: <http://journal.frontiersin.org/article/10.3389/fpls.2015.00254/abstract>

- Fulcher, N., and Sablowski, R. (2009). Hypersensitivity to DNA damage in plant stem cell niches. *Proc. Natl. Acad. Sci. U.S.A.* 106, 20984–20988. doi: 10.1073/pnas.0909218106
- Furukawa, T., Curtis, M. J., Tominey, C. M., Duong, Y. H., Wilcox, B. W., Aggoune, D., et al. (2010). A shared DNA-damage-response pathway for induction of stem-cell death by UVB and by gamma irradiation. *DNA Repair* 9, 940–948. doi: 10.1016/j.dnarep.2010.06.006
- Gális, I., Šimek, P., Sasaki, M., Horiguchi, T., Fukuda, H., Matsuoka, K., et al. (2006). A novel R2R3 MYB transcription factor NtMYBJS1 is a methyl jasmonate-dependent regulator of phenylpropanoid-conjugated biosynthesis in tobacco. *Plant J.* 46, 573–592 doi: 10.1111/j.1365-313X.2006.02719.x
- Garcia, V., Bruchet, H., Camescasse, D., Granier, F., Bouchez, D., and Tissier, A. (2003). AtATM is essential for meiosis and the somatic response to DNA damage in plants. *Plant Cell* 15, 119–132. doi: 10.1105/tpc.006577
- Gardner, G., Lin, C., Tobin, E. M., Loerher, H., and Brinkman, D. (2009). Photobiological properties of the inhibition of etiolated *Arabidopsis* seedling growth by ultraviolet-B irradiation. *Plant Cell Environ.* 32, 1573–1583. doi: 10.1111/j.1365-3040.2009.02021.x
- Garinis, G. A., Mitchell, J. R., Moorhouse, M. J., Hanada, K., De Waard, H., Vandepitte, D., et al. (2005). Transcriptome analysis reveals cyclobutane pyrimidine dimers as a major source of UV-induced DNA breaks. *EMBO J.* 24, 3952–3962. doi: 10.1038/sj.emboj.7600849
- Gavrieli, Y., Sherman, Y., and Ben-Sasson, S. A. (1992). Identification of programmed cell death *in situ* via specific labeling of nuclear DNA fragmentation. *J. Cell. Biol.* 119, 493–501 doi: 10.1083/jcb.119.3.493
- Hada, M., Iida, Y., and Takeuchi, Y. (2000). Action spectra of DNA photolyases for photorepair of cyclobutane pyrimidine dimers in sorghum and cucumber. *Plant Cell Physiol.* 41, 644–648. doi: 10.1093/pcp/41.5.644
- Hidema, J., Kumagai, T., and Sutherland, B. M. (2000). UV radiation-sensitive norin 1 rice contains defective cyclobutane pyrimidine dimer photolyase. *Plant Cell* 12, 1569–1578. doi: 10.1105/tpc.12.9.1569
- Higaki, T., Goh, T., Hayashi, T., Kutsuna, N., Kadota, Y., Hasezawa, S., et al. (2007). Elicitor-induced cytoskeletal rearrangement relates to vacuolar dynamics and execution of cell death: *in vivo* imaging of hypersensitive cell death in tobacco BY-2 cells. *Plant Cell Physiol.* 48, 1414–1425. doi: 10.1093/pcp/pcm109
- Ioki, M., Takahashi, S., Nakajima, N., Fujikura, K., Tamaoki, M., Saji, H., et al. (2008). An unidentified ultraviolet-B-specific photoreceptor mediates transcriptional activation of the cyclobutane pyrimidine dimer photolyase gene in plants. *Planta* 229, 25–36. doi: 10.1007/s00425-008-0803-4
- Jiang, L., Wang, Y., Bjorn, L. O., and Li, S. (2011). UV-B-induced DNA damage mediates expression changes of cell cycle regulatory genes in *Arabidopsis* root tips. *Planta* 233, 831–841. doi: 10.1007/s00425-010-1340-5
- Kadota, Y., Furuchi, T., Sano, T., Kaya, H., Gunji, W., Murakami, Y., et al. (2005). Cell-cycle-dependent regulation of oxidative stress responses and Ca^{2+} permeable channels NtTPC1A/B in tobacco BY-2 cells. *Biochem. Biophys. Res. Commun.* 336, 1259–1267. doi: 10.1016/j.bbrc.2005.09.004
- Kumagai-Sano, F., Hayashi, T., Sano, T., and Hasezawa, S. (2006). Cell cycle synchronization of tobacco BY-2 cells. *Nat. Protoc.* 1, 2621–2627. doi: 10.1038/nprot.2006.381
- Kusano, M., Tohge, T., Fukushima, A., Kobayashi, M., Hayashi, N., Otsuki, H., et al. (2011). Metabolomics reveals comprehensive reprogramming involving two independent metabolic responses of *Arabidopsis* to UV-B light. *Plant J.* 67, 354–369. doi: 10.1111/j.1365-313X.2011.04599.x
- Kwon, Y. I., Abe, K., Endo, M., Osakabe, K., Ohtsuki, N., Nishizawa-Yokoi, A., et al. (2013). DNA replication arrest leads to enhanced homologous recombination and cell death in meristems of rice OsRecQL4 mutants. *BMC Plant Biol.* 13:62. doi: 10.1186/1471-2229-13-62
- Lo, H. L., Nakajima, S., Ma, L., Walter, B., Yasui, A., Ethell, D. W., et al. (2005). Differential biologic effects of CPD and 6-4PP UV-induced DNA damage on the induction of apoptosis and cell-cycle arrest. *BMC Cancer* 5:135. doi: 10.1186/1471-2407-5-135
- Lopes, M., Foiani, M., and Sogo, J. M. (2006). Multiple mechanisms control chromosome integrity after replication fork uncoupling and restart at irreparable UV lesions. *Mol. Cell.* 21, 15–27. doi: 10.1016/j.molcel.2005.11.015
- Lytvyn, D. I., Yemets, A. I., and Blume, Y. B. (2010). UV-B overexposure induces programmed cell death in a BY-2 tobacco cell line. *Environ. Exp. Bot.* 68, 51–57. doi: 10.1016/j.envexpbot.2009.11.004
- Mannuss, A., Trapp, O., and Puchta, H. (2012). Gene regulation in response to DNA damage. *Biochim. Biophys. Acta* 1819, 154–165. doi: 10.1016/j.bbagen.2011.08.003
- Matsuoka, K., Demura, T., Galis, I., Horiguchi, T., Sasaki, N., Tashiro, G., et al. (2004). A comprehensive gene expression analysis toward the understanding of growth and differentiation of tobacco BY-2 cells. *Plant Cell Physiol.* 45, 1280–1289. doi: 10.1093/pcp/pch155
- Menke, M., Chen, I., Angelis, K. J., and Schubert, I. (2001). DNA damage and repair in *Arabidopsis thaliana* as measured by the comet assay after treatment with different classes of genotoxins. *Mutat. Res.* 493, 87–93. doi: 10.1016/S1383-5718(01)00165-6
- Nagata, T., Nemoto, Y., and Hasezawa, S. (1992). Tobacco By-2 cell line as the “HeLa” cell in the cell biology of higher plants. *Int. Rev. Cytol.* 132, 1–30. doi: 10.1016/S0074-7696(08)62452-3
- Nakajima, S., Sugiyama, M., Iwai, S., Hitomi, K., Otoshi, E., Kim, S. T., et al. (1998). Cloning and characterization of a gene (UVR3) required for photorepair of 6-4 photoproducts in *Arabidopsis thaliana*. *Nucleic Acids Res.* 26, 638–644. doi: 10.1093/nar/26.2.638
- Ohno, R., Kadota, Y., Fujii, S., Sekine, M., Umeda, M., and Kuchitsu, K. (2011). Cryptogein-Induced cell cycle arrest at G2 phase is associated with inhibition of cyclin-dependent kinases, suppression of expression of cell cycle-related genes and protein degradation in synchronized tobacco BY-2 cells. *Plant Cell Physiol.* 52, 922–932. doi: 10.1093/pcp/pcp042
- Ortolan, T. G., and Menck, C. F. (2013). UVB-induced cell death signaling is associated with G1-S progression and transcription inhibition in primary human fibroblasts. *PLoS ONE* 8:e76936. doi: 10.1371/journal.pone.0076936
- Perennes, C., Glab, N., Guglieni, B., Doutriaux, M. P., Phan, T. H., Planchais, S., et al. (1999). Is arcA3 a possible mediator in the signal transduction pathway during agonist cell cycle arrest by salicylic acid and UV irradiation? *J. Cell Sci.* 112, 1181–1190.
- Radziejewski, A., Vlieghe, K., Lammens, T., Berckmans, B., Maes, S., Jansen, M. A., et al. (2011). Atypical E2F activity coordinates PHR1 photolyase gene transcription with endoreduplication onset. *EMBO J.* 30, 355–363. doi: 10.1038/embj.2010.313
- Ries, G., Buchholz, G., Frohnmyer, H., and Hohn, B. (2000). UV-damage-mediated induction of homologous recombination in *Arabidopsis* is dependent on photosynthetically active radiation. *Proc. Natl. Acad. Sci. U.S.A.* 97, 13425–13429. doi: 10.1073/pnas.230251897
- Roy, S. (2014). Maintenance of genome stability in plants: repairing DNA double strand breaks and chromatin structure stability. *Front. Plant Sci.* 5:487. doi: 10.3389/fpls.2014.00487
- Sakamoto, A., Lan, V. T., Hase, Y., Shikazono, N., Matsunaga, T., and Tanaka, A. (2003). Disruption of the AtREV3 gene causes hypersensitivity to ultraviolet B light and gamma-rays in *Arabidopsis*: implication of the presence of a translesion synthesis mechanism in plants. *Plant Cell* 15, 2042–2057. doi: 10.1105/tpc.012369
- Sakamoto, A. N., Lan, V. T., Puripunyanich, V., Hase, Y., Yokota, Y., Shikazono, N., et al. (2009). A UVB-hypersensitive mutant in *Arabidopsis thaliana* is defective in the DNA damage response. *Plant J.* 60, 509–517. doi: 10.1111/j.1365-313X.2009.03974.x
- Sano, T., Higaki, T., Handa, K., Kadota, Y., Kuchitsu, K., Hasezawa, S., et al. (2006). Calcium ions are involved in the delay of plant cell cycle progression by abiotic stresses. *FEBS Lett.* 580, 597–602. doi: 10.1016/j.febslet.2005.12.074
- Sano, T., Higaki, T., Oda, Y., Hayashi, T., and Hasezawa, S. (2005). Appearance of actin microfilament ‘twist peaks’ in mitosis and their function in cell plate formation, as visualized in tobacco BY-2 cells expressing GFP-fimbrin. *Plant J.* 44, 595–605 doi: 10.1111/j.1365-313X.2005.02558.x
- Shiloh, Y., and Ziv, Y. (2013). The ATM protein kinase: regulating the cellular response to genotoxic stress, and more. *Nat. Rev. Mol. Cell. Biol.* 14, 197–210. doi: 10.1038/nrm3546
- Sierro, N., Battey, J. N. D., Ouadi, S., Bakaher, N., Bovet, L., Willig, A., et al. (2014). The tobacco genome sequence and its comparison with those of tomato and potato. *Nat. Commun.* 5, 3833. doi: 10.1038/ncomms4833
- Smetana, O., Siroky, J., Houlne, G., Opatrný, Z., and Chaboute, M. E. (2012). Non-apoptotic programmed cell death with paraptotic-like features in bleomycin-treated plant cells is suppressed by inhibition of ATM/ATR pathways or NtE2F overexpression. *J. Exp. Bot.* 63, 2631–2644. doi: 10.1093/jxb/err439

- Takahashi, S., Nakajima, N., Saji, H., and Kondo, N. (2002). Diurnal change of cucumber CPD photolyase gene (*CsPHR*) expression and its physiological role in growth under UV-B irradiation. *Plant Cell Physiol.* 43, 342–349. doi: 10.1093/pcp/pcf038
- Takahashi, S., Sakamoto, A., Sato, S., Kato, T., Tabata, S., and Tanaka, A. (2005). Roles of *Arabidopsis AtREV1* and *AtREV7* in translesion synthesis. *Plant Physiol.* 138, 870–881. doi: 10.1104/pp.105.060236
- Takasawa, R., Nakamura, T., Mori, T., and Tanuma, S. (2005). Differential apoptotic pathways in human keratinocyte HaCaT Cells exposed to UVB and UVC. *Apoptosis* 10, 1121–1130. doi: 10.1007/s10495-005-0901-8
- Takeuchi, A., Yamaguchi, T., Hidema, J., Strid, A., and Kumagai, T. (2002). Changes in synthesis and degradataion of Rubisco and LHCII with leaf age in rice (*Oryza sativa* L.) growing under supplementary UV-B radiation. *Plant Cell Environ.* 25, 695–706 doi: 10.1046/j.1365-3040.2002.00844.x
- Takeuchi, Y., Inoue, T., Takemura, K., Hada, M., Takahashi, S., Ioki, M., et al. (2007). Induction and inhibition of cyclobutane pyrimidine dimer photolyase in etiolated cucumber (*Cucumis sativus*) cotyledons after ultraviolet irradiation depends on wavelength. *J. Plant Res.* 120, 365–374. doi: 10.1007/s10265-006-0065-9
- Takeuchi, Y., Murakami, M., Nakajima, N., Kondo, N., and Nikaido, O. (1996). Induction and repair of damage to DNA in cucumber cotyledons irradiated with UV-B. *Plant Cell Physiol.* 37, 181–187. doi: 10.1093/oxfordjournals.pcp.a028930
- Teranishi, M., Nakamura, K., Morioka, H., Yamamoto, K., and Hidema, J. (2008). The native cyclobutane pyrimidine dimer photolyase of rice is phosphorylated. *Plant Physiol.* 146, 1941–1951. doi: 10.1104/pp.107.110189
- Yasuhara, H., and Kitamoto, K. (2014). Aphidicolin-induced nuclear elongation in tobacco BY-2 cells. *Plant Cell Physiol.* 55, 913–927. doi: 10.1093/pcp/pcu026
- Yoshiyama, K., Conklin, P. A., Huefner, N. D., and Britt, A. B. (2009). Suppressor of gamma response 1 (*SOG1*) encodes a putative transcription factor governing multiple responses to DNA damage. *Proc. Natl. Acad. Sci. U.S.A.* 106, 12843–12848. doi: 10.1073/pnas.0810304106
- Yoshiyama, K. O., Kobayashi, J., Ogita, N., Ueda, M., Kimura, S., Maki, H., et al. (2013a). ATM-mediated phosphorylation of SOG1 is essential for the DNA damage response in *Arabidopsis*. *EMBO Rep.* 14, 817–822. doi: 10.1038/embor.2013.112
- Yoshiyama, K. O., Sakaguchi, K., and Kimura, S. (2013b). DNA damage response in plants: conserved and variable response compared to animals. *Biology* 2, 1338–1356. doi: 10.3390/biology2041338

Conflict of Interest Statement: The authors declare that the research was conducted in the absence of any commercial or financial relationships that could be construed as a potential conflict of interest.

Copyright © 2015 Takahashi, Kojo, Kutsuna, Endo, Toki, Isoda and Hasezawa. This is an open-access article distributed under the terms of the Creative Commons Attribution License (CC BY). The use, distribution or reproduction in other forums is permitted, provided the original author(s) or licensor are credited and that the original publication in this journal is cited, in accordance with accepted academic practice. No use, distribution or reproduction is permitted which does not comply with these terms.



DDM1 and ROS1 have a role in UV-B induced- and oxidative DNA damage in *A. thaliana*

Julia I. Qüesta^{†‡}, Julieta P. Fina[†] and Paula Casati^{*}

Centro de Estudios Fotosintéticos y Bioquímicos, Universidad Nacional de Rosario, Rosario, Argentina

Edited by:

Alma Balestrazzi, University of Pavia, Italy

Reviewed by:

Suleyman I. Allakhverdiev, Russian Academy of Sciences, Russia
Barbara Hohn, Friedrich Miescher Institute for Biomedical Research, Switzerland

***Correspondence:**

Paula Casati, Centro de Estudios Fotosintéticos y Bioquímicos, Universidad Nacional de Rosario, Suipacha 531, 2000 Rosario, Argentina
e-mail: casati@cefobi-conicet.gov.ar

†Present address:

Julia I. Qüesta, Cell and Developmental Biology, John Innes Centre, Norwich, UK

[‡]These authors have contributed equally to this work.

Absorption of UV-B by DNA induces the formation of covalent bonds between adjacent pyrimidines. In maize and arabidopsis, plants deficient in chromatin remodeling show increased DNA damage compared to WT plants after a UV-B treatment. However, the role of enzymes that participate in DNA methylation in DNA repair after UV-B damage was not previously investigated. In this work, we analyzed how chromatin remodeling activities that have an effect on DNA methylation affects the repair of UV-B damaged DNA using plants deficient in the expression of *DDM1* and *ROS1*. First, we analyzed their regulation by UV-B radiation in arabidopsis plants. Then, we demonstrated that *ddm1* mutants accumulated more DNA damage after UV-B exposure compared to Col0 plants. Surprisingly, *ros1* mutants show less CPDs and 6-4PPs than WT plants after the treatment under light conditions, while the repair under dark conditions is impaired. Transcripts for two photolyases are highly induced by UV-B in *ros1* mutants, suggesting that the lower accumulation of photoproducts by UV-B is due to increased photorepair in these mutants. Finally, we demonstrate that oxidative DNA damage does not occur after UV-B exposure in arabidopsis plants; however, *ros1* plants accumulate high levels of oxoproducts, while *ddm1* mutants have less oxoproducts than Col0 plants, suggesting that both *ROS1* and *DDM1* have a role in the repair of oxidative DNA damage. Together, our data provide evidence that both *DDM1* and *ROS1*, directly or indirectly, participate in UV-B induced- and oxidative DNA damage repair.

Keywords: UV-B, DNA repair, chromatin remodeling, DNA methylation, arabidopsis

INTRODUCTION

Because of their sessile condition, plants are inevitably exposed to ultraviolet-B radiation (UV-B, 290–315 nm); this energetic radiation causes direct damage to DNA, proteins, lipids, and RNA (Britt, 1996; Jansen et al., 1998; Gerhardt et al., 1999; Casati and Walbot, 2004). Absorption of UV-B by DNA induces the formation of covalent bonds between adjacent pyrimidines, giving rise to cyclobutane pyrimidine dimers (CPD) and, to a lesser extent, pyrimidine (6-4) pyrimidone photoproducts (6-4PPs) (Friedberg et al., 1995). These lesions disrupt base pairing and block DNA replication and transcription if photoproducts persist, or result in mutations if photoproducts are bypassed by error-prone DNA polymerases (Britt, 1996). Accumulation of such lesions must be prevented to maintain genome integrity, plant growth and seed viability. Thus, plants have not only developed mechanisms that filter or absorb UV-B to protect them against DNA damage (Mazza et al., 2000; Bieza and Lois, 2001), but also have different DNA repair systems to remove or tolerate DNA lesions (Hays, 2002; Bray and West, 2005; Kimura and Sakaguchi, 2006). At the genome level, the accessibility of DNA is determined by the structure of chromatin, which is subjected to epigenetic regulation. The structure of chromatin can be remodeled by three distinct processes, including covalent modifications of histones, such as phosphorylation, acetylation, methylation, ubiquitylation, sumoylation; ATP-dependent reorganization and

positioning of DNA-histones; and methylation of DNA cytosine residues (Verbsky and Richards, 2001; Eberharter and Becker, 2002; Pfluger and Wagner, 2007; Vaillant and Paszkowski, 2007).

In plants, DNA methylation regulates different epigenetic phenomena, including transcriptional silencing of transposons and transgenes, defense against pathogens, regulation of imprinting as well as silencing of genes (Vongs et al., 1993; Jeddelloh et al., 1999; Bender, 2004; Chan et al., 2005; Vanyushin and Ashapkin, 2011; Yaish et al., 2011). *DECREASE IN DNA METHYLATION1 (DDM1)*, is an ATP-dependent SWI2/SNF2 chromatin remodeling factor that is required for normal patterns of genomic DNA methylation in arabidopsis (Vongs et al., 1993; Jeddelloh et al., 1999). Mutations in *DDM1* result in a rapid loss of cytosine methylation at heterochromatic repetitive sequences and a gradual depletion of methylation at euchromatic low-copy sequences over successive generations (Kakutani et al., 1996). In *ddm1* heterochromatin, DNA methylation is lost and methylation of lysine 9 is largely replaced by methylation of lysine 4 (Gendrel et al., 2002). In addition, *DDM1* maintains 5S rDNA methylation patterns while silencing transcription through 5S rDNA intergenic spacers (IGS) (Kurihara et al., 2008). *DDM1* also regulates gene imprinting, transposon, gene and transgene silencing, and possibly the occurrence of paramutations (Jeddelloh et al., 1998; Vielle-Calzada et al., 1999; Hirochika et al., 2000). In *ddm1* plants, there is a significant DNA decondensation at centromeric

and pericentromeric regions rich in repetitive sequences and transposons; and in these mutants, some transposons become transcriptionally active or even undergo transposition (Hirochika et al., 2000; Miura et al., 2001; Singer et al., 2001; Mittelsten Scheid et al., 2002; Soppe et al., 2002; Fransz et al., 2003; Lippman et al., 2003; Probst et al., 2003; Slotkin and Martienssen, 2007; Mirouze et al., 2009; Tsukahara et al., 2009). DDM1 apparently stabilizes the activity of transposons; one of the *ddm1*-induced abnormalities was shown to be caused by insertion of CAC1, an endogenous CACTA family transposon (Miura et al., 2001). *ddm1* plants are also sensitive to NaCl stress and are deficient in DNA repair by methyl methane sulfonate (Yao et al., 2012); DDM1 participates in homologous recombination, and plants deficient in the expression of this gene show sensitivity to γ and UV-C radiation; demonstrating that DDM1 plays a role in response to DNA damage (Shaked et al., 2006).

Biochemical and genetic evidences have shown that plants possess DNA glycosylases that specifically remove 5-meC from DNA, initiating its replacement by unmethylated cytosine through a base excision repair process (Gehring et al., 2009; Roldan-Arjona and Ariza, 2009; Zhu, 2009). The *in vivo* functions of plant 5-meC DNA glycosylases are not fully understood, but they seem to contribute to the stability and flexibility of the plant epigenome. Plant 5-meC DNA glycosylases comprise a subfamily of atypical HhH-GPD enzymes, examples of enzymes in this group are the arabidopsis proteins ROS1 (repressor of silencing 1), DME (Demeter), DML2, and DML3 (Demeter-like proteins 2 and 3) (Choi et al., 2002; Gong et al., 2002; Penterman et al., 2007; Ortega-Galisteo et al., 2008). ROS1 was identified in a screen for mutants with increased silencing of the repetitive RD29ALUC transgene (Gong et al., 2002). Together with paralogs DML2 and DML3, ROS1 is needed to regulate the DNA methylation pathway at discrete regions across the plant genome, and probably protect the genome from excess methylation (Penterman et al., 2007; Zhu et al., 2007; Ortega-Galisteo et al., 2008). ROS1 and its homologs are bifunctional DNA glycosylases/lyases that cleave the phosphodiester backbone at the 5-meC removal site by b-elimination, generating a 3' phospho a,b-unsaturated aldehyde at the strand break (Agius et al., 2006; Gehring et al., 2006; Morales-Ruiz et al., 2006; Penterman et al., 2007; Ortega-Galisteo et al., 2008). The final reaction product generated by ROS1 is a single-nucleotide gap flanked by 3'-phosphate and 5'-phosphate termini. The phosphate group present at the 3' end of the single-nucleotide gap generated by ROS1 is removed by a DNA 3' phosphatase (Martínez-Macías et al., 2012). Finally, a yet unknown DNA polymerase must fill this gap with an unmethylated cytosine before a DNA ligase can seal the remaining nick. In addition to 5-meC, ROS1 also excise with less efficiency its deamination product thymine (5-methyluracil) from T_G mispairs, but do not show detectable activity on either C_G pairs or U_G mispairs; and ROS1 activity is facilitated at mismatched 5-meC residues (Morales-Ruiz et al., 2006; Ponferrada-Marín et al., 2009). The *ros1* mutation increases the telomere length in arabidopsis (Liu et al., 2010b); however, *ros1* mutants have not previously shown any differential response in DNA repair when compared to WT plants (Liu et al., 2010a).

We have previously demonstrated that arabidopsis plants deficient in 4 chromatin remodeling proteins NFC4, SDG26, HAM1, and HAM2 show more damaged DNA than WT plants after 4 h of UV-B exposure (Campi et al., 2012). In addition, plants treated with an inhibitor of histone acetyltransferases, cumin, previous to the UV-B treatment show deficiencies in DNA repair; demonstrating that histone acetylation is important during DNA repair in arabidopsis. These results showed that chromatin remodeling, and histone acetylation in particular, are essential during DNA repair by UV-B; demonstrating that both genetic and epigenetic effects control DNA repair in plants. However, the role of enzymes that participate in DNA methylation in DNA repair after UV-B damage has not been investigated yet. Therefore, the aim of this work was to analyze the role of chromatin remodeling proteins that have a role in DNA methylation in the repair of CPDs and 6-4PPs using plants deficient in the expression of *DDM1* and *ROS1*. First, we analyzed their regulation by UV-B radiation in WT plants. Then, using plants with decreased transcript levels of *DDM1* and *ROS1*, we demonstrated that *ddm1* mutants accumulated more DNA damage after UV-B exposure compared to Col0 WT plants. Surprisingly, *ros1* mutants show less CPDs and 6-4PPs than Col0 plants after the treatment under light conditions, while the repair under dark conditions is impaired. Transcripts for two photolyases are highly induced by UV-B in *ros1* mutants, suggesting that the lower accumulation of photoproducts by UV-B is due to increased photorepair in these mutants. Finally, we here demonstrate that oxidative DNA damage does not occur after UV-B exposure in arabidopsis plants; however, *ros1* plants accumulate high levels of oxoproducts, while *ddm1* mutants have less oxoproducts than Col0 plants, suggesting that both ROS1 and DDM1 have a role in the repair of oxidative DNA damage. Together, our data provide evidence that both *DDM1* and *ROS1*, directly or indirectly, participate in UV-B induced- and oxidative DNA damage repair.

RESULTS

UV-B REGULATION OF *DDM1* AND *ROS1*, MUTANT ANALYSIS AND PHYSIOLOGICAL EFFECTS

Chromatin remodeling has previously been shown to be crucial for UV-B damage repair in plants (Casati et al., 2006; Campi et al., 2012). Different chromatin landscapes control the accessibility of the DNA repair machinery to damaged DNA. In several organisms, a major factor affecting chromatin accessibility is DNA methylation. Therefore, we sought to determine if enzymes that have a role in DNA methylation participate in UV-B damage repair in arabidopsis. Provided that *ros1* and *ddm1* mutants were previously reported to contain altered levels of DNA methylation in their genomes (Kakutani et al., 1996; Xia et al., 2006), they confer an adequate system to analyze how DNA methylation affects the repair of UV-B induced DNA lesions. *A. thaliana* mutants defective in *DDM1* and *ROS1* were identified in the SALK collection. For *ros1*, two independent T-DNA insertional lines, SALK_135293 and SALK_045303, with insertions in the 3' UTR and the 16th exon, respectively, were identified by a PCR screen using gene-specific primers and one specific primer for the T-DNA left border (**Figures S1, S2** and **Table S1** in Supplementary Material). Insertional inactivation of

ROS1 in both lines was confirmed by RT-PCR (**Figures S1, S2**). For the *DDM1* gene, two independent T-DNA insertional lines, SALK_000590 and SALK_093009 (*ddm1-10*, Jordan et al., 2007), with insertions in the 16th exon and the 15th intron, respectively, were identified by a PCR screen using gene-specific primers and one specific primer for the T-DNA left border (**Figure S3** and **Table S1** in Supplementary Material). Decreased expression of *DDM1* in both lines was confirmed by RT-PCR (**Figure S4** in Supplementary Material). *ddm1* mutants show hypomethylation in several regions of the DNA; in particular, the *AtMu1* transposon, which is usually methylated and its transposase is not transcribed in WT plants, it is actively transcribed when it is hypomethylated in *ddm1* mutants (Singer et al., 2001). **Figure S5** in Supplementary Material shows that *AtMu1* is highly transcribed in the SALK_093009 mutant, while is not expressed in the Col0 plants. In addition, because DNA hypomethylation induces the misregulation of the expression of diverse genes, *ddm1* mutants show an abnormal phenotype, with small and curved leaves (Kakutani et al., 1996). The SALK_093009 mutant has already been described to show a *ddm1* mutant phenotype, showing up-regulation of genes as a consequence of hypomethylated DNA (Jordan et al., 2007). In addition, **Figure S5** shows that both the SALK_093009 and the SALK_000590 mutants have a similar phenotype as that described for other *ddm1* mutants (Vongs et al., 1993; Jordan et al., 2007). The SALK_000590 mutants also show high expression of *AtMu1* and a similar phenotype as that of SALK_093009 plants (not shown), suggesting that both mutants are probably deficient in DNA methylation. It is important to mention that we have not tested the methylation profile of the SALK_093009 and the SALK_000590 mutants, but we are confident, according to the observed phenotypes, transcription activation of *AtMu1* transposon and the published data (Vongs et al., 1993; Kakutani et al., 1996; Singer et al., 2001; Jordan et al., 2007) that the two mutants behave as methylation deficient.

We first investigated the effects of UV-B on physiological parameters in *ddm1* and *ros1* mutants. UV-B induces flavonoid accumulation such as anthocyanins and other UV sunscreens in many plants (Li et al., 1993; Landry et al., 1995; Ormrod et al., 1995). After a 4 h-UV-B treatment, the concentration of these molecules was 1.76-fold higher than under control conditions in Col0 plants. Similar increases were observed for the two *ros1* mutants analyzed (1.63- and 1.73-fold, respectively; **Figure 1A**). On the contrary, plants with decreased levels of *DDM1* transcript have altered accumulation of UV sunscreen photoprotectors. *ddm1* mutants showed a significantly higher increase in the level of these pigments after the UV-B treatment (2.24 and 2.16-fold increase, respectively; **Figure 1A**). Moreover, when pigment levels were compared in baseline control conditions in the absence of UV-B, *ddm1* mutants showed already elevated flavonoid levels similar to those in Col0 plants after the UV-B treatment. In addition, UV-B sensitivity was analyzed by inhibition of primary root elongation assays (Tong et al., 2008). One day after the end of the UV-B treatment, both Col0 and *ros1* seedlings showed a slight although significant decrease in primary root elongation compared to untreated plants (**Figure 1B**). However, 2 days after the treatment, *ros1* plants showed a lower decrease

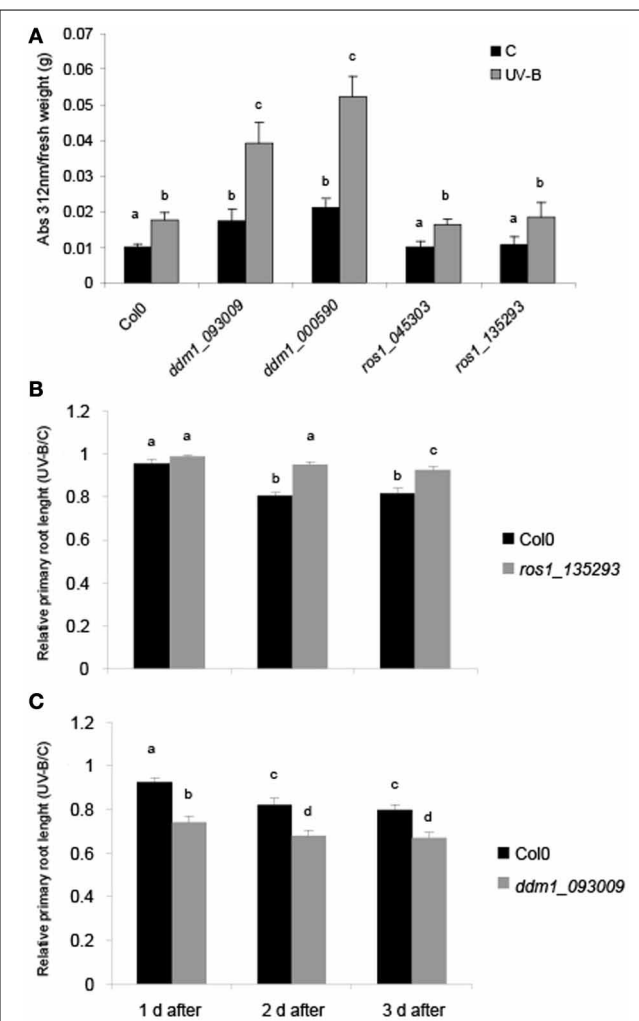


FIGURE 1 | Physiological responses in *ddm1* and *ros1* mutants after UV-B exposure. **(A)** Total UV-B absorbing compounds were assayed after 4 h UV-B (UV-B) compared to untreated controls (C) in Col0 plants, and *ddm1* and *ros1* mutants. Measurements are the average of six adult leaves from six different plants. **(B and C)** Graph of average root lengths in Col0, *ros1* **(B)** and *ddm1* **(C)** mutants up to 3 days after a UV-B treatment. Error bars represent S.E.M. Statistical significance was analyzed using ANOVA, Tukey test with $P < 0.05$; differences from the control are marked with different letters.

in primary root growth than Col0 plants. In contrast, *ddm1* seedlings showed a significant higher inhibition of root elongation by UV-B than Col0 plants (**Figure 1C**). Together, these results suggest that *ddm1* mutants are more sensitive to UV-B radiation than Col0 plants; while *ros1* mutants are less responsive to this radiation.

Previously, four arabidopsis chromatin remodeling genes *NFC4*, *SDG26*, *HAM1* and *HAM2* were reported to be induced by UV-B; and plants deficient in the expression of these genes all showed increased accumulation of CPDs compared to WT plants of the Col0 ecotype when exposed with UV-B light (Campi et al., 2012). Therefore, we investigated if *DDM1* and *ROS1* were also regulated by this radiation. 4-weeks-old Col0 (WT) plants

grown in the absence of UV-B were exposed under UV-B lamps for 4 h in a growth chamber. After the treatment, leaf tissue was collected for RNA extraction and qRT-PCR analysis. Contrary to the up-regulation reported for *NFC4*, *SDG26*, *HAM1* and *HAM2*, **Figure 2** shows that *DDM1* and *ROS1* are significantly down regulated by UV-B. The transcript of the arabidopsis CPD photolyase *UVR2* (*At1g12370*), a UV-B inducible gene, was used as a positive control.

OPPOSING IMPACT OF *ROS1* AND *DDM1* ON UV-B DNA DAMAGE REPAIR IN ARABIDOPSIS

To test the participation of *ROS1* and *DDM1* in UV-B-damaged DNA repair, 4-weeks-old Col0, *ros1* and *ddm1* plants were irradiated with UV-B for 4 h. Leaf samples from control and treated plants were collected immediately after the treatment under light conditions that allow photoreactivation. Genomic DNA was extracted to evaluate CPD abundance after UV-B exposure, both in Col0 and mutant plants (**Figures 3A,B**). CPD levels were measured by an immunological sensitive assay; this assay detects CPDs by monoclonal antibodies specifically raised against them. 1.5 µg of DNA was used for each sample, as that there is a linear relationship of signal values of UV-B treated samples vs. the corresponding amounts of DNA loaded up to 2 µg of DNA (Lario et al., 2011). In the absence of UV-B, the steady state levels of CPDs in Col0 and mutant plants were similar [about 200 intensity of the optical density (IOD) in all samples; **Figure 3B**]. After 4 h UV-B exposure, unrepaired lesions accumulated in all plants (**Figure 3A**) CPD levels in *ddm1* mutants were significantly higher than in Col0 (**Figures 3A,B**). Interestingly, *ros1* mutants showed only a minor, although still significant increased accumulation of CPDs after the UV-B treatment. Consistent with the lack of UV-B sensitivity observed in the root elongation assay, *ros1* plants accumulate lower levels of CPDs than Col0 (**Figures 3A,B**). These results confirm the participation of *ROS1* and *DDM1* in UV-B damage repair and also evidence the opposing effects of these two proteins in UV-B response.

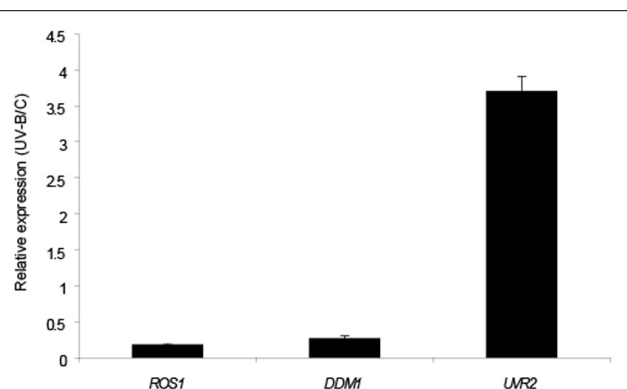


FIGURE 2 | Relative transcript levels of *A. thaliana* *ROS1* and *DDM1* genes measured by qRT-PCR. Plants were irradiated with UV-B light for 4 h (UV-B) or kept under control conditions (C) as indicated in Materials and Methods. *CPK3* transcript was used for normalization and *UVR2* as a control of a UV-B inducible gene. Data show mean values ± S.E.M. of at least three independent experiments.

6-4PPs constitute around 25% of the DNA damage induced by UV-B radiation (Britt, 1996). We investigated how 6-4 photoproducts were accumulated in *ddm1* and *ros1* mutants. As observed for CPD accumulation, *ddm1* plants accumulated significant higher levels of 6-4PPs than Col0 plants after a 4 h-UV-B treatment, while *ros1* mutants showed lower accumulation of these products under the same conditions (**Figure 3C**).

ddm1 AND *ros1* MUTANTS HAVE ALTERED LEVELS OF DNA REPAIR TRANSCRIPTS

The evidence of a role of *DDM1* and *ROS1* in UV-B damage repair prompted us to investigate their involvement in the regulation of the expression of DNA repair genes. UV-B-induced DNA damage repair is accomplished by two main pathways: nucleotide excision repair (NER) and photoreactivation (PR). Therefore, we measured the transcript levels of some selected NER and PR genes before and after UV-B exposure. First, we evaluated the expression of 2 photolyase genes: *UVR2*, encoding a CPD photolyase, and *UVR3*, encoding a 6-4 photoproduct photolyase (*At3g15620*). **Figure 4** and **Figure S6** in Supplementary Material show that both genes were up-regulated by UV-B radiation in Col0 plants after the treatment; however, *ddm1* mutants constitutively expressed high levels of both photolyases. In previous studies using different mutants that are deficient in homologous recombination and repair of damaged DNA with methylmethane sulphonate, such as *abo4* (a mutant in the DNA pol ε, Yin et al., 2009), *rfc1* (a mutant in the DNA replication factor C1; Liu et al., 2010a), and *polα* (a mutant in the DNA pol α, Liu et al., 2010b), DNA repair transcripts were highly and constitutively expressed, suggesting that in these mutants DNA repair-related genes were spontaneously induced. We hypothesize that a similar situation occurs in *ddm1* plants. In contrast, *ros1* mutants contained wild type amounts of *UVR2* and *UVR3* transcripts in the absence of UV-B and showed higher levels of both transcripts after the UV-B treatment compared to Col0 (**Figure 4** and **Figure S6**). Thus, the lower accumulation of CPDs in *ros1* mutants after the UV-B treatment may be a result of increased photolyases activity.

On the other hand, we analyzed the expression of the NER genes *UVR7* (encoding ERCC1, a DNA excision repair protein, *At3g05210*), *UVH1* (encoding the RAD1 endonuclease, *At5g41150*), and *UVH6* (encoding a protein similar to the human helicase XPD, *At1g03190*). All these transcripts were induced by UV-B in the Col0 background, and this was also true for *ros1* mutants. However, after UV-B exposure the induction of *UVR7* was 3-fold higher in *ros1* plants compared to Col0 (**Figure 4** and **Figure S6**). In *ddm1* mutants, high basal expression of these genes was detected under control conditions, as previously observed for the photolyases. Finally, we analyzed the expression of the 8-oxoguanine DNA glycosylase gene *OGG1* (*At1g21710*), a member of the arabidopsis base excision repair (BER) system. Although the expression of this gene was similar in Col0 and the mutants under control conditions, Col0 showed decreased levels of *OGG1* after 4 h UV-B treatment, not measured in either mutant (**Figure 4**).

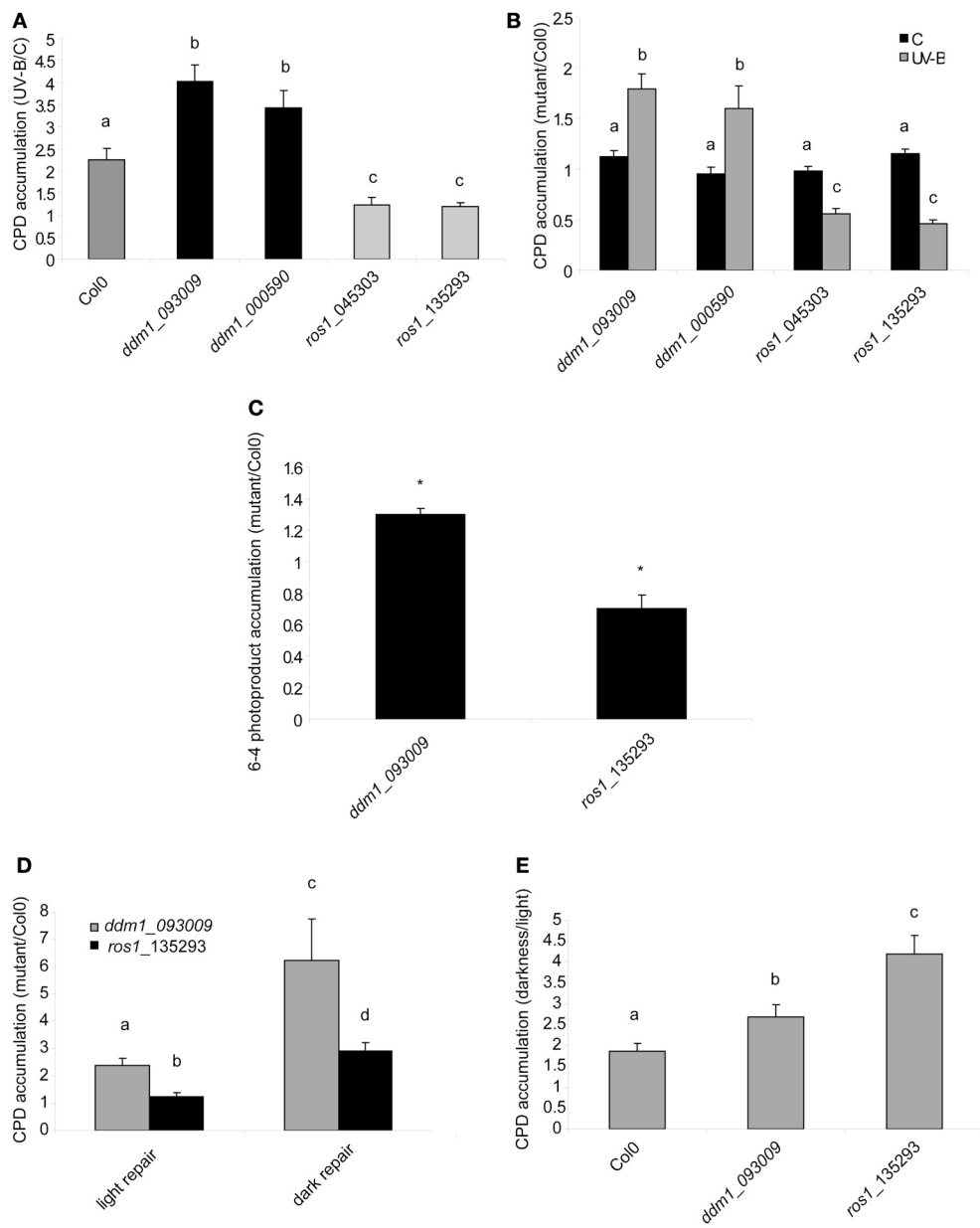


FIGURE 3 | CPD and 6-4PPs levels in the DNA of Col0, ddm1 and ros1 arabidopsis plants. (A) CPD levels in DNA of UV-B treated Col0, ddm1, and ros1 plants for 4 h, relative to levels under control conditions without UV-B (C). **(B)** CPD levels in DNA of ddm1 and ros1 plants relative to Col0 plants under control conditions without UV-B (C) and after a 4 h-UV-B treatment (UV-B). **(C)** 6-4PPs levels in DNA of ddm1 and ros1 plants relative to Col0 plants after a 4 h-UV-B treatment. **(D)** CPD levels in DNA of ddm1 and ros1 plants relative to Col0 plants after a recovery period in the absence of UV-B

for 2 h. Experiments were done under conditions that allowed photorepair in the light (light) or under dark conditions (dark). **(E)** CPD levels in DNA of Col0, ddm1 and ros1 plants after a recovery period in the absence of UV-B for 2 h in the light relative to levels after recovery under dark conditions. Results represent the average \pm S.E.M. of six independent biological replicates. Different letters denote statistical differences applying ANOVA tests using Sigma Stat 3.1. Asterisks denote statistical differences applying Student's t test ($P < 0.05$).

LOWER ACCUMULATION OF CPDs IN ros1 MUTANTS ARE PROBABLY A CONSEQUENCE OF INCREASED LEVELS OF PHOTOLYASES AFTER UV-B EXPOSURE

To analyze that the decreased UV-B sensitivity of ros1 mutants is due to increased photolyases activity, we tested the repair of CPDs in the dark and in the light after 2 h of recovery in the absence

of UV-B. As expected, all plants repaired CPD damage better in the light, when photoreactivation occurs, than in the dark, when photoreactivation is absent (Figure 3E). After 2 h recovery in the light, ros1 plants showed similar levels of CPDs as Col0 plants as a result of photoreactivation (Figure 3D). However, recovery in the dark was significantly compromised (Figures 3D,E). This

result demonstrates that the low levels of CPDs accumulated in the light are probably a consequence of the higher expression of photolyases after UV-B exposure.

On the other hand, *ddm1* mutants still showed higher CPD accumulation than Col0 plants after 2 h recovery under both conditions, demonstrating that these mutants have a defect in DNA repair, probably due to a deficiency in chromatin remodeling, as already reported for other types of DNA damage (Shaked et al., 2006; Yao et al., 2012; **Figure 3D**). It is interesting to note that *ddm1* plants were more affected in the dark than in the light repair (**Figure 3D**), the reason for this may be probably because different proteins participate in the NER repair machinery (the main dark CPD repair system), while photoreactivation requires the action of only one protein, the photolyase. Therefore, chromatin remodeling activities may be more important in the dark repair, which replace the damaged DNA with new, undamaged nucleotides, to allow to spatially accommodate the different proteins that participate in this process.

Together, our results suggest that chromatin remodeling deficient *ddm1* plants have increased CPD accumulation by UV-B because DNA repair mechanisms, in particular NER proteins, may require chromatin remodeling by this enzyme for their activities. On the contrary, *ros1* mutants are also deficient in CPD dark repair, but have high photoreactivation probably as a result of increased expression of *UVR2* and *UVR3*.

UV-B DOES NOT INDUCE THE ACCUMULATION OF OXIDIZED BASES IN THE DNA OF ARABIDOPSIS PLANTS, BUT *ddm1* AND *ros1* MUTANTS ARE AFFECTED IN OXIDATIVE DAMAGE REPAIR

The results presented in **Figure 4** suggest that both *ddm1* and *ros1* mutants are deficient in CPD dark repair. In plants, dark pathways

fall into two major categories: NER and BER (Britt, 1996). The BER involves the removal of a single damaged base through the action of one of many lesion-specific glycosylases, which leaves the DNA sugar-phosphate backbone intact. Glycosylases and endonucleases specific for cyclobutane dimers have been observed in bacteria and bacteriophages and have been useful as diagnostic agents for the assay of UV-induced damage (Friedberg et al., 1995). On the other hand, UV-B radiation has been described to alter reactive oxygen species metabolism (Hidet et al., 2013). A wide variety of oxidative damage products are induced in DNA by hydroxyl radicals, superoxide, and nitric oxide (Britt, 1996). The most significant oxidized base is 8-hydroxyguanine (8-oxodG); thus, we investigated if UV-B produces base oxidation in arabidopsis. For this aim, we analyzed the accumulation of 8-oxodG after a 4 h UV-B treatment in Col0, *ddm1* and *ros1* mutants. Interestingly, Col0 plants did not accumulate 8-oxodG after the UV-B treatment (**Figure 5**). Moreover, the accumulation of 8-oxodG was neither changed in *ddm1* nor in *ros1* mutants after UV-B. However, both mutants showed significantly different accumulation of this DNA oxidation product compared to Col0 plants (**Figure 5**). For *ros1*, 8-oxodG accumulation was higher than Col0 plants (**Figure 5**). Despite that ROS1 is a glycosyltransferase of the BER repair system that has been described to remove 5-meC and T mismatched to G (Morales-Ruiz et al., 2006), its activity using oxidized bases as substrates has not been previously determined. On the other hand, *ddm1* mutants showed significantly lower levels of 8-oxodG than Col0 plants (**Figure 5**). This is in contrast to which was previously reported for other types of DNA damage, such as treatment with UV-C, γ -radiation and methyl methane sulfonate (Shaked et al., 2006; Yao et al., 2012), and our results in the repair of photoproducts by UV-B (**Figure 3**), where these mutants show higher levels of DNA damage than WT plants. In particular, *ros1* mutants show altered levels of the other 5-meC glycosylases *DML2*, *DML3* and *DME1* (**Figure S7** in Supplementary Material). Therefore, it is possible that this increase in the accumulation of 8-oxodG may be due

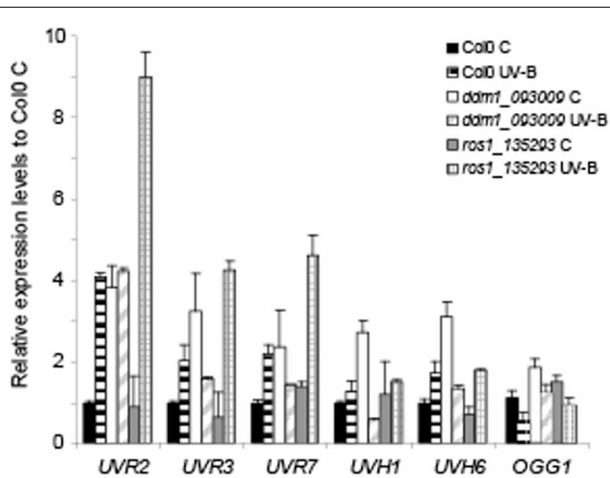


FIGURE 4 | Relative expression of DNA repair transcripts by RT-qPCR in Col0, *ddm1* (*ddm1_093009* line) and *ros1* (*ros1_135293* line). Levels of *UVR2*, *UVR3*, *UVR7*, *UVH1*, *UVH6*, and *OGG1* were assayed in arabidopsis plants that were irradiated with UV-B for 4 h (UV-B) or were kept under control conditions without UV-B (control, C). Expression values are relative to the values in Col0 plants under control conditions in the absence of UV-B. The *CPK3* transcript was used as a control. Data show mean values \pm S.E.M. of at least three independent experiments.

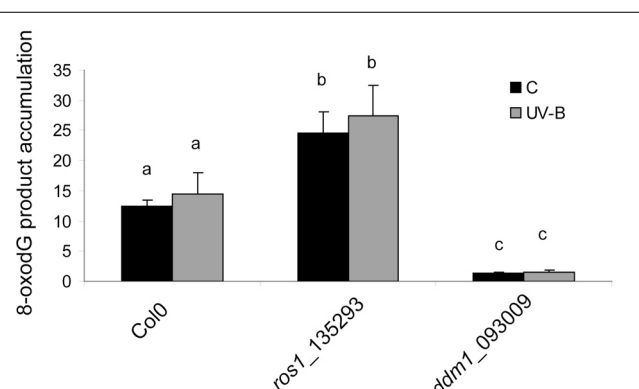


FIGURE 5 | 8-oxodG levels in the DNA of Col0, *ros1* and *ddm1* arabidopsis plants. Plants were assayed under control conditions (C) and after a 4 h UV-B treatment (UV-B). Results represent the average \pm S.E.M. of six independent biological replicates. Different letters denote statistical differences applying ANOVA tests using Sigma Stat 3.1.

to altered expression of different glycosylases in these mutants. Together, our data provide evidence that both *DDM1* and *ROS1*, directly or indirectly, participate in oxidative DNA damage repair in arabidopsis.

DISCUSSION

Absorption of UV-B by DNA induces the formation of covalent bonds between adjacent pyrimidines with the formation of CPDs and 6-4PPs (Friedberg et al., 1995); overaccumulation of these lesions must be prevented to maintain genome integrity, plant growth and seed viability. Plants have evolved mechanisms that filter or absorb UV-B to protect against DNA damage (Mazza et al., 2000; Bieza and Lois, 2001), and also have DNA repair systems to remove DNA lesions (Hays, 2002; Bray and West, 2005; Kimura and Sakaguchi, 2006). The genome of plants is organized into chromatin, which limits the accessibility of DNA, affecting the rates of processes such as DNA recombination and repair. The disruption of the interactions of nucleosome–DNA or the remodeling of chromatin can stimulate or repress DNA repair. In yeast, RAD54, RAD26 and RDH54, which all belong to the switch2/sucrose non-fermenting2 (Swi2/Snf2) superfamily, participate in meiosis and also in various aspects of DNA repair, for example in homologous recombination and in nucleotide excision and transcription-coupled repair (Eisen et al., 1995; Klein, 1997; Shinohara et al., 1997). In arabidopsis, the Swi2/Snf2-related SWR1 complex, which deposits histone H2A.Z, is important for DNA repair (Rosa et al., 2013). Mutations in genes for different subunits of the SWR1 complex cause hypersensitivity to various DNA damaging agents; and even without additional genotoxic stress, these mutants show symptoms of DNA damage accumulation (Rosa et al., 2013). In maize, chromatin remodeling has been implicated in UV-B responses. Transgenic maize plants knockdown for chromatin remodeling genes were found to be acutely sensitive to UV-B at doses that do not cause visible damage to maize lacking flavonoid sunscreens (Casati et al., 2006). In maize and arabidopsis, plants deficient in chromatin remodeling show increased DNA damage compared to WT plants after a UV-B treatment (Campi et al., 2012). However, the role of enzymes that participate in DNA methylation in DNA repair after UV-B damage was not previously investigated yet. Therefore, in this work, we analyzed the role of enzymes that participate in DNA methylation in the repair of CPDs and 6-4PPs using mutant plants in *DDM1* and *ROS1*.

First, we analyzed the expression of both *DDM1* and *ROS1* by UV-B radiation in arabidopsis. Interestingly, both genes are repressed after the treatment, suggesting that *DDM1* and *ROS1* may have a role in UV-B responses. Therefore, their function in UV-B responses was investigated. In plants, the first line of defense when exposed to UV-B is the synthesis of protective pigments like flavonoids and UV-B absorbing pigments. In our experiments, UV-B absorbing pigments levels increased in Col0, *ddm1* and *ros1* mutants after the UV-B treatment; however, when pigment levels were compared in baseline control conditions in the absence of UV-B, *ddm1* mutants showed already elevated flavonoid levels similar to those in Col0 plants after the UV-B treatment. This demonstrates that arabidopsis plants deficient in

chromatin remodeling are affected in the accumulation of UV-absorbing compounds, similarly as previously described in maize and arabidopsis chromatin remodeling deficient plants (Casati et al., 2006; Campi et al., 2012). In addition, *ddm1* seedlings showed a significantly higher inhibition of root elongation by UV-B than Col0 plants; while *ros1* roots were less affected by UV-B than those from Col0 plants. Together, these results suggest that *ddm1* mutants are more sensitive to UV-B radiation than Col0 plants; whereas *ros1* mutants are less responsive to this radiation.

In addition, we demonstrated that *ddm1* mutants accumulated more damaged DNA after UV-B exposure compared to Col0 plants. Previous studies have shown that *ddm1* plants have increased sensitivity to γ and UV-C radiation, they are susceptible to NaCl stress and are also deficient in DNA repair by methyl methane sulfonate (Shaked et al., 2006; Yao et al., 2012). Moreover, *DDM1* participates in homologous recombination (Shaked et al., 2006). These data, in agreement with our results, demonstrate that *DDM1* plays a role in response to DNA damage. The *ddm1* mutants used in our experiments show high expression of the *AtMu1* transposase, which is not expressed in the Col0 plants, demonstrating that these mutants have deficient methylation in some DNA regions (Singer et al., 2001). It is interesting that *ddm1* plants constitutively express high levels of DNA repair enzymes, similarly as other mutants deficient in DNA repair (Yin et al., 2009; Liu et al., 2010a,b), suggesting that in all these mutants DNA repair-related genes were spontaneously induced. However, these increased expression levels do not correlate with increased DNA repair; therefore, *DDM1* may participate directly in DNA repair, and not through the regulation of the expression of DNA repair genes. A comparison of mutants in *DDM1* and *MET1*, a gene encoding a cytokine methyltransferase, suggested that DNA damage response is affected essentially by chromatin structure, while cytosine methylation was less critical (Shaked et al., 2006). Therefore, we suggest that *DDM1* is important in chromatin remodeling during DNA repair of UV-B induced pyrimidine dimers.

In contrast, *ddm1* plants show significantly lower levels of 8-oxodG than Col0 plants. *DDM1* has been shown to increase meiotic recombination in both male and female lineages, but the effect is not equal throughout the genome (Melamed-Bessudo and Levy, 2012). In these mutants, euchromatic regions exhibit high rates of meiotic recombination, whereas no changes are found in heterochromatic centric and pericentric areas; demonstrating the involvement of *DDM1* and chromatin remodeling in genome maintenance. *DDM1* regulates histone H3 and DNA methylation; upon loss of *DDM1* activity, a 70% reduction in DNA methylation is induced, promoting chromatin decondensation (Jeddeloh et al., 1999; Probst et al., 2003). Therefore, the DNA demethylation *per se* or altered chromatin remodeling could make the DNA more accessible to the BER repair system, as similarly suggested for homologous recombination enzymes (Melamed-Bessudo and Levy, 2012). Interestingly, the expression levels *OGG1*, an 8-oxoguanine DNA glycosylase of the BER, is similar in *ddm1* and *Col0* plants, so increased repair of 8-oxodG cannot be explained by changes in the activity of this enzyme. However, we cannot rule out that other glycosylases

or repair enzymes may be up-regulated in the *ddm1* mutants, for example by activation of silent genes from hypomethylated chromosomes.

On the other hand, in our experiments, *ros1* showed less CPDs and 6-4PPs than Col0 plants after a UV-B treatment under light conditions; however, CPD accumulation after a 2 h recovery in the dark was higher in the mutants than in Col0. The results presented here show that transcripts for two photolyases, *UVR2* (a CPD photolyase) and *UVR3* (a 6-4PPs photolyase) are highly induced by UV-B in *ros1*, suggesting that the lower accumulation of photoproducts by UV-B may be due to increased photorepair in these mutants. This higher photorepair correlates with lower inhibition of primary root elongation by UV-B, suggesting that these mutants have higher UV-B tolerance than WT plants. On the contrary, *ros1* plants accumulate elevated levels of 8-oxodG in the DNA; therefore, ROS1 may have a role in the repair of oxidative DNA damage. Interestingly, ROS1 is a DNA glycosylase that has been described to remove 5-meC and T mismatched to G (Morales-Ruiz et al., 2006), but its activity using oxidized bases as substrates has not been previously determined. Several *ros1* suppressors have been identified, including replication protein A2 (RPA2A/ROR1) (Xia et al., 2006), DNA polymerase α (Liu et al., 2010b), DNA polymerase ϵ (Yin et al., 2009) and TOUSLED (Wang et al., 2007). These mutants release the TGS of 35S-NPTII and increase the expression of transcriptionally active information, but they do not change the DNA methylation state when mutated. All *ros1* suppressors described above are sensitive to DNA damage, they respond to the damage with constitutive expression of DNA damage related genes, and most of them also have a high homologous recombination rate (Xia et al., 2006; Wang et al., 2007; Yin et al., 2009), suggesting that the silencing of chromatin is closely related with DNA replication, DNA repair and homologous recombination (Probst et al., 2009). However, with the exception that *ros1* mutation increases the telomere length in arabidopsis (Liu et al., 2010b), *ros1* mutants have not previously shown any differential response in DNA repair when compared to WT plants (Liu et al., 2010a). Our results suggest that *in vivo*, ROS1 may also have a role in the repair of 8-oxodG. Alternatively, a mutation in ROS1 may affect the expression of other glycosylases specific for 8-oxodG, similarly as determined for the *UVR2* and *UVR3* photolyases in this work. *ros1* plants show altered levels of the other 5-meC glycosylases *DML2*, *DML3* and *DME1*; thus, it is possible that this increase in the accumulation of 8-oxodG may be due to altered expression levels of different glycosylases in these mutants.

We have previously demonstrated that chromatin remodeling is essential during DNA repair by UV-B (Campi et al., 2012). In particular, because histone H3 and H4 acetylation is increased by UV-B (Casati et al., 2008), the effect of histone acetylation on DNA repair was previously analyzed, and our results demonstrated that when plants are pre-treated with curcumin, a histone acetylase inhibitor, DNA repair was impaired (Campi et al., 2012). Interestingly, in *sdg26* mutants (*SDG26* encodes a histone methyltransferase), a curcumin treatment previous to UV-B irradiation induced a significantly higher accumulation of CPDs than curcumin-treated WT plants. Therefore, a deficiency

in the expression of a histone methyltransferase interferes directly or indirectly with the DNA damage repair mediated by histone acetylation, suggesting that both processes, histone acetylation and methylation, act synergistically during UV-B induced damage repair. In this manuscript, we show that enzymes that participate in DNA methylation are also important during DNA repair by UV-B, demonstrating that both genetic and epigenetic effects control DNA repair in plants.

Together, the results presented here demonstrate the participation of DDM1 and ROS1 in DNA repair after UV-B damage and oxidation. We propose that, in *ddm1* mutants, DNA demethylation *per se* or altered chromatin remodeling could affect accessibility to DNA repair systems. On the contrary, we suggest that in *ros1* mutants, lower accumulation of photoproducts is due to increased levels of photolyases by UV-B. Finally, ROS1, besides its demonstrated role as a 5-meC glycosylase, it could also act as an oxoprotectant glycosidase.

MATERIALS AND METHODS

PLANT MATERIAL, GROWTH CONDITIONS AND IRRADIATION PROTOCOLS

The *A. thaliana* ecotype Columbia (Col0) was used for all the experiments. The T-DNA insertion mutants were obtained from the SALK T-DNA insertion mutant collection (Alonso et al., 2003). Mutants lines used are shown in Figures S1–S4 in Supplemental data. Arabidopsis plants were sown directly on soil and placed at 4°C in the dark. After 3 days, pots were transferred to a greenhouse and plants were grown at 22°C under a 16 h/8 h light/dark regime. Plants were exposed 4 h to UV-B radiation (315 nm) from UV-B bulbs (2 W m⁻² UV-B and 0.65 W m⁻² UV-A, Bio-Rad, Hercules, California) in a growth chamber, both in the presence or the absence of white light, and control plants were treated with the same plants covered with a polyester film (0.04 W m⁻² UV-B, 0.4 W m⁻² UV-A). Adult leaf samples from 4-weeks-old plants were collected immediately after irradiation, or 2 h after the end of the UV-B treatment, both under light and under dark conditions.

IDENTIFICATION OF INSERTIONAL T-DNA MUTANTS

The genotype of plants with T-DNA constructs was determined using a PCR-based approach. Initial screening was performed using genomic DNA isolated from leaves by a modified cetyl-trimethyl-ammonium bromide (CTAB) method (Sambrook and Russel, 2001) and three combinations of primers. Two primers hybridize to specific genomic sequences (Table S1) and one primer is located inside the left border of the T-DNA. The presence or absence of the T-DNA insertion in the genes allowed the identification of homozygous, heterozygous and WT plants.

RT-PCR for expression analyses in the knockout T-DNA lines were carried out in a 25 μ l final volume containing 1X buffer Taq DNA polymerase, 3 mM MgCl₂, 0.2 mM dNTP, 0.25 μ M of each primer, 0.625 U Taq DNA polymerase (Invitrogen, Carlsbad, California). Cycling were performed under the following conditions: 2 min denaturation at 95°C, 35 cycles of 10 s denaturation at 95°C, 15 s annealing at 57°C, 30 s amplification at 72°C and a final 7 min amplification at 72°C. RT-PCR products were

separated on a 1% (w/v) agarose gel and stained with SYBR Safe (Invitrogen).

QUANTITATIVE RT-PCR

Total RNA was isolated from about 100 mg of tissue using the TRIzol reagent (Invitrogen) as described by the Manufacturer's Protocol. The RNA was incubated with RNase-free DNase I (1 U/ml) following the protocol provided by the manufacturer to remove possible genomic DNA. Then, RNA was reverse-transcribed into first-strand cDNA using SuperScript II reverse transcriptase (Invitrogen) and oligo-dT as a primer. The resultant cDNA was used as a template for qPCR amplification in a MiniOPTICON2 apparatus (Bio-Rad), using the intercalation dye SYBRGreen I (Invitrogen) as a fluorescent reporter and Platinum Taq Polymerase (Invitrogen). Primers for each of the genes under study were designed using the PRIMER3 software (Rozen and Skaletsky, 2000) in order to amplify unique 150–250 bp products (Table S2 in Supplementary Material). Amplification conditions were carried out under the following conditions: 2 min denaturation at 94°C; 40 cycles at 94°C for 10 s, 57°C for 15 s, and 72°C for 30 s, followed by 10 min extension at 72°C. Three replicates were performed for each sample. Melting curves for each PCR were determined by measuring the decrease of fluorescence with increasing temperature (from 65 to 98°C). PCR products were run on a 2% (w/v) agarose gel to confirm the size of the amplification products and to verify the presence of a unique PCR product. Gene expressions were normalized to the *A. thaliana* calcium dependent protein kinase3 (CPK3, Table S2). The expression of this gene has been previously reported to remain unchanged by UV-B (Ulm et al., 2004).

DNA DAMAGE ANALYSIS

The induction of CPD, 6-4 photoproducts and 8-oxodG was determined using an assay described in detail previously (Stapleton et al., 1993), using monoclonal antibodies specific to CPDs (TDM-2), 6-4 photoproducts (64M-2) and 8-oxodG (N45.1 obtained from Cosmo Bio Co., Ltd., Japan). After the treatments, plant samples (0.1 g) were collected and immediately immersed in liquid nitrogen and stored at –80°C. The 1.5 µg (for CPD assays), 20 µg (for 6-4 photoproduct assays) and 2 µg (for 8-oxodG assays) of the extracted DNA by a modified cetyl-trimethyl-ammonium bromide (CTAB) method was denatured in 0.3 M NaOH for 10 min and sextuplicate biological replicates were dot blotted onto a nylon membrane (Perkin Elmer Life Sciences, Waltham, Massachusetts). The membrane was incubated for 2 h at 80°C and then it was blocked in TBS (20 mM Tris-HCl, pH 7.6, 137 mM NaCl) containing 5% dried milk for 1 h at room temperature or overnight at 4°C. The blot was then washed with TBS and incubated with the different antibodies (1:2000 in TBS) overnight at 4°C with agitation. Unbound antibody was washed away and secondary antibody (BioRad) conjugated to alkaline phosphatase (1:3000) was added. The blot was then washed several times followed by the addition of the detection reagents NBT and BCIP. Quantification was achieved by densitometry of the dot blot using ImageQuant software version 5.2. DNA concentration was fluorometrically determined using the Qubit dsDNA assay kit (Invitrogen), and checked in a 1%

(w/v) agarose gels after quantification. DNA concentration was determined spectrophotometrically at 260 and 280 nm in the microplate reader (Biotek XS Power Wave) using the KC Junior computer program, and checked in a 1% (w/v) agarose gel after quantification.

ROOT LENGTH MEASUREMENTS

Petri dish-grown seedlings, surface-sterilized seeds were grown on MS growth medium and were held vertical in a growth chamber. Then, seedlings were UV-B treated for 2 h and kept in the absence of UV-B for 3 days. Plates were photographed before the treatment, and 24, 48, and 72 h after the end of the treatment, and the images were analyzed using the ImageJ program. Root lengths were determined by measuring the length of a line traced along the root.

PIGMENT MEASUREMENTS

UV-absorbing pigments (absorbance at 312 nm) were determined as described in Casati and Walbot (2004).

STATISTICAL ANALYSIS

Statistical analysis was done using ANOVA models (Tukey test) using untransformed data with Sigma Stat 3.1.

AUTHOR CONTRIBUTIONS

Julia I. Questa, Julieta Fina and Paula Casati designed the experiments and analyzed the data. Julia I. Questa and Julieta Fina did the experiments. Paula Casati wrote the article. Julia I. Questa, Julieta Fina and Paula Casati edited the manuscript.

ACKNOWLEDGMENTS

We thank the Arabidopsis Biological Resource Center (ABRC, Columbus, OH) that provided seed stocks. This research was supported by FONCyT grants PICT 2007-00711 and 2010-00105 to Paula Casati. Paula Casati is a member of the Researcher Career of the Consejo Nacional de Investigaciones Científicas y Técnicas (CONICET).

SUPPLEMENTARY MATERIAL

The Supplementary Material for this article can be found online at: <http://www.frontiersin.org/journal/10.3389/fpls.2013.00420/abstract>

Figure S1 | (A) Location of the T-DNA insertion in the *ROS1* gene (SALK_135293 line). Exons are represented by blue boxes, introns by thin black lines and the UTR regions by light gray boxes. The T-DNA insertion is indicated as a triangle. **(B)** Analysis of the PCR products separated in 1% (w/v) agarose gels. The PCR reactions were done using genomic DNA from Col0 and SALK_135293 plants. Lanes 1 show the PCR products obtained for a WT plant using the SALK_135293 F and SALK_135293 R primers; while lanes 2 show the PCR products obtained for homozygous mutant plants using the Lb and SALK_13293 R primers. **(C)** Transcript levels were evaluated by RT-PCR followed by agarose gels on cDNAs obtained from RNA extracted from the mutant or WT lines. Amplifications were performed using *ROS1* F and *ROS1* R primers, which are specific for the *ROS1* transcript. As a control, primers for the *RPL10B* transcript were used.

Figure S2 | (A) Location of the T-DNA insertion in the *ROS1* gene (SALK_045303 line). Exons are represented by blue boxes, introns by thin black lines and the UTR regions by light gray boxes. The T-DNA insertion is indicated as a triangle. **(B)** Analysis of the PCR products separated in 1% (w/v) agarose gels. The PCR reactions were done using genomic DNA from Col0 and SALK_045303 plants. Lanes 1 show the PCR products obtained for a WT plant using the SALK_045303 F and SALK_045303 R primers; while lanes 2 show the PCR products obtained for homozygous mutant plants using the Lb and SALK_045303 F primers. **(C)** Transcript levels were evaluated by RT-PCR followed by agarose gels on cDNAs obtained from RNA extracted from the mutant or WT lines. Amplifications were performed using *ROS1* F and *ROS1* R primers, which are specific for the *ROS1* transcript. As a control, primers for the *RPL10B* transcript were used.

Figure S3 | (A, C) Location of the T-DNA insertion in the *DDM1* gene (SALK_000590 **(A)** and SALK_093009 **(C)** lines). Exons are represented by blue boxes, introns by thin black lines and the UTR regions by light gray boxes. The T-DNA insertion is indicated as a triangle. **(B)** Analysis of the PCR products separated in 1% (w/v) agarose gels. The PCR reactions were done using genomic DNA from Col0 and SALK_000590 plants. Lanes 1 show the PCR products obtained for a WT plant using the SALK_000590 F and SALK_000590 R primers; while lanes 2 show the PCR products obtained for homozygous mutant plants using the Lb and SALK_000590 F primers. **(D)** Analysis of the PCR products separated in 1% (w/v) agarose gels. The PCR reactions were done using genomic DNA from Col0 and SALK_093009 plants. Lanes 1 show the PCR products obtained for a WT plant using the SALK_093009 F and SALK_093009 R primers; while lanes 2 show the PCR products obtained for homozygous mutant plants using the Lb and SALK_093009 R primers.

Figure S4 | Expression of *DDM1* transcripts in Col0 plants and *ddm1* mutants. Transcript levels were evaluated by RT-PCR followed by agarose

gels **(A)** and RT-qPCR **(B)** on cDNAs obtained from RNA extracted from the mutant or WT lines. Amplifications were performed using DDM1 F and DDM1 R primers, which are specific for the *DDM1* transcript. As controls, primers for the *RPL10B* **(A)** and *CPK3* **(B)** transcripts were used. **(B)** Expression values are relative to the values in Col0 plants. Data show mean values ± S.E.M. of at least three independent experiments.

Figure S5 | Phenotypes of *ddm1* mutants. (A) Images of 4-weeks-old Col0 and SALK_093009 plants. **(B)** Images of 6-weeks-old Col0 and SALK_093009 plants. **(C)** Analysis of *AtMu1* transposase expression in Col0 and SALK_093009 plants. Transcript levels were evaluated by RT-PCR followed by agarose gels on cDNAs obtained from RNA extracted from the mutant or WT lines.

Figure S6 | Relative expression of DNA repair transcripts by RT-qPCR in Col0, *ddm1* (*ddm1_000509* line) and *ros1* (*ros1_045303* line). Levels of *UVR2*, *UVR3*, *UVR7*, *UVH1*, *UVH6*, and *OGG1* were assayed in arabidopsis plants that were irradiated with UV-B for 4 h (UV-B) or were kept under control conditions without UV-B (control). Expression values are relative to the values in Col0 plants under control conditions in the absence of UV-B. The *CPK3* transcript was used as a control. Data show mean values ± S.E.M. of at least three independent experiments.

Figure S7 | Relative expression of DNA glycosidase transcripts by RT-qPCR in *ros1* plants. Levels of *DML2*, *DML3* and *DME1* were assayed in arabidopsis plants that were irradiated with UV-B for 4 h (UV-B) or were kept under control conditions without UV-B (control). Expression values are relative to the values in Col0 plants under control conditions in the absence of UV-B. The *CPK3* transcript was used as a control. Data show mean values ± S.E.M. of at least three independent experiments.

Table S1 | Primers used for identification of homozygous mutant lines.

Table S2 Primers used for RT-qPCR.

REFERENCES

- Agius, E., Kapoor, A., and Zhu, J.-K. (2006). Role of the Arabidopsis DNA glycosylase-lyase ROS1 in active DNA demethylation. *Proc. Natl. Acad. Sci. U.S.A.* 103, 11796–11801. doi: 10.1073/pnas.0603563103
- Alonso, J. M., Stepanova, A. N., Leisse, T. J., Kim, C. J., Chen, H., Shinn, P., et al. (2003). Genome-wide insertional mutagenesis of *Arabidopsis thaliana*. *Science* 301, 653–657. doi: 10.1126/science.1086391
- Bender, J. (2004). DNA methylation and epigenetics. *Annu. Rev. Plant Biol.* 55, 41–68. doi: 10.1146/annurev.arplant.55.031903.141641
- Bieza, K., and Lois, R. (2001). An *Arabidopsis* mutant tolerant to lethal ultraviolet-B levels shows constitutively elevated accumulation of flavonoids and other phenolics. *Plant Physiol.* 126, 1105–1115. doi: 10.1104/pp.126.3.1105
- Bray, C., and West, C. (2005). DNA repair mechanisms in plants: crucial sensors and effectors for the maintenance of genome integrity. *New Phytol.* 168, 511–528. doi: 10.1111/j.1469-8137.2005.01548.x
- Britt, A. B. (1996). DNA damage and repair in plants. *Annu. Rev. Plant Physiol. Plant Mol. Biol.* 4, 75–100. doi: 10.1146/annurev.arplant.47.1.75
- Campi, M., D'Andrea, L., Emiliani, J., and Casati, P. (2012). Participation of chromatin-remodeling proteins in the repair of ultraviolet-B-damaged DNA. *Plant Physiol.* 158, 981–995. doi: 10.1104/pp.111.191452
- Casati, P., Campi, M., Chu, F., Suzuki, N., Maltby, D., Guan, S., et al. (2008). Histone acetylation and chromatin remodeling are required for UV-B-dependent transcriptional activation of regulated genes in maize. *Plant Cell* 20, 827–842. doi: 10.1105/tpc.107.056457
- Casati, P., Stapleton, A. E., Blum, J. E., and Walbot, V. (2006). Genome-wide analysis of high altitude maize and gene knock-down stocks implicates chromatin remodeling proteins in responses to UV-B. *Plant J.* 46, 613–627. doi: 10.1111/j.1365-313X.2006.02721.x
- Casati, P., and Walbot, V. (2004). Crosslinking of ribosomal proteins to RNA in maize ribosomes by UV-B and its effects on translation. *Plant Physiol.* 136, 3319–3332. doi: 10.1104/pp.104.047043
- Chan, S. W. L., Henderson, I. R., and Jacobsen, S. E. (2005). Gardening the genome: DNA methylation in *Arabidopsis thaliana*. *Nat. Rev. Genet.* 6, 590–590. doi: 10.1038/nrg1664
- Choi, Y., Gehring, M., Johnson, L., Hannon, M., Harada, J. J., Goldberg, R. B., et al. (2002). DEMETER, a DNA glycosylase domain protein, is required for endosperm gene imprinting and seed viability in arabidopsis. *Cell* 110, 33–42. doi: 10.1016/S0092-8674(02)00807-3
- Eberharter, A., and Becker, P. B. (2002). Histone acetylation: a switch between repressive and permissive chromatin. Second in review on chromatin dynamics.
- Eisen, J. A., Sweder, K. S., and Hanawalt, P. C. (1995). Evolution of the SNF2 family of proteins: subfamilies with distinct sequences and functions. *Nucleic Acids Res.* 23, 2715–2723. doi: 10.1093/nar/23.14.2715
- Fransz, P., Soppe, W., and Schubert, I. (2003). Heterochromatin in interphase nuclei of *Arabidopsis thaliana*. *Chromosome Res.* 11, 227–240. doi: 10.1023/A:1022835825899
- Friedberg, E. C., Walker, G. C., and Siede, W. (1995). *DNA Repair and Mutagenesis*. Washington, DC: American Society For Microbiology.
- Gehring, M., Huh, J. H., Hsieh, T. F., Penterman, J., Choi, Y., Harada, J. J., et al. (2006). DEMETER DNA glycosylase establishes MEDEA polycomb gene self-imprinting by allele-specific demethylation. *Cell* 124, 495–506. doi: 10.1016/j.cell.2005.12.034
- Gehring, M., Reik, W., and Henikoff, S. (2009). DNA demethylation

- by DNA repair. *Trends Genet.* 25, 82–90. doi: 10.1016/j.tig.2008.12.001
- Gendrel, A.-V., Lippman, Z., Yordan, C., Colot, V., and Martienssen, R. A. (2002). Dependence of heterochromatic histone H3 methylation patterns on the Arabidopsis gene DDM1. *Science* 297, 1871–1873. doi: 10.1126/science.1074950
- Gerhardt, K. E., Wilson, M. I., and Greenberg, B. M. (1999). Tryptophan photolysis leads to a UVB-induced 66 kDa photoproduct of ribulose-1,5-bisphosphate carboxylase/oxygenase (Rubisco) *in vitro* and *in vivo*. *Photochem. Photobiol.* 70, 49–56. doi: 10.1562/0031-8655(1999)070<0049:TPLTAU>2.3.CO;2
- Gong, Z., Morales-Ruiz, T., Ariza, R. R., Roldán-Arjona, T., David, L., and Zhu, J. K. (2002). ROS1, a repressor of transcriptional gene silencing in Arabidopsis, encodes a DNA glycosylase/lyase. *Cell* 111, 803–814. doi: 10.1016/S0092-8674(02)01133-9
- Hays, J. B. (2002). *Arabidopsis thaliana*, a versatile model system for study of eukaryotic genome-maintenance functions. *DNA Repair* 1, 579–600. doi: 10.1016/S1568-7864(02)00093-9
- Hideg, E., Jansen, M. A. K., and Strid, A. (2013). UV-B exposure, ROS, and stress: inseparable companions or loosely linked associates? *Trends Plant. Sci.* 18, 107–115. doi: 10.1016/j.tplants.2012.09.003
- Hirochika, H., Okamoto, H., and Kakutani, T. (2000). Silencing of retrotransposons in arabidopsis and reactivation by the ddm1 mutation. *Plant Cell* 12, 357–369. doi: 10.1105/tpc.12.3.357
- Jansen, M. A. K., Gaba, V., and Greenberg, B. M. (1998). Higher plants and UV-B radiation: balancing damage, repair and acclimation. *Trends Plant. Sci.* 3, 131–135. doi: 10.1016/S1360-1385(98)01215-1
- Jeddeloh, J. A., Bender, J., and Richards, E. J. (1998). The DNA methylation locus DDM1 is required for maintenance of gene silencing in Arabidopsis. *Genes Dev.* 12, 1714–1725. doi: 10.1101/gad.12.11.1714
- Jeddeloh, J. A., Stokes, T. L., and Richards, E. J. (1999). Maintenance of genomic methylation requires a SWI2/SNF2-like protein. *Nat. Genet.* 22, 94–97. doi: 10.1038/8803
- Jordan, N. D., West, J. P., Bottley, A., Sheikh, M., and Furner, I. (2007). Transcript profling of the hypomethylated hog1 mutant of Arabidopsis. *Plant Mol. Biol.* 65, 571–586. doi: 10.1007/s11103-007-9221-4
- Kakutani, T., Jeddeloh, J. A., Flowers, S. K., Munakata, K., and Richards, E. J. (1996). Developmental abnormalities and epimutations associated with DNA hypomethylation mutations. *Proc. Natl. Acad. Sci. U.S.A.* 93, 12406–12411. doi: 10.1073/pnas.93.22.12406
- Kimura, S., and Sakaguchi, K. (2006). DNA repair in plants. *Chem. Rev.* 106, 753–766. doi: 10.1021/cr040482n
- Klein, H. L. (1997). RDH54, a RAD54 homologue in *Saccharomyces cerevisiae*, is required for mitotic diploid-specific recombination and repair and for meiosis. *Genetics* 147, 1533–1543.
- Kurihara, Y., Matsui, A., Kawashima, M., Kamimura, E., Ishida, J., Morosawa, T., et al. (2008). Identification of the candidate genes regulated by RNA-directed DNA methylation in Arabidopsis. *Biochem. Biophys. Res. Commun.* 376, 553–557. doi: 10.1016/j.bbrc.2008.09.046
- Landry, L. G., Chapple, C. C. S., and Last, R. L. (1995). Arabidopsis mutants lacking phenolic sunscreens exhibit enhanced ultraviolet-B injury and oxidative damage. *Plant Physiol.* 109, 1159–1166. doi: 10.1104/pp.109.4.1159
- Lario, L. D., Ramirez-Parra, E., Gutierrez, C., Casati, P., and Spampinato, C. P. (2011). Regulation of plant MSH2 and MSH6 genes in the UV-B induced DNA damage response. *J. Exp. Bot.* 62, 2925–2937. doi: 10.1093/jxb/err001
- Li, J. Y., Oulee, T. M., Raba, R., Amundson, R. G., and Last, R. L. (1993). Arabidopsis flavonoid mutants are hypersensitive to UV-B irradiation. *Plant Cell* 5, 171–179. doi: 10.1105/tpc.5.2.171
- Lippman, Z., May, B., Yordan, C., Singer, T., and Martienssen, R. (2003). Distinct mechanisms determine transposon inheritance and methylation via small interfering RNA and histone modification. *PLoS Biol.* 1:E67. doi: 10.1371/journal.pbio.0000067
- Liu, Q., Wang, J., Miki, D., Xia, R., Yu, W., He, J., et al. (2010a). DNA replication factor C1 mediates genomic stability and transcriptional gene silencing in Arabidopsis. *Plant Cell* 22, 2336–2352. doi: 10.1105/tpc.110.076349
- Liu, J., Ren, X., Yin, H., Wang, Y., Xia, R., Wang, Y., et al. (2010b). Mutation in the catalytic subunit of DNA polymerase a influences transcriptional gene silencing and homologous recombination in Arabidopsis. *Plant J.* 61, 36–45. doi: 10.1111/j.1365-313X.2009.04026.x
- Martínez-Macías, M. I., Qian, W., Miki, D., Pontes, O., Liu, Y., Tang, K., et al. (2012). A DNA 30 phosphatase functions in active DNA demethylation in Arabidopsis. *Mol. Cell* 45, 357–370. doi: 10.1016/j.molcel.2011.11.034
- Mazza, C. A., Boccalandro, H. E., Giordano, C. V., Battista, D., Scopel, A. L., and Ballaré, C. L. (2000). Functional significance and induction by solar radiation of ultraviolet-absorbing sunscreens in field-grown soybean crops. *Plant Physiol.* 122, 117–125. doi: 10.1104/pp.122.1.117
- Melamed-Bessudo, C., and Levy, A. A. (2012). Deficiency in DNA methylation increases meiotic crossover rates in euchromatic but not in heterochromatic regions in Arabidopsis. *Proc. Natl. Acad. Sci. U.S.A.* 109, E981–E988. doi: 10.1073/pnas.1120742109
- Mirouze, M., Reinders, J., Bucher, E., Nishimura, T., Schneeberger, K., Ossowski, S., et al. (2009). Selective epigenetic control of retrotransposition in Arabidopsis. *Nature* 461, 427–430. doi: 10.1038/nature08328
- Mittelsten Scheid, O., Probst, A. V., Afsar, K., and Paszkowski, J. (2002). Two regulatory levels of transcriptional gene silencing in Arabidopsis. *Proc. Natl. Acad. Sci. U.S.A.* 99, 13659–13662. doi: 10.1073/pnas.202380499
- Miura, A., Yonebayashi, S., Watanabe, K., Toyama, T., Shimada, H., and Kakutani, T. (2001). Mobilization of transposons by a mutation abolishing full DNA methylation in Arabidopsis. *Nature* 411, 212–214. doi: 10.1038/35075612
- Morales-Ruiz, T., Ortega-Galisteo, A. P., Ponferrada-Marín, M. I., Martínez-Macías, M. I., Ariza, R. R., and Roldán-Arjona, T. (2006). DEMETER and REPRESSOR OF SILENCING 1 encode 5-methylcytosine DNA glycosylases. *Proc. Natl. Acad. Sci. U.S.A.* 103, 6853–6858. doi: 10.1073/pnas.0601109103
- Ormrod, D. P., Landry, L. G., and Conklin, P. L. (1995). Short-term UV-B radiation and ozone exposure effects on aromatic secondary metabolite accumulation and shoot growth of flavonoid-deficient arabidopsis mutants. *Physiol. Plant.* 93, 602–610. doi: 10.1111/j.1399-3054.1995.tb05106.x
- Ortega-Galisteo, A. P., Morales-Ruiz, T., Ariza, R. R., and Roldán-Arjona, T. (2008). Arabidopsis DEMETER-LIKE proteins DML2 and DML3 are required for appropriate distribution of DNA methylation marks. *Plant Mol. Biol.* 67, 671–681. doi: 10.1007/s11103-008-9346-0
- Penterman, J., Zilberman, D., Huh, J. H., Ballinger, T., Henikoff, S., and Fischer, R. L. (2007). DNA demethylation in the Arabidopsis genome. *Proc. Natl. Acad. Sci. U.S.A.* 104, 6752–6757. doi: 10.1073/pnas.0701861104
- Pfluger, J., and Wagner, D. (2007). Histone modifications and dynamic regulation of genome accessibility in plants. *Curr. Opin. Plant Biol.* 10, 645–652. doi: 10.1016/j.pbi.2007.07.013
- Ponferrada-Marín, M. I., Roldán-Arjona, T., and Ariza, R. R. (2009). ROS1 5-methylcytosine DNA glycosylase is a slow-turnover catalyst that initiates DNA demethylation in a distributive fashion. *Nucleic Acids Res.* 37, 4264–4274. doi: 10.1093/nar/gkp390
- Probst, A. V., Dunleavy, E., and Almouzni, G. (2009). Epigenetic inheritance during the cell cycle. *Nat. Rev. Mol. Cell Biol.* 10, 192–206. doi: 10.1038/nrm2640
- Probst, A. V., Fransz, P. F., Paszkowski, J., and Mittelsten Scheid, O. (2003). Two means of transcriptional reactivation within heterochromatin. *Plant J.* 33, 743–749. doi: 10.1046/j.1365-313X.2003.01667.x
- Roldán-Arjona, T., and Ariza, R. R. (2009). “DNA demethylation,” in *DNA and RNA Modification Enzymes: Comparative Structure, Mechanism, Functions, Cellular Interactions and Evolution*, ed H. Grosjean (Austin, TX: Landes Bioscience), 149–161.
- Rosa, M., Von Harder, M., Cigliano, R. A., Schlöglhofer, P., and Mittelsten Scheid, O. (2013). The Arabidopsis SWR1 chromatin-remodeling complex is important for DNA repair, somatic recombination, and meiosis. *Plant Cell* 25, 1990–2001. doi: 10.1105/tpc.112.104067
- Rozen, S., and Skaletsky, H. (2000). Primer3 on the WWW for general users and for biologist programmers. *Methods Mol. Biol.* 132, 365–386. doi: 10.1385/1-59259-192-2:365
- Sambrook, J., and Russell, D. W. (2001). *Molecular Cloning – A Laboratory Manual*. New York, NY: Cold Spring Harbor Laboratory Press.
- Shaked, H., Avivi-Ragolsky, N., and Levy, A. A. (2006). Involvement of

- the Arabidopsis SWI2/SNF2 chromatin remodeling gene family in DNA damage response and recombination. *Genetics* 173, 985–994. doi: 10.1534/genetics.105.051664
- Shinohara, M., Shita-Yamaguchi, E., Buerstedde, J. M., Shinagawa, H., Ogawa, H., and Shinohara, A. (1997). Characterization of the roles of the *Saccharomyces cerevisiae RAD54* gene and a homologue of *RAD54*, *RDH54/TID1*, in mitosis and meiosis. *Genetics* 147, 1545–1556.
- Singer, T., Yordan, C., and Martienssen, R. A. (2001). Robertson's mutator transposons in *A. thaliana* are regulated by the chromatin-remodeling gene *Decrease in DNA Methylation (DDM1)*. *Genes Dev.* 15, 591–602. doi: 10.1101/gad.193701
- Slotkin, R. K., and Martienssen, R. (2007). Transposable elements and the epigenetic regulation of the genome. *Nat. Rev. Genet.* 8, 272–285. doi: 10.1038/nrg2072
- Soppe, W. J. J., Jasencakova, Z., Houben, A., Kakutani, T., Meister, A., Huang, M. S., et al. (2002). DNA methylation controls histone H3 lysine 9 methylation and heterochromatin assembly in Arabidopsis. *EMBO J.* 21, 6549–6559. doi: 10.1093/emboj/cdf657
- Stapleton, A. E., Mori, T., and Walbot, V. (1993). A simple and sensitive antibody-based method to measure UV-induced DNA damage in *Zea mays*. *Plant Mol. Biol. Rep.* 11, 230–236. doi: 10.1007/BF02669850
- Tong, H., Leisure, C. D., Hou, X., Yuen, G., Briggs, W., and He, Z. H. (2008). Role of root UV-B sensing in *Arabidopsis* early seedling development. *Proc. Natl. Acad. Sci. U.S.A.* 105, 21039–21044. doi: 10.1073/pnas.0809942106
- Tsukahara, S., Kobayashi, A., Kawabe, A., Matthieu, O., Miura, A., and Kakutani, T. (2009). Bursts of retrotransposition reproduced in Arabidopsis. *Nature* 461, 423–426. doi: 10.1038/nature08351
- Ulm, R., Baumann, A., Oravecz, A., Mate, Z., Adam, E., Oakeley, E. J., et al. (2004). Genome-wide analysis of gene expression reveals function of the bZIP transcription factor HY5 in the UV-B response of Arabidopsis. *Proc. Natl. Acad. Sci. U.S.A.* 101, 1397–1402. doi: 10.1073/pnas.0308044100
- Vaillant, I., and Paszkowski, J. (2007). Role of histone and DNA methylation in gene regulation. *Curr. Opin. Plant Biol.* 10, 528–533. doi: 10.1016/j.pbi.2007.06.008
- Vanyushin, B. F., and Ashapkin, V. V. (2011). DNA methylation in higher plants: past, present and future. *Biochim. Biophys. Acta* 1809, 360–368. doi: 10.1016/j.bbagen.2011.04.006
- Verbsky, M. L., and Richards, E. J. (2001). Chromatin remodeling in plants. *Curr. Opin. Plant Biol.* 4, 494–500. doi: 10.1016/S1369-5266(00)00206-5
- Vielle-Calzada, J. P., Thomas, J., Spillane, C., Coluccio, A., Hoeppner, M. A., and Grossniklaus, U. (1999). Maintenance of genomic imprinting at the Arabidopsis medea locus requires zygotic DDM1 activity. *Genes Dev.* 13, 2971–2982. doi: 10.1101/gad.13.22.2971
- Vongs, A., Kakutani, T., Martienssen, R. A., and Richards, E. J. (1993). *Arabidopsis thaliana* DNA methylation mutants. *Science* 260, 1926–1928. doi: 10.1126/science.8316832
- Wang, Y., Liu, J., Xia, R., Wang, J., Shen, J., Cao, R., et al. (2007). The protein kinase TOUSLED is required for maintenance of transcriptional gene silencing in Arabidopsis. *EMBO Rep.* 8, 77–83. doi: 10.1038/sj.emboj.7400852
- Xia, R., Wang, J., Liu, C., Wang, Y., Zhai, J., Liu, J., et al. (2006). ROR1/RPA2A, a putative replication protein A2, functions in epigenetic gene silencing and in regulation of meristem development in Arabidopsis. *Plant Cell* 18, 85–103. doi: 10.1105/tpc.105.037507
- Yaish, M. W., Colasanti, J., and Rothstein, S. J. (2011). The role of epigenetic processes in controlling flowering time in plants exposed to stress. *J. Exp. Bot.* 62, 3727–3735. doi: 10.1093/jxb/err177
- Yao, Y., Bilicheck, A., Golubov, A., and Kovalchuk, I. (2012). *ddm1* plants are sensitive to methyl methane sulfonate and NaCl stresses and are deficient in DNA repair. *Plant Cell Rep.* 31, 1549–1561. doi: 10.1007/s00299-012-1269-1
- Yin, H., Zhang, X., Liu, J., Wang, Y., He, J., Yang, T., et al. (2009). Epigenetic regulation, somatic homologous recombination, and abscisic acid signaling are influenced by DNA polymerase {epsilon} mutation in Arabidopsis. *Plant Cell* 21, 386–402. doi: 10.1105/tpc.108.061549
- Zhu, J., Kapoor, A., Sridhar, V. V., Agius, F., and Zhu, J. K. (2007). The DNA glycosylase/lyase ROS1 functions in pruning DNA methylation patterns in Arabidopsis. *Curr. Biol.* 17, 54–59. doi: 10.1016/j.cub.2006.10.059
- Zhu, J. K. (2009). Active DNA demethylation mediated by DNA glycosylases. *Annu. Rev. Genet.* 43, 143–166. doi: 10.1146/annurev-genet-102108-134205

Conflict of Interest Statement: The authors declare that the research was conducted in the absence of any commercial or financial relationships that could be construed as a potential conflict of interest.

Received: 22 August 2013; accepted: 02 October 2013; published online: 21 October 2013.

*Citation: Questa JI, Fina JP and Casati P (2013) DDM1 and ROS1 have a role in UV-B induced- and oxidative DNA damage in *A. thaliana*. Front. Plant Sci. 4:420. doi: 10.3389/fpls.2013.00420*

This article was submitted to Plant Physiology, a section of the journal Frontiers in Plant Science.

Copyright © 2013 Questa, Fina and Casati. This is an open-access article distributed under the terms of the Creative Commons Attribution License (CC BY). The use, distribution or reproduction in other forums is permitted, provided the original author(s) or licensor are credited and that the original publication in this journal is cited, in accordance with accepted academic practice. No use, distribution or reproduction is permitted which does not comply with these terms.



Mitogen-activated protein kinase signal transduction and DNA repair network are involved in aluminum-induced DNA damage and adaptive response in root cells of *Allium cepa* L.

Brahma B. Panda * and V. Mohan M. Achary[†]

Molecular Biology and Genomics Laboratory, Department of Botany, Berhampur University, Berhampur, India

Edited by:

Alma Balestrazzi, University of Pavia, Italy

Reviewed by:

Reinhard Kunze, Freie Universität Berlin, Germany

Alma Balestrazzi, University of Pavia, Italy

Mattia Donà, Gregor Mendel Institute of Plant Molecular Biology, Austria

***Correspondence:**

Brahma B. Panda, Molecular Biology and Genomics Laboratory, Department of Botany, Berhampur University, Bhanj Bihar, Berhampur 760007 India
e-mail: panda.brahma@gmail.com

†Present address:

V. Mohan M. Achary, Plant Molecular Biology Group, International Centre for Genetic Engineering and Biotechnology, New Delhi, India

In the current study, we studied the role of signal transduction in aluminum (Al^{3+})-induced DNA damage and adaptive response in root cells of *Allium cepa* L. The root cells *in planta* were treated with Al^{3+} (800 μM) for 3 h without or with 2 h pre-treatment of inhibitors of mitogen-activated protein kinase (MAPK), and protein phosphatase. Also, root cells *in planta* were conditioned with Al^{3+} (10 μM) for 2 h and then subjected to genotoxic challenge of ethyl methane sulfonate (EMS; 5 mM) for 3 h without or with the pre-treatment of the aforementioned inhibitors as well as the inhibitors of translation, transcription, DNA replication and repair. At the end of treatments, roots cells were assayed for cell death and/or DNA damage. The results revealed that Al^{3+} (800 μM)-induced significant DNA damage and cell death. On the other hand, conditioning with low dose of Al^{3+} induced adaptive response conferring protection of root cells from genotoxic stress caused by EMS-challenge. Pre-treatment of roots cells with the chosen inhibitors prior to Al^{3+} -conditioning prevented or reduced the adaptive response to EMS genotoxicity. The results of this study suggested the involvement of MAPK and DNA repair network underlying Al-induced DNA damage and adaptive response to genotoxic stress in root cells of *A. cepa*.

Keywords: adaptive response, DNA damage, DNA repair, genome protection, MAP kinase, metabolic inhibitors, signal transduction

INTRODUCTION

Plant genome is under constant stress from endogenous as well as exogenous factors. Plants being sedentary are uniquely equipped with innate mechanisms that help them to adapt to environmental changes. Plant genome integrity is maintained by specific cellular repair functions, among which some are known to be highly conserved during evolution (Roldan-Arjona and Ariza, 2009). DNA damage, if not repaired properly, results in genomic perturbation adversely affecting the plant development, productivity and genetic diversity (Tuteja et al., 2009; Balestrazzi et al., 2011). Recently, genetic and biochemical analysis have considerably advanced our understanding of DNA repair processes and their involvement in genotoxic stress response and signaling in plants (Ulm, 2003; Bray and West, 2005). Often, plants are known to display cross-adaptation to abiotic and genotoxic stresses (Panda et al., 2013).

The mitogen-activated protein kinase (MAPK) cascade comprising the MAPKKK-MAPKK-MAPK module is one of the major routes that mediates transduction of extra cellular stimuli to intracellular responses, which has been shown in yeast (Thevelein, 1994) and mammalian cells (Kyriakis and Avruch, 2001). MAPKs are the intracellular mediators of signals that shuttle between the cytoplasm and the nucleus targeting several

transcription factors (Hirt, 2000; Yang et al., 2003a). MAPK phosphatases (MKPs) through dephosphorylation of both tyrosine and serine/threonine residues, are known to inactivate MAPK cascades with high specificity (Camps et al., 2000; Keyse, 2000). MKPs are also implicated in DNA damage response mediated by MAPK pathway (Ulm et al., 2001). Ataxia telangiectasia-mutated (ATM) and ATM-Rad3-related (ATR) kinases that are activated by DNA damage are considered central to the DNA damage response (Hurley and Bunz, 2007). DNA double strand breaks (DSBs) have been reported to activate ATM kinase, which in turn activate the downstream signaling pathways leading to transient arrest of the cell cycle and inhibition of DNA replication facilitating DNA repair (Mannuss et al., 2012). ATM is also activated by oxidative stress (Watters, 2003). On the other hand, the ATR kinase is activated by stalled replication forks, which can occur spontaneously or upon exposure to UV-irradiation or hydroxyurea (Mannuss et al., 2012). ATR regulates the slowing of the cell cycle during S phase and the G2/M progression (Abraham, 2001). In plant cells, DNA-damage activates ATM and ATR kinases via the WEE1 serine/threonine kinase transiently arresting the cell-cycle and allowing cells to repair DNA damage prior to initiation of mitosis (De Schutter et al., 2007). However, the proteins that initially sense DNA damage and initiate the signaling

response are currently unknown. Poly(ADP-ribose) polymerase (PARP) and DNA-dependent protein kinase (DNA-PK) have long been proposed as DNA damage sensors. PARP is activated by DNA break, which in turn depending on the severity of the damage and amplitude of activation, can lead to either repair or programmed cell death (PCD) in cells (Briggs and Bent, 2011). PARPs and poly(ADP ribose) glycohydrolases (PARGs) are the main enzymes responsible for the posttranslational modification known as poly(ADP-ribosyl)ation implicated in DNA damage response (Briggs and Bent, 2011). These enzymes play important roles in tolerance to genotoxic stress, DNA repair, PCD, transcription, and cell cycle control in plants (Adams-Phillips et al., 2010). Current knowledge on DNA damage response emerging from plants also suggests that strand breaks trigger the DNA damage response by inducing the expression of molecular markers associated with DNA damage repair, such as the PARP, RAD51, and breast cancer (BRCA) family members (Vanderauwera et al., 2011).

The role of reactive oxygen species (ROS) in the activation of MAPK-pathways, DNA damage response, and DNA repair networks has been suggested (Varnova et al., 2002; Yang et al., 2003b). Heavy metals (Cd^{2+} , Cu^{2+} , Pb^{2+} , Zn^{2+}) are also known to activate signal transduction pathways through the ROS-mediated MAPK pathways (Jonak et al., 2004; Lin et al., 2005; Liu et al., 2010). Aluminum (Al^{3+}) is a light metal that induces DNA damage through triggering the oxidative burst (Achary et al., 2012). The involvement of checkpoint regulators such as TANMEI/ALUMINUM TOLERANT2 (ALT2) and ataxia telangiectasia-mutated (ATM) and ATM-Rad3-related (ATR) kinases in the Al-dependent root growth inhibition and cell cycle arrest in *Arabidopsis thaliana* has been suggested (Rounds and Larsen, 2008; Nezames et al., 2012). Furthermore, we have recently demonstrated the role of ROS in Ca^{2+} channel signal transduction underlying Al^{3+} -induced DNA damage and adaptive response (Achary et al., 2013). Also, in this study, we have shown that the Al^{3+} induces adaptive response to genotoxic stress in root cells of *A. cepa* failing to uphold the cell cycle checkpoint arrest mechanism in the underlying DNA damage and response. Furthermore, our earlier study also suggests unknown alternate pathway(s) involving the MAPK signal transduction and DNA repair network (Achary et al., 2013).

In sequel to our earlier studies (Achary and Panda, 2010; Achary et al., 2012, 2013), in the present study we investigated the involvement of MAPK signaling in DNA repair network in the Al^{3+} -induced DNA damage and adaptive response to genotoxic stress in root cells of *A. cepa* L.

MATERIALS AND METHODS

ASSAY SYSTEMS

Bulbs of onion (*Allium cepa* L., $2n = 16$) were used as the test system. Bulbs were procured from the local farmers. Hand-picked bulbs of uniform size were scrapped so that the apices of the root primordial were exposed and their dry scales peeled off. Bulbs were then surface sterilized by rinsing in 1% sodium hypochlorite solution followed by 70% ethanol and set for rooting in sterilized moist sand in dark. After 2 days, bulbs with 2–3 cm long roots were washed in running tap water for 5–10 min and

then subjected to the chosen treatments. The experiments were conducted at room temperature $25 \pm 1^\circ\text{C}$ in dark.

TEST CHEMICALS AND EXPERIMENTAL SOLUTIONS

The major chemicals used in the current experiments include: Aluminum chloride (AlCl_3 , HiMedia, India), ethyl methanesulfonate (EMS, HiMedia, Mumbai), and actinomycin D (ACD), 3-aminobenzamide (3-AB), 2-aminopurine (2-AP), aphidicolin (APH), caffeine (CAF), cycloheximide (CHX), cantharidin (CAN, 2,3-dimethyl-7-oxabicyclo[2.2.1] heptane-2,3-dicarboxylic anhydride), endothall, (ENT, 7-oxabicyclo[2.2.1] heptane-2,3-dicarboxylic acid), LY-294002 (LY), PD-98059 (PD), and sodium orthovanadate (SOV), were all procured from Sigma-Aldrich, USA. Stock solutions of the chemicals were prepared in distilled water. Chemicals that were not easily dissolved in water were first dissolved in a small volume of dimethyl sulfoxide (DMSO) and then diluted with distilled water. Experimental solution of AlCl_3 was adjusted to pH 4.5 rendering the metal in the soluble form (Al^{3+}) available for plant-uptake (Kochian et al., 2004).

EXPERIMENTAL DESIGN AND TREATMENT PROTOCOL

Treatments were carried out by placing the onion bulbs on 30 mL glass test tubes (Borosil®, Mumbai) with roots dipped in the experimental solutions. Depending on the specific objectives, experiments were conducted following two different treatment protocols as described as below.

Experiment I: Effect of kinase and phosphatase inhibitors on Al^{3+} -induced cell death and DNA damage in root cells of *A. cepa* L.

Bulbs of *A. cepa* with growing roots (2–3 cm long) were treated with Al^{3+} (800 μM) at pH 4.5 for 3 h either without or with prior treatment with the kinase inhibitors: LY (1–4 μM), PD (2.5–7.5 μM), and 2-AP (5–20 μM); protein phosphatase inhibitors: SOV (10–50 μM), ENT (10–50 μM), and CAN (5–20 μM) for 2 h. Appropriate water and DMSO controls were maintained under identical conditions for comparison. At the end of the treatments, cell death and DNA damage by the Comet assay were assayed in the excised roots (Figure 1).

Experiment II: Effect of kinase, phosphatase, and metabolic inhibitors on Al^{3+} -induced adaptive response to genotoxic stress in root cells of *A. cepa* L.

Bulbs of *A. cepa* with growing roots (2–3 cm long) were first conditioned by a 2 h treatment with Al^{3+} 10 μM (pH 4.5), and after a 2 h inter-treatment interval, were subjected to

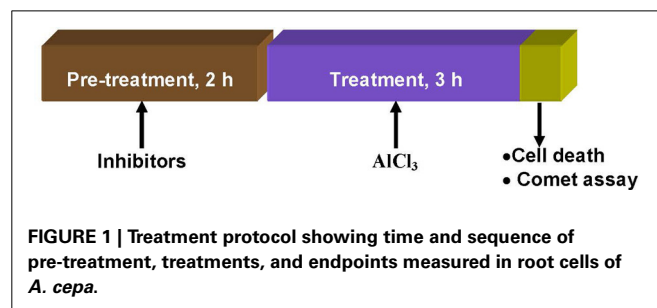


FIGURE 1 | Treatment protocol showing time and sequence of pre-treatment, treatments, and endpoints measured in root cells of *A. cepa*.

challenge-treatment for 3 h by EMS 5 mM without or with pre-treatments of kinase inhibitors: LY (1, 2 μ M), PD (2.5, 5 μ M), 2-AP (10, 20 μ M); protein phosphatase inhibitors: SOV (25, 50 μ M); ENT (25, 50 μ M), CAN (10, 20 μ M); *de novo* translation inhibitor: CHX (1, 5 μ M); transcriptional inhibitor ACD (5, 10 μ M); PARP inhibitor: 3-AB (5, 10 μ M), post-transcriptional repair inhibitor: CAF (10, 20 μ M); repair replication polymerase inhibitor: APH (5, 10 μ M) for 2 h, administered prior to Al³⁺ conditioning at low non-toxic treatments. All the treatments were terminated by washing of the intact roots in running tap water for at least 10 min. At the end of treatments, batches of roots from different groups were processed immediately for Comet assay (**Figure 2**). Appropriate negative (water and DMSO) and positive (inhibitor + EMS and inhibitor + low dose Al³⁺) controls were maintained and handled alike. The above pre-treatment concentrations of kinase, phosphatase, and metabolic inhibitors were chosen on the basis of pilot experiments that revealed little or no influence on EMS-induced DNA damage.

CELL DEATH

For determination of cell death, control, and treated bulbs with intact roots were stained with 0.25% (w/v) aqueous solution of Evans blue (HiMedia, Mumbai) for 15 min (Baker and Mock, 1994). After washing the roots, batches of 10 stained root tips of equal length (10 mm) were excised and soaked in 3 mL of N, N-dimethylformamide (Merck, Mumbai) for 1 h at room temperature. The absorbance of Evans blue released was measured spectrophotometrically at 600 nm.

COMET ASSAY

For alkaline comet assay, bulbs with intact roots of *A. cepa* from different treatments were thoroughly washed in running tap water. Comet assay on excised roots was carried out following the protocol described earlier (Achary and Panda, 2010). Analysis of DNA damage by Comet assay was performed on the nuclei isolated from root cells belonging to the elongation or differentiation root zones (**Figure 3**). An Olympus BX51 microscope fitted with a fluorescence attachment (using the excitation filter 515–560 nm and barrier filter 590 nm) and a Cohu camera and Kinetic Komet™ Imaging Software 5.5 (Andor™ Technology, www.andor.com) was employed for comet analysis. Two slides prepared from 20 roots were examined for each treatment. At least, 50 comets were scored from each slide. The comet images

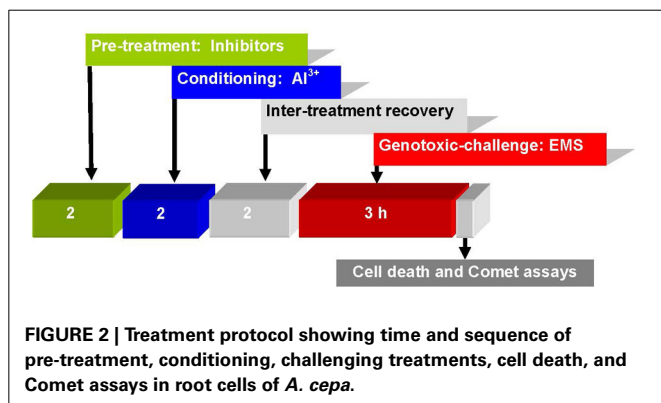


FIGURE 2 | Treatment protocol showing time and sequence of pre-treatment, conditioning, challenging treatments, cell death, and Comet assays in root cells of *A. cepa*.

obtained from roots of *A. cepa* were visualized and captured at 100 \times magnifications, respectively. Out of a number of parameters available in the software, comets were analyzed on the basis of the Olive tail moment, OTM (Kumaravel et al., 2000). The entire process of the comet assay was carried out in dim or yellow light.

STATISTICAL ANALYSIS

All the experiments with the exception to genotoxic assay were replicated thrice, whereas experiments with genotoxic assay were repeated at least once in order to establish the reproducibility of the results. Pooled data were statistically analyzed using analysis of variance (ANOVA), followed by Tukey's honestly significant difference (HSD) test (Daniel, 1995) employing the Windows®7/Microsoft Excel 2003 computer package.

Protection conferred by kinase and phosphatase inhibitor on Al³⁺-induced cell death and DNA-damage were calculated as percent of relative decrease from Al³⁺ (800 μ M; positive control). Furthermore, adaptive response was assessed on the basis of protection calculated as percent of relative decrease of DNA damage as compared with that of the positive controls (EMS-challenge). Likewise, prevention of adaptive response induced by kinase, phosphatase and metabolic repair inhibitors was calculated as percent of the relative increase in the above values as compared to corresponding Al³⁺-conditioning plus EMS challenge (Achary and Panda, 2010).

RESULTS

EFFECT OF INHIBITORS OF PROTEIN KINASE AND PHOSPHATASE ON AI³⁺-INDUCED CELL DEATH AND DNA DAMAGE

First of all it was established that the inhibitors at the chosen pre-treatment concentrations in par with the corresponding controls

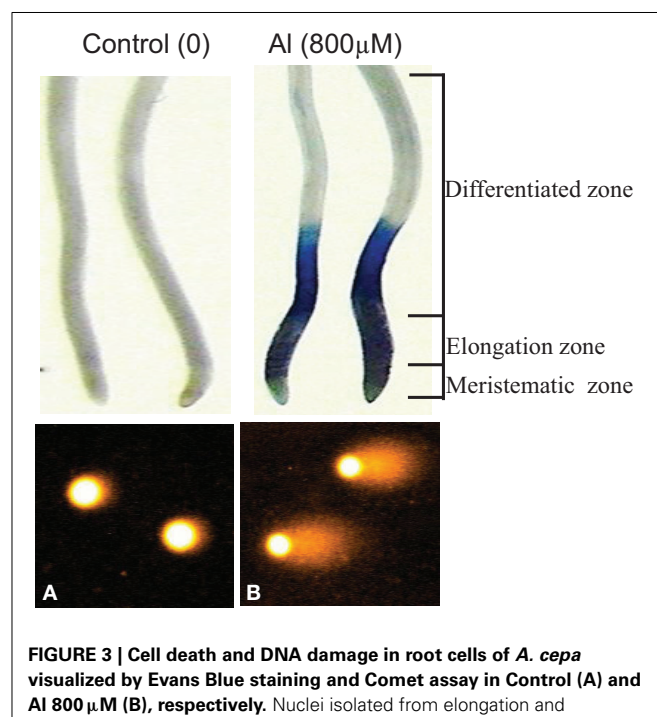


FIGURE 3 | Cell death and DNA damage in root cells of *A. cepa* visualized by Evans Blue staining and Comet assay in Control (A) and Al 800 μ M (B), respectively. Nuclei isolated from elongation and differentiation zones were analyzed for DNA damage by Comet assay.

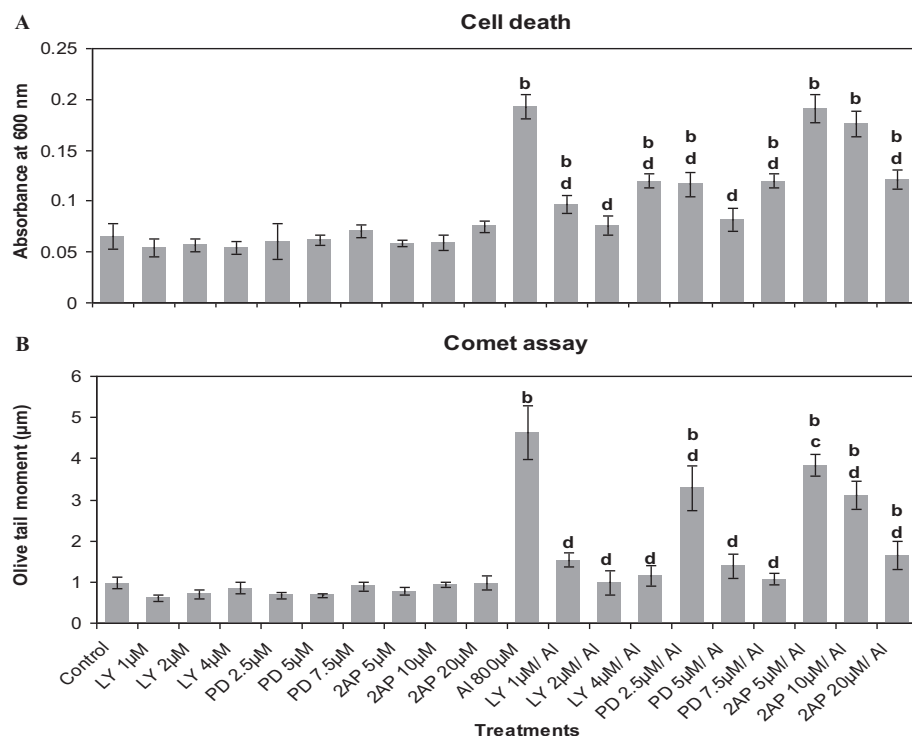


FIGURE 4 | Pre-treatment of MAPK inhibitors: LY (LY-294002) 1–4 μM; PD (PD-98059) 2.5–7.5 μM and protein kinase inhibitor: 2AP (2-aminopurine) 5–20 μM prevented Al³⁺-induced cell death (A) and

DNA damage (B) in root tissue of *A. cepa*. Increase significant compared to control at $p \leq 0.01$ (b); decrease significant compared to Al³⁺ 800 μM at $p \leq 0.05$ (c) or 0.01 (d).

(water or DMSO) did not induce cell death or DNA damage in root cells of *A. cepa* (Figure 4). There was no difference between water and DMSO controls nor DMSO showed any effect on the treatments (data not shown). On the contrary, Al³⁺ (800 μM) induced cell death and DNA damage significantly ($p \leq 0.01$). Al³⁺-induced cell death or DNA damage was significantly counteracted when the roots were pre-treated with the protein kinase inhibitors LY at the doses of 1, 2, and 4 μM (49.82, 60.5, and 37.7%); PD at the doses of 2.5, 5, and 7.5 μM (39.49, 57.73, and 37.7%) and 2-AP only at the dose of 20 μM (37%) that offered protection against cell death to different extents. However, 2-AP at the two lower concentrations (5 and 10 μM) failed to affect the cell death induced by Al³⁺ (800 μM). Likewise, pre-treatments with the chosen inhibitors conferred significant protection ($p \leq 0.05$ or 0.01) against Al³⁺-induced DNA-damage in root cells (66.97, 78.61, and 75.3% inhibition by LY 1, 2, and 4 μM; 29.26, 70.14, and 77% inhibition by PD 2.5, 5, and 7.5 μM, and 17.04, 33.03, and 64.52% inhibition by 2-AP 5, 10, and 20 μM, respectively). Among the tested MAPK-inhibitors, 2-AP was the least effective in countering cell death or DNA damage induced by Al³⁺ (800 μM) (Figure 4). Similarly, pre-treatment with the protein phosphatase inhibitors (ENT 25, 50 μM and CAN 5, 10, and 20 μM) significantly protected roots from Al³⁺-induced cell death (10.6, 23.6 and 5.9, 10.6, and 23.6% protection), and DNA damage (28.3, 35.7, and 29.1, 36, and 61.9%) (Figure 5). On the other hand, SOV at doses of 10–50 μM and the ENT at the lowest dose of 10 μM apparently

were ineffective in preventing Al³⁺-induced cell death or DNA damage.

EFFECT OF INHIBITORS OF PROTEIN KINASE AND PHOSPHATASE ON Al³⁺-INDUCED GENOTOXIC ADAPTATION TO EMS

Comet analysis revealed that LY (1, 2 μM), PD (2.5, 5 μM) or 2-AP (10, 20 μM) did not significantly affect the DNA damage induced by Al³⁺ (10 μM) in root cells of *A. cepa* as compared to that in the control (Figure 6). EMS at the dose of 5 mM significantly induced ($p \leq 0.01$) DNA damage. The kinase and phosphatase inhibitors at the tested concentrations had little or no effect on EMS-induced DNA damage (data not shown for sake of brevity). Al³⁺-conditioning significantly ($p \leq 0.01$) protected against the EMS-induced DNA damage that accounted for 69.83% genomic protection. Pre-treatments of protein kinase inhibitors LY (1, 2 μM), PD (2.5, 5 μM) and 2-AP (10, 20 μM) significantly ($p \leq 0.01$) abolished the Al-induced adaptive response against EMS-challenge that was evident by the recurrence of the DNA damage (58.07 and 67.1% under treatment with LY at 1, 2 μM; 52.77 and 65.45% under treatment with PD at 2.5, 5 μM; 40.06 and 45.38% under treatment with 2-AP at 10, 20 μM). Noteworthy was that of all protein kinase inhibitors LY (2 μM) and PD (5 μM) were the most effective to abolish the Al-adaptive response against EMS-challenge (Figure 6). On the contrary, the protein phosphatase inhibitors SOV (25, 50 μM), ENT (25, 50 μM), and CAN (10, 20 μM) proved ineffective to counter the Al-induced

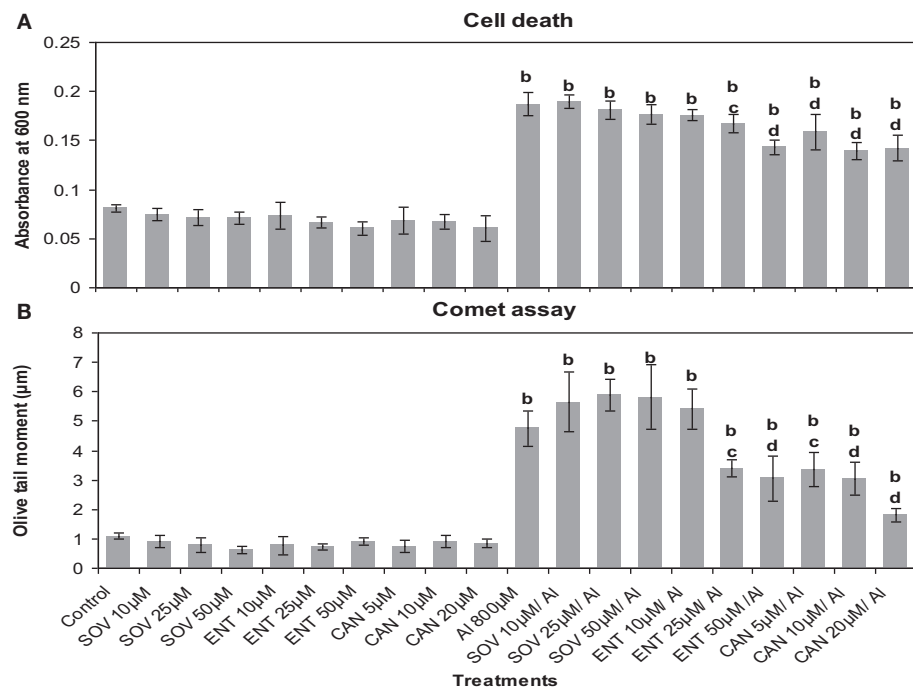


FIGURE 5 | Pre-treatment of protein phosphatase inhibitors: SOV (Na_2VO_4) 10–50 μM ; ENT (endothall) 10–50 μM ; CAN (cantharidin) 5–20 μM prevented Al-induced cell death (A) and DNA damage (B) in

root tissue of *A. cepa*. Increase significant compared to control at $p \leq 0.01$ (b); decrease significant compared to Al^{3+} 800 μM at $p \leq 0.05$ (c) or 0.01 (d).

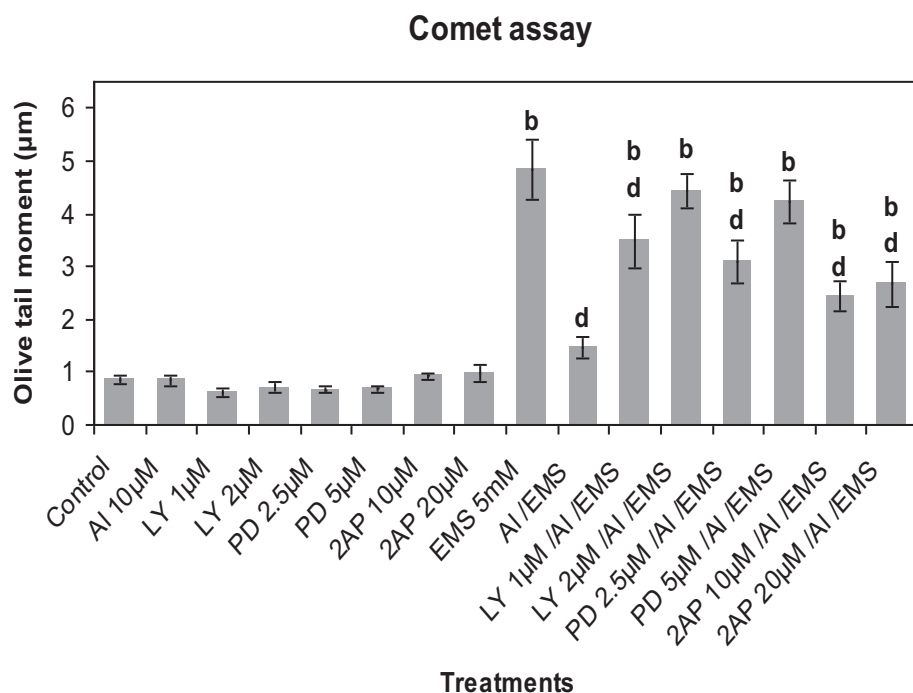


FIGURE 6 | Pre-treatments of protein kinase inhibitors: LY (LY-294002) 1 and 2 μM ; PD (PD-98059) 2.5 and 5 μM ; 2-AP (2-aminopurine) 10 and 20 μM , prevented Al-induced adaptive response to DNA damage

induced by EMS 5 mM in root meristems of *A. cepa*. Increase significant compared to control (0) at $p \leq 0.01$ (b); decrease significant compared to EMS challenge at $p \leq 0.01$ (d).

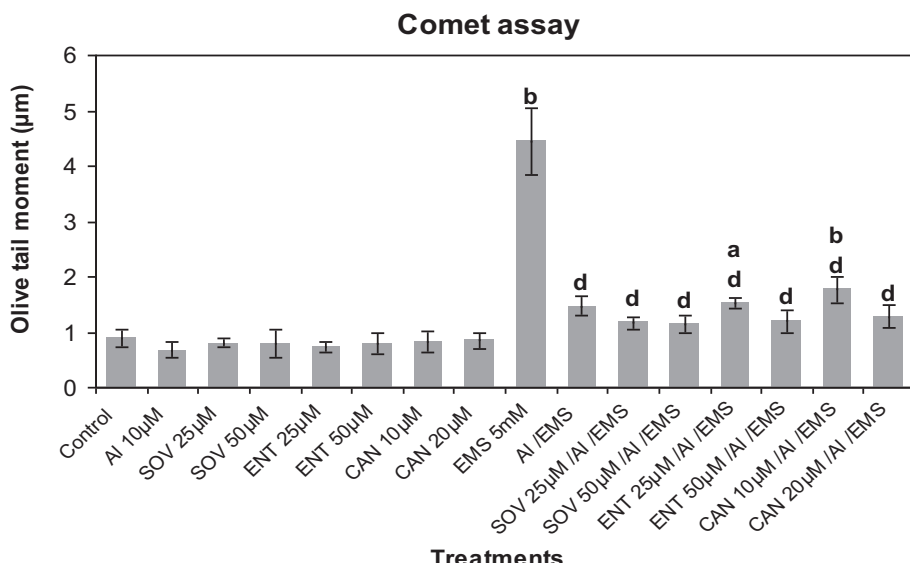


FIGURE 7 | Pre-treatments of protein phosphatase inhibitors SOV (Na_2VO_4) 25 and 50 μM ; ENT (endothall) 25 and 50 μM ; CAN (cantharidin) 10 and 20 μM prevented Al-induced adaptive response to

DNA damage induced by EMS 5 mM in root meristems of *A. cepa*.

Increase significant compared to control (0) at $p \leq 0.05$ (a) or 0.01 (b); decrease significant compared to EMS-challenge at $p \leq 0.1$ (d).

adaptive response to EMS-genotoxicity, revealed in Comet assay (Figure 7).

EFFECT OF METABOLIC INHIBITORS ON Al^{3+} -INDUCED GENOTOXIC ADAPTATION TO EMS

Comet assay revealed that CHX (1, 5 μM), ACD (5, 10 μM), 3AB (5, 10 μM), CAF (10, 20 μM), and APH (5, 10 μM) did not cause any observable DNA damage (Figure 8). The metabolic inhibitors at the tested concentrations did not show significant effect on the EMS-induced DNA damage. Al^{3+} -conditioning (10 μM) conferred 72.33% genomic protection against the EMS-challenge. Pre-treatment with CHX (1, 5 μM), ACD (5, 10 μM), 3-AB (5, 10 μM), CAF (10, 20 μM), and APH (5, 10 μM) prior to Al^{3+} -conditioning abolished the genomic protection significantly ($p \leq 0.05$ or 0.01) to different extents (74.65, 68.63% under treatment with CHX at 1, 5 μM ; 60.89, 59.15% under treatment with ACD at 5, 10 μM ; 34.98, 65.56% under treatment with 3AB at 5, 10 μM ; 35.11, 54.83% under treatment with CAF at 10, 20 μM ; and 45.4, 36.28% under treatment with APH at 5, 10 μM).

DISCUSSION

MODULATION OF Al^{3+} -INDUCED CELL DEATH AND DNA-DAMAGE

Earlier we have reported that Al^{3+} ($\geq 100 \mu\text{M}$) induces DNA damage revealing the involvement of ROS generated through the Al-triggered oxidative burst (Achary and Panda, 2010; Achary et al., 2012). Cell death (Figure 3) assayed by the Evans Blue staining method indicates disintegration of the plasma membrane caused by Al^{3+} (Baker and Mock, 1994). The Evans Blue stain method has been shown to be a reliable measure of the PCD in rice seedlings subjected to Zn-stress (Chang et al., 2005). The involvement of signal transduction in ROS-mediated cell death or DNA damage so far has not been established. Eukaryotic MAPK

cascades have evolved to transduce environmental and developmental signals into adaptive and programmed responses. MAPK cascades relay and amplify signals via three types of reversibly phosphorylated kinases (MAPKKK, MAPKK, and MAPK) leading to the phosphorylation of substrate proteins, whose altered activities mediate a wide array of responses, including changes in gene expression (Mishra et al., 2006; Rodriguez et al., 2010). Several reports suggest activation of MAPK by H_2O_2 (Varnova et al., 2002; Pitzschke and Hirt, 2006). In the present study, intact roots of *A. cepa* were pre-treated with protein kinase inhibitors including LY, PD, and 2-AP prior to challenge with Al^{3+} (800 μM). LY is an inhibitor of mammalian PI3 kinase, and its plant homologue VPS34-type is associated with the membrane trafficking (Davies et al., 2006; Vermeer et al., 2006). PD is a specific inhibitor of MAPKK (Alessi et al., 1995; Davies et al., 2006). The adenine analog 2AP, is a protein kinase inhibitor that inhibits the cyclin-dependent kinase (CDK) (Vesely et al., 1994; Huang et al., 2003). Also, 2-AP is a potent inhibitor of the double-stranded RNA (dsRNA)-activated protein kinase (PKR), a critical mediator of apoptosis (Kaufman, 1999). In the current study, LY, PD, and 2-AP significantly diminished Al-induced cell death and DNA damage (Figure 4) to different extents (LY > PD > 2-AP). Dephosphorylation of the MAPKs by specific phosphatases plays a critical role in their inactivation (Schenk and Snaar-Jagalska, 1999). SOV is an inhibitor of protein tyrosine phosphatase, whereas ENT and CAN are the inhibitors of serine/threonine protein phosphatase. ENT and CAN inhibit mammalian protein phosphatase 1 (PP1) and protein phosphatase 2A (PP2A), respectively (Li and Casida, 1992; Erdödi et al., 1995). Of these inhibitors, ENT only at 25, 50 μM and CAN at all the concentrations, 5–20 μM , significantly prevented the Al^{3+} -induced cell death and DNA damage. SOV, on the

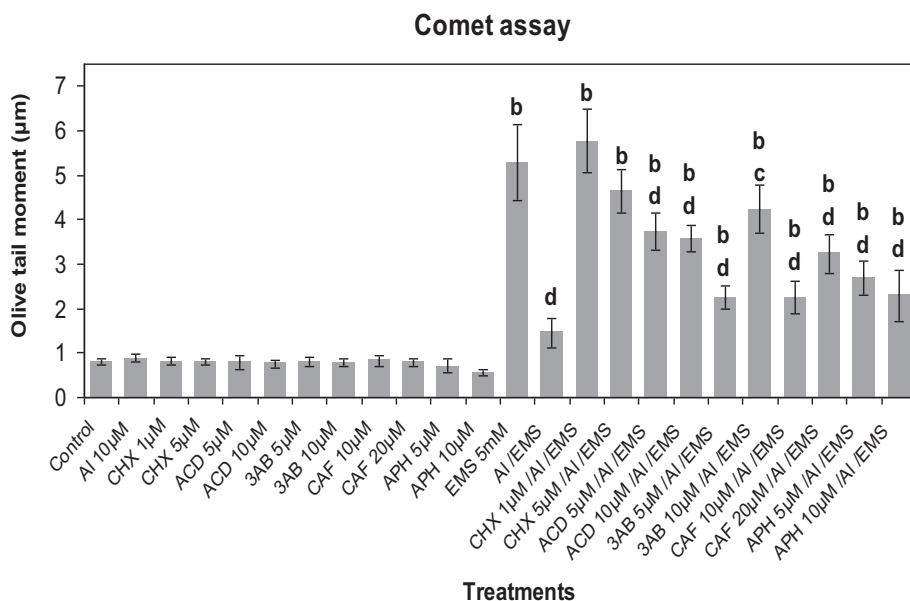


FIGURE 8 | Pre-treatments of inhibitors of protein synthesis: CHX (cycloheximide) 1 and 5 μ M; transcription: ACD (actinomycin D) 5 and 10 μ M; PARP: 3AB (3-aminobenzamide) 5 and 10 μ M; post-transcriptional repair: CAF (caffeine) 10 and 20 μ M; replication

repair: APH (aphidicolin) 5 and 10 μ M prevented Al-induced adaptive response to DNA damage induced by EMS 5 mM in root meristems of *A. cepa*. Increase significant compared to control (0) at $p \leq 0.01$ (b); decrease significant compared to EMS-challenge at $p \leq 0.05$ (c) or 0.1 (d).

contrary, was ineffective to counter the Al^{3+} -induced cell death and DNA damage (Figure 5). The above inhibitors have been reported to diminish the Cu^{2+} - or Zn^{2+} -induced cell death in rice (*Oryza sativa*) root tissue (Chang et al., 2005; Hung et al., 2007). Furthermore, CAN is reported to counteract against the vanadate-induced MAPK activation in rice roots (Lin et al., 2005). Therefore, the findings of the present study suggested the involvement of MAPK-pathway in the Al^{3+} -induced cell death and DNA damage.

ROLE OF SIGNAL TRANSDUCTION IN Al^{3+} -INDUCED ADAPTIVE RESPONSE TO GENOTOXIC STRESS

Perception of stress cues and relay of the signals that trigger adaptive responses are the key steps in plant stress tolerance (Chinnusamy et al., 2004). The MAPK pathways that regulate growth, death, differentiation, proliferation, and stress responses are highly conserved in eukaryotes including plants (Nakagami et al., 2005; Zhang et al., 2006). The ROS mediated oxidation of amino acid residues alters properties of specific cellular proteins involved in signal transduction, such as protein kinases, protein phosphatases, and transcription factors (Gordeeva et al., 2003). Studies have revealed the DNA repair machinery adaptively responds to oxidative or nitrosative stress, both *in vitro* and *in vivo* (Ramana et al., 1998). Metals including As^{3+} (Rao et al., 2011), Cd^{2+} (Jonak et al., 2004; Liu et al., 2010), Cr^{6+} (Ding et al., 2009), Cu^{2+} (Yeh et al., 2003; Jonak et al., 2004), Ni^{2+} (Chen et al., 2007), and Zn^{2+} (Lin et al., 2005) are known to activate MAPKs in a variety of plant species, which are believed to be mediated by ROS (Leonard et al., 2004; Nakagami et al., 2005). In our earlier studies, we have demonstrated that Al^{3+} at low conditioning doses, comparable to oxidative agents such as prauquat,

rose bengal, or salicylic acid, induce adaptive response conferring genomic protection from the genotoxicity of methylmercury chloride (MMCl) or EMS (Patra et al., 2003; Achary and Panda, 2010). As revealed by the current study, the treatment protocol (Figure 2) comprising of the treatments administered at different time intervals ruled out the possibility of any direct interference of Al^{3+} on the stability or activity of EMS. EMS being an alkylating agent can directly damage DNA as a result of depurination. Earlier, we have demonstrated the involvement of both ROS and Ca^{2+} -channel in Al^{3+} -induced adaptive response to genotoxic stress (Achary and Panda, 2010; Achary et al., 2013). Al^{3+} has been reported to activate a MAP kinase like protein in cell suspension cultures of *Coffea arabica* (Martínez-Estevez et al., 2001; Arroyo-Serralta et al., 2005). In the present study, the inhibitors of MAP kinase (Figure 6) significantly prevented the Al^{3+} -induced adaptive response to genotoxic challenge of EMS in the order LY > PD > 2-AP. Treatment with 2-AP has been shown to cause cells to bypass chemical- and radiation-induced cell cycle arrest through yet unidentified mechanisms that promote cell survival (Huang et al., 2003). On the other hand, in the current study the protein phosphatase inhibitors such as SOV, ENT, and CAN were shown to be least effective in preventing the Al^{3+} -induced adaptive response to genotoxic challenge of EMS (Figure 7). DNA-damaging agents are known to activate the protein kinases, triggering a protein phosphorylation cascade leading to the activation of transcription factors, which in turn alter gene expression (Yang et al., 2003b). Several genes are expressed in response to the Al-stress in *Arabidopsis* (Ezaki et al., 2004). A recent microarray analysis has revealed a total of 256 Al-responsive genes comprising 1.1% of the 24,000 genes of *Arabidopsis* genome of which 94 genes have been shown to be up-regulated and 162 have been observed

to be down-regulated (Goodwin and Sutter, 2009). Furthermore, a proteomic analysis of primary tomato root tissue has identified 49 Al-stress responsive proteins (Zhou et al., 2009). Interestingly, *WAK1* (cell wall-associated receptor kinase 1) has been one of the early pathogenesis related (PR) genes that expresses WAK proteins in response to Al^{3+} in *Arabidopsis* (Sivaguru et al., 2003). Interestingly, many of the genes induced by Al^{3+} are also the common genes induced by oxidative stress, metal stress, and pathogen infection (Cruz-Ortega and Ownby, 1993; Hamel et al., 1998; Mitheofer et al., 2004). Therefore, the findings of the present study suggested involvement of the MAPK cascade-mediated signal transduction in the Al^{3+} -induced adaptive response to genotoxic stress.

ROLE OF DNA-DAMAGE REPAIR NETWORK IN AI-INDUCED ADAPTIVE RESPONSE TO GENOTOXIC STRESS

To gain insight into the possible role of DNA damage response in the Al^{3+} -induced adaptive response to genotoxic stress, metabolic inhibitors including CHX, ACD (Zhang et al., 2003), APH (Spadari et al., 1982), and CAF (Gascoigne et al., 1981), inhibitors of *de novo* translation, and *de novo* transcription, replication- and post-replication repair in eukaryotes, respectively, were used in the subsequent experiments of the current study (**Figure 7**). APH, an inhibitor of the mammalian polymerases α and δ (Wright et al., 1994), has been shown to inhibit plant polymerase α -like activity (Sala et al., 1980, 1981). CAF, a radio-protectant (Singh and Kesvan, 1991), has been reported to inhibit ATM/ATR (Sarkaria et al., 1999), delay replication fork progression and enhance homologous recombination (Johansson et al., 2006). 3-AB inhibits the synthesis of poly(ADP-ribose) by the enzyme PARP, which requires NAD as a substrate (Purnell and Whish, 1980). In the present study, CHX was found to be the most effective in removing Al^{3+} -induced adaptive response to genotoxicity of EMS that was followed by 3-AB, ACD, CAF and APH (**Figure 8**). CHX being an inhibitor of *de novo* protein synthesis machinery has been observed to be the most effective in eliminating the adaptive response against genotoxic and DNA damage (Angelis et al., 2000; Patra et al., 2003). Studies using ACD and CHX have demonstrated that *de novo* transcription and translation are necessary for the activation of certain kinases at the levels of transcription and translation in tobacco cell suspension cultures treated with fungal elicitors (Zhang et al., 2000). The ROS-induced adaptive response (oxi-adaptive response) to H_2O_2 , bleomycin, and methyl methanesulfonate in HeLa cells is mediated by the base excision repair (BER) of the toxic apurinic/apyrimidinic (AP) sites and DNA strand break lesions that are attributed to the activation of AP endonuclease, APE-1 (Ramana et al., 1998). 3-AB has been shown to abolish the Al^{3+} -induced adaptive response to genotoxic stress imposed by MMCl in plant cells (Patra et al., 2003). Earlier, we have demonstrated that Al^{3+} at concentrations as low as 5–10 μM caused neither DNA damage nor cell cycle arrest thereby ruling out any involvement of ATR kinase, which is one of the key components of DNA damage response pathway (Rounds and Larsen, 2008; Nezames et al., 2012; Achary et al., 2013). On the contrary, the findings of the present study suggested involvement of the MAPK-DNA repair network in the Al^{3+} -induced adaptive response to

genotoxic stress by possibly overriding the DNA damage response pathway.

The results of the current study underscored the biphasic mode of Al^{3+} that it induced DNA damage in high concentration (800 μM), and in low concentration (10 μM) induced adaptive response, conferring genomic protection from EMS-challenge. The involvement of the same MAPK-DNA repair network in the induction of DNA damage as well as adaptive response is suggested.

AUTHOR CONTRIBUTIONS

Whereas Brahma B. Panda is responsible to develop the research concept, design the experiments, interpretation of the results, obtain financial support, and writing the manuscript, V. Mohan M. Achary has executed the experiments and recorded the results.

ACKNOWLEDGMENTS

The authors are thankful to the Berhampur University for administrative support and facilities to conduct research in the Department of Botany. Funding support provided by the Ministry of Science and Technology, Government of India (Project No. SR/SO/PS07/2004) as well as by University Grants Commission, New Delhi (Emeritus Fellowship No. F.6-6/2013-14/EMERITUS-2013-14-GEN-2681/SA-II) awarded to BBP is acknowledged. Thanks are also due to Prof. N. L. Parinandi of the Ohio State University College of Medicine, Columbus, USA who has kindly corrected the manuscript and helped with discussion.

REFERENCES

- Abraham, R. T. (2001). Cell cycle checkpoint signaling through the ATM and ATR kinases. *Genes Dev.* 15, 2177–2196. doi: 10.1101/gad.914401
- Achary, V. M. M., and Panda, B. B. (2010). Aluminium-induced DNA-damage and adaptive response to genotoxic stress in plant cells are mediated through reactive oxygen intermediates. *Mutagenesis* 25, 201–209. doi: 10.1093/mutage/gep063
- Achary, V. M. M., Parinandi, N. L., and Panda, B. B. (2012). Aluminum induces oxidative burst, cell wall NADH peroxidase activity, and DNA damage in root cells of *Allium cepa* L. *Environ. Mol. Mutagen.* 53, 550–560. doi: 10.1002/em.21719
- Achary, V. M. M., Parinandi, N. L., and Panda, B. B. (2013). Calcium channel blockers protect against aluminium-induced DNA damage and block adaptive response to genotoxic stress in plant cells. *Mutat. Res.* 751, 130–138. doi: 10.1016/j.mrgentox.2012.12.008
- Adams-Phillips, L., Briggs, A. G., and Bent, A. F. (2010). Disruption of poly(ADPrabolation) mechanisms alters responses of *Arabidopsis* to biotic stress. *Plant Physiol.* 152, 267–280. doi: 10.1104/pp.109.148049
- Alessi, D. R., Cuenda, A., Cohen, P., Dudley, D. T., and Saltiel, A. R. (1995). PD 098059 is a specific inhibitor of the activation of mitogen-activated protein kinase kinase *in vitro* and *in vivo*. *J. Biol. Chem.* 270, 27489–27494. doi: 10.1074/jbc.270.46.27489
- Angelis, K. J., McGuffie, M., Menke, M., and Schubert, I. (2000). Adaptation to alkylation damage in DNA measured by comet assay. *Environ. Mol. Mutagen.* 36, 146–150. doi: 10.1002/1098-2280(2000)36:2<146::AID-EM9>3.0.CO;2-5
- Arroyo-Serralta, G. A., Kú-González, A., Hernández-Sotomayor, S. M. T., and Aguilar, J. Z. (2005). Exposure to toxic concentrations of aluminum activates a MAPK-like protein in cell suspension cultures of *Coffea arabica*. *Plant Physiol. Biochem.* 43, 27–35. doi: 10.1016/j.plaphy.2004.12.003
- Baker, C. J., and Mock, N. M. (1994). An improved method for monitoring cell death in cell suspension and leaf disc assays using Evan's blue. *Plant Cell Tissue Org. Cult.* 39, 7–12. doi: 10.1007/BF00037585
- Balestrazzi, A., Confalonieri, M., Macovei, A., Dona, M., and Carbonera, D. (2011). Genotoxic stress and DNA repair in plants: emerging functions and tools for

- improving crop productivity. *Plant Cell Rep.* 30, 287–295. doi: 10.1007/s00299-010-0975-9
- Bray, C. M., and West, C. E. (2005). DNA repair mechanisms in plants: crucial sensors and effectors for the maintenance of genome integrity. *New Phytol.* 168, 511–528. doi: 10.1111/j.1469-8137.2005.01548.x
- Briggs, A. G., and Bent, A. F. (2011). Poly(ADP-ribosylation) in plants. *Trends Plant Sci.* 16, 372–380. doi: 10.1016/j.tplants.2011.03.008
- Camps, M., Nichols, A., and Arkinstall, S. (2000). Dual specificity phosphatases: a gene family for control of MAP kinase function. *FASEB J.* 14, 6–16. Available online at: <http://www.fasebj.org/content/14/1/6.full>
- Chang, H.-B., Lin, C.-W., and Huang, H.-J. (2005). Zinc induced cell death in rice (*Oryza sativa* L.) roots. *Plant Growth Regul.* 46, 261–266. doi: 10.1007/s10725-005-0162-0
- Chen, P.-Y., Huang, T.-L., and Huang, H.-J. (2007). Early events in the signalling pathway for the activation of MAPKs in rice roots exposed to nickel. *Funct. Plant Biol.* 34, 995–1001. doi: 10.1071/FP07163
- Chinnusamy, V., Schumaker, K., and Zhu, J.-K. (2004). Molecular genetic perspectives on cross-talk and specificity in abiotic stress signalling in plants. *J. Exp. Bot.* 55, 225–236. doi: 10.1093/jxb/erh005
- Cruz-Ortega, R., and Ownby, J. D. (1993). A protein similar to PR (pathogenesis related) proteins is elicited by metal toxicity in wheat roots. *Physiol. Plant.* 89, 211–219. doi: 10.1111/j.1399-3054.1993.tb01808.x
- Daniel, W. W. (1995). *Biostatistics: A foundation for Analysis in the Health Sciences*. New York: John Wiley.
- Davies, D. R., Bindschedler, L. V., Strickland, T. S., and Bolwell, G. P. (2006). Production of reactive oxygen species in *Arabidopsis thaliana* cell suspension cultures in response to an elicitor from *Fusarium oxysporum*: implications for basal resistance. *J. Exp. Bot.* 57, 1817–1827. doi: 10.1093/jxb/erj216
- De Schutter, K., Joubes, J., Cools, T., Verkest, A., Corellou, F., Babiyuchuk, E., et al. (2007). *Arabidopsis* WEE1 kinase controls cell cycle arrest in response to activation of the DNA integrity checkpoint. *Plant Cell* 19, 211–225. doi: 10.1105/tpc.106.045047
- Ding, H., Tan, M. P., Zhang, C., Zhang, Z., Zhang, A., and Kang, Y. (2009). Hexavalent chromium (VI) stress induces mitogen-activated protein kinase activation mediated by distinct signal molecules in roots of *Zea mays* L. *Environ. Exp. Bot.* 67, 328–334. doi: 10.1016/j.envebot.2009.08.007
- Erdödi, F., Toth, B., Hirano, K., Hirano, M., Hartshorne, D. J., and Gergely, P. (1995). Endothall thioamide inhibits protein phosphatases-1 and -2A *in vivo*. *Am. J. Physiol.* 269, 1176–1184.
- Ezaki, B., Suzuki, M., Motoda, H., Kawamura, M., Nakashima, S., and Matsumoto, H. (2004). Mechanism of gene expression of *Arabidopsis* glutathione S-transferase, *AtGST1* and *AtGST11* in response to aluminum stress. *Plant Physiol.* 134, 1672–1682. doi: 10.1104/pp.103.037135
- Gascoigne, E. W., Robinson, A. C., and Harris, W. J. (1981). The effect of caffeine upon cell survival and post-replication repair of DNA after treatment of BHK 21 cells with either UV irradiation or N-methyl N-nitrosoguanidine. *Chem. Biol. Interact.* 36, 107–116. doi: 10.1016/0009-2797(81)90032-6
- Goodwin, S. B., and Sutter, T. R. (2009). Microarray analysis of *Arabidopsis* genome response to aluminum stress. *Biol. Plant.* 53, 85–99. doi: 10.1007/s10535-009-0012-4
- Gordeeva, A. V., Zvyagilskaya, R. A., and Labas, Y. A. (2003). Cross-talk between reactive oxygen species and calcium in living cells. *Biochemistry (Mosc.)* 68, 1077–1080. doi: 10.1023/A:1026398310003
- Hamel, F., Breton, C., and Houde, M. (1998). Isolation and characterization of wheat aluminum-regulated genes: possible involvement of aluminum as a pathogenesis response elicitor. *Planta* 205, 531–538. doi: 10.1007/s004250050352
- Hirt, H. (2000). *MAP kinases in Plant Signal Transduction*. Berlin: Springer-Verlag. doi: 10.1007/978-3-540-49166-8
- Huang, S., Qu, L. K., Cuddihy, A. R., Ragheb, R., Taya, Y., and Koromilas, A. E. (2003). Protein kinase inhibitor 2-aminopurine overrides multiple genotoxic stress-induced cellular pathways to promote cell survival. *Oncogene* 22, 3721–3733. doi: 10.1038/sj.onc.1206490
- Hung, W. C., Huang, D. D., Chein, P. S., Yeh, C. M., Chen, P. Y., Chi, W. C., et al. (2007). Protein tyrosine dephosphorylation during copper-induced cell death in rice roots. *Chemosphere* 69, 55–62. doi: 10.1016/j.chemosphere.2007.04.073
- Hurley, P. J., and Bunz, F. (2007). ATM and ATR: components of an integrated circuit. *Cell Cycle* 6, 414–417. doi: 10.4161/cc.6.4.3886
- Johansson, F., Lagerqvist, A., Filippi, S., Palitti, F., Erixon, K., Helleday, T., et al. (2006). Caffeine delays replication fork progression and enhances UV-induced homologous recombination in Chinese hamster cell lines. *DNA Rep.* 5, 1449–1458. doi: 10.1016/j.dnarep.2006.07.005
- Jonak, C., Nakagami, H., and Hirt, H. (2004). Heavy metal stress activation of distinct mitogen-activated protein kinase pathways by copper and cadmium. *Plant Physiol.* 136, 32763283. doi: 10.1104/pp.104.045724
- Kaufman, R. J. (1999). Double-stranded RNA-activated protein kinase mediated virusinduced apoptosis: a new role for an old actor. *Proc. Natl. Acad. Sci. U.S.A.* 96, 11693–11695. doi: 10.1073/pnas.96.21.11693
- Keyse, S. M. (2000). Protein phosphatases and the regulation of mitogen-activated protein kinase signalling. *Curr. Opin. Cell Biol.* 12, 186–192. doi: 10.1016/S0955-0674(99)00075-7
- Kochian, L. V., Hoekenga, O. A., and Pineros, M. A. (2004). How do crop plants tolerate acid soil? Mechanisms of aluminum tolerance and phosphorous deficiency. *Annu. Rev. Plant Biol.* 55, 459–493. doi: 10.1146/annurev.arplant.55.031903.141655
- Kumaravel, T. S., Vilhar, B., Faux, S. P., and Jha, A. N. (2000). Comet Assay measurements: a perspective. *Cell Biol. Toxicol.* 25, 53–64. doi: 10.1007/s10565-007-9043-9
- Kyriakis, J. M., and Avruch, J. (2001). Mammalian mitogen-activated protein kinase signal transduction pathways activated by stress and inflammation. *Physiol. Rev.* 81, 807–869. doi: 10.1152/physrev.00028.2011
- Leonard, S. S., Harris, G. K., and Shi, X. (2004). Metal-induced oxidative stress and signal transduction. *Free Radic. Biol. Med.* 37, 1921–1942. doi: 10.1016/j.freeradbiomed.2004.09.010
- Li, Y. M., and Casida, J. E. (1992). Cantharidin-binding protein: identification as protein phosphatase 2A. *Proc. Natl. Acad. Sci. U.S.A.* 89, 11867–11870. doi: 10.1073/pnas.89.24.11867
- Lin, C. W., Chang, H. B., and Huang, H. J. (2005). Zinc induces mitogen-activated protein kinase activation mediated by reactive oxygen species in rice roots. *Plant Physiol. Biochem.* 43, 963–968. doi: 10.1016/j.plaphy.2005.10.001
- Liu, X. M., Kim, K. E., Kim, K. C., Nguyen, X. C., Han, H. J., Jung, M. S., et al. (2010). Cadmium activates *Arabidopsis* MPK3 and MPK6 via accumulation of reactive oxygen species. *Phytochemistry* 71, 614–618. doi: 10.1016/j.phytochem.2010.01.005
- Mannuss, A., Trapp, O., and Puchta, H. (2012). Gene regulation in response to DNA damage. *Biochem. Biophys. Acta* 1819, 154–165. doi: 10.1016/j.bbaram.2011.08.003
- Martínez-Estévez, M., Loyola-Vargas, V. M., and Hernández-Sotomayor, S. M. T. (2001). Aluminum increases phosphorylation of particular proteins in cellular suspension cultures of coffee (*Coffea arabica*). *J. Plant Physiol.* 158, 1375–1379. doi: 10.1078/0176-1617-00623
- Mishra, N. S., Tuteja, R., and Tuteja, N. (2006). Signaling through MAP kinase networks in plants. *Arch. Biochem. Biophys.* 452, 55–68. doi: 10.1016/j.abb.2006.05.001
- Mitheofer, A., Schulze, B., and Boland, W. (2004). Biotic and heavy metal stress response in plants: evidence for common signals. *FEBS Lett.* 566, 1–5. doi: 10.1016/j.febslet.2004.04.011
- Nakagami, H., Pitzschke, A., and Hirt, H. (2005). Emerging MAP kinase pathways in plant stress signaling. *Trends Plant Sci.* 10, 339–346. doi: 10.1016/j.tplants.2005.05.009
- Nezames, C. D., Sjogren, C. A., Barajas, J. F., and Larsen, P. B. (2012). The *Arabidopsis* cell cycle checkpoint regulators TANMEI/ALT2 and ATR mediate the active process of aluminum-dependent root growth inhibition. *Plant Cell* 24, 608–621. doi: 10.1105/tpc.112.095596
- Panda, B. B., Achary, V. M. M., Mahanty, S., and Panda, K. K. (2013). “Plant adaptation to abiotic and genotoxic stress: relevance to climate change and evolution,” in *Climate Change and Abiotic Stress Tolerance*, eds N. Tuteja and S. S. Gill (Weinheim: Wiley-VCH), 251–294.
- Patra, J., Sahoo, M. K., and Panda, B. B. (2003). Persistence and prevention of aluminium- and paraquat- induced adaptive response to methyl mercuric chloride in plant cells *in vivo*. *Mutat. Res.* 538, 51–61. doi: 10.1016/S1383-5718(03)00085-8
- Pitzschke, A., and Hirt, H. (2006). Mitogen-activated protein kinases and reactive oxygen species signaling in plants. *Plant Physiol.* 141, 351–356. doi: 10.1104/pp.106.079160
- Purnell, M. R., and Whish, W. J. (1980). Novel inhibitors of poly(ADP-ribose) synthetase. *Biochem. J.* 185, 775–777.

- Ramana, C. V., Boldogh, I., Izumi, T., and Mitra, S. (1998). Activation of apurinic/pyrimidinic endonuclease in human cells by reactive oxygen species and its correlation with their adaptive response to genotoxicity of free radicals. *Proc. Natl. Acad. Sci. U.S.A.* 95, 5061–5066. doi: 10.1073/pnas.95.9.5061
- Rao, K. P., Vani, G., Kumar, K., Wankhede, D. P., Misra, M., Gupta, M., et al. (2011). Arsenic stress activates MAP kinase in rice roots and leaves. *Arch. Biochem. Biophys.* 506, 73–82. doi: 10.1016/j.abb.2010.11.006
- Rodriguez, M. C. S., Petersen, M., and Mundy, J. (2010). Mitogen-activated protein kinase signaling in plants. *Annu. Rev. Plant. Biol.* 61, 621–649. doi: 10.1146/annurev-arplant-042809-112252
- Roldan-Arjona, T., and Ariza, R. R. (2009). Repair and tolerance of oxidative DNA damage in plants. *Mutat. Res.* 681, 169–179. doi: 10.1016/j.mrrev.2008.07.003
- Rounds, M. A., and Larsen, P. B. (2008). Aluminum-dependent root-growth inhibition in *Arabidopsis* results from AtATR-regulated cell cycle arrest. *Curr. Biol.* 18, 1495–1500. doi: 10.1016/j.cub.2008.08.050
- Sala, F., Galli, M. G., Levi, M., Burroni, D., Parisi, B., Pedrali-Noy, G., et al. (1981). Functional roles of the plant α -like and γ -like DNA polymerases. *FEBS Lett.* 124, 112–118. doi: 10.1016/0014-5793(81)80064-6
- Sala, F., Parisi, B., Burroni, D., Amilena, A. R., Pedrali-Noy, G., and Spadari, S. (1980). Specific and reversible inhibition by aphidicolin of the α -like DNA polymerase of plant cells. *FEBS Lett.* 117, 93–98. doi: 10.1016/0014-5793(80)80920-3
- Sarkaria, J. N., Busby, E. C., Tibbetts, R. S., Roos, P., Taya, Y., Karnitz, L. M., et al. (1999). Inhibition of ATM and ATR kinase activities by the radiosensitizing agent, caffeine. *Cancer Res.* 59, 4375–4382.
- Schenk, P. W., and Snaar-Jagalska, B. E. (1999). Signal perception and transduction: the role of protein kinases. *Biochim. Biophys. Acta* 1449, 1–24. doi: 10.1016/S0167-4889(98)00178-5
- Singh, S. P., and Kesvan, P. C. (1991). Biochemical effects of heat shock and caffeine on postirradiation oxic and anoxic damage in barley seeds of low and high water content. *Int. J. Radiat. Biol.* 59, 1227–1236. doi: 10.1080/09553009114551101
- Sivaguru, M., Ezaki, B., He, Z.-H., Tong, H., Osawa, H., Baluska, F., et al. (2003). Aluminum-induced gene expression and protein localization of a cell wall-associated receptor kinase in *Arabidopsis*. *Plant Physiol.* 132, 2256–2266. doi: 10.1104/pp.103.022129
- Spadari, S., Sala, F., and Pedrali-Noy, G. (1982). Aphidicolin: a specific inhibitor of nuclear DNA replication in eukaryotes. *Trends Biochem. Sci.* 7, 29–32. doi: 10.1016/0968-0004(82)90061-5
- Thevelein, J. M. (1994). Signal transduction in yeast. *Yeast* 10, 1753–1790. doi: 10.1002/yea.320101308
- Tuteja, N., Ahmed, P., Panda, B. B., and Tuteja, R. (2009). Genotoxic stress in plants: shedding light on DNA damage, repair and DNA repair helicases. *Mutat. Res.* 681, 134–149. doi: 10.1016/j.mrrev.2008.06.004
- Ulm, R. (2003). “Molecular genetics of genotoxic stress signalling in plants,” in *Plant Responses to Abiotic Stress*, eds H. Hirt and K. Shinozaki (Berlin: Springer-Verlag), 217–240. doi: 10.1007/978-3-540-39402-0_9
- Ulm, R., Revenkova, E., di Sansebastiano, G.-P., Bechtold, N., and Paszkowski, J. (2001). Mitogen-activated protein kinase phosphatase is required for genotoxic stress relief in *Arabidopsis*. *Genes Dev.* 15, 699–709. doi: 10.1101/gad.192601
- Vanderauwera, S., Suzuki, N., Miller, G., van de Cotte, B., Morsa, S., Ravanat, J.-L., et al. (2011). Extracellular protection of chromosomal DNA from oxidative stress. *Proc. Natl. Acad. Sci. U.S.A.* 108, 1711–1716. doi: 10.1073/pnas.1018359108
- Varnova, E., Inze, D., and Breusegem, F. V. (2002). Signal transduction during oxidative stress. *J. Exp. Bot.* 53, 1227–1236. doi: 10.1093/jexbot/53.372.1227
- Vermeer, J. E., Van Leeuwen, W., Tobena-Santamaría, R., Laxalt, A. M., Jones, D. R., Divecha, N., et al. (2006). Visualization of PtdIns3P dynamics in living plant cells. *Plant J.* 47, 687–700. doi: 10.1111/j.1365-313X.2006.02830.x
- Vesely, J., Havlicek, L., Strand, M., Blow, J. J., Donella-Deanna, A., Pinna, L., et al. (1994). Inhibition of cyclin-dependent kinases by purine analogues. *Eur. J. Biochem.* 224, 771–786. doi: 10.1111/j.1432-1033.1994.00771.x
- Watters, D. J. (2003). Oxidative stress in ataxia telangiectasia. *Redox Rep.* 8, 23–29. doi: 10.1179/135100003125001206
- Wright, G. E., Hubscher, U., Khan, N. N., Focher, F., and Verri, A. (1994). Inhibitor analysis of calf thymus DNA polymerases alpha, delta and epsilon. *FEBS Lett.* 14, 128–130. doi: 10.1016/0014-5793(94)80254-8
- Yang, J., Yu, Y., and Duerksen-Hughes, P. J. (2003a). Protein kinases and their involvement in the cellular responses to genotoxic stress. *Mutat. Res.* 543, 31–58. doi: 10.1016/S1383-5742(02)00069-8
- Yang, J., Yu, Y., Hamrick, H. E., and Duerksen-Hughes, P. J. (2003b). ATM, ATR and DNA-PK: initiators of the cellular genotoxic stress responses. *Carcinogenesis* 24, 1571–1580. doi: 10.1093/carcin/bgg137
- Yeh, C.-M., Hung, W.-C., and Huang, H.-J. (2003). Copper treatment activates mitogen-activated protein kinase signalling in rice. *Physiol. Plant.* 119, 392–399. doi: 10.1034/j.1399-3054.2003.00191.x
- Zhang, S., Liu, Y., and Klessig, D. F. (2000). Multiple levels of tobacco WIPK activation during the induction of cell death by fungal elicitors. *Plant J.* 23, 339–347. doi: 10.1046/j.1365-313X.2000.00780.x
- Zhang, T., Liu, Y., Yang, T., Zhang, L., Xu, S., Xue, L., et al. (2006). Diverse signals converge at MAPK cascades in plant. *Plant Physiol. Biochem.* 44, 274–283. doi: 10.1016/j.plaphy.2006.06.004
- Zhang, Y., Wolf, G. W., Bhat, K., Jin, A., Allio, T., Burkhardt, W. A., et al. (2003). Ribosomal protein L11 negatively regulates oncogene MDM2 and mediates a p53-dependent ribosomal-stress checkpoint pathway. *Mol. Cell Biol.* 23, 8902–8912. doi: 10.1128/MCB.23.23.8902-8912.2003
- Zhou, S., Sauvé, R., and Thannhauser, T. W. (2009). Proteome changes induced by aluminium stress in tomato roots. *J. Exp. Bot.* 60, 1849–1857. doi: 10.1093/jxb/erp065

Conflict of Interest Statement: The authors declare that the research was conducted in the absence of any commercial or financial relationships that could be construed as a potential conflict of interest.

Received: 30 January 2014; **accepted:** 19 May 2014; **published online:** 05 June 2014.
Citation: Panda BB and Achary VMM (2014) Mitogen-activated protein kinase signal transduction and DNA repair network are involved in aluminum-induced DNA damage and adaptive response in root cells of *Allium cepa* L.. *Front. Plant Sci.* 5:256. doi: 10.3389/fpls.2014.00256

This article was submitted to Plant Physiology, a section of the journal Frontiers in Plant Science.

Copyright © 2014 Panda and Achary. This is an open-access article distributed under the terms of the Creative Commons Attribution License (CC BY). The use, distribution or reproduction in other forums is permitted, provided the original author(s) or licensor are credited and that the original publication in this journal is cited, in accordance with accepted academic practice. No use, distribution or reproduction is permitted which does not comply with these terms.



Emerging Importance of Helicases in Plant Stress Tolerance: Characterization of *Oryza sativa* Repair Helicase XPB2 Promoter and Its Functional Validation in Tobacco under Multiple Stresses

Shailendra Raikwar¹, Vineet K. Srivastava¹, Sarvajeet S. Gill², Renu Tuteja¹ and Narendra Tuteja^{1,3*}

¹ Plant Molecular Biology Group, International Centre for Genetic Engineering and Biotechnology, New Delhi, India, ² Stress Physiology and Molecular Biology Lab, Centre for Biotechnology, Maharshi Dayanand University, Rohtak, India, ³ Amity Institute of Microbial Technology, Amity University, Noida, India

OPEN ACCESS

Edited by:

Alma Balestrazzi,
University of Pavia, Italy

Reviewed by:

Irene Murgia,
Università degli Studi di Milano, Italy
Susana Araújo,
Universidade Nova de Lisboa,
Portugal

*Correspondence:

Narendra Tuteja
ntuteja@amity.edu;
narendra@icgeb.res.in

Specialty section:

This article was submitted to
Plant Physiology,
a section of the journal
Frontiers in Plant Science

Received: 12 February 2015

Accepted: 20 November 2015

Published: 16 December 2015

Citation:

Raikwar S, Srivastava VK, Gill SS, Tuteja R and Tuteja N (2015) Emerging Importance of Helicases in Plant Stress Tolerance: Characterization of *Oryza sativa* Repair Helicase XPB2 Promoter and Its Functional Validation in Tobacco under Multiple Stresses. *Front. Plant Sci.* 6:1094.

doi: 10.3389/fpls.2015.01094

Genetic material always remains at the risk of spontaneous or induced damage which challenges the normal functioning of DNA molecule, thus, DNA repair is vital to protect the organisms against genetic damage. Helicases, the unique molecular motors, are emerged as prospective molecules to engineer stress tolerance in plants and are involved in nucleic acid metabolism including DNA repair. The repair helicase, XPB is an evolutionary conserved protein present in different organisms, including plants. Availability of few efficient promoters for gene expression in plants provoked us to study the promoter of XPB for better understanding of gene regulation under stress conditions. Here, we report the *in silico* analysis of novel stress inducible promoter of *Oryza sativa* XPB2 (*OsXPB2*). The *in vivo* validation of functionality/activity of *OsXPB2* promoter under abiotic and hormonal stress conditions was performed by *Agrobacterium*-mediated transient assay in tobacco leaves using *OsXPB2::GUS* chimeric construct. The present research revealed that *OsXPB2* promoter contains cis-elements accounting for various abiotic stresses (salt, dehydration, or cold) and hormone (Auxin, ABA, or MeJA) induced GUS expression/activity in the promoter-reporter assay. The promoter region of *OsXPB2* contains CACG, GTAACG, CACGTG, CGTCA CCGCCGCGCT cis acting-elements which are reported to be salt, dehydration, cold, MeJA, or ABA responsive, respectively. Functional analysis was done by *Agrobacterium*-mediated transient assay using agroinfiltration in tobacco leaves, followed by GUS staining and fluorescence quantitative analyses. The results revealed high induction of GUS activity under multiple abiotic stresses as compared to mock treated control. The present findings suggest that *OsXPB2* promoter is a multi-stress inducible promoter and has potential applications in sustainable crop production under abiotic stresses by regulating desirable pattern of gene expression.

Keywords: agroinfiltration, rice, helicases, *OsXPB2* promoter, abiotic stress, tobacco

INTRODUCTION

Essentially vital for all living organisms, the unique molecular motors, helicases unwind the duplex nucleic acids (i.e., DNA, RNA, or RNA-DNA hybrid) by using the free energy of ATP-binding/hydrolysis. Helicases remains present everywhere during the processing of nucleic acid in the cell and also emerged as potential candidate molecules for engineering abiotic stress tolerance in plants. Environmental cues continuously threaten the genomic integrity of all living organisms therefore in order to maintain the integrity of genome almost all the organisms throughout evolution contain robust DNA repair and recombination pathways to repair/remove or to tolerate lesions (Singh et al., 2011). Recent helicase research supports the potential of DNA/RNA helicases to counteract the adverse effect of various abiotic stress factors (Gill et al., 2014). OsXPB2 is a member of highly conserved helicase super family 2 (SF2), in eukaryotes and it plays a vital role in DNA metabolism such as transcription and repair (Umate et al., 2011). XPB also known as ERCC3 and RAD25 is a 3'-5' DNA helicase and it is an essential subunit of the eukaryotic basal transcription factor complex TFIH [contains seven subunits (XPB, XPD, p62, p52, p44, p34, and TTDA)] (Schaeffer et al., 1993). XPB facilitates initiation of RNA polymerase II transcription and nucleotide excision repair (NER) by unwinding dsDNA around a DNA lesion. It has been reported that helicases play important roles in cell metabolic processes, including plant growth and development (Ribeiro et al., 1998; Costa et al., 2001). Various helicases have been known to function in providing abiotic stress tolerance to plants and few of them like *PDH45*, *MCM6*, and *p68* have been reported to contain stress inducible promoters (Sanan-Mishra et al., 2005; Luo et al., 2009; Dang et al., 2011a,b; Tajrishi and Tuteja, 2011; Gill et al., 2013; Tuteja et al., 2013; Banu et al., 2014). Therefore, exploitation of stress inducible promoters of candidate helicase genes can further complement the stress tolerance potential of crop plants.

In the present scenario, the *in silico* analysis of sequenced plant genome has become a routine to study and predict the promoter sequences (upstream of the 5' end of the gene) and their contributing cis-acting elements. However, the demonstration of promoter activity is essential in order to confirm the functions of putative cis-elements. It is well-known that inducible promoters have broad biotechnological applications in the regulation of stress-related genes that are activated as a result of abiotic and biotic stresses (Kasuga et al., 1999; Oettgen, 2001). The inducible plant promoters based on their responsiveness, can be categorized as responsive to endogenous signals (plant hormones), external stimuli (biotic and abiotic stresses), and chemical stimuli. The promoters harbor various cis-regulatory elements and play vital role in the plant gene expression and regulation. Gene regulation can occur during different stages of gene expression and the most important point of control is RNA transcription. The promoter of Cauliflower mosaic virus (CaMV) 35S and its derivatives are used frequently for constitutive expression of transgene in plants and to achieve higher transgene expression (Odell et al., 1985; Battraw and Hall, 1990). However, the constitutive expression of functional genes/transcription

factors in genetically engineered plants sometimes results in undesirable phenotype like growth inhibition or significant yield penalty (Capell et al., 1998; Liu et al., 1998; Kasuga et al., 1999; Hsieh et al., 2002). Therefore, the inducible promoters which can drive the expression of foreign genes under specific stresses can be of prime importance in engineering tolerance potential of crop plants (Kasuga et al., 1999). These inducible and tissue-specific promoters are central to the study of gene regulatory networks in plant (Huda et al., 2013; Oettgen, 2001). Different helicases like *PDH45*, *MCM6*, *SUV3*, *p68*, and *BAT1* are shown to be upregulated by abiotic stresses including salinity, dehydration, wounding, and low temperature and their overexpression conferred stress tolerance in plants (Sanan-Mishra et al., 2005; Tran et al., 2010; Tuteja et al., 2013, 2014a,b; Manjulatha et al., 2014).

Helicases are an intriguing aspect of the plant response to various stress factors but their potential has so far been poorly explored. Therefore, the functional validation of the upstream regulatory part or promoter of the DNA repair helicase OsXPB2 gene is important for understanding its regulation under stress conditions. Thus, the isolation and functional characterization of OsXPB2 promoter with respect to abiotic stresses and hormonal treatments may be of potential importance for engineering stress tolerance. The results presented in this report suggest that OsXPB2 promoter can be a convincing tool that can be used as stress-inducible promoter for engineering crops with higher tolerance against abiotic stresses.

MATERIALS AND METHODS

In Silico Analysis of Promoter

The 1000 bp promoter sequence upstream of the start codon of the OsXPB2 gene (ID: Os01g49680; <http://rice.plantbiology.msu.edu/>) was retrieved from the rice genome database and *cis*-elements in the promoter were analyzed using PLANTCARE (<http://bioinformatics.psb.ugent.be/webtools/plantcare/html/>) and PLACE (<http://www.dna.affrc.go.jp/PLACE/>) database.

Amplification of OsXPB2 Promoter and Development of Chimeric Promoter-Reporter Construct

Genomic DNA was isolated from the leaves of *Oryza sativa* (Var. IR 64) by CTAB method and 30× dilution of genomic DNA was used as template for the amplification of OsXPB2 promoter. Sequences of DNA adaptors and primers used for promoter amplification are OsXPB2FW: AA CTGCAGAGACCCAGTGAAGCCAACACCCATTAA, OsXPB2 RV: ATGGATCCAACAT GGC CGG AAG CCC TGG AGC. The amplified fragment was cloned into pJET2.1 vector (Thermo Scientific). Subsequently the promoter was cloned into pCAMBIA-1391Z (promoter less vector) at PstI and BamHI restriction sites (Figure 1A, Supplementary Figure 1). The OsXPB2 promoter cloned in pCAMBIA-1391Z was transformed in *Agrobacterium tumefaciens* (LBA4404) and confirmed by colony PCR using OsXPB2 promoter specific primers.

Agrobacterium-Mediated Transient Assay

Agrobacterium-mediated transient assay was performed to study the expression of *OsXPB2* promoter using the method described by Yang et al. (2000). Fully expanded leaves of tobacco (*Nicotiana tabacum* cv. USA) plants were agro-infiltrated by using 500 µl of bacterial suspension with 1 ml syringe into the abaxial surface of intact leaf. After 3 days, leaves were used for the stress and mock treatment analysis.

Stress Treatments

Agro-infiltrated leaf discs were soaked in petri dishes filled with 200 mM NaCl, 20% PEG (Polyethylene glycol), 5 µM ABA, 10 µM MeJA, or 10 µM NAA, respectively, and incubated for 1, 6, 12, or 24 h at room temperature. For cold stress, agro-infiltrated leaf discs were incubated at 4°C and the samples were collected at 1, 6, 12, and 24 h. Similarly, CaMV35S::GUS fusion construct transformed leaf discs were treated with H₂O and used as mock treated control.

Histochemical GUS Staining and GUS Activity Quantification

GUS histochemical staining was performed using the method described earlier (Jefferson et al., 1987). The protein extraction (Bradford, 1976) and GUS fluorometric analysis was done using the method described earlier (Huda et al., 2013).

Statistical Analysis

Statistically significant differences between mean values were analyzed by Student's *t*-test (*P* ≤ 0.05).

RESULTS

Isolation of *OsXPB2* Promoter from Rice and Analysis of C/S-Acting Elements

OsXPB2 promoter was amplified using promoter specific primer pairs as described earlier (Supplementary Figures 1A–C). Cis-acting elements present in the *OsXPB2* promoter

TABLE 1 | Predictions of cis-elements present in *OsXPB2* promoter using PLANT CARE and PLACE database analysis.

Element	Position	Database ID	Strand	Expected function
CCGCC-box	427	PC	—	Meristem specific activation
CGTCA-motif	811	PC	+	MeJA-responsiveness
TGACG-motif	628	PC	+	MeJA-responsiveness
Skn-1_motif	627	PC	—	Endosperm expression
Circadian	204	PC	+	circadian control
AC-1	119	PC	+	Enhanced xylem expression and repressed phloem
CAAT-box	60	PC	+	Promoter and enhancer regions
TC-rich repeats	52	PC	+	Defense and stress responsiveness
CACTFTPPCA1	517	(P)S000449	+	Mesophyll expression module
CGACGOSAMY3	718	(P)S000205	+	Expression during sugar starvation
box S	459	PC	+	Elicitation; wounding and pathogen response
ABRELATERD1	46	(P) S000414	—	Early responsive to dehydration
ARFAT	824	(P) S000270	—	Auxin response factor(ARF)
ASF1MOTIFCAMV	629	(P) S000024	+	ASF-1 binding site" in CaMV 35S promoter
BS1EGCCR	882	(P) S000352	+	Vascular expression
CBFHV	49	(P) S000497	—	Dehydration-responsive element (DRE)
CCAATBOX1	165	(P) S000030	+	Heat shock protein genes
GCCCCORE	612	(P) S000430	+	Ethylene-responsive element
	921			
	950			
	961			
GT1CONSENSUS	861	(P) S000198	+	SA-inducible gene expression
MYB2CONSENSUSAT	70	(P) S000409	+	Dehydration-response
MYBCORE	152	(P) S000176	+	Responsive to water stress
MYCCONSENSUSAT	211	(P) S000407	+	Cold response
	384			
	567			
PREATPRODH	647	(P) S000450	—	Hypoosmolarity-responsive element
RGATAOS	254	(P) S000191	+	Phloem-specific
TAAAGSTKST1	863	(P) S000387	+	Guard cell-specific
TATCCACHVAL21	42	(P) S000416	+	GA response
WRKY71OS	629	(P) S000447	+	Transcriptional repressor of the gibberellins signaling pathway
Motif IIb	961	PC	+	Abscisic acid responsive element

region as identified by *in silico* analysis are listed in **Table 1**. The promoter region has a transcription start site TATA (TACAAA, consensus TTCC) and CCAAT box at position –55 and –61 base pair, respectively (**Table 1**). The sequence analysis suggests that several cis-elements including defense and stress responsiveness (TC-rich repeats), early responsive to dehydration (ABRELATERD1), dehydration responsive elements (CBFHV), heat shock protein responsive element (CCAATBOX1), cold response (MYC CONSENSUSAT), and element responsive to water stress (MYBCORE) are present in the *OsXPB2* promoter sequence (**Table 1**). The sequence also contains hormone responsive cis-acting elements like MeJ responsive CGTCA-motif, GCCCORE ethylene responsive element, GT1CONSENSUS SA response element and ABA responsive elements (e.g., Motif IIb). BS1EGCCR and skn-1 motifs are also identified to be associated with vascular tissue specificity and endosperm expression, respectively (**Table 1**). The cis-regulatory elements such as meristem specific (CCGTCC-box) element, wounding and pathogen response (box-s) element, phloem specific (RGATAOS), guard cell specific (TAAAGSTKST1), and mesophyll expression elements (CACTFTPPCA1) are also present in the sequence (**Table 1**).

Cloning of *OsXPB2* Promoter and Its Activity in Tobacco Leaves

The *OsXPB2* promoter was cloned into pCAMBIA-1391Z and the clones were confirmed by PCR and restriction analysis (Supplementary Figures 1A–C). Different stress responsive cis-elements are shown in the *OsXPB2* promoter sequence (Supplementary Figure 2). The fusion construct *OsXPB2::GUS* was transiently expressed in tobacco leaves and it was used to check the promoter inducibility under different abiotic and hormonal stress conditions at different time points to study time course of GUS activity. To check whether the isolated promoter region of *OsXPB2* possesses active promoter functions, the tobacco leaves agro-infiltrated with *OsXPB2::GUS* or CaMV35S::GUS (as control) were mock treated (**Figures 1B,C**). There was no blue color development in the mock treated *OsXPB2* promoter and very low level of GUS expression and activity was recorded (**Figures 1B,J**). The CaMV35S::GUS was also given mock treatment and an intense blue coloration developed at different time points suggesting very high GUS activity (**Figures 1C,J**). The activity of *OsXPB2* promoter was analyzed under different abiotic stress (Salt, PEG, or cold) conditions by transient assay (**Figures 1D–F**). Histochemical staining revealed that the GUS expression increased at 12–24 h as compared to 1 and 6 h (**Figure 1D**). The effect of PEG stress varied for the *OsXPB2* promoter; the blue staining was detected at 1–6 h of stress treatment, but the intensity of the blue color gradually increased from 12 to 24 h, and similar trend was also observed in the quantitative GUS activity (**Figures 1E,J**). Under cold stress treatment at the early time period 1–6 h, slight blue coloration was detected and increase in the blue color intensity was present at 24 h (**Figures 1E,J**). These results reveal that *OsXPB2* promoter is a

stress inducible promoter and it mainly responds to osmotic and cold stresses.

Leaf disks were also incubated with different hormones (NAA, ABA, or MeJA) and differential pattern in GUS activity was noted (**Figures 1G–I**). The GUS expression driven by *OsXPB2* promoter under NAA treatment showed moderate blue color at 1–12 h and slight increase was noted at 24 h and the corresponding GUS activity was also recorded (**Figures 1G,J**). It is interesting to note that in the ABA treatment the blue color was intense in the initial time period and it sustained up to 24 h and the GUS activity recorded was also high (**Figures 1H,J**). Furthermore, in the MeJA treated leaves the blue color developed but the variation in the blue color did not differ much up to 24 h, and the corresponding GUS activity was recorded (**Figures 1I,J**). The observed variation in GUS expression levels may be due to difference in response of cis-acting elements of *OsXPB2* promoter.

DISCUSSION

Helicases, the motor proteins have vast potential as modulators of stress responses in plants. The new emerging role of helicases in engineering plant abiotic stress tolerance has encouraged studying the associated promoters for better understanding of gene regulation under stressful conditions. At present, constitutive and inducible promoters are widely used for the expression of candidate genes and their functional analysis. However, the constitutive expression of transgene may lead to homology-dependent gene silencing. Therefore, the exploitation of inducible promoters may be a vital tool for spatial and temporal gene expression under stress. In this study, we have presented important information regarding the complex regulation of rice helicase promoter in response to different abiotic stresses. Recent report regarding the function of *OsXPB2* gene in DNA damage and the concomitant activation of TC-NER pathway in response to γ -radiation and salinity stress emphasizes the importance of helicases in abiotic stress tolerance (Macovei et al., 2014). Therefore, the identification and functional validation of cis-elements is crucial in understanding the regulation of promoter and its possible exploitation in transgenic research. It is well-established that the putative regulatory elements in plant promoters can be easily identified using *in silico* analysis (Pujade-Renaud et al., 2005; Wei-Min et al., 2005; Huda et al., 2013). The analysis of cis-regulatory elements present in the promoter regions have received special attention as they provide insights into gene regulation and plant signaling under stress conditions. Further, *Agrobacterium*-mediated transient expression assay is a widely accepted method for *in vivo* quantitative analysis of plant promoters and cis-element/trans-factor interactions (Yang et al., 2000). The analysis of the expression of GUS reporter gene in *OsXPB2::GUS* revealed abiotic and hormonal regulation of GUS expression.

Brosché et al. (2002) reported that the promoter of XPD helicase of *Arabidopsis thaliana* contains multiple cis-elements [ACGT, ACCTA, H-box, myeloblastosis (Myb), Myb recognition element (MRE), SET binding factor 1 (SBF-1) and TCA-element, salicylic acid-responsive element] and has implication in light

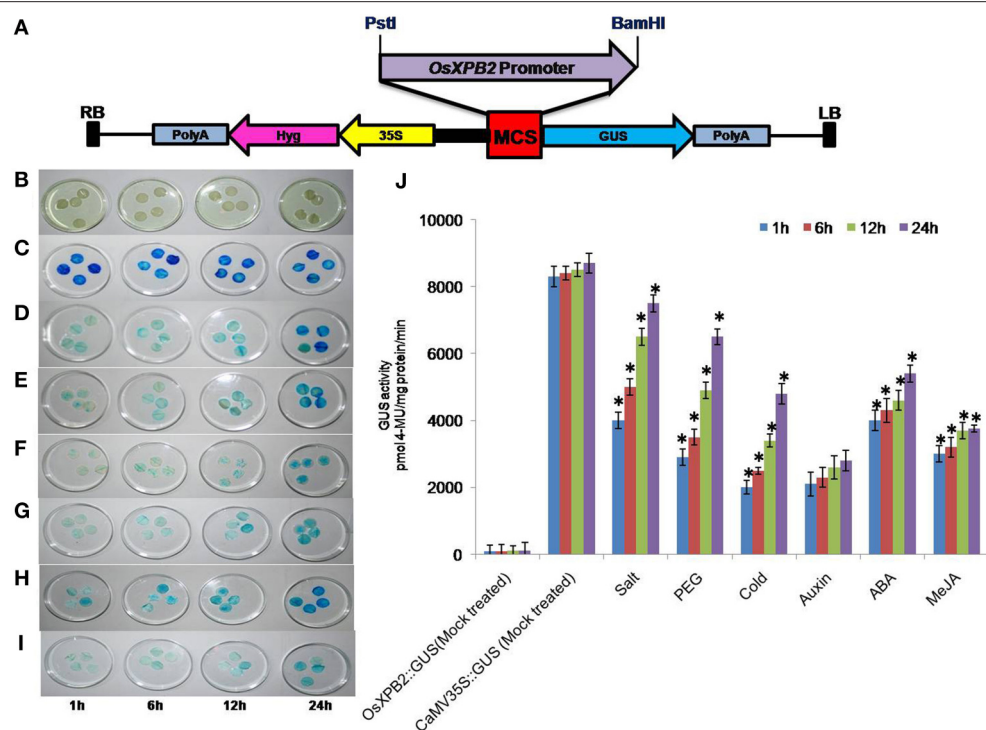


FIGURE 1 | (A) Schematic representation of OsXPB2 promoter cloned in pCAMBIA1391Z vector (promoter less vector) at PstI and Bam-HI sites for measuring GUS activity and agro-infiltration. **(B–J)** time course of OsXPB2 promoter-GUS expression analysis in the agro-infiltrated tobacco leaves in response to abiotic stress [200 mM salt, 20% PEG, cold (4°C) stress] and phytohormones [MeJA (10 μM), ABA (5 μM), and auxin (10 μM)]. Histochemical GUS staining of OsXPB2 promoter::GUS treated with water (mock treated) **(B)**, CaMV35S::GUS water (mock treated) **(C)**, OsXPB2::GUS NaCl **(D)**, PEG **(E)**, cold **(F)**, Auxin **(G)**, MeJA **(H)**, ABA **(I)**, comparison of GUS activity determined in protein extracts (*in vitro*) **(J)**. Data of four independent agro-infiltrated leaves were measured, and each experiment was replicated four times. Error bars on the graphic represent (±SD). *P < 0.05 differ significantly from their respective controls according to Student's paired *t*-test.

regulation and in UV stress response. It has also been reported that *AtXPD* gene was among some DNA repair genes that are hypomethylated in the promoter region (Boyko et al., 2010). Hypomethylation was reported to be correlated with permissive chromatin histone modification and increased *AtXPD* expression (Boyko et al., 2010). The significance of few cis-regulatory elements like G-box and ABREs combinations have also shown that stress-responsive genes are regulated by multiple transcription factors (Abe et al., 1997; Liu et al., 2014; Wang et al., 2014). Therefore, functional analysis of cis-regulatory elements is crucial to understand the regulatory gene networks in stress-responsive pathways. Our present study demonstrates the presence of different stress responsive cis-elements in *OsXPB2* promoter that are associated with tissue-specific expression, meristem specific, endosperm specific expression, defense and stress responsiveness, vascular expression, phloem specific, guard cell specific, and mesophyll expression module. The presence of these tissue-specific expression regulatory elements indicates the association of *OsXPB2* gene to a wide range of cellular processes which still requires validation. In addition, the *in silico* analysis of *OsXPB2* promoter suggests the presence of salt or dehydration responsive cis-acting elements in the sequence.

In vivo analysis of *OsXPB2::GUS* construct revealed that GUS expression was induced by different abiotic stresses and

OsXPB2 promoter was able to drive GUS expression when agro-infiltrated in tobacco leaves treated with NaCl, PEG or cold stress. The presence of multiple copies of the NAC like element (5'-CACG-3') in the upstream region of *OsXPB2* gene might be responsible for salt induced expression. Tran et al. (2004) reported that NAC-type transcription factors regulate salt responsive genes in an ABA-dependent manner. Salt stress was also shown to induce several NAC genes in rice (Hu et al., 2006). It has been reported that *OsNAC5* salt inducible NAC transcription factor which binds to the NAC recognition core sequence (CACG) of *OsLEA3* promoter, when overexpressed, showed improved salt tolerance (Takasaki et al., 2010).

Furthermore, the PEG and ABA treatment leads to higher GUS activity. A significant increase in ABA levels has been observed in response to dehydration stress. Previous reports also support that most dehydration-inducible genes are induced by ABA (Chandler and Robertson, 1994; Shinozaki et al., 2003). The upstream region of *OsXPB2* gene also contains multiple cold responsive elements, e.g., MYC CONSENSUSAT (CACGTG). Chinnusamy et al. (2003) reported that cold stress induced ICE1 binds to MYC cis-elements of the CBF promoter in *Arabidopsis* and it induces the expression of CBF, which regulates the COR genes and imparts cold acclimation.

Plant hormones are known to mediate the defense processes against pathogenic attack and herbivores (Ohshima et al., 1990). Furthermore, phytohormones like salicylate, jasmonates, and ethylene are reported to be involved in plant responses to various stresses (Ohshima et al., 1990). It is well-established that phytohormone auxin regulates several physiological processes such as apical dominance, shoot elongation, lateral root initiation, vascular differentiation, embryo patterning etc. (Davies, 1995) and enhances the transcription of various genes (Aux/IAA, GH3, and SAUR gene family members) (Abel and Theologis, 1996). In the present study, we have identified auxin responsive cis-regulatory elements in *OsXPB2* promoter sequence and high GUS expression was observed in the agro-infiltrated tobacco leaves. Jasmonates including MeJA and JA are also key signaling molecules for diverse developmental processes from seed germination to fruit ripening and senescence (Wasternack and Hause, 2002). The GCC or G-box elements, CGTCA motif and TGACG motif are required for MeJA-inducible expression of different genes. The role of JA in response to various abiotic stresses has been reported in a number of studies (Clarke et al., 2009; Yoon et al., 2009; Brossa et al., 2011). The analysis of GUS expression in response to MeJA indicates that the cis-elements present in *OsXPB2* promoter may have positive regulatory role toward stress tolerance.

In the present study, using histochemical analysis (qualitative and quantitative) we have demonstrated that the *OsXPB2*

promoter is able to drive GUS reporter gene expression in response to abiotic stress and hormonal treatments. The cis-elements identified in *OsXPB2* promoter together with the data from GUS reporter gene expression profiles under different abiotic stresses, support that *OsXPB2* promoter is stress responsive. The transient assay results along with GUS fluorometric assay results show that the *OsXPB2* promoter triggers high levels of GUS expression under abiotic and hormonal treatment stresses. Our data collectively suggest that the *OsXPB2* promoter analyzed in the present study could be potentially used to drive transgenes based on its responsiveness to different abiotic stresses including the genotoxic stress for the crop improvement.

ACKNOWLEDGMENTS

The research of NT's laboratory is partially supported by Department of Biotechnology (DBT), Govt. of India, New Delhi. We thank Dr. Anca Macovei for reading the manuscript.

SUPPLEMENTARY MATERIAL

The Supplementary Material for this article can be found online at: <http://journal.frontiersin.org/article/10.3389/fpls.2015.01094>

REFERENCES

- Abe, H., Yamaguchi-Shinozaki, K., Urao, T., Iwasaki, T., Hosokawa, D., and Shinozaki, K. (1997). Role of arabidopsis MYC and MYB homologs in drought- and abscisic acid-regulated gene expression. *Plant Cell* 9, 1859–1868. doi: 10.1101/tpc.9.10.1859
- Abel, S., and Theologis, A. (1996). Early genes and auxin action. *Plant Physiol.* 111, 9–17. doi: 10.1104/pp.111.1.9
- Banu, S. A., Huda, K. M. K., and Tuteja, N. (2014). Isolation and functional characterization of the promoter of a DEAD-box helicase *Psp68* using *Agrobacterium*-mediated transient assay. *Plant Signal. Behav.* 9:e28992. doi: 10.4161/psb.28992
- Battraw, M. J., and Hall, T. C. (1990). Histochemical analysis of CaMV 35S promoter-glucuronidase gene expression in transgenic rice plants. *Plant Mol. Biol.* 15, 527–538. doi: 10.1007/BF00017828
- Boyko, A., Blelvin, T., Yao, Y., Golubov, A., Bilichak, A., Ilnytskyy, Y., et al. (2010). Transgenerational adaptation of *Arabidopsis* to stress requires DNA methylation and the function of Dicer-like proteins. *PLoS ONE* 5:e9514. doi: 10.1371/journal.pone.0009514
- Bradford, M. M. (1976). A rapid and sensitive method for the quantitation of microgram quantities of protein utilizing the principle of protein-dye binding. *Anal. Biochem.* 72, 248–254. doi: 10.1016/0003-2697(76)90527-3
- Brosché, M., Schuler, M. A., Kalbina, I., Connor, L., and Strid, A. (2002). Gene regulation by low level UV-B radiation: identification by DNA array analysis. *Photochem. Photobiol. Sci.* 1, 656–664. doi: 10.1039/B202659G
- Brossa, R., Lopez-Carbonell, M., Jubany-Mari, T., and Alegre, L. (2011). Interplay between abscisic acid and jasmonic acid and its role in water-oxidative stress in wild-type, ABA-deficient, JA-deficient, and ascorbate-deficient Arabidopsis plants. *J. Plant Growth Regul.* 30, 322–333. doi: 10.1007/s00344-011-9194-z
- Capell, T., Escobar, C., Liu, H., Burtin, D., Lepri, O., and Christou, P. (1998). Over-expression of the oat arginine decarboxylase cDNA in transgenic rice (*Oryza sativa* L.) affects normal development patterns *in vitro* and results in putrescine accumulation in transgenic plants. *Theor. Appl. Genet.* 97, 246–254. doi: 10.1007/s001220050892
- Chandler, P. M., and Robertson, M. (1994). Gene-expression regulated by abscisic acid and its relation to stress tolerance. *Annu. Rev. Plant Physiol. Plant Mol. Biol.* 45, 113–141. doi: 10.1146/annurev.pp.45.06194.000553
- Chinnusamy, V., Ohta, M., Kanrar, S., Lee, B.-H., Hong, X., Agarwal, M., et al. (2003). ICE1: a regulator of cold-induced transcriptome and freezing tolerance in *Arabidopsis*. *Genes Dev.* 17, 1043–1054. doi: 10.1101/gad.1077503
- Clarke, S. M., Cristescu, S. M., Miersch, O., Harren, F. J. M., and Wasternack, C. (2009). Jasmonates act with salicylic acid to confer basal thermo tolerance in *Arabidopsis thaliana*. *New Phytol.* 182, 175–187. doi: 10.1111/j.1469-8137.2008.02735.x
- Costa, R. M., Morgante, P. G., Berra, C. M., Nakabashi, M., Bruneau, D., Bouchez, D., et al. (2001). The participation of AtXPB1, the XPB/RAD25 homologue gene from *Arabidopsis thaliana*, in DNA repair and plant development. *Plant J.* 28, 385–395. doi: 10.1046/j.1365-313X.2001.01162.x
- Dang, H. Q., Tran, N. Q., Gill, S. S., Tuteja, R., and Tuteja, N. (2011a). A single subunit MCM6 from pea promotes salinity stress tolerance without affecting yield. *Plant Mol. Biol.* 76, 19–34. doi: 10.1007/s11103-011-9758-0
- Dang, H. Q., Tran, N. Q., Tuteja, R., and Tuteja, N. (2011b). Promoter of a salinity and cold stress-induced MCM6 DNA helicase from pea. *Plant Signal. Behav.* 6, 1006–1008. doi: 10.4161/psb.6.7.15502
- Davies, P. J. (1995). *Plant Hormones, Physiology, Biochemistry and Molecular Biology*, 2nd Edn. Dordrecht: Kluwer.
- Gill, S. S., Gill, R., Tuteja, R., and Tuteja, N. (2014). Genetic engineering of crops: a ray of hope for enhanced food security. *Plant Signal. Behav.* 9:e28545. doi: 10.4161/psb.28545
- Gill, S. S., Tajrishi, M., Madan, M., and Tuteja, N. (2013). A DESD-box helicase functions in salinity stress tolerance by improving photosynthesis and antioxidant machinery in rice (*Oryza sativa* L. cv. PB1). *Plant Mol. Biol.* 82, 1–22. doi: 10.1007/s11103-013-0031-6
- Hsieh, T. H., Lee, J. T., Yang, P. T., Chiu, L. H., Charng, Y. Y., Wang, Y. C., et al. (2002). Heterology expression of the *Arabidopsis* C-repeat/dehydration

- response element binding factor 1 gene confers elevated tolerance to chilling and oxidative stresses in transgenic tomato. *Plant Physiol.* 129, 1086–1094. doi: 10.1104/pp.003442
- Hu, H., Dai, M., Yao, J., Xiao, B., Li, X., Zhang, Q., et al. (2006). Overexpressing a NAM, ATAF, and CUC (NAC) transcription factor enhances drought resistance and salt tolerance in rice. *Proc. Natl. Acad. Sci. U.S.A.* 103, 12987–12992. doi: 10.1073/pnas.0604882103
- Huda, K. M., Banu, M. S., Pathi, K. M., and Tuteja, N. (2013). Reproductive organ and vascular specific promoter of the rice plasma membrane Ca^{2+} ATPase mediates environmental stress responses in plants. *PLoS ONE* 8:e57803. doi: 10.1371/journal.pone.0057803
- Jefferson, R. A., Kavanagh, T. A., and Bevan, M. W. (1987). GUS fusions: β -glucuronidase as a sensitive and versatile gene fusion marker in higher plants. *EMBO J.* 6, 3901–3907.
- Kasuga, M., Liu, Q., Miura, S., Yamaguchi-Shinozaki, K., and Shinozaki, K. (1999). Improving plant drought, salt, and freezing tolerance by gene transfer of a single stress-inducible transcription factor. *Nat. Biotechnol.* 17, 287–291. doi: 10.1038/7036
- Liu, N., Ding, Y., and Fromm, M. (2014). Avramova Z. Different gene-specific mechanisms determine the ‘revised response’ memory transcription patterns of a subset of *A. thaliana* dehydration stress responding genes. *Nucleic Acids Res.* 42, 5556. doi: 10.1093/nar/gku220
- Liu, Q., Kasuga, M., Sakuma, Y., Abe, H., Miura, S., Yamaguchi-Shinozaki, K., et al. (1998). Two transcription factors, DREB1 and DREB2, with an EREBP/AP2 DNA binding domain separate two cellular signal transduction pathways in drought- and low-temperature- responsive gene expression, respectively, in Arabidopsis. *Plant Cell* 10, 1391–1406. doi: 10.1105/tpc.10.8.1391
- Luo, Y., Liu, Y. B., Dong, Y. X., Gao, X. Q., and Zhang, X. S. (2009). Expression of a putative alfalfa helicase increases tolerance to abiotic stress in Arabidopsis by enhancing the capacities for ROS scavenging and osmotic adjustment. *J. Plant Physiol.* 166, 385–394. doi: 10.1016/j.jplph.2008.06.018
- Macovei, A., Garg, B., Raikwar, S., Balestrazzi, A., Carbonera, D., Buttafava, A., et al. (2014). Synergistic exposure of rice seeds to different doses of γ -ray and salinity stress resulted in increased antioxidant enzyme activities and gene-specific modulation of TC-NER pathway. *Biomed Res. Int.* 2014:676934. doi: 10.1155/2014/676934
- Manjulatha, M., Sreevaths, R., Kumar, A. M., Sudhakar, C., Prasad, T. G., Tuteja, N., et al. (2014). Overexpression of a pea DNA helicase (PDH45) in peanut (*Arachis hypogaea* L.) confers improvement of cellular level tolerance and productivity under drought stress. *Mol. Biotechnol.* 56, 111–125. doi: 10.1007/s12033-013-9687-z
- Odell, J. T., Nagy, F., and Chua, N. H. (1985). Identification of DNA sequences required for activity of the cauliflower mosaic virus 35S promoter. *Nature* 313, 810–812. doi: 10.1038/313810a0
- Oettgen, P. (2001). Transcriptional regulation of vascular development. *Circ. Res.* 89, 380–388. doi: 10.1161/hh1701.095958
- Ohshima, M., Itoh, H., Matsuoka, M., Murakami, T., and Ohashi, Y. (1990). Analysis of stress-induced or salicylic acid induced expression of the pathogenesis-related 1a protein gene in transgenic tobacco. *Plant Cell* 2, 95–106. doi: 10.1105/tpc.2.2.95
- Pujade-Renaud, V., Sanier, C., Cambillau, L., Pappusamy, A., Jonese, H., Ruengsri, N., et al. (2005). Molecular characterization of new members of the *Hevea brasiliensis* hevein multigene family and analysis of their promoter region in rice. *Biochim. Biophys. Acta* 1727, 151–161. doi: 10.1016/j.bbapplied.2004.12.013
- Ribeiro, D. T., Machado, C. R., Costa, R. M., Praekelt, U. M., Van Sluys, M. A., and Menck, C. F. (1998). Cloning of a cDNA from *Arabidopsis thaliana* homologous to the human XPB gene. *Gene* 208, 207–213. doi: 10.1016/S0378-1119(97)00656-2
- Sanan-Mishra, N., Pham, X. H., Sopory, S. K., and Tuteja, N. (2005). Pea DNA helicase 45 overexpression in tobacco confers high salinity tolerance without affecting yield. *Proc. Natl. Acad. Sci. U.S.A.* 102, 509–514. doi: 10.1073/pnas.0406485102
- Schaeffer, L., Roy, R., Humbert, S., Moncollin, V., Vermeulen, W., Hoeijmakers, J. H., et al. (1993). DNA repair helicase: a component of BTF2 (TFIIH) basic transcription factor. *Science* 260, 58–63. doi: 10.1126/science.8465201
- Shinozaki, K., Yamaguchi-Shinozaki, K., and Seki, M. (2003). Regulatory network of gene expression in the drought and cold stress responses. *Curr. Opin. Plant Biol.* 6, 410–417. doi: 10.1016/S1369-5266(03)00092-X
- Singh, S. K., Roy, S., Choudhury, S. R., and Sengupta, D. N. (2011). DNA repair and recombination in higher plants insights from comparative genomics of Arabidopsis and rice. *BMC Genomics* 11:443. doi: 10.1186/1471-2164-11-443
- Tajirishi, M. M., and Tuteja, N. (2011). Isolation and *in silico* analysis of promoter of a high salinity stress-regulated pea DNA helicase 45. *Plant Signal Behav.* 6, 1447–1450. doi: 10.4161/psb.6.10.17106
- Takasaki, H., Maruyama, K., Kidokoro, S., Ito, Y., Fujita, Y., Shinozaki, K., et al. (2010). The abiotic stress responsive NAC-type transcription factor OsNAC5 regulates stress-inducible genes and stress tolerance in rice. *Mol. Genet. Genomics* 284, 173–183. doi: 10.1007/s00438-010-0557-0
- Tran, L. S. P., Nakashima, K., Sakuma, Y., Simpson, S. D., Fujita, Y., Maruyama, K., et al. (2004). Isolation and functional analysis of Arabidopsis stress-Inducible NAC transcription factors that bind to a drought-responsive cis-element in the early responsive to dehydration stress1 Promoter. *Plant Cell* 16, 2481–2498. doi: 10.1105/tpc.104.022699
- Tran, N. Q., Dang, H. Q., Tuteja, R., and Tuteja, N. (2010). A single subunit MCM6 from pea forms homohexamer and functions as DNA helicase. *Plant Mol. Biol.* 74, 327–336. doi: 10.1007/s11103-010-9675-7
- Tuteja, N., Banu, M. S. A., Huda, K. M. K., Gill, S. S., Jain, P., Pham, X. H., et al. (2014a). Pea p68, a DEAD-box helicase, provides salinity stress tolerance in transgenic tobacco by reducing oxidative stress and improving photosynthesis machinery. *PLoS ONE* 9:e98287. doi: 10.1371/journal.pone.0098287
- Tuteja, N., Sahoo, R. K., Garg, B., and Tuteja, R. (2013). OsSUV3 dual helicase functions in salinity stress tolerance by maintaining photosynthesis and antioxidant machinery in rice (*Oryza sativa* L. cv. IR64). *Plant J.* 76, 115–127. doi: 10.1111/tpj.12277
- Tuteja, N., Sahoo, R. K., Huda, K. M. K., Tula, S., and Tuteja, R. (2014b). OsBAT1 augments salinity stress tolerance by enhancing detoxification of ROS and expression of stress-responsive genes in transgenic rice. *Plant Mol. Biol. Rep.* 33, 1192–1209. doi: 10.1007/s11105-014-0827-9
- Umate, P., Tuteja, N., and Tuteja, R. (2011). Genome-wide comprehensive analysis of human helicases. *Commun. Integr. Biol.* 4, 118–137. doi: 10.4161/cib.13844
- Wang, X., Yan, Y., Li, Y., Chu, X., Wu, C., and Guo, X. (2014). GhWRKY40, a multiple stress-responsive cotton WRKY gene, plays an important role in the wounding response and enhances susceptibility to *Ralstonia solanacearum* infection in transgenic *Nicotiana benthamiana*. *PLoS ONE* 9:e93577. doi: 10.1371/journal.pone.0093577
- Wasternack, C., and Hause, B. (2002). Jasmonates and octadecanoids: signals in plant stress responses and plant development. *Prog. Nucl. Acid Res. Mol. Biol.* 72, 165–221. doi: 10.1016/S0079-6603(02)72070-9
- Wei-Min, L., Zhi-Xing, W., Wu, P., and Shi Rong, J. (2005). Cloning and characterization of the light-inducible Gacab promoter from *Gossypium arboreum*. *Agric. Biotechnol.* 2, 17–22. doi: 10.1079/CJB200547
- Yang, Y., Li, R., and Qi, M. (2000). *In vivo* analysis of plant promoters and transcription factors by agroinfiltration of tobacco leaves. *Plant J.* 22, 543–551. doi: 10.1046/j.1365-313x.2000.00760.x
- Yoon, J. Y., Hamayun, M., Lee, S. K., and Lee, I. J. (2009). Methyl jasmonate alleviated salinity stress in soybean. *J. Crop Sci. Biotech.* 12, 63–68. doi: 10.1007/s12892-009-0060-5
- Conflict of Interest Statement:** The authors declare that the research was conducted in the absence of any commercial or financial relationships that could be construed as a potential conflict of interest.
- Copyright © 2015 Raikwar, Srivastava, Gill, Tuteja and Tuteja. This is an open-access article distributed under the terms of the Creative Commons Attribution License (CC BY). The use, distribution or reproduction in other forums is permitted, provided the original author(s) or licensor are credited and that the original publication in this journal is cited, in accordance with accepted academic practice. No use, distribution or reproduction is permitted which does not comply with these terms.*



Genomic stability in response to high versus low linear energy transfer radiation in *Arabidopsis thaliana*

Neil D. Huefner^{1,2}, Kaoru Yoshiyama¹, Joanna D. Friesner^{1,2}, Phillip A. Conklin^{1,2} and Anne B. Britt^{1,2 *}

¹ Department of Plant Biology, University of California at Davis, Davis, CA, USA

² Graduate Program in Genetics, University of California at Davis, Davis, CA, USA

Edited by:

Alma Balestrazzi, University of Pavia, Italy

Reviewed by:

Igor Kovalchuk, University of Lethbridge, Canada

Nabil I. Elsheery, Tanta University, Egypt

***Correspondence:**

Anne B. Britt, Department of Plant Biology, University of California at Davis, 1002 Life Sciences, One Shields Avenue, Davis, CA 95616, USA

e-mail: abritt@ucdavis.edu

Low linear energy transfer (LET) gamma rays and high LET HZE (high atomic weight, high energy) particles act as powerful mutagens in both plants and animals. DNA damage generated by HZE particles is more densely clustered than that generated by gamma rays. To understand the genetic requirements for resistance to high versus low LET radiation, a series of *Arabidopsis thaliana* mutants were exposed to either 1GeV Fe nuclei or gamma radiation. A comparison of effects on the germination and subsequent growth of seedlings led us to conclude that the relative biological effectiveness (RBE) of the two types of radiation (HZE versus gamma) are roughly 3:1. Similarly, in wild-type lines, loss of somatic heterozygosity was induced at an RBE of about a 2:1 (HZE versus gamma). Checkpoint and repair defects, as expected, enhanced sensitivity to both agents. The "replication fork" checkpoint, governed by ATM, played a slightly more important role in resistance to HZE-induced mutagenesis than in resistance to gamma induced mutagenesis.

Keywords: ATM, ATR, double-strand breaks, genomic instability, KU80, LIG4, radiation

INTRODUCTION

The function of a cell, its capacity to proliferate, and ultimately, its viability, are under constant threat from a diverse array of DNA damaging agents and events. Although any lesion can have deleterious effects on an organism, double strand breaks (DSBs) are among the most dangerous types of DNA damage a cell can sustain. The threat such a lesion poses to an organism is influenced by several important factors. The site of damage and the phase of the cell-cycle in which the damage occurs impact both a cell's response to DSBs and their consequences (Rothkamm et al., 2003; Delacote and Lopez, 2008; Goodarzi et al., 2010). Furthermore, while some DSBs are relatively simple, more complex breaks may arise from secondary damage to the DNA backbone, damage to bases adjacent to the DSB, or the presence of multiple breaks in close proximity. Such variation in DSB complexity also plays an important role in governing the repair of these lesions (Mladenov et al., 2009).

Ionizing radiation (IR) is a particularly potent DNA damaging agent that produces single strand breaks, oxidized bases, abasic sites, and DSBs of varying complexity (McGrath and Williams, 1966; Lehnert, 2008). The efficiency with which an ionizing particle transfers its energy to the medium it passes through, termed linear energy transfer (LET), plays an important role in the nature of the DNA damage caused by exposure to IR (Zirkle et al., 1952). Low LET particles, such as gamma rays and X-rays, deposit their energy inefficiently as they pass through a cell, resulting in widely scattered damage (Costes et al., 2007). Such damage is generally repaired via base excision or nucleotide excision repair in a largely error-free manner (Ward and Chen, 1998). High-LET particles, such as accelerated nucleons or high charge, high energy (HZE) particles, deposit their energy much more efficiently along a discreet track as they pass through matter, resulting in significantly more complex, clustered damage along the track (Goodhead, 1988;

Nikjoo et al., 1998, 1999; Sutherland et al., 2001; Costes et al., 2007; Hada and Georgakilas, 2008). In human cell lines, the distribution of DSBs induced by HZE has been shown to lie along a well defined path through the nucleus, whereas gamma-induced DSBs are widely scattered; furthermore, HZE-induced γ-H2AX foci are often so closely packed, that individual foci are difficult to discern (Karlsson and Stenerlow, 2004; Costes et al., 2007). Although life on Earth's surface is largely protected from exposure to high-LET radiation, its hazards are still of significant concern, particularly in the planning of long-duration space missions. Moreover, the damage sustained as a result of exposure to either low or high-LET radiation exhibits similarities with the damage caused by other more common DSB-inducing agents, and may provide insight into the response to and repair of such lesions.

To investigate the immediate and long-term impacts high versus low-LET radiation have on plants, we employed the various DNA repair-deficient and cell-cycle checkpoint-deficient lines in the model plant *Arabidopsis thaliana*. ATM (ataxia-telangiectasia, mutated) and ATR (ATM and Rad3-related), members of the phosphoinositide-3-kinase-related protein kinase (PIKK) family, play important roles in governing the transcriptional response to DNA breakage and in the induction of cell-cycle arrest (Durocher and Jackson, 2001; Khanna and Jackson, 2001; Sancar et al., 2004; Culligan et al., 2006). While ATM and ATR have been shown to recognize DSBs and stalled replication forks respectively, it is clear that both kinases play important roles in the IR-induced DNA-damage response (Chen et al., 1999; Gatei et al., 2000; Abraham, 2001; Friesner et al., 2005; Ismail et al., 2005). Given the distinct nature of the lesions these proteins target, we were interested in the role these checkpoint genes play in responding to DNA damage of variable complexity as induced by exposure to high versus low-LET radiation. Lines lacking *DNA ligase IV* (*LIG4*) or *KU70*, important players in the canonical nonhomologous end-joining

(NHEJ) repair pathway, were also utilized to probe the importance of NHEJ and alternative repair pathways in the response to damage done by high and low-LET radiation.

MATERIALS AND METHODS

PLANT LINES

The following DNA repair-deficient and cell-cycle checkpoint-deficient alleles were used in our root growth assay: *atm-1* (Garcia et al., 2003), *atr-3* (Culligan et al., 2004), *lig4-1* (Friesner and Britt, 2003), and *ku80-1* (Friesner and Britt, 2003); all of which are in the *Ws* ecotype.

For our sectoring assay, we searched the Arabidopsis Information Resource (TAIR) database to identify alleles that might serve as an albino marker. The *APG3* gene (*albino/pale green mutant 3*), located near the telomere of chromosome III, is essential in chloroplast development (Motohashi et al., 2007). Seedlings deficient for *APG3* arrest development shortly after germination; as the name implies, cells deficient for *APG3* lack pigment and are easily distinguished from those that retain a wild-type copy of the *APG3* gene. A line harboring a T-DNA insertion in *APG3* was ordered from the Arabidopsis Biological Resource Center (Syngenta stock “CS16118”; McElver et al., 2001). This particular allele, *apg3-2*, was selected both because the T-DNA construct used in generating this particular line imparts resistance to the herbicide Basta, and because of its clear and consistent albino phenotype; the presence of the Basta resistance (*BAR*) gene in this construct afforded us the ability to select for just those plants carrying the albino marker. To introduce the *APG3* albino marker into our repair-deficient and checkpoint-deficient lines, we tried where possible, to choose alleles that did not already carry the *BAR* gene. We crossed *apg3-2* with *atm-1* (Garcia et al., 2003), *atr-2* (Culligan et al., 2004), *lig4-3* (Hefner et al., 2003, 2006), and *ku80-1* (Friesner and Britt, 2003); the ecotype of *apg3-2* and *atr-2* is *Col*, that of *atm-1* and *ku80-1* is *Ws*, and that of *lig4-3* is *Ler*.

IONIZING RADIATION

High-LET radiation treatments were administered at the NASA Space Radiation Laboratory (NSRL) at Brookhaven National Laboratory (BNL) (Upton, NY) using accelerated ^{56}Fe nucleons with a beam size diameter of 20 cm and a dose rate of 7 Gy min $^{-1}$. Following irradiation, samples remained at the NSRL facility for approximately 30 m until deactivated.

Low-LET, gamma radiation treatments were carried out at BNL using a ^{137}Cs source in the Controlled Environment Radiation Facility at a dose rate of up to 6 Gy min $^{-1}$. A subset of the gamma radiation treatments done on samples for the albino sectoring assay were carried out using an alternate ^{137}Cs source (Institute of Toxicology and Environmental Health, University of California, Davis, CA, USA) with a dose rate of 7 Gy min $^{-1}$.

PREPARATION OF SAMPLES USED IN ROOT GROWTH AND SECTORING ASSAYS

Four to six days prior to irradiation, seeds used in the root growth assay were surface sterilized using a 20% bleach solution; sterilized seeds and seeds used in the sectoring assay were aliquoted, suspended in ddH₂O, and stored at 4°C. Seeds were shipped overnight, on ice, to BNL where they were again stored at 4°C

until the time of IR treatment. Samples were irradiated (See “Ionizing Radiation” above) with the doses indicated in the text and figures. Following treatment, the samples were repacked on ice and shipped overnight to the University of California, Davis. Upon arrival, seeds used in the sectoring assay were sown on soil (Sunshine Mix #1; Sungro, Bellevue, WA, USA) at a density of ~0.2 seeds cm $^{-2}$ and placed in the growth chamber under clear plastic domes to maintain high humidity; seeds used in the root growth assay were sown on 1 × nutritive MS (Sigma-Aldrich, Saint Louis, MO, USA) Phytoagar (PlantMedia, Dublin, OH, USA) plates, pH 5.9, and placed vertically in the growth chamber. Seeds were grown under a simulated 16 h day/8 h night cycle using light from cool-white lamps (100–150 $\mu\text{mol m}^{-2} \text{s}^{-1}$) filtered through Clear UV-filtering Protect-O-Sleeves (McGill Electrical Product Group, Rosemont, IL, USA). Plastic domes were partially removed from seeds used in the sectoring assay 3 days after sowing and fully removed after 5 days.

MEASUREMENT OF ROOT LENGTH

Digital images of the plated seeds were taken eight days after transfer to the growth chamber. The length of the primary root was determined using the public domain, image-processing program, ImageJ.

QUANTIFICATION OF APG3 SECTORS

Because the *apg3-2* allele imparts resistance to the herbicide Basta, we were able to significantly reduce the number of plants it was necessary to screen for sectoring. Roughly 2 w after sowing, the number of healthy seedlings was determined. Plants were then treated with Basta (Finale, AgrEvo Environmental Health, Montvale, NJ, USA) and the number of resistant plants was determined in the following days. Resistant plants were scored for the presence of albino sectors approximately 3 weeks after sowing. The leaves of each plant were gently manipulated in order to inspect underlying leaves. Sectors were white or pale green in color, could be traced toward or along the petiole, and exhibited a relatively clear and well-defined boundary between the sector and the neighboring tissue; leaves that were clearly unhealthy or grossly deformed were not scored for sectors. While the number of Basta resistant plants might have been used to calculate such a frequency directly, the fact that in the case of the *atm-1* mutant, this insertion allele also carries Basta resistance, and so seedlings in the next generation, after selection for Basta resistance, would be expected to segregate 2 *apg3-2* het:1 *APG3-2* $^{+/+}$. To correct for this, seeds were collected from a heterozygous parent, and the frequency of hets for *apg3-2* was corrected for in the next generation. To estimate the frequency of sectoring in the progeny of heterozygous *APG3* $^{+/+}$ plants, we divided the number of plants with a sector by two-thirds the total number of healthy seedlings present 2 weeks after sowing.

RESULTS AND DISCUSSION

THE BIOLOGICAL EFFECTIVENESS OF HZE ^{56}Fe PARTICLES IS APPROXIMATELY 3-FOLD GREATER THAN THAT OF ^{137}Cs GAMMA RAYS WITH RESPECT TO INHIBITION OF PRIMARY ROOT GROWTH

To test the relative impact of high- versus low-LET radiation on root growth, a process governed by both cell division and cell

expansion, seeds were irradiated with either high-LET ^{56}Fe particles (HZE) or low-LET ^{137}Cs gamma rays. The length of the primary root 8 days after planting (DAP), relative to the length in unirradiated seeds, is shown in **Figure 1**. Consistent with previously published data, exposure to increasingly higher doses of gamma radiation results in increased inhibition of root elongation (Jiang et al., 1997). A similar, though more pronounced trend is observed in seeds exposed to HZE. At doses of 100 Gy HZE or higher, root elongation appears to be almost completely inhibited in wild-type lines, though seeds irradiated at such doses are still capable of germination, indicating that the treated embryos remain alive.

Relative biological effectiveness (RBE), defined as the absorbed dose of radiation of a standard type (e.g. gamma) divided by the absorbed dose of radiation type “*x*” that causes the same amount of biological damage, offers a means of comparing how damaging different types of radiation are, given the same amount of absorbed energy; the larger the RBE for a type of radiation, the more damaging the radiation per unit energy deposited (Failla and Henshaw, 1931). The RBE of HZE versus gamma radiation was estimated by interpolating the dose response data to determine the dose at which the length of the primary root is reduced to 37% that of the untreated control ($ID_{1/e}$; **Table 1**). In the case of both our

Table 1 | Relative biological effectiveness of HZE versus gamma radiation with respect to root hypersensitivity.

Line	$ID_{1/e}$ (Gy)		
	$^{56}\text{Fe-HZE}$	$^{137}\text{Cs-}\gamma$	RBE (ID_γ / ID_{HZE})
Wild-type (Ws)	43.9	130.1	2.97
<i>atm-1</i>	22.8	82.9	3.63
<i>atr-3</i>	39.0	81.6	2.09
<i>lig4-1</i>	27.1	65.8	2.43
<i>ku80-1</i>	19.0	40.2	2.12

$ID_{1/e}$ = Dose required to inhibit growth of primary root to 37% that of the untreated control.

wild-type and mutant lines, the effect of HZE on primary root growth is significantly greater than that of gamma rays. The biological effectiveness of HZE versus gamma in our repair-deficient lines is slightly lower than observed in wild-type. Somewhat more variance is observed in our checkpoint-deficient lines. Lines deficient for ATM exhibit a slight increase in root sensitivity to HZE versus gamma radiation relative to wild-type (RBE = 3.63 versus 2.97), while lines deficient for ATR exhibit a slight decrease in their relative HZE sensitivity (2.09). Whether this shift in root hypersensitivity is a function of cell death resulting from a failed checkpoint induction, or from prolonged cell-cycle arrest is unclear from the root growth data.

GENOMIC INSTABILITY IN SEEDS EXPOSED TO HZE ^{56}Fe PARTICLES IS GREATER THAN THAT OBSERVED IN SEEDS EXPOSED TO ^{137}Cs GAMMA RAYS

While the root hypersensitivity assay indicates that exposure to HZE has a more pronounced effect, per Gy on the growth of seedlings than does exposure to gamma radiation, it fails to shed much light on long-term effects on genomic stability. In order to address the impact HZE and gamma radiation have on the integrity of the genome, we employed a sectoring assay to test for loss of heterozygosity (LOH) in treated seeds (Preuss and Britt, 2003). An albino marker gene (*apg3*) near the tip of chromosome III was introduced to a series of DNA repair defective lines and checkpoint defective lines. While seedlings homozygous for the albino marker arrest and die shortly after germination, untreated seedlings heterozygous for the marker appear phenotypically identical to wild-type. Loss of the wt allele marker in a heterozygous single cell, whether as a result of aneuploidy, loss of the distal portion of the chromosome, or mutation of the wild-type allele, followed by production of mutant cell files via cell division, results in the production of an albino sector (**Figure 2**, inset). The frequency with which these sectors occur within a population provides a measure of genomic stability (Yoshiyama et al., 2009).

As expected, under normal conditions, genomic stability in wild-type plants appears quite high. To obtain an estimate of the rate of spontaneous LOH at the *APG3* locus in wild-type plants, 900 untreated plants were scored for the presence of an albino sector. Of the 900 plants scored, none exhibited the presence of

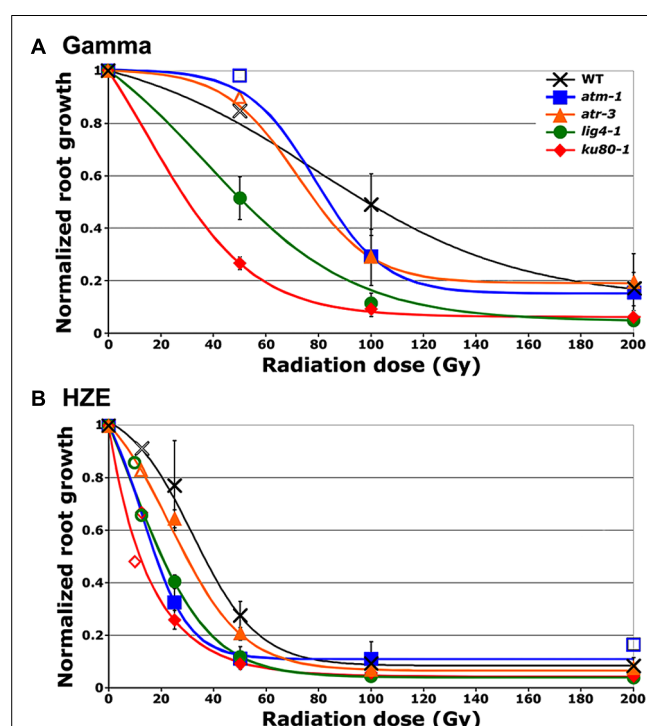


FIGURE 1 | Relative root growth of irradiated seeds 8 days after treatment. (A) Gamma treatment. (B) HZE treatment. Data points reflect results from three ($n = 3$) biological replicates in the case of *atm*, and *atr* and four ($n = 4$) biological replicates in the case of wild-type, *lig4* and *ku80* (Doses for which only a single biological replicate was performed are displayed as hollow data points.). Rootlengths from an average of 29 seedlings were scored per line, per treatment, per replicate. Lines represent interpolation of the data, fit to a sigmoid curve. Error bars depict standard error of the mean, as calculated and plotted by Microsoft Excel.

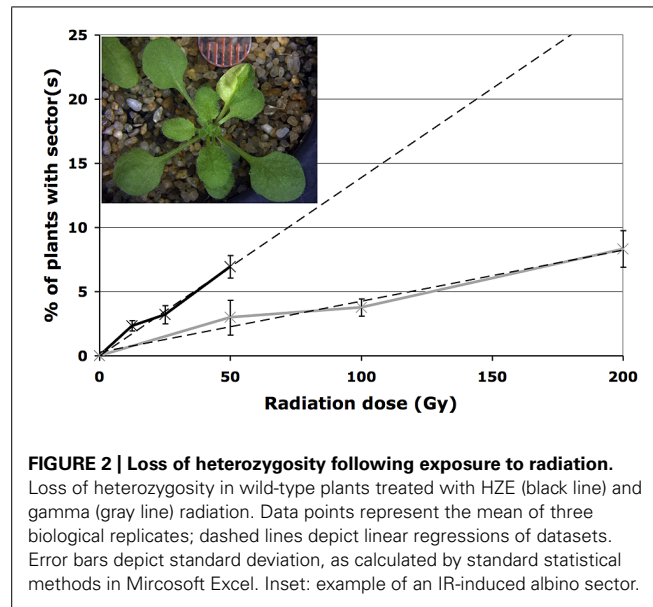


FIGURE 2 | Loss of heterozygosity following exposure to radiation.
Loss of heterozygosity in wild-type plants treated with HZE (black line) and gamma (gray line) radiation. Data points represent the mean of three biological replicates; dashed lines depict linear regressions of datasets. Error bars depict standard deviation, as calculated by standard statistical methods in Microsoft Excel. Inset: example of an IR-induced albino sector.

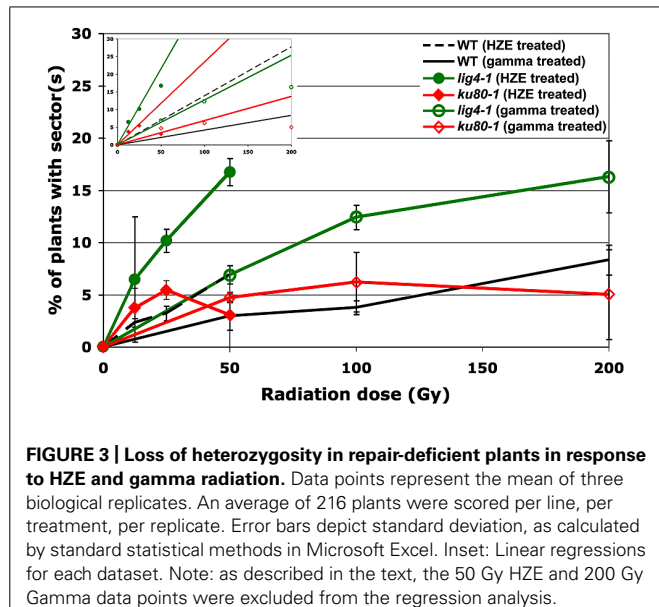


FIGURE 3 | Loss of heterozygosity in repair-deficient plants in response to HZE and gamma radiation. Data points represent the mean of three biological replicates. An average of 216 plants were scored per line, per treatment, per replicate. Error bars depict standard deviation, as calculated by standard statistical methods in Microsoft Excel. Inset: Linear regressions for each dataset. Note: as described in the text, the 50 Gy HZE and 200 Gy Gamma data points were excluded from the regression analysis.

a sector, suggesting a rate of spontaneous LOH per plant for this particular allele of less than 0.1%.

In seeds treated with low doses of either HZE or gamma radiation, sectoring increases with dose in a roughly linear, positive fashion (**Figure 2**). However, plants treated with higher doses are very small, and exhibit decreasing frequencies of sectoring/plant, perhaps simply because fewer cells are sampled per plant. Sectoring frequency in seeds treated with ^{56}Fe particles was consistently higher than that observed in seeds treated with gamma rays; these results are consistent with the observation that in human cells, clustered damage generated by Fe ions leads to increases in chromosome breakage and genomic instability (Asaithamby et al., 2011). To obtain an estimate of the biological effectiveness of HZE versus gamma radiation, in the context of long-term genomic stability, linear regressions were generated from the sectoring data (**Figures 2 and 3, inset**). Regressions were constrained such that they passed through the origin, and the ratio of the slopes from the HZE and gamma datasets was determined. In wild-type plants, a 3.33-fold increase in sectoring was observed in seeds treated with HZE as compared to those treated with gamma rays (**Table 2**). In the case of *lig4* and *ku80*, the 50 Gy gamma and 200 Gy HZE data points were omitted in the regression analysis due to a drop-off in sectoring at higher doses as discussed in the following section.

LINES DEFECTIVE IN DNA DSB REPAIR EXHIBIT A DECREASE IN GENOMIC STABILITY

Given the significant roles LIG4 and the KU70/KU80 heterodimer play in NHEJ (Friesner and Britt, 2003), we sought to determine the importance of these factors in maintaining genomic stability during the repair of IR-induced DSBs. As in the case of wild-type, at low doses, our *lig4* and *ku80* lines exhibited a roughly linear increase in the frequency of sectoring with exposure to increased levels of radiation; however, unlike our wild-type line, a significant drop-off in sectoring was observed at higher doses of either HZE or gamma radiation (**Figure 3**). Again, we believe this is due to the

very small size of the repair-defect plants after irradiation at these doses.

Of the mutant lines tested, plants lacking LIG4 exhibited the highest rate of sectoring following exposure to IR (**Table 2**). Although research has demonstrated that DSBs can be rejoined in the absence of LIG4, its role as the primary ligase involved in NHEJ is well documented (Grawunder et al., 1998; Tsukamoto and Ikeda, 1998; Junop et al., 2000; Friesner and Britt, 2003; van Attikum et al., 2003; Huefner et al., 2011). The increased rate of LOH in *lig4* is almost certainly the result of persistent DSBs present during cell division; whether the structure of these breaks precludes other ligases from rejoining the broken ends, or the ends are repaired in a more error-prone fashion is unclear. KU80, another important component of NHEJ, also appears to be involved in maintaining genomic stability following exposure to IR. Other work has shown that while the KU complex plays an important role in governing the size of deletions and insertions at DSB

Table 2 | Relative biological effectiveness of HZE versus gamma radiation with respect to LOH.

Slope of Linear Regression "y = mx" (fraction of <i>APG3</i> \pm plants with visible sector/Gy)			
Line	m (^{56}Fe -HZE)	m (^{137}Cs - γ)	RBE (m _{HZE} /m _y)
Wild-type	0.1389	0.0417	3.33
<i>atm-1</i>	0.2626	0.1024	2.56
<i>atr-2</i>	0.3079	0.0784	3.93
<i>lig4-3</i>	0.4292	0.1268	3.38
<i>ku80-1</i>	0.2343	0.0686	3.42

Calculations were made as described in the text, where RBE of HZE relative to gamma is taken as the ratio of slopes (m_{HZE}/m_y) for the linear regressions of the sectoring versus dose datasets forced through the origin.

repair sites and in stabilizing broken ends prior to ligation, end-joining can still occur in its absence (Ma et al., 2003; Boboila et al., 2010; Huefner et al., 2011). It is likely, therefore, that a relatively large portion of the broken DNA ends generated by IR are ultimately rejoined in our *ku80* line resulting in the more moderate increase in sectoring observed in *ku80* plants as compared to *lig4* plants.

THE RELATIVE IMPORTANCE OF ATM AND ATR IN MAINTAINING GENOMIC STABILITY DIFFERS IN RESPONSE TO HZE VERSUS GAMMA RADIATION

As with our DNA repair-deficient lines, a significant increase in sectoring was observed in our checkpoint-deficient lines relative to wild-type (Figure 4). Such an increase is consistent with the role ATM and ATR play in governing the DSB driven, early G2/M phase arrest. Failure to properly arrest cells in response to DSBs could result in the presence of persistent DSBs during cell division, thereby leading to aneuploidy and LOH (Garcia et al., 2003; Culigan and Britt, 2008). ATM and ATR function synergistically in response to IR-induced DNA damage, functioning in some ways redundantly and in other ways distinctly to activate downstream targets, trigger cell-cycle arrest, and help drive DNA repair. In light of the fact that ATM is thought to respond directly to DSBs via interaction with proteins associated with the breaks (Bakkenist and Kastan, 2003; Lee and Paull, 2005), whereas ATR is thought to respond to the presence of persistent single-stranded DNA (ssDNA) (Burrows and Elledge, 2008; Cimprich and Cortez, 2008), we were interested in whether ATM and ATR function differently in maintaining genomic stability in response to the damage caused by HZE versus gamma radiation.

atm-1 seeds exposed to gamma radiation exhibit a 2.5-fold increase in the frequency of sectoring as compared to wild-type (calculated from the slopes reported in Table 2). A more moderate increase in sectoring, 1.9-fold, was observed in our *atr* line, suggesting that while both ATM and ATR play a role in maintaining genomic stability in response to gamma radiation exposure, ATM

is of greater relative importance. In seeds exposed to HZE particles, an increase in sectoring was again observed in both *atm* and *atr* relative to wild-type. Fold increases of 1.9 and 2.2 were observed for *atm* and *atr* respectively, indicating a reversal in the relative importance of ATM and ATR in mitigating LOH in HZE versus gamma treated seeds, although these differences are small. Quantification of the RBE of HZE versus gamma, in terms of genomic stability, in our checkpoint-deficient lines demonstrates a decrease in the relative importance of ATM in response to HZE radiation as compared to wild-type (2.6 and 3.3, respectively), and an increase in the relative importance of ATR (3.9). Based on the LOH data, it appears that ATR plays a more important role in responding to the complex, clustered damage induced by HZE particles than it does in responding to damage induced by exposure to gamma radiation.

Given that ATR responds to persistent ssDNA, one possible explanation for the increased importance ATR plays in response to HZE treatment, is that more ssDNA is produced directly upon exposure to HZE particles. Multiple nicks to the DNA backbone in close proximity to one another may produce significant stretches of ssDNA in conjunction with DSBs not typically present in breaks generated by low-LET radiation. Alternatively, ssDNA may also be produced secondarily in HZE treated cells as the cell attempts to repair the clustered damage via resection of damaged ends or excision of damaged nucleotides. In cells deficient for ATR, imposition of cell-cycle arrest in HZE treated cells may be abrogated or delayed, resulting in enhanced loss of heterozygosity in cells that divide before the damage can be resolved. This may also provide insight into the observation that relative to both wild-type and *atm*, root growth in *atr* is slightly more resistant to HZE treatment, given that affected cells, while incurring greater damage to the genome, may still be capable of cell division and expansion.

CONCLUSION

Our results demonstrate a clear difference in the sensitivity of *Arabidopsis* to high- versus low-LET radiation. Data from both our root hypersensitivity and LOH assays indicate that the RBE of HZE radiation is between two and four times that of gamma radiation. The increased sensitivity of plants to HZE suggests that not only the quantity, but also the complexity of DSBs induced by IR play an import part in determining the efficiency and accuracy of DNA repair. A significant decrease in the genomic stability of *KU80*-deficient and *LIG4*-deficient lines in response to both HZE and gamma radiation reflects the importance of C-NHEJ in the repair of both simple and complex DSBs.

While it is unclear what additional factors may be unique to or of special importance in the repair DSBs induced by one class of radiation versus another, it is apparent that the relative importance of ATM versus ATR shifts in response to HZE versus gamma radiation. The increased relative importance of ATR versus ATM in responding to damage induced by HZE suggests that treatment with high-LET radiation results, either directly or indirectly, in a significant increase in the amount of ssDNA in the cell. Given the differences in the composition of DNA damage induced by HZE and gamma radiation, it will be interesting to determine what

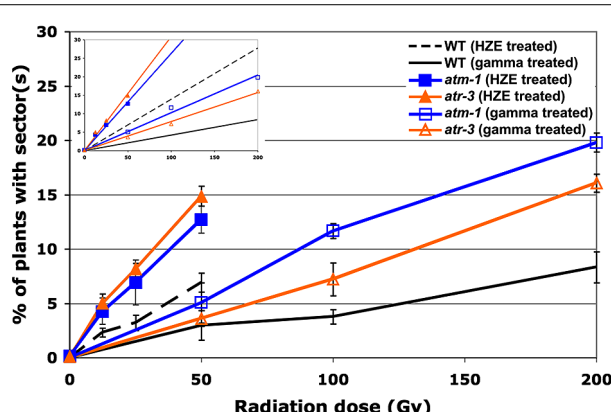


FIGURE 4 | Loss of heterozygosity in cell-cycle checkpoint-deficient plants in response to HZE and gamma radiation. Data points represent the mean of three biological replicates. Error bars depict standard deviation, calculated as before via Microsoft Excel. Inset: Linear regressions for each dataset.

other differences exist in a cell's response to both types of IR. Differences in response at the transcriptomics level are addressed in the accompanying paper.

ACKNOWLEDGMENTS

Experimental design by Anne B. Britt, preparation of albino reporter lines by Neil D. Huefner, irradiations and scoring performed by Anne B. Britt, Neil D. Huefner, and Joanna D. Friesner, scoring of albino sectors by Neil D. Huefner, scoring of root growth by Anne B. Britt, Neil D. Huefner, Phillip A. Conklin, Kaoru Yoshiyama, text and figures prepared by Neil D. Huefner with edits by Anne B. Britt. This work was funded by grants from NASA Fundamental Space Radiation Biology Program (Grant # NNA04CL13G) and DOE SC Office of Basic Energy Sciences (award # FG02-05ER15668). We gratefully acknowledge the assistance of the staff and faculty at Brookhaven National Labs/National Space Radiation Labs. including Adam Russek, Peter Guida, Richard Sautkulis, and the late Betsy Sutherland.

REFERENCES

- Abraham, R. T. (2001). Cell cycle checkpoint signaling through the ATM and ATR kinases. *Genes Dev.* 15, 2177–2196. doi: 10.1101/gad.914401
- Asaithamby, A., Hu, B., and Chen, D. J. (2011). Unrepaired clustered DNA lesions induce chromosome breakage in human cells. *Proc. Natl. Acad. Sci. U.S.A.* 108, 8293–8298. doi: 10.1073/pnas.1016045108
- Bakkenist, C. J., and Kastan, M. B. (2003). DNA damage activates ATM through intermolecular autophosphorylation and dimer dissociation. *Nature* 421, 499–506. doi: 10.1038/nature01368
- Boboila, C., Jankovic, M., Yan, C. T., Wang, J. H., Wesemann, D. R., Zhang, T., et al. (2010). Alternative end-joining catalyzes robust IgH locus deletions and translocations in the combined absence of ligase 4 and Ku70. *Proc. Natl. Acad. Sci. U.S.A.* 107, 3034–3039. doi: 10.1073/pnas.0915067107
- Burrows, A. E., and Elledge, S. J. (2008). How ATR turns on: topBP1 goes on ATRIP with ATR. *Genes Dev.* 22, 1416–1421. doi: 10.1101/gad.1685108
- Chen, G., Yuan, S. S., Liu, W., Xu, Y., Trujillo, K., Song, B., et al. (1999). Radiation-induced assembly of Rad51 and Rad52 recombination complex requires ATM and c-Abl. *J. Biol. Chem.* 274, 12748–12752. doi: 10.1074/jbc.274.18.12748
- Cimprich, K. A., and Cortez, D. (2008). ATR: an essential regulator of genome integrity. *Nat. Rev. Mol. Cell Biol.* 9, 616–627. doi: 10.1038/nrm2450
- Costes, S. V., Ponomarev, A., Chen, J. L., Nguyen, D., Cucinotta, F. A., and Barcellos-Hoff, M. H. (2007). Image-based modeling reveals dynamic redistribution of DNA damage into nuclear sub-domains. *PLoS Comput. Biol.* 3:e155. doi: 10.1371/journal.pcbi.0030155
- Culligan, K., Tissier, A., and Britt, A. (2004). ATR regulates a G2-phase cell-cycle checkpoint in *Arabidopsis thaliana*. *Plant Cell* 16, 1091–1104. doi: 10.1105/tpc.018903 tpc.018903
- Culligan, K. M., and Britt, A. B. (2008). Both ATM and ATR promote the efficient and accurate processing of programmed meiotic double-strand breaks. *Plant J.* 55, 629–638. doi: 10.1111/j.1365-313X.2008.03530.x
- Culligan, K. M., Robertson, C. E., Foreman, J., Doerner, P., and Britt, A. B. (2006). ATR and ATM play both distinct and additive roles in response to ionizing radiation. *Plant J.* 48, 947–961. doi: 10.1111/j.1365-313X.2006.02931.x
- Delacote, F., and Lopez, B. S. (2008). Importance of the cell cycle phase for the choice of the appropriate DSB repair pathway, for genome stability maintenance: the trans-S double-strand break repair model. *Cell Cycle* 7, 33–38. doi: 10.4161/cc.7.1.5149
- Durocher, D., and Jackson, S. P. (2001). DNA-PK, ATM and ATR as sensors of DNA damage: variations on a theme? *Curr. Opin. Cell Biol.* 13, 225–231. doi: 10.1016/S0955-0674(00)00201-5
- Failla, G., and Henshaw, P. S. (1931). The relative biological effectiveness of X-rays and gamma rays. *Radiology* 17, 1–43. doi: 10.1148/17.1.1
- Friesner, J., and Britt, A. B. (2003). Ku80- and DNA ligase IV-deficient plants are sensitive to ionizing radiation and defective in T-DNA integration. *Plant J.* 34, 427–440. doi: 10.1046/j.1365-313X.2003.01738.x
- Friesner, J. D., Liu, B., Culligan, K., and Britt, A. B. (2005). Ionizing radiation-dependent gamma-H2AX focus formation requires ataxia telangiectasia mutated and ataxia telangiectasia mutated and Rad3-related. *Mol. Biol. Cell* 16, 2566–2576. doi: 10.1091/mbc.E04-10-0890
- Garcia, V., Bruchet, H., Camescasse, D., Granier, F., Bouchez, D., and Tissier, A. (2003). AtATM is essential for meiosis and the somatic response to DNA damage in plants. *Plant Cell* 15, 119–132. doi: 10.1105/tpc.006577
- Gatei, M., Young, D., Cerosaletti, K. M., Desai-Mehta, A., Spring, K., Kozlov, S., et al. (2000). ATM-dependent phosphorylation of nibrin in response to radiation exposure. *Nat. Genet.* 25, 115–119. doi: 10.1038/75508
- Goodarzi, A. A., Jeggo, P., and Lobrich, M. (2010). The influence of heterochromatin on DNA double strand break repair: getting the strong, silent type to relax. *DNA Repair (Amst.)* 9, 1273–1282. doi: 10.1016/j.dnarep.2010.09.013
- Goodhead, D. T. (1988). Spatial and temporal distribution of energy. *Health Phys.* 55, 231–240. doi: 10.1097/00004032-198808000-00015
- Gravunder, U., Zimmer, D., Fugmann, S., Schwarz, K., and Lieber, M. R. (1998). DNA ligase IV is essential for V(D)J recombination and DNA double-strand break repair in human precursor lymphocytes. *Mol. Cell.* 2, 477–484. doi: 10.1016/S1097-2765(00)80147-1
- Hada, M., and Georgakilas, A. G. (2008). Formation of clustered DNA damage after high-LET irradiation: a review. *J. Radiat. Res. (Tokyo)* 49, 203–210. doi: 10.1269/jrr.07123
- Hefner, E., Huefner, N., and Britt, A. B. (2006). Tissue-specific regulation of cell-cycle responses to DNA damage in *Arabidopsis* seedlings. *DNA Repair (Amst.)* 5, 102–110. doi: 10.1016/j.dnarep.2005.08.013
- Hefner, E., Preuss, S. B., and Britt, A. B. (2003). *Arabidopsis* mutants sensitive to gamma radiation include the homologue of the human repair gene ERCC1. *J. Exp. Bot.* 54, 669–680. doi: 10.1093/jxb/erg069
- Huefner, N. D., Mizuno, Y., Weil, C. F., Korf, I., and Britt, A. B. (2011). Breadth by depth: expanding our understanding of the repair of transposon-induced DNA double strand breaks via deep-sequencing. *DNA Repair (Amst.)* 10, 1023–1033. doi: 10.1016/j.dnarep.2011.07.011
- Ismail, I. H., Nyström, S., Nygren, J., and Hammarsten, O. (2005). Activation of ataxia telangiectasia mutated by DNA strand break-inducing agents correlates closely with the number of DNA double strand breaks. *J. Biol. Chem.* 280, 4649–4655. doi: 10.1074/jbc.M411588200
- Jiang, C. Z., Yen, C. N., Cronin, K., Mitchell, D., and Britt, A. B. (1997). UV- and gamma-radiation sensitive mutants of *Arabidopsis thaliana*. *Genetics* 147, 1401–1409.
- Junop, M. S., Modesti, M., Guarne, A., Ghirlando, R., Gellert, M., and Yang, W. W. (2000). Crystal structure of the Xrc4 DNA repair protein and implications for end joining. *EMBO J.* 19, 5962–5970. doi: 10.1093/emboj/19.22.5962
- Karlsson, K. H., and Stenerlow, B. (2004). Focus formation of DNA repair proteins in normal and repair-deficient cells irradiated with high-LET ions. *Radiat. Res.* 161, 517–527. doi: 10.1667/RR3171
- Khanna, K. K., and Jackson, S. P. (2001). DNA double-strand breaks: signaling, repair and the cancer connection. *Nat. Genet.* 27, 247–254. doi: 10.1038/85798
- Lee, J. H., and Paull, T. T. (2005). ATM activation by DNA double-strand breaks through the Mre11-Rad50-Nbs1 complex. *Science* 308, 551–554. doi: 10.1126/science.1108297
- Lehnert, S. (2008). *Biomolecular Action of Ionizing Radiation*. New York: Taylor & Francis.
- Ma, J. L., Kim, E. M., Haber, J. E., and Lee, S. E. (2003). Yeast Mre11 and Rad1 proteins define a Ku-independent mechanism to repair double-strand breaks lacking overlapping end sequences. *Mol. Cell. Biol.* 23, 8820–8828. doi: 10.1128/MCB.23.23.8820-8828.2003
- McElver, J., Tzafrir, I., Aux, G., Rogers, R., Ashby, C., Smith, K., et al. (2001). Insertional mutagenesis of genes required for seed development in *Arabidopsis thaliana*. *Genetics* 159, 1751–1763.
- McGrath, R. A., and Williams, R. W. (1966). Reconstruction in vivo of irradiated *Escherichia coli* deoxyribonucleic acid; the rejoicing of broken pieces. *Nature* 212, 534–535. doi: 10.1038/212534a0
- Mladenov, E., Kalev, P., and Anachkova, B. (2009). The complexity of double-strand break ends is a factor in the repair pathway choice. *Radiat. Res.* 171, 397–404. doi: 10.1667/RR1487.1
- Motohashi, R., Yamazaki, T., Myouga, F., Ito, T., Ito, K., Satou, M., et al. (2007). Chloroplast ribosome release factor 1 (AtcpRF1) is essential for chloroplast development. *Plant Mol. Biol.* 64, 481–497. doi: 10.1007/s11103-007-9166-7

- Nikjoo, H., O'Neill, P., Terrissol, M., and Goodhead, D. T. (1999). Quantitative modelling of DNA damage using Monte Carlo track structure method. *Radiat. Environ. Biophys.* 38, 31–38. doi: 10.1007/s004110050135
- Nikjoo, H., Uehara, S., Wilson, W. E., Hoshi, M., and Goodhead, D. T. (1998). Track structure in radiation biology: theory and applications. *Int. J. Radiat. Biol.* 73, 355–364. doi: 10.1080/095530098142176
- Preuss, S. B., and Britt, A. B. (2003). A DNA-damage-induced cell cycle checkpoint in *Arabidopsis*. *Genetics* 164, 323–334.
- Rothkamm, K., Kruger, I., Thompson, L. H., and Lobrich, M. (2003). Pathways of DNA double-strand break repair during the mammalian cell cycle. *Mol. Cell. Biol.* 23, 5706–5715. doi: 10.1128/MCB.23.16.5706-5715.2003
- Sancar, A., Lindsey-Boltz, L. A., Unsal-Kacmaz, K., and Linn, S. (2004). Molecular mechanisms of mammalian DNA repair and the DNA damage checkpoints. *Annu. Rev. Biochem.* 73, 39–85. doi: 10.1146/annurev.biochem.73.011303.073723
- Sutherland, B. M., Bennett, P. V., Schenk, H., Sidorkina, O., Laval, J., Trunk, J., et al. (2001). Clustered DNA damages induced by high and low LET radiation, including heavy ions. *Phys. Med.* 17(Suppl. 1), 202–204.
- Tsukamoto, Y., and Ikeda, H. (1998). Double-strand break repair mediated by DNA end-joining. *Genes Cells* 3, 135–144. doi: 10.1046/j.1365-2443.1998.00180.x
- van Attikum, H., Bundoock, P., Overmeer, R. M., Lee, L. Y., Gelvin, S. B., and Hooykaas, P. J. (2003). The *Arabidopsis* AtLIG4 gene is required for the repair of DNA damage, but not for the integration of *Agrobacterium* T-DNA. *Nucleic Acids Res.* 31, 4247–4255. doi: 10.1093/nar/gkg458
- Ward, I. M., and Chen, J. (1998). “Nature of lesions formed by ionizing radiation,” in *DNA Damage and Repair: DNA Repair in Higher Eukaryotes*, eds J. A. Nickoloff and M. F. Hoekstra (Totowa, NJ: Humana Press), 65–84.
- Yoshiyama, K., Conklin, P. A., Huefner, N. D., and Britt, A. B. (2009). Suppressor of gamma response 1 (SOG1) encodes a putative transcription factor governing multiple responses to DNA damage. *Proc. Natl. Acad. Sci. U.S.A.* 106, 12843–12848. doi: 10.1073/pnas.0810304106
- Zirkle, R. E., Marchbank, D. F., and Kuck, K. D. (1952). Exponential and sigmoid survival curves resulting from alpha and x irradiation of *Aspergillus* spores. *J. Cell. Physiol. Suppl.* 39, 78–85.

Conflict of Interest Statement: The authors declare that the research was conducted in the absence of any commercial or financial relationships that could be construed as a potential conflict of interest.

Received: 05 February 2014; accepted: 28 April 2014; published online: 20 May 2014.

Citation: Huefner ND, Yoshiyama K, Friesner JD, Conklin PA and Britt AB (2014) Genomic stability in response to high versus low linear energy transfer radiation in *Arabidopsis thaliana*. *Front. Plant Sci.* 5:206. doi: 10.3389/fpls.2014.00206

This article was submitted to Plant Physiology, a section of the journal *Frontiers in Plant Science*.

Copyright © 2014 Huefner, Yoshiyama, Friesner, Conklin and Britt. This is an open-access article distributed under the terms of the Creative Commons Attribution License (CC BY). The use, distribution or reproduction in other forums is permitted, provided the original author(s) or licensor are credited and that the original publication in this journal is cited, in accordance with accepted academic practice. No use, distribution or reproduction is permitted which does not comply with these terms.



High atomic weight, high-energy radiation (HZE) induces transcriptional responses shared with conventional stresses in addition to a core “DSB” response specific to clastogenic treatments

Victor Missirian^{1†}, Phillip A. Conklin^{1†}, Kevin M. Culligan², Neil D. Huefner¹ and Anne B. Britt^{1*}

¹ Department of Plant Biology, University of California Davis, Davis, CA, USA

² Department of Molecular, Cellular, and Biomedical Sciences, University of New Hampshire, Durham, NH, USA

Edited by:

Alma Balestrazzi, University of Pavia, Italy

Reviewed by:

Nicholas Provert, University of Toronto, Canada

Wanda Waaterworth, University of Leeds, UK

***Correspondence:**

Anne B. Britt, Department of Plant Biology, University of California Davis, One Shields Avenue, Davis, CA 95616, USA

e-mail: abritt@ucdavis.edu

[†]Co-first authors.

Plants exhibit a robust transcriptional response to gamma radiation which includes the induction of transcripts required for homologous recombination and the suppression of transcripts that promote cell cycle progression. Various DNA damaging agents induce different spectra of DNA damage as well as “collateral” damage to other cellular components and therefore are not expected to provoke identical responses by the cell. Here we study the effects of two different types of ionizing radiation (IR) treatment, HZE (1 GeV Fe²⁶⁺ high mass, high charge, and high energy relativistic particles) and gamma photons, on the transcriptome of *Arabidopsis thaliana* seedlings. Both types of IR induce small clusters of radicals that can result in the formation of double strand breaks (DSBs), but HZE also produces linear arrays of extremely clustered damage. We performed these experiments across a range of time points (1.5–24 h after irradiation) in both wild-type plants and in mutants defective in the DSB-sensing protein kinase ATM. The two types of IR exhibit a shared double strand break-repair-related damage response, although they differ slightly in the timing, degree, and ATM-dependence of the response. The ATM-dependent, DNA metabolism-related transcripts of the “DSB response” were also induced by other DNA damaging agents, but were not induced by conventional stresses. Both Gamma and HZE irradiation induced, at 24 h post-irradiation, ATM-dependent transcripts associated with a variety of conventional stresses; these were overrepresented for pathogen response, rather than DNA metabolism. In contrast, only HZE-irradiated plants, at 1.5 h after irradiation, exhibited an additional and very extensive transcriptional response, shared with plants experiencing “extended night.” This response was not apparent in gamma-irradiated plants.

Keywords: DNA repair, double-strand breaks, transcriptomics, stress, cell-cycle, ionizing radiation, HZE, gamma radiation

INTRODUCTION

Programmed responses to DNA damage include the induction of repair, recombination, mutagenesis, cell cycle arrest, and cell death. These responses vary with the quality and quantity of the damage induced, with the phase of the cell cycle (Jazayeri et al., 2006), and with cell type (Shi et al., 1997). Damage response can also be influenced by environmental inputs (Shor et al., 2013), the age of the organism (Goukassian et al., 2000; Gredilla et al., 2012; Garm et al., 2013), and even the time of day (Ramsey and Ellisen, 2011; Gaddameedhi et al., 2012). A thorough knowledge of damage response provides insight into the mechanisms that promote genetic stability. In addition, comparative studies of damage response (the study of response to different agents, in different environments, or in different cell types) inform us as to how organisms balance the benefits of error-free repair vs. the risks engendered by cell death, growth arrest, inappropriate repair and ectopic recombination.

DNA damage response (DDR) is highly complex, involving the regulation of gene expression at all mechanistic levels and affecting the expression of thousands of genes. For this reason, DDR is an excellent subject for proteomic and transcriptomics approaches. Studies (largely focused on *Arabidopsis* seedlings) of both the transcriptomic and the phenotypic consequences of a variety of DNA damaging agents (Chen et al., 2003; Ulm and Nagy, 2005; Culligan et al., 2006; Kim, 2006; Ricaud et al., 2007; Cools et al., 2011; Mannuss et al., 2012) have led to the conclusion that different DNA damaging agents induce very different phenotypic and transcriptomic responses. This is worth considering in depth, as all significant types of DNA damage might be naively expected to have very similar immediate physiological consequences, for example, the blockage of transcription and replication. Observed differences in response to DNA damaging agents may not be due to response to DNA damage *per se*. All “DNA damaging agents” also damage other cellular components, and

some may act as signals (i.e., UV-B, ROS) that invoke responses unrelated to DNA repair. The ability of a species or cell to cope -or not- with this “collateral damage” can in some instances determine the difference between life and death- as exemplified by the role of protein-protective compounds in conferring extreme radioresistance in some bacteria (Daly et al., 2007).

In this study we focus on the quantitative, qualitative, and temporal differences in transcriptional response to two different types of ionizing radiation (IR): gamma photons, which have low rates of linear energy transfer (LET), and relativistic Fe nuclei (here termed HZE), a high LET form of IR. Interest in the differences in biological response to these two forms of IR has risen as long-term manned missions beyond the shielding effects the Earth’s atmosphere and magnetic field- to the moon and to Mars- have been increasingly contemplated.

Gamma photons interact weakly with matter- a large fraction of gamma photons will pass through a cell’s nucleus without losing any of their energy at all. However, some fraction of photons, during their transit across the cell, will interact indiscriminately with the cell’s molecules via Compton scattering. In this process, a small fraction of the photon’s energy will be transferred to an atom, inducing the ejection of a high-energy electron. The ejected electron will proceed to lose its energy through interactions with many additional atoms, producing many additional radicals. This energy will be lost quickly (on the order of 10^{-6} s), resulting in “clusters” of ionization events. Typically, 2–5 radicals are induced per cluster along a track length of 4–5 nm- on the order of the diameter of DNA (2 nm). It is the clustered nature of the formation of radicals that distinguishes the damage induced by IR from the damage induced by radical-forming chemicals (such as hydrogen peroxide or heavy metals), which produce isolated radicals (nicely reviewed in Ward, 1998). Isolated radicals, on interaction with DNA, induce singly damaged sites, which can be corrected via excision repair, using the undamaged strand as a template for error-free repair. In contrast, excision repair is not an option for DNA that has suffered the formation of closely spaced damage on both strands of the DNA. Thus, although all types of molecules in the cell are damaged by IR, in eukaryotic cells the biological effects of IR (mutation, cell cycle arrest, and cell death) are ascribed to the induction of clustered lesions in DNA.

Relativistic (near light-speed) Fe²⁶⁺ nuclei also induce high-energy electrons and so produce these scattered “handfuls” of clustered radicals. However, *in addition*, as this pinpoint charge source travels through the cell, it *continuously* displaces high-energy electrons from molecules along its path. Thus, this high LET particle (170 keV/ μ , in contrast to gamma radiation’s average of 0.2 keV/ μ) lays down a very dense and continuous cylinder of radicals as it crosses the cell. DNA molecules in the direct path of these particles are inevitably damaged at multiple sites. This produces a pattern of co-located multiply damaged sites- a continuous linear array of clusters on neighboring DNA molecules, facilitating the formation of deletions, inversions, and translocations. Isolated clusters and singly damaged sites occur also, at molecules in the less dense “penumbra” of secondary electrons generated at the periphery of the particle’s path (Magee and Chatterjee, 1980).

IR interacts indiscriminately with all molecules, and so damages all molecules. Researchers focus on DNA damage because DNA is uniquely low copy number and hence irreplaceable, and because the radiosensitivity of DNA repair and response mutants clearly indicates that DNA repair plays a central role in alleviating the mutagenic, carcinogenic, and toxic effects of IR. However, the very dense and collocated track of radicals laid down by HZE, and the inevitable damage to proteins, protein complexes, and membranes may have significant physiological effects that have not yet been characterized.

The effects of gamma radiation on plant growth, development, and mutation have, in contrast, been extensively described in several plant species. Most recently attention has focused on the *Arabidopsis* embryo and seedling, where gamma radiation has been shown to induce programmed cell death, cell cycle arrest, premature differentiation, and mutation (Preuss and Britt, 2003; Hefner et al., 2006; Fulcher and Sablowski, 2009; Furukawa et al., 2010). These effects are enhanced in mutants defective in DSB repair (via NHEJ pathways) (West et al., 2000; Tamura et al., 2002; Friesner and Britt, 2003; Hefner et al., 2003; Heacock et al., 2007; Fulcher and Sablowski, 2009), suggesting that clustered lesions are responsible for most of the effects of gamma radiation. Gamma radiation has also been shown (again, in the *Arabidopsis* seedling) to induce a robust transcriptional response, in which DNA and RNA metabolism genes are over-represented (Culligan et al., 2006; Ricaud et al., 2007). These same repair genes—most involved in HR- are also induced by treatment with bleomycin (BLM, an agent that induces clustered damage) plus mitomycin C (MMC, an inter-strand crosslinking agent) (Chen et al., 2003; Roa et al., 2009). Induction of these repair-related transcripts requires the DSB-sensing protein kinase ATM, suggesting that this is a direct response to the induction of DSBs. The transcriptional effects of HZE, in contrast, have not been described in any plant species.

Here we compare the time course (from 1.5 to 24 h after irradiation) of the transcriptional response to gamma radiation vs. HZE. We find that both agents strongly induce, a set of double-strand-break-repair-related transcripts, although the intensity and the degree of ATM-dependence of the response differs with the two types of radiation. We also describe the induction of additional transcripts, without known roles in DNA repair, induced specifically by HZE, which may reflect a response to damage to other (non-chromosomal) cellular components. Lastly, we contrast the transcriptional response to both types of IR to previously published data sets describing responses to a wide variety of more conventional stresses.

MATERIALS AND METHODS

GROWTH AND IRRADIATION OF SEEDLINGS

Eight days prior to irradiation, wild-type Ws and *atm-1* seeds were surface sterilized using a 20% bleach solution and then plated on 1 × MS, Phytoagar (PlantMedia, BioWorld, Dublin, OH). These plates were placed on ice and shipped to Brookhaven National Labs (BNL) where they were placed at 4°C. Five days prior to irradiation, the plates were placed vertically in a 21°C growth chamber in the BNL Controlled Environment Facility, where plants grew under cool white lamps (16 h day) until the

time of irradiation. For irradiation, plates were moved either to the Controlled Environment Radiation Facility for exposure to gamma radiation (100 Gy at 7 Gy/min), or to the National Space Radiation Laboratory (NSRL) for exposure to accelerated 1 GeV/n ^{56}Fe particles (30 Gy at 7 Gy/min). NSRL is located on the BNL campus. Plants exposed to ^{56}Fe particles were placed in a lighted hood for approximately 30 min, at which time the samples were considered to be deactivated and safe for return to the growth chamber, where they remained until time of harvest. Both facilities are located on the BNL campus.

PREPARATION OF TISSUE FOR MICROARRAY ANALYSIS

Whole wt seedlings were harvested 1.5, 3, 6, 12, and 24 h after treatment, frozen in liquid Nitrogen, and stored at -80°C . *atm-1* seedlings were harvested in parallel, though seedlings were not collected at 3 h. Isolated total RNA samples were processed as recommended by the manufacturer (Affymetrix GeneChip Expression Analysis Technical Manual, Affymetrix Inc.). Approximately 30–40 plants were harvested and pooled together for total RNA extraction (RNeasy Mini-Prep; Qiagen, Valencia, CA, USA). Eluted total RNAs were quantified with a portion of the recovered total RNA adjusted to a final concentration of $1.25 \mu\text{g } \mu\text{l}^{-1}$.

RNA quality control, cRNA production and hybridization were performed at U.C. Irvine's Microarray Core Facility using the following protocol: All starting total RNA samples were quality assessed prior to beginning target preparation/processing steps by running out a small amount of each sample (typically 25–250 ng well $^{-1}$) onto a RNA Lab-On-A-Chip (Caliper Technologies Corp., Mountain View, CA, USA) that was evaluated on an Agilent Bioanalyzer 2100 (Agilent Technologies, Palo Alto, CA, USA). Single-stranded and then double-stranded cDNA was synthesized from the poly(A)+ mRNA present in the isolated total RNA (typically 10 μg total RNA starting material for each sample reaction) using the SuperScript double-stranded cDNA synthesis kit (Invitrogen, Carlsbad, CA, USA) and poly(T) nucleotide primers that contained a sequence recognized by T7 RNA polymerase. A portion of the resulting double-stranded cDNA was used as a template to generate biotin-tagged cRNA from the Affymetrix GeneChip IVT labeling kit, and 15 μg of the resulting biotin-tagged cRNA was fragmented to an average strand length of 100 bases (range 35–200 bases) following prescribed protocols (Affymetrix GeneChip Expression Analysis Technical Manual). Subsequently, 10 μg of this fragmented target cRNA was hybridized at 45°C with rotation for 16 h (Affymetrix GeneChip Hybridization Oven 640) to probe sets present on an Affymetrix ATH1 array. The GeneChip arrays were washed and then stained with SAPE (streptavidin–phycoerythrin) on an Affymetrix Fluidics Station 450, followed by scanning on a GeneChip Scanner 3000. The results were quantified and analyzed using GCOS 1.2 software (Affymetrix Inc.) with default values (scaling, target signal intensity = 500; normalization, all probe sets; parameters, all set at default values).

DIFFERENTIAL EXPRESSION ANALYSIS OF MICROARRAY DATA

Normalization of microarray data was performed using the R (Team, 2012) package RMA (Irizarry et al., 2003) for

ATH1 arrays (including those from our own experiments) and the package BufferedMatrixMethods (Benjamin Milo Bolstad. BufferedMatrix: A matrix data storage object held in temporary files. R package version 1.22.0. <<http://www.bmbolstad.com>>) for 1.0R tiling arrays (none of which were from our own experiments). Any 1.0F arrays were excluded from analysis. Sets of differentially expressed transcripts were determined using the R package Limma (Smyth, 2005), applying a significance threshold of adjusted *p*-value < 0.05 [*p*-values of differential expression were adjusted using the Benjamini–Hochberg multiple testing method, which should control the expected false discovery rate (Benjamini and Hochberg, 1995)].

ELIMINATION OF TRANSCRIPTS RESPONSIVE TO CIRCADIAN AND DEVELOPMENTAL EFFECTS

Irradiated wild-type seedlings were collected at 1.5, 3, 6, 12, and 24 h after irradiation. Irradiated *atm-1* seedlings were collected at 1.5, 6, 12, and 24 h after irradiation. Unirradiated controls were collected only at 1.5 and 24 h. For this reason, in the majority of our figures, fold-induction by IR is illustrated, effects discussed, and conclusions drawn solely based on the data from the 1.5 to 24 h time points. In addition, transcripts with fold induction (or suppression) of 2-fold or less are not considered in this manuscript, though the interested reader can access that data online (XXXcite source site). In some Supplementary Figures (Figures S2, S4, S5, S6), the intermediary time points are included in order to allow the reader to roughly determine the duration and peak of the effects. In order to avoid possible confounding effects of circadian influences on these intermediary data sets, transcripts known to be subject to strong circadian regulation [2-fold or more (Covington and Harmer, 2007), 586 transcripts] have been deleted from consideration throughout this paper, as have transcripts that differ 2-fold or more between the unirradiated 1.5 and 24 h controls (685 transcripts). These two deleted gene sets share 85 transcripts. These gene sets are listed in Table S1, and, again, the reader can access the unredacted data set online.

As an additional check for possible diurnal effects stemming from the absence of a control for each intermediary time point, we extended the expression profiles in selected figures to include the circadian time series expression profiles on which our circadian filtering method was based (Covington and Harmer, 2007) as well as time series expression profiles for the diurnal regulation of 7-to-9-day-old Landsberg erecta seedlings under a light/dark cycle (16 h day, 8 h night) that matched our own growth conditions (Michael et al., 2008). Circadian and diurnal profiles were scaled- separately, and for each transcript- so that the minimum (or maximum, depending on the figure) fold change would be zero.

HIERARCHICAL CLUSTERING AND VISUALIZATION OF EXPRESSION PROFILES (DENDROGRAMS)

Hierarchical clustering of transcripts with a fold change > 2 and an adjusted *p*-value < 0.05 in at least one of the 1.5 or 24-h timepoints/treatments was performed with the use of the program Cluster 3.0. Average-linkage clustering of genes was calculated with a correlation cutoff of 0.8 and an exponent of 1.0. The resulting clusters were visualized with the use of the

program TreeView as previously described (Eisen et al., 1998). Cluster 3.0 and Treeview software is available at <http://rana.lbl.gov/EisenSoftware.htm>.

SEMI-QUANTITATIVE PCR

To determine the dose response for key DSB repair transcripts *BRCA1* and *RAD51*, semiquantitative RT-PCR was performed on cDNA isolated from 5 day old seedlings 1.5 h after completion 100 Gy gamma radiation at a dose rate of 1.8 Gy/min. The seedlings were frozen in liquid N₂ and RNA was immediately isolated with Trizol reagent (Invitrogen). Two micrograms of the total RNA was reverse transcribed with Superscript III (Invitrogen) according to the manufacturer's protocol. Semiquantitative PCR was conducted with the Bio-Rad C1000 thermocycler using 22 cycles. The primers used for *BRCA1* and *Rad51* are:

BRCA1F2 (GGATGGGAAGAGAACTCAAGTGC),
BRCA1rtR2 (GTTGCTCGTCTTCCTTCGATGG),
Rad51AF1 (GGTGTTGCTTACTCCGAGGAAGG), and
Rad51ArtR1 (CAGCCACACCAAACCATCTGCTAAC).
Elf4A was used as a loading control with primers
elf4A-1 (CTCTCGCAATCTCGCTCTCTCTT) and
elf4A-5 (TCATAGATCTGGCTTGAAAC).

EXTERNAL SOURCES OF MICROARRAY DATA

Our expression data on HZE and Gamma radiation was compared against existing microarray experiments for the treatment of Arabidopsis with a variety of individual abiotic or biotic stresses. We included data on Cold, Heat, Drought, Salt, Osmotic, Genotoxic (Bleomycin, a DSB-inducing agent, plus Mitomycin C, a crosslinking agent), UV-B, and Wounding, from the AtGenExpress abiotic stress data set (Kilian et al., 2007). In addition, we compared against data for stress treatments with Paraquat (De Coninck et al., 2013), *Pseudomonas syringae* (with and without the effector AvrRpt2) (Zheng et al., 2012), Hydroxyurea (Cools et al., 2011), and Extended Night (the extension of the length of night- via a delayed dawn, rather than an early sunset) (Usadel et al., 2008).

GENE ONTOLOGY ENRICHMENT ANALYSIS

Gene Ontology (Ashburner et al., 2000) enrichment analysis was performed using DAVID (Huang da et al., 2009a,b).

HEAT-MAPS DISPLAYING OVERLAPS BETWEEN SETS OF "TOP 100" INDUCED TRANSCRIPTS

Top 100 gene sets were computed by ranking the set of all significantly up-regulated (or down-regulated) transcripts by fold change. Significance was determined by an adjusted *p*-value cut-off of 0.05. In addition, transcripts that did not have at least one dedicated ATH1 probe set, that is, a probe set that is uniquely associated with that transcript, were excluded from consideration. For Paraquat, the one stress whose transcriptional response was measured using a tiling 1.0R array, we also excluded transcripts that were not represented in the tiling 1.0R microarray. Since a small percentage of transcripts that have a dedicated ATH1 probe set are not present in the tiling 1.0R array, there is

a slight amount of additional bias in computing "top 100" overlaps between the other stresses and Paraquat (relative to the "top 100" overlaps among the other stresses themselves). If the filtering process described above resulted in less than 100 transcripts for a given experimental condition, then that experimental condition was not included in the heat-map in question.

RESULTS

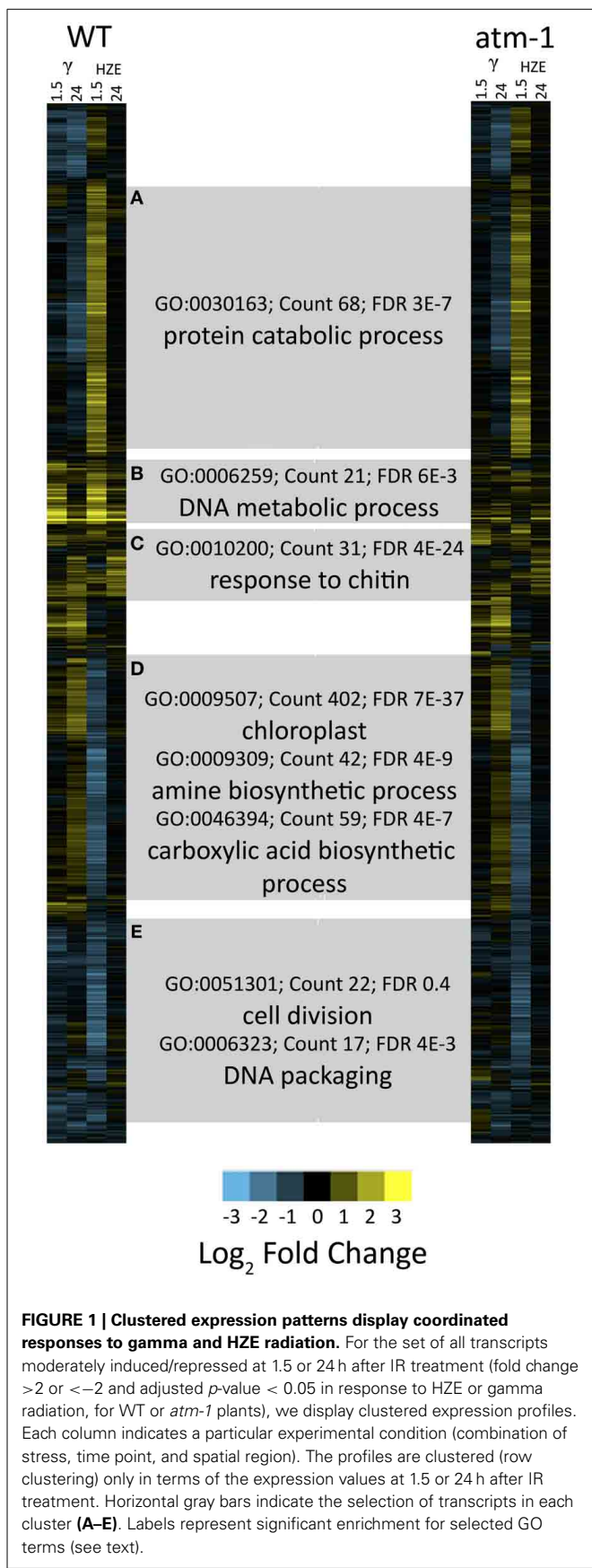
RESULTS SECTION 1: OVERVIEW

In order to compare the effects of gamma radiation to those of HZE, we exposed wild-type (ecotype Ws) 5-day-old seedlings to doses of these agents that were nearly biologically equivalent in their short-term effects on root growth. These doses (100 Gy gamma radiation, 30 Gy 1GeV/nucleon Fe²⁶⁺) were sufficient to induce a transient arrest of root growth, and had some long-term effects on development, fertility, or genetic stability (see accompanying paper). For those familiar with the effects of IR, these doses may appear to be extremely large, and Arabidopsis, therefore, would appear to be extremely radio-resistant. However, the Arabidopsis genome is small (135 Mb) in comparison with the human genome (3.2 Gb). Thus, a 100 Gy gamma radiation dose in Arabidopsis would generate the same number of DSBs as a 4 Gy dose in humans (where the LD₅₀ is 5 Gy) (Mole, 1984).

ATM is a protein kinase required in eukaryotes for recognition and signaling of DSBs (Shiloh and Ziv, 2013). Earlier work with gamma radiation has established that ATM regulates many, but not all, aspects of gamma radiation response in Arabidopsis (Garcia et al., 2003; Friesner et al., 2005; Vespa et al., 2005, 2007; Culligan et al., 2006; Jazayeri et al., 2006; Fulcher and Sablowski, 2009; Yoshiyama et al., 2009; Adachi et al., 2011; Amiard et al., 2011). In order to specifically identify HZE-induced responses that are regulated by ATM, we also performed this analysis in the T-DNA insertion mutant *atm-1*. For the mutant, time points were taken at 1.5, 6, 12, and 24 h after irradiation. Unirradiated controls for both of these genotypes were collected at 1.5 and 24 h after irradiation.

"Fold induction or repression," as described in this paper, refers to relative levels of transcripts of the 1.5, 3, 6, and 12 h irradiated vs. the unirradiated control (collected at the 1.5 h time point). The 24 h point was compared to unirradiated controls collected at 24 h after irradiation. Because of our lack of controls for circadian variation in gene expression for some intermediary time points, we filtered out genes known to be subject to circadian regulation (a set of approximately 600 genes that were classified as circadian-regulated and varied in expression by 2-fold or more 24–68 h after the transfer of seedlings into continuous light) (Covington and Harmer, 2007). Similarly, we also filtered out a set of approximately 600 transcripts that were found to be significantly differentially expressed (by 2-fold or more) between our 1.5 and 24 h control. A complete list of these excluded transcripts is presented in Table S1. In order to further limit the effects of diurnal regulation, we restricted the majority of our figures to include data from only the 1.5 to 24-h time points after IR treatment. More details are provided in the Materials and Methods.

The dendrogram in Figure 1 represents all transcripts induced or repressed with 2-fold change and an adjusted *p*-value < 0.05 in



either IR treatment at either the 1.5 or 24-h time points. We clustered these transcripts, via *xcluster*, by their expression values at both time points after irradiation, in WT and *atm-1* plants, and then we visualized their expression profiles across the same set of time points. We also provide a Supplementary Figure (Figure S6) that extends the expression profiles in **Figure 1** to include the middle time points (3, 6, and 12 h after IR treatment). Here we present an overview of the major regulatory clusters in **Figure 1**, their induction by specific agents, and their regulation by ATM. These observations will be discussed in more detail in Results sections Responses Shared by HZE and Gamma Radiation and Comparison of the Transcriptional Response to HZE with that Induced by Other Stressors.

Cluster D represents 1336 transcripts *repressed* by HZE (but not by gamma radiation) in an ATM-independent manner. Among these transcripts, the GO category “Chloroplast” (GO:0009507~chloroplast) is highly overrepresented (FDR 7e-37, 411 genes). This same cluster is also significantly repressed for transcripts involved in both amine and carboxylic acid “biosynthetic processes” (GO:0009309~amine biosynthetic process, FDR 4e-9, 42 genes; GO:0046394~carboxylic acid biosynthetic process, FDR 4e-7, 59 genes). The uniquely HZE-induced Cluster A representing 1357 transcripts is overrepresented in “protein catabolic process” (FDR 3e-7, 68 genes). This cluster of induced transcripts follows the same time course as cluster D (see also Figure S6), and like D, is ATM-independent. This suggests that the two clusters (including suppression of amino acid biosynthesis, suppression of protein synthesis, and the induction of degradation of protein) may represent a coordinated response to a single stimulus. In section Results, we revisit this HZE-specific association with protein catabolism.

Cluster C (349 transcripts) of later-induced, largely ATM-dependent transcripts has its peak expression around 6 h for HZE (Figure S6), while its expression is apparent only at 24 h after gamma radiation. This cluster is overrepresented in “response to chitin” (GO:0010200~response to chitin, FDR 4e-24, 31 genes), and the “defense response” (GO:0006952~defense response, FDR 2e-9, 50 genes) both of which overlap strongly with “programmed cell death” (GO:0012501~programmed cell death, FDR 0.07, 14 genes).

Cluster B consists of 424 rapidly induced ATM-dependent transcripts that peak at 1.5 h (the first data point taken) for both types of radiation. These are overrepresented for “DNA metabolic process” (GO:0006259~DNA metabolic process, FDR 6e-3, 21 genes). This cluster contains the most highly induced set of transcripts.

Cluster E (1248 transcripts) includes the suppression of cell-cycle progression-related transcripts (GO:0051301~cell division, FDR 0.4, 22 genes; GO:0006323~DNA packaging, FDR 4e-3, 17 genes). The suppression of these transcripts occurs in response to Gamma radiation and (to a greater degree) in response to HZE. This suppression appears to be ATM-dependent in response to gamma radiation but less so in response to HZE. This cluster is discussed in greater depth in section Effects on Cell Cycle Progression. Previously published work with Gamma-irradiated mutants indicates that cell cycle arrest

may be induced either by ATM or by ATR (Culligan et al., 2006).

Gamma radiation, HZE, and Bleomycin/MMC (“Genotoxic stress” induce an ATM-dependent DSB response that is not observed in plants treated with conventional stressors

IR, at these doses, is a stress not found in the natural environment, and it is unlikely that plants have evolved a response to IR *per se*. The transcriptional responses observed here and elsewhere (Culligan et al., 2006; De Schutter et al., 2007; Ricaud et al., 2007) must represent a response to a class of damage (i.e., DSBs, or oxidized cellular components) that is also generated by a more “conventional” stressor (biotic or abiotic), or via an endogenous genomic stress (such as the induction of breaks in meiosis, or transposable element activity). For this reason we compared the transcripts induced by both forms of IR with previously published data describing the transcripts induced by a variety of other abiotic stresses, plus one biotic stress (infection by *Pseudomonas syringae*). Our results are presented in **Figure 6**. This heatmap visualizes (via treeview) the clustered (via xcluster) expression profiles of the set of all transcripts induced 1.5 or 24 h after IR treatment (with \log_2 fold change >2 and adjusted *p*-value <0.05 in Gamma radiation or HZE, and in WT or *atm-1* plants) across a variety of environmental challenges (Kilian et al., 2007; Usadel et al., 2008; Cools et al., 2011; Zheng et al., 2012; De Coninck et al., 2013) (**Figure 6**, additional information about each of the experimental conditions is presented in Table S3). While there is very little overlap between the effects of IR and that of most conventional stresses, Gamma radiation and HZE share a strong ATM-dependent overlap with “Genotoxic Stress” (simultaneous treatment with both the DSB-inducing agent Bleomycin and the crosslinking agent MMC). ATM is a key component of the response to repair double-stranded breaks (Culligan et al., 2006;

Ricaud et al., 2007), and so the observed ATM-dependent overlap of the transcriptional responses to these three DSB-inducing agents probably reflects a response to DSBs *per se*, rather than collateral damage specific to each agent. This figure also reveals some induction—perhaps simply to a lesser degree, of the DSB response by the DNA damaging agents UV-B and hydroxyurea. However, **Figure 6** does not reveal a conventional stress (i.e., drought, cold, infection) that provokes this “DSB response.”

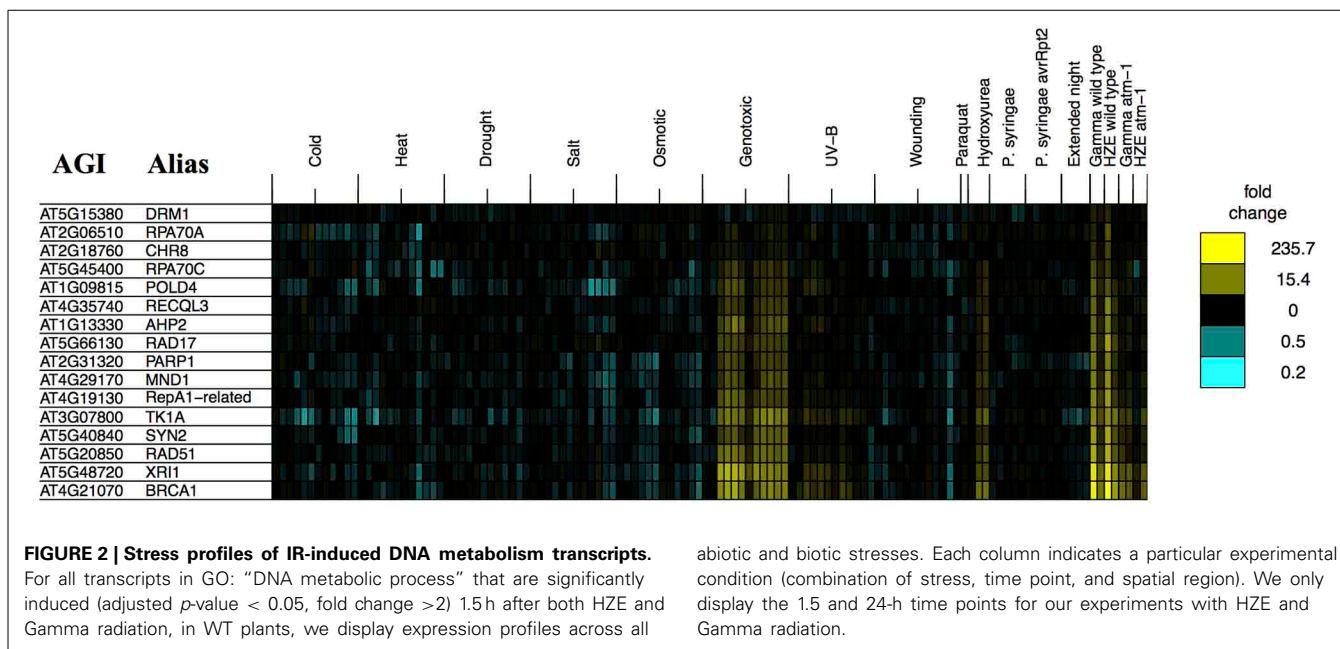
The analysis described above (**Figure 6**) provides a general overview that makes it easy to visualize major similarities between general responses to IR and various other stresses. In order to determine whether *any* of our queried stresses induce specific transcripts known to be involved in DSB repair, we took the set of transcripts from the “DNA Metabolic Process” GO category that were induced in the early response to both forms of IR (**Table 1**) and searched for their induction by other stresses (**Figure 2**). We found that these specific, largely HR-related transcripts were induced by UV-B and hydroxyurea (an inhibitor of dNTP synthesis). Both of these agents are known to induce replication blocks. Replication blocks can be repaired via homologous recombination and can lead to the formation of one-ended DSBs, which also must be repaired by HR. For this reason it is not surprising to find that these agents induce HR-related transcripts.

However, it is interesting to see that none of the other biotic or abiotic stresses investigated here invokes the DSB response. We might further speculate, based on this, that these stresses do not induce significant levels of DSBs or replication blocks, in spite of the fact that many stresses induce the production of ROS in plants (Suzuki et al., 2012; Choudhury et al., 2013). Strikingly, Paraquat treatment itself, a very potent source of ROS, did not induce the DSB response. Given that there clearly is a programmed DSB response in Arabidopsis, the “DSB response” may reflect an evolutionary adaption to some other DSB-inducing event-

Table 1 | Gamma radiation and HZE share an overrepresentation of DNA metabolic transcripts at 1.5 h after IR.

agi	GW	HW	GA	HA	Description
At4g21070	7.4	7.9	3.3	0.6	BRCA1 ubiquitination, transcription, cell cycle
At5g48720	7.0	7.1	2.5	1.0	XRI1 x-ray induced 1 interacts with MND1
At5g20850	5.3	5.4	1.6	0.3	RAD51 homology search/base pairing during HR
At5g40840	4.8	5.3	1.2	0.2	SYN2: sister chromatid cohesion 1 homolog 2
At3g07800	4.3	4.3	1.8	-0.2	TK1A Thymidine kinase 1A
At4g19130	4.2	4.8	0.8	-0.1	RPA1E replication factor-A protein 1-related (Akliilu et al., 2014)
At4g29170	3.9	4.4	0.4	-0.1	Mnd1: interacts with AHP2 in synapse formation
At2g31320	3.6	3.9	0.4	0.0	PARP1 poly(ADP-ribose) polymerase 1
At5g66130	3.6	5.0	0.5	0.2	RAD17
At1g13330	3.2	4.0	0.4	-0.1	AHP2 Hop2 homolog
At4g35740	3.1	4.1	0.2	0.6	RecQL3 helicase
At1g09815	3.0	2.6	0.4	-0.2	POLD4 polymerase delta 4
At5g45400	2.3	1.8	0.3	-0.6	RPA70C/RPA1C replication factor-A protein 1-related
At2g18760	1.4	2.1	0.2	0.3	CHR8 chromatin remodeling 8
At2g06510	1.2	2.6	0.1	0.4	RPA70A/RPA1A replication protein A
At5g15380	1.1	1.2	0.1	0.2	DRM1 domains rearranged methylase 1

Significantly induced (fold change >2 , adjusted p-value <0.05) transcripts by gamma radiation and HZE at 1.5 h after IR in GO: DNA Metabolic Process. Fold Enrichment is shown under each treatment. G = gamma radiation, H = HZE, W = WT, A = atm-1. Log₂ fold induction is shown.



perhaps the induction of DSBs by naturally occurring external chemical agents not tested here. Induction of both DSBs and HR-related transcripts has also been observed during the very early stages of seed imbibition (Waterworth et al., 2010), and may reflect the accumulation of these lesions during desiccation and rehydration. Alternatively, DSBs might be induced endogenously, without environmental influences- through the activation of transposable element activity, or the programmed induction of DSBs that occurs during meiosis. However, our results indicate that DSBs, or at least the DSB response, are not induced by the conventional stresses tested here.

We did observe some overlap between IR (but not “genotoxic stress”) and certain abiotic stresses- these are described further in section Comparison of the Transcriptional response to HZE with that Induced by Other Stressors.

RESPONSES SHARED BY HZE AND GAMMA RADIATION

The shared response at 1.5 h is overrepresented for transcripts related to DNA metabolism

HZE and gamma radiation induce both singly damaged sites and clustered lesions in DNA, which lead to DSBs. However, our two treatments differ in both the severity of the clustering in DNA and the quantity of the remaining non-clustered damage. A comparison of the transcriptomic effects of the two treatments can help us identify which genes are candidates for the repair of lesions induced by both agents. Thus, we compared the specific set of transcripts induced by HZE at 1.5 h after treatment (adjusted *p*-value < 0.05, at least 2-fold induction) to that induced by gamma radiation, in wild type plants (Figure 3A). We found that of a total of 280 gamma radiation-induced and 1169 HZE-induced transcripts, only 160 transcripts were shared. This is surprisingly small degree of overlap, and suggests that plants irradiated with the two different agents receive significantly different spectra of damage.

Of the 160 shared transcripts, 16 fall into the “DNA Metabolism” GO category (GO:0006259~DNA metabolic process). This is the most overrepresented category among the shared transcripts at this time point (Figure 3B). The majority of these induced DNA Metabolism genes play a role in the repair of DSBs via homologous recombination (Table 1). Other transcripts that we might expect to be induced by IR, such as components required for nonhomologous end-joining, for nucleotide excision repair, or for the base excision repair of oxidized bases, were not found among the shared transcripts, but were observed to be induced (at significant but rather low amplitude) in the HZE-treated plants (Table 2, see section Effects on Cell Cycle Progression for further discussion). This suggests that basal levels of expression for these genes may be sufficient for plants irradiated at this dose of gamma, while the same is not true for HZE.

Human homologs of transcripts induced by both forms of IR

Transcriptional induction provides clues to the recruitment of proteins required for a given cellular process. While many different metabolic processes may be induced in response to HZE and gamma radiation, a DSB repair is clearly a shared response (Table 1). Taking advantage of the high conservation of DNA repair proteins among eukaryotes, this dataset may allow us to identify novel DSB response proteins in both Arabidopsis and mammals. Using BLAST, we found that 72 of the 160 shared transcripts induced by both forms of radiation shared homology with human proteins (*e*-value < 1e-6) (Table S2). Many of these transcripts are known to be involved in DSB repair, DNA replication, DNA methylation, and cell cycle control in humans and Arabidopsis (highlighted). AT5g49110, annotated as an unknown protein in Arabidopsis, was found to be homologous to a human protein annotated as “PREDICTED: Fanconi anemia group I protein.” Fanconi anemia is a genetic disorder

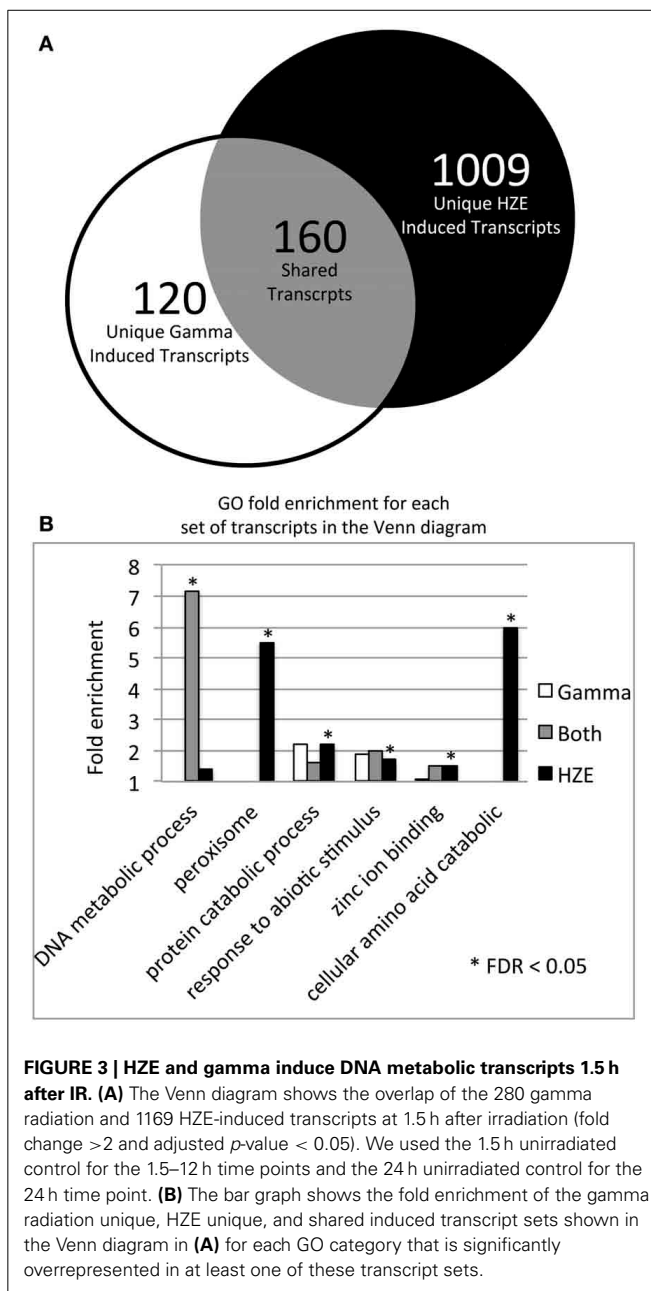


FIGURE 3 | HZE and gamma induce DNA metabolic transcripts 1.5 h after IR. (A) The Venn diagram shows the overlap of the 280 gamma radiation and 1169 HZE-induced transcripts at 1.5 h after irradiation (fold change >2 and adjusted p -value <0.05). We used the 1.5 h unirradiated control for the 1.5–12 h time points and the 24 h unirradiated control for the 24 h time point. **(B)** The bar graph shows the fold enrichment of the gamma radiation unique, HZE unique, and shared induced transcript sets shown in the Venn diagram in **(A)** for each GO category that is significantly overrepresented in at least one of these transcript sets.

linked to defects in DNA repair—particularly the repair of inter-strand crosslinks (Kim and D’Andrea, 2012). Our results provide additional support for the prediction that this protein is involved in the DSB response.

HZE-treated plants exhibit a greater dependence on ATM for the induction of DSB-repair-related transcripts

At the doses used here (100 Gy gamma radiation and 30 Gy HZE, which have equivalent effects on root growth) the level of expression of DSB-repair-related transcripts at 1.5 h is of a similar order of magnitude (Table 1, Figure 4A). The fact that HZE treatment deposits less energy but triggers similar levels of induction of these genes may reflect a difference in either the efficiency per Gray of

induction (or the time required for repair) of DSBs induced by this agent. In order to determine whether transcript induction increases with the level of damage incurred, we measured the effect of an increasing dose of gamma radiation on the fold-induction of the repair genes *BRCA1* and *RAD51*. We found that the transcriptional response of these two genes does indeed scale up with IR dose (Figure S1). Thus, the level of expression of these characteristic HR genes might be used as a proxy for not only the presence but also the frequency of DSBs.

DSB repair-related transcripts are induced rapidly by both agents (Figure 4A) and this induction is more heavily dependent on ATM in the early time-points (Figures 4B–D). The ATM dependence of the early response suggests recognition and signaling of DSBs. In contrast, the continued expression of these transcripts at 24 h (Figure 2) appears to be completely ATM-independent (Figures 4C,D). Although both gamma and HZE induce DSB repair transcripts to a similar degree (Figure 4A) this induction is far more ATM-dependent in HZE-irradiated cells (Figures 4C,D). This suggests that ATR may play a more important role in activation of DSB repair in gamma-irradiated plants than it does in HZE-irradiated plants. It is possible that gamma radiation triggers more replication stress than HZE, thus activating an ATR-dependent (rather than ATM-dependent) DNA repair pathway. We discuss this possibility below.

Effects on cell cycle progression

Cyclin transcripts are similarly suppressed by both gamma radiation and HZE at 1.5 h after irradiation. This presumably reflects an the suppression of cell cycle progression. This effect is largely, but not entirely, alleviated by 24 h post-IR (Figure S4). *CycB1;1*, an exceptional cyclin known to be highly induced by gamma radiation (Culligan et al., 2006) is also induced by HZE (Figure S4).

In order to determine whether cells were accumulating in a particular phase of the cell cycle, we looked at expression levels of transcripts associated with S or M phase (identified in sucrose-starved synchronized *Arabidopsis* cells) (Menges et al., 2005) (Figures 5B,C). As we see in Figure S5, both gamma radiation and HZE-treated seedlings exhibit suppression of transcripts associated with both M or S phase, indicating that neither phase of the cell cycle is progressing normally. By 24 h, HZE-treated seedlings are slightly repressing some transcripts associated with S or M phase, but nearly back to unperturbed levels of expression. In contrast, at 24 h gamma-irradiated seedlings have begun to hyperexpress many S phase associated transcripts (in a partially-ATM-dependent manner) (Figure 5B), suggesting that, at 24 h, cells of gamma irradiated plants may be overrepresented for S phase. It is possible that this reflects the accumulation of cells, at earlier time points, at an S- or intra-S checkpoint.

The notion that gamma-irradiated seedlings are undergoing replication stress is also consistent with our observation of the stronger induction of *Wee1* in gamma-irradiated plants vs. HZE-irradiated plants, at 1.5 h (Figure 5A). *WEE1* is protein kinase involved in adaptation to replication stress in plants (Cools et al., 2011) which is induced during S phase in the HU-stressed cell,

Table 2 | "DNA metabolic response" transcripts induced by HZE, but not Gamma irradiation at 1.5 h after IR.

agi	Description	GW 1.5	HW 1.5	GA 1.5	HA 1.5
At1g80850	3-mA glycosylase-like, BER	2.0	3.2	0.9	0.35
At5g16630	XPC, damage recognition for NER	1.1	2.5	0.81	2.3
At1g02670	P-loop helicase	1.2	4.9	0.87	1.5
At2g13840	DNA polymerase-like	0.87	2.3	0.93	2.1
At1g30480	DRT111, HR	1.74	2.5	1.1	1.5
At1g49980	Y-family polymerase, dinB like	1.4	2.6	1	1.2
At3g02540	RAD23-3, ubiquitination	1.1	3.5	1	2.8
At4g36050	Endo/exonuclease family	1	2.6	0.87	3.2
At2g30350	uvrC-like, organellar NER?	0.87	3.2	0.7	3.0
At5g14620	DMT7/DRM2 DNA methyltransferase	1	2.6	0.7	1.5
At5g57160	LIG4, NHEJ	1.9	2.3	0.87	1.3
At1g80420	XRCC1, BER, DNA demethylation	0.57	4	0.81	3.7
At4g31150	Endonuclease V family	0.93	2.3	0.87	1.9
At3g12710	3-mA glycosylase-like, BER	1.1	2.1	0.66	1.5
At5g58720	SMR (Small MutS Related)	0.93	2.8	1	2.3

The 15 transcripts are observed among the 1009 transcripts that are significantly induced (fold change >2, adjusted p-value < 0.05) at 1.5 h after treatment by HZE (HW1.5) but not Gamma radiation (GW1.5). Log₂ fold induction or repression is shown. G = gamma radiation, H = HZE, W = WT, A = atm-1.

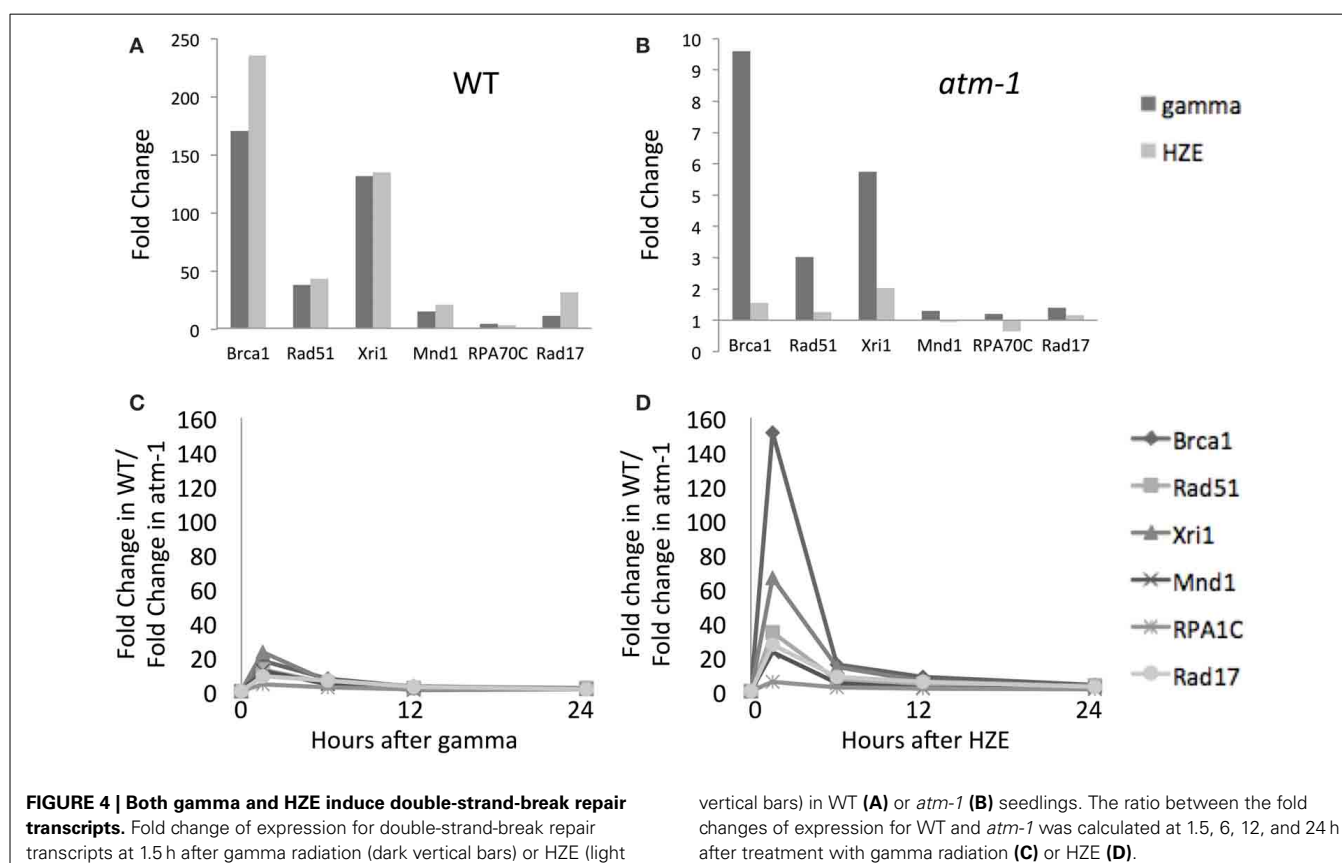


FIGURE 4 | Both gamma and HZE induce double-strand-break repair transcripts. Fold change of expression for double-strand-break repair transcripts at 1.5 h after gamma radiation (dark vertical bars) or HZE (light vertical bars) in WT (A) or *atm-1* (B) seedlings. The ratio between the fold changes of expression for WT and *atm-1* was calculated at 1.5, 6, 12, and 24 h after treatment with gamma radiation (C) or HZE (D).

allowing it to proceed through S phase without an extended delay, and preventing the premature cellular differentiation that is observed in permanently arrested meristematic cells. The effects observed on cell-cycle related transcripts are muted, but not entirely absent in the *atm-1* mutant.

The difference in expression of the above markers is consistent with the hypothesis that gamma radiation is inducing a replication stress not incurred by HZE-treated cells. It should be noted that approximately 50% of the energy deposited by a 1 GeV/n Fe ion is thought to be deposited with the 9 nm

“core” of the particle’s path—the remaining 50% of its energy would produce a “penumbra” of high-energy electrons similar to those produced by gamma radiation (Magee and Chatterjee, 1980). Given that we have applied 30 Gy of HZE vs. 100 Gy of gamma radiation, we would expect that relatively little (15 Gy vs. 100 Gy) of the Fe ion’s energy is deposited in the “dispersed clusters” characteristic of gamma radiation rather than along the path of the particle. In short, the amount of HZE-induced damage to DNA not within the core radius of the particle would be expected to be only 15% that induced by gamma radiation. Thus, gamma radiation, at 100 Gy, may be generating more replication blocks than HZE at 30 Gy. While DNA in the path of the HZE particle’s core radius is extensively damaged, and this damage is difficult to repair, a replication block is still a replication block regardless of the multiplicity of lesions at a particular site.

A set of HZE-specific induced transcripts involved in DNA metabolism

While a large number of genes in the “DNA metabolic process” GO category are induced in response to both HZE and gamma radiation at the 1.5-h time point (**Table 1**), an additional 16 genes in this category are induced in response to HZE but not Gamma radiation at the same time point (**Table 2**). These transcripts are known (LIG4) or predicted to participate in a variety of DNA-related processes (BER, NER, NHEJ, DNA methylation) and vary in their dependence on ATM. Also at 1.5 h, we observe a large number of transcripts induced by HZE but not Gamma; these are ATM-independent. We will discuss this general response in the next section.

COMPARISON OF THE TRANSCRIPTIONAL RESPONSE TO HZE WITH THAT INDUCED BY OTHER STRESSORS

Visualization of transcriptomic overlaps between ionizing radiation and other abiotic and biotic stresses

GO category overrepresentation is a useful way to sift through transcriptomics data in the hope of identifying the metabolic nature of the response to a given stress. While we made use of GO enrichment throughout our own analysis, we acknowledge that it has its limitations. Significant enrichment of a GO category is not a guarantee of the activation of a particular biological process, nor will it reveal the reason for which that process is activated. A complementary approach to understanding the biological processes activated by a given stress is to consider the overlap between the transcriptional response under scrutiny and published responses to other stresses. If there is significant overlap between the transcripts induced by IR and those induced by a different, more thoroughly studied stress, then we can leverage our understanding of the plant’s response to the other stress in order to make inferences about IR. This approach may be particularly useful when investigating an “unnatural” stress such as high dose rate IR. We would expect the plant to lack evolved responses specific to IR and thus be limited to “sampling” the programmed responses to natural stresses, according to similarities in the inflicted damage.

With this goal in mind, we considered the extent to which the transcriptional responses to HZE and gamma radiation resemble the responses to a range of different abiotic and biotic stresses.

To test for shared transcriptional responses, we visualized (via treeview) the clustered (via xcluster) expression profiles of the set of all transcripts induced at 1.5 or 24 h after IR treatment (with \log_2 fold change >2 and adjusted p -value <0.05 in Gamma radiation or HZE, and in WT or *atm-1* plants) and compared these to a transcript sets induced by a wide variety of abiotic and biotic stresses (**Figure 6**). Specifically, we first clustered these transcripts across their IR-induced expression profiles, and then we extended the profiles to include the expression patterns across the abiotic and biotic stress conditions. The IR-induced transcripts fall roughly into several clusters, three of which are consistent with a shared programmed response between HZE and (1) DSB-inducing agents, (2) extended night, and (3) multiple conventional stresses. Figure S3 displays the corresponding clustered expression profiles for all IR-repressed transcripts, using the same cutoff parameters.

The results from **Figure 6** suggest that seedlings subjected to DSB-inducing Gamma radiation or radiomimetic chemicals- to an extent that transiently inhibits growth- induce few of the transcripts commonly expressed by seedlings subjected to other abiotic stresses. Thus, the response to these DSB-inducing agents appears to be relatively unique. However, treatment with HZE (but not gamma radiation or “genotoxic agents”) did induce some transcripts that are similarly induced by “Extended night” (Cluster 2 of **Figure 6**). The term “Extended night” refers to the plant’s response to the extension of the length of night- via a delayed dawn, rather than an early sunset (Usadel et al., 2008). This similarity between extended night and HZE response is limited to early time points (1.5 and 3 h) after HZE treatment, but includes all reported time points of extended night. This “Extended night-like response” induced by HZE is not ATM-dependent (**Figure 6**), and, again, is not observed in gamma radiation or BLM+MMC-treated plants- strongly suggesting that this response is not the result of DSB induction, but is instead due to some other lesion(s) induced specifically by HZE.

Treatment with HZE and Gamma also induced a set of transcripts (absent in “genotoxic agents”) that are similarly induced across a wide variety of conventional stresses (Cluster 3 of **Figure 6**: cold, drought, salt, osmotic, UV-B, and wounding). Here, we define “conventional” as stresses that we perceive to be more commonly occurring in nature. This similarity is limited to the late response to HZE and Gamma (24 h) but is more clearly observable in the early responses to conventional stresses (0.5–6 h). The fact that this shared response is dependent on the presence of ATM in the IR-treated plants is surprising given the fact that, in plants, ATM is known exclusively for its role in the response to DSBs. Extending the profiles of transcripts in Cluster 3 (IR + multiple conventional abiotic stresses) to include all time points for IR treatment shows strong induction at 6 and 12 h after HZE but not Gamma radiation, suggesting that this particular set of transcripts is induced earlier in response to HZE vs. gamma radiation (Figure S2). The relative strength of the IR signal vs. the circadian and diurnal time series suggest to us that any circadian or diurnal bias at the middle time points would not affect our overall conclusions. We have extended Figure S2 to include previously published circadian and diurnal time series profiles in order to aid the reader in drawing their own conclusions.

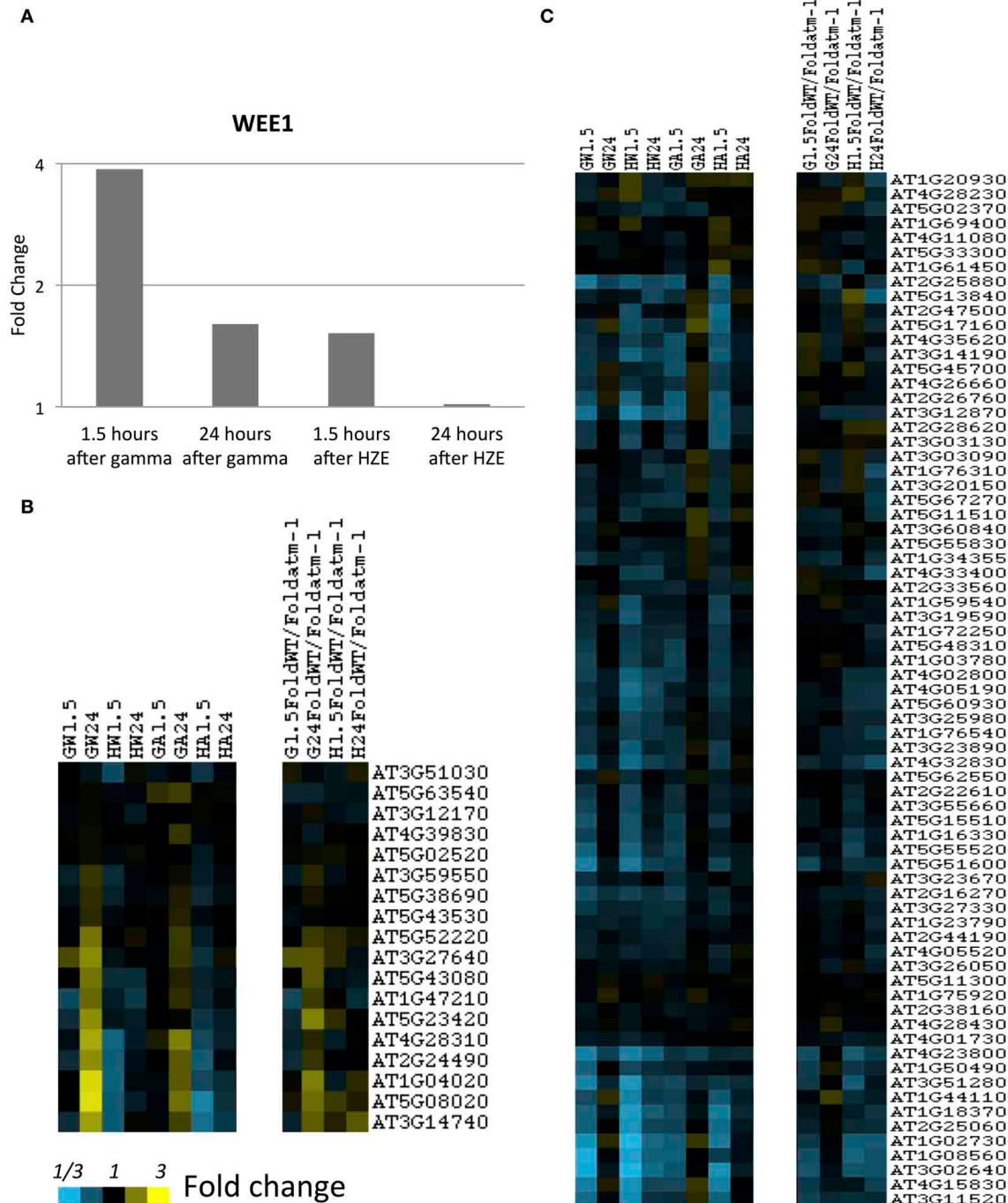


FIGURE 5 | S-and-M-phase-specific transcripts at 1.5 and 24 h after gamma or HZE. (A) Fold change of expression of Wee1 was calculated at 1.5 and 24 h after IR. Fold-change of expression was also calculated for **(B)** S-phase specific, or **(C)** M-phase specific transcripts (Menges et al., 2005) at 1.5 and 24 h after gamma radiation in WT (GW1.5 and GW24), 1.5

and 24 h after HZE in WT (HW1.5 and HW24), 1.5 and 24 h after gamma radiation in *atm-1* (GA1.5 and GA24), and 1.5 and 24 h after HZE (HA1.5 and HA24). In addition, we reported the ratio between the fold changes of expression for WT and *atm-1* at 1.5 and 24 h after treatment by HZE or gamma radiation.

The fact that transcripts with similar expression patterns in response to IR also had very similar expression patterns across the other stress conditions suggest that these sets of transcripts are coordinately regulated in response to both IR and the other stresses. We hypothesize that these sets of co-expressed transcripts

comprise distinct transcriptional programs that evolved in response to naturally occurring stresses but can also be triggered when unnatural stresses, such as HZE and gamma radiation, induce patterns of damage or signals in the plant that resemble those induced by the naturally occurring stresses. We follow

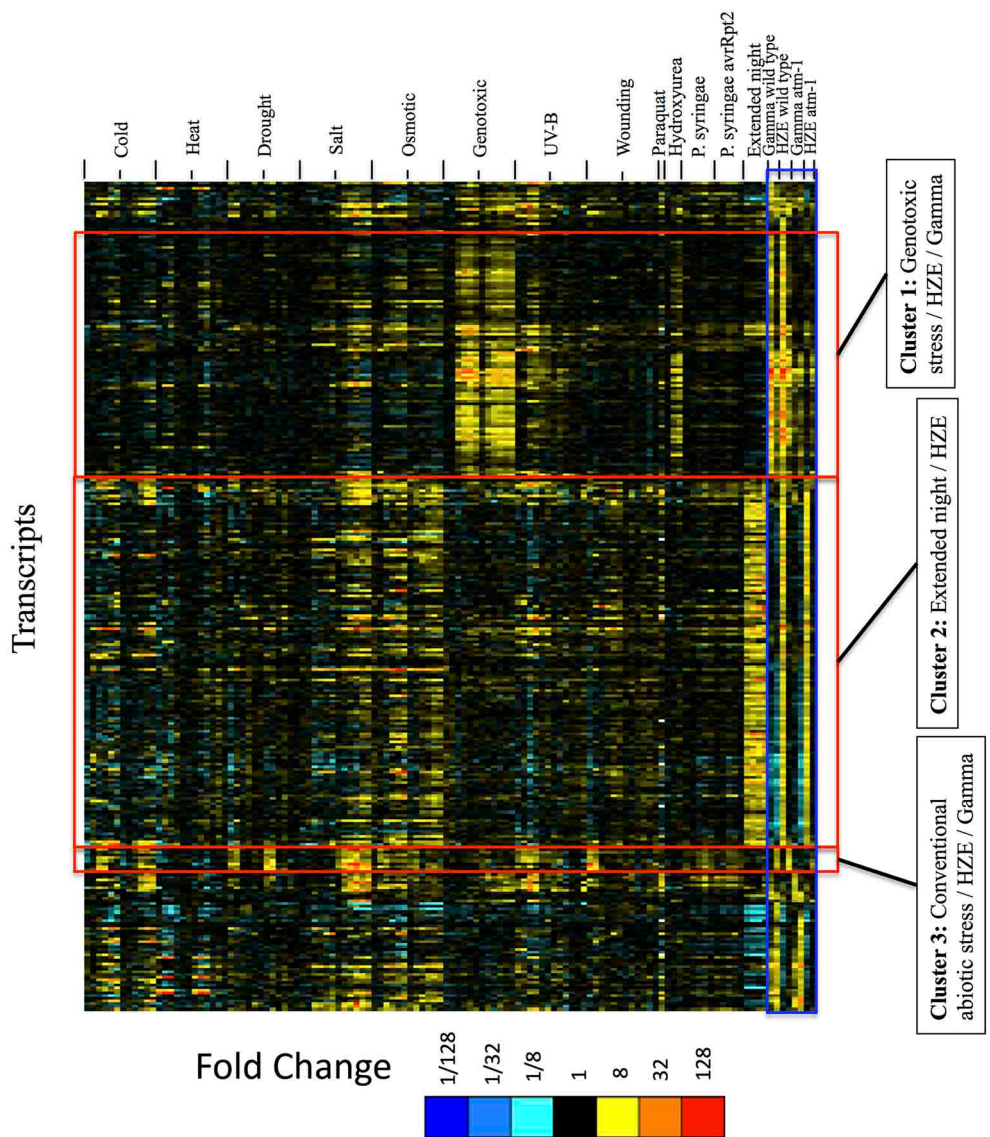


FIGURE 6 | Expression profiles of IR-induced transcripts, across abiotic and biotic stresses, clustered by the expression profiles across IR experimental conditions only. For the set of all transcripts strongly induced at 1.5 or 24 h after IR treatment (fold change >4 and adjusted *p*-value < 0.05 in response to HZE or gamma radiation, for WT or *atm-1* plants), we display

expression profiles across all abiotic and biotic stresses. These profiles are clustered (row clustering) only in terms of the expression values at 1.5 or 24 h after IR treatment. Each column indicates a particular experimental condition (combination of stress, time point, and spatial region). We only display the 1.5 and 24-h time points for our experiments with HZE and Gamma radiation.

up this hypothesis in the context of the two candidate IR-induced programmed responses shared with extended night and conventional stress in subsections Transcripts Strongly Induced in Response to Extended Night are also Induced in an Early ATM-Independent Transcriptional Response to HZE and HZE Triggers an ATM-Dependent Transcriptional Response that is also Induced by Several Conventional Abiotic Stresses.

Transcripts strongly induced in response to extended night are also induced in an early ATM-independent transcriptional response to HZE

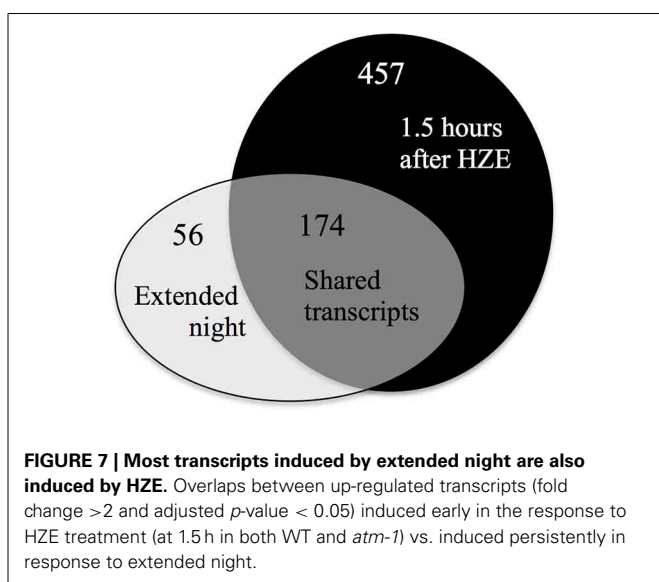
Extended night is known to trigger a variety of biological processes, many of them resulting from a shortage of energy stores in

the form of carbon. Leaf starch accumulates during the day but most of it is gone by the end of the night (Zeeman et al., 2007; Usadel et al., 2008). In an extended night, the plants respond to lack of stored energy in two ways: (a) by slowing growth and (b) by looking for alternative internal sources of energy. Extended night results in a three-fold decrease in the level of trehalose-6-phosphate (T6P) (Lunn et al., 2006), an important positive regulator of growth (Delatte et al., 2011; Schluemann et al., 2012), as well as the induction of genes associated with amino acid catabolism (Usadel et al., 2008). In addition, fatty acid beta-oxidation- a process by which lipids are broken down for energy- has been shown to be a key component of the response to extended night (Kunz et al., 2009). In this section, we present

evidence that many of the above processes are transcriptionally active in the early response to HZE treatment as well as in the response to extended night.

To characterize the full extent of the shared induction between these two stresses, we identified commonalities using a fixed criterion for induction, specifically a fold change cutoff of 2 and an adjusted *p*-value cutoff of 0.05. Under these settings, we identified a set of 457 transcripts that were induced at 1.5 h after HZE treatment of wt or *atm-1* plants. Applying the same cutoffs to published data on transcriptional response to extended night, we found 230 transcripts were induced across all four of the time points. There is an overlap of 174 induced genes between these two transcript sets (**Figure 7**). 83 of transcripts are present in the 136 genes in Cluster 2 of **Figure 6**, 158 overlap with the 1357 genes in cluster A from **Figure 1** (which was described earlier as being overrepresented for the GO category “protein catabolic process”). The fact that the majority of the transcripts persistently induced in response to extended night were also induced in the early response to HZE (**Figure 7**) suggests that HZE treatment triggers most components of the transcriptional program for response to extended night.

GO enrichment analysis of this set of 174 shared genes suggests that several of the biological processes that are associated with the response to extended night are also transcriptionally activated in the early response to HZE treatment. These processes reflect the catabolism of cellular components, including “fatty acid beta-oxidation” (GO:0006635, 25.0-fold enrichment, FDR 5.9E-2, 5 genes) together with “peroxisome” (GO:0005777, 6.3-fold enrichment, FDR 2.5E0, 6 genes), the peroxisome being a site of fatty-acid beta-oxidation in plants. We also found strong enrichment of “cellular amino acid catabolic process” (GO:0009063, 15.9-fold enrichment, FDR 3.6E-1, 5 genes). These enrichment results suggest that increased catabolism of fatty acids and amino acids is part of the early response to HZE treatment- a response not induced by other DSB-inducing agents.

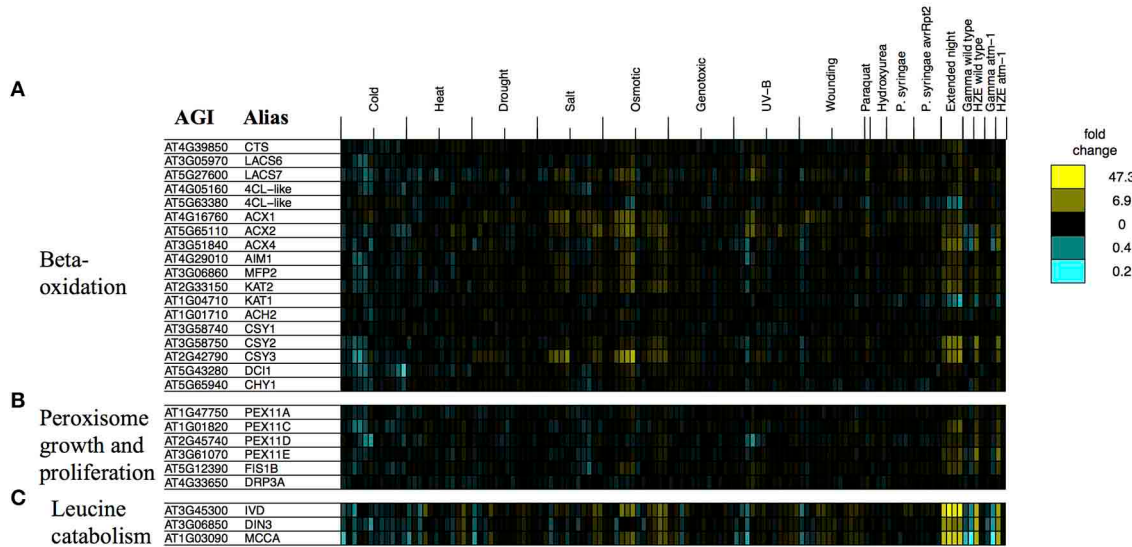


We examined the expression profiles of a number of transcripts associated with beta-oxidation that were compiled in a review study (Baker et al., 2006) (we excluded any transcripts that did not pass our circadian and developmental filtering criteria, which are described in the Materials and Methods). Consistent with the activation of fatty acid beta-oxidation, we observe strong induction of many of the beta-oxidation associated transcripts described in this study (**Figure 8A**).

Fatty-acid beta-oxidation is known to occur in the peroxisomes (including glyoxysomes), although there is a body of evidence (Masterson and Wood, 2000) suggesting that it also occurs in the mitochondria. Given the proposed increase in fatty acid beta-oxidation under extended night (and HZE) treatment, one might consider whether it would be accompanied by an increase in the number of peroxisomes. The placement of excised leaves of *Pisum sativum* in the dark for 3–11 days results in an increase in the number of peroxisomes (Pastori and Delrio, 1994), suggesting that extended night treatment might have a similar effect on *Arabidopsis*. We found that a group of transcripts associated with peroxisome growth or proliferation (Lingard et al., 2008) tended to be induced both in the early response to HZE and persistently in response to extended night. **Figure 8B** illustrates the regulation by stress of genes associated with peroxisome growth (elongation) or proliferation (fission), in one or more of three studies (Lingard and Trelease, 2006; Orth et al., 2007; Lingard et al., 2008). Overexpression of individual PEX11 homologs PEX11a and PEX11c-e has been shown to increase peroxisome elongation and/or duplication; studies disagree on whether the same is true for PEX11b (Lingard and Trelease, 2006; Orth et al., 2007). Subsequent studies suggest that PEX11c-e, FIS1b, and DRP3a all work together to coordinate fission of elongated peroxisomes (Lingard et al., 2008). Again, we found that most of these transcripts (we excluded any transcripts that did not pass our circadian and developmental filtering criteria, which are described in the Materials and Methods) were persistently induced in response to extended night and induced in the early response to HZE (**Figure 8B**), suggesting that peroxisome growth and proliferation occurs both in the response to extended night and in the early response to HZE. This proliferation may occur to facilitate beta-oxidation of fatty acids.

We also tested the expression profiles of a set of co-expressed transcripts associated with leucine degradation that were compiled by Mentzen et al. (2008) (we excluded any transcripts that did not pass our circadian and developmental filtering criteria, which are described in the Materials and Methods). For all tested transcripts, we found strong induction in the early response to HZE as well as strong, persistent induction in response to extended night (**Figure 8C**).

While the causal basis for the exceptional similarities between the transcription response to extended night and the early ATM-independent response to HZE remain obscure, we can offer two hypotheses: (a) HZE-treated cells are, for some reason, starving. Perhaps this form of radiation, at this intensity of dose, disrupts mitochondrial or chloroplast function? or (b) The extensive induction of catabolic processes for both lipids and proteins might reflect the degradation of damaged cellular components.

**FIGURE 8 | Stress profiles of transcripts associated with extended night.**

For transcripts related to key biological processes that appear to be transcriptionally activated in response to both HZE (early response) and extended night- **(A)** beta-oxidation, **(B)** peroxisome growth and proliferation,

and **(C)** leucine catabolism- we display expression profiles across all abiotic and biotic stresses. Each column indicates a particular experimental condition (combination of stress, time point, and spatial region). We only display the 1.5 and 24-h time points for our experiments with HZE and Gamma radiation.

HZE triggers an ATM-dependent transcriptional response that is also induced by several conventional abiotic stresses

As described above, **Figure 6** is a dendrogram generated by sorting by the patterns of expression of all transcripts that are induced 1.5 or 24 h after either IR treatment, in WT or *atm-1* plants. This dendrogram was then extended, without further sorting, to include similar data sets from transcriptomics studies of other more conventional stresses. Here we focus on Cluster 3 of this dendrogram- a set of 9 transcripts induced 24 h, but not 1.5 h, after treatment by HZE or gamma radiation. Although the observed induction of these transcripts is clearly ATM-dependent, in response to gamma radiation, the same is only true for half of the transcripts, in response to HZE. All of these 9 genes also belong to **Figure 1**'s Cluster C, a late-expressed, ATM-dependent cluster of 349 transcripts. Like Cluster C, these 9 genes are highly enriched for “response to chitin” (GO:0010200, 27.6-fold enrichment, FDR 4.9E1, 2 genes) and “defense response” (GO:0006952, 5.1-fold enrichment, FDR 6.2E1, 3 genes) (via the GO DAVID enrichment tool). Consistent with the high enrichment of Cluster 3 for the GO categories for “defense response” and “response to chitin,” we found that a large percentage of these 9 induced genes were induced in response to *P. syringae*, a much larger percentage than for the rest of the strongly IR-induced transcripts. However, this cluster of genes was more strongly induced by a wide variety of stresses, most noticeably cold, salt, wounding, and UV-B.

The (partial) ATM-dependence of the shared response to IR and conventional abiotic stress described above suggests that ATM might possibly play a role in triggering this suite of transcripts in response to conventional abiotic stress treatments. This would be surprising, given that ATM is only known in plants for its role in the response to DNA damage. But such a hypothesis

may be consistent with the observations in animal systems for which ATM has been shown to be activated by not only DSBs, but also stimuli such as ROS (Guo et al., 2010) and chromatin hyper-acetylation (Sun et al., 2005; Kaidi and Jackson, 2013). Another hypothesis for the ATM-dependence of this response, which might not necessarily negate the first, is that IR induces some effect on the cell that, in the absence of ATM, derails the plant’s normal course of recovery and so results in a suppression of the observed conventional stress program. Such an effect could involve IR-specific patterns of DNA damage, which ATM could counter by its role in the processing and repair of DSBs.

CONCLUSIONS

In this paper, we compare the transcriptomic response to HZE vs. those of other DSB-inducing agents, and then compare that to previously published data sets describing response to a variety of conventional stresses. Some subtle differences were observed between gamma radiation and HZE (section Responses Shared by HZE and Gamma Radiation) which can probably be ascribed to differences in the quantity or quality of DSBs generated by each agent; HZE-generated breaks are expected to be more complex and thus more difficult to repair.

More interestingly, comparison of 3 DSB-inducing treatments: gamma radiation, IR, and a combination of Bleomycin and Mitomycin C (a crosslinking agent), vs. a wide variety of conventional stresses shows that the response to these DSB-inducing agents is a unique “DSB response”- it is very robust, intense, of rather short duration (less than a day), and it is *not* induced by conventional stresses. Thus, this is not a generic response to stress, but a response to a specific lesion in DNA. It has been suggested that DSBs might be generated by conventional stresses in plants, as a wide variety of stresses are known to induce ROS. However,

we see here that treatment with Paraquat, a notorious source of ROS that shunts electrons from donors (such as NADPH or Photosystem I) directly to oxygen to produce superoxide does not induce the “DSB response.” Careful observation of the transcripts induced in the DSB response (cluster B, **Figure 1**) indicates that two other stresses- UV-B and HU, already identified as DNA damaging agents, also induce the DSB response, though at low amplitude, suggesting that these agents induce DSBs at some low frequency (**Figure 2**).

HZE and gamma radiation both displayed some overlap with a set of transcripts induced by a variety of conventional stresses, particularly at later time points (**Figures 6** and S2). These may reflect downstream effects of stress on plant cells, rather than similarities of the immediate effects of each of these stressors. It is interesting that these late-time point commonalities are partially ATM-dependent in HZE and completely ATM-dependent in Gamma (ATM-dependence has not been tested in other stresses). It is somewhat surprising that the shared stress response would be partially or completely eliminated by a defect in ATM- one would guess that a defect in DDR would enhance the stress induced by DNA damage. We should bear in mind, however, that stress response, at least in plants, should not be seen as a set of counter-productive actions resulting from a breakdown of cell function. What appear to be toxic effects of IR [for example cell death (Fulcher and Sablowski, 2009; Furukawa et al., 2010)] are actually ATM-governed orderly responses to DSB-inducing agents. It will be interesting to learn more about the regulators of these “shared stress response” transcripts.

A remarkable similarity was observed between ATM-independent transcriptional response to HZE and the response to extended night. The extended night response in plants is a response to lack of sugar- leaves store away just enough carbohydrates to make it through to dawn. It seems unlikely that HZE-treated cells are starving at 1.5 h after irradiation, but it is possible that HZE treatment has rendered the energy-producing organelles dysfunctional. The starvation response involves the cannibalization of non-carbohydrate cellular components (proteins and lipids), and we do observe up-regulation of these pathways in HZE-treated plants. It is also possible that the cells are not actually starved, but are instead recycling damaged cellular components.

Do our results inform our understanding of space radiation biology? Yes and no. The identification of a set of transcripts very specifically induced by DSB-inducing agents, and the over-representation of repair factors among this set, suggests that the remaining genes of unknown function will also be enriched for this process. Given that many of these have obvious human homologs, this data set undoubtedly includes candidates for previously undiscovered repair functions.

The relevance of the observed HZE-specific responses to space radiation biology are more obscure given the very high dose rate applied here. We ascribe these responses to collateral damage to non-DNA components of the cell, but both our dose (approximately 100× that predicted for a mission to Mars) and dose rate (received in 4 min rather than 4 years) are very high. At more realistic doses damage to membranes and proteins may be slight enough that up-regulation of enzymes that promote “recycling”

is not required. On the other hand, it is possible that a single HZE track may generate sufficient damage to provoke such a response- at our dose (30 Gy) we estimate that about 65 particles crossed the nucleus. Given the 30× larger amount of DNA in a human cell, the equivalent amount (though not concentration) of damage would be generated by only 2 or 3 HZE tracks. A recently published transcriptomics study using human fibroblasts and employing a maximum dose of 1 Gy of 1 GeV Fe nuclei (an equivalent dose to ours, if corrected for genome size) also demonstrated both a shared (with gamma radiation) response focused on what the authors describe as “BRCA1-centric repair” and a unique HZE signature. The unique signature was also overrepresented for transcripts related to “pro-inflammatory acute phase response signaling” (Ding et al., 2013). It is interesting that the HZE-specific response in both plants and in animals is overrepresented- albeit slightly- for disease response.

ACCESSION NUMBERS

All of our microarray data has been deposited in the Gene Expression Omnibus (<http://www.ncbi.nlm.nih.gov/geo>) with the accession number [GSEXXXX].

ACKNOWLEDGMENTS

Experimental design and analysis by Anne B. Britt, Phillip A. Conklin, and Victor Missirian, irradiations performed by Kevin M. Culligan and Neil D. Huefner, RNA extraction by Kevin M. Culligan, text and figures prepared by Victor Missirian, Phillip A. Conklin, and Anne B. Britt. This work was funded by grants to Anne B. Britt from NASA Fundamental Space Radiation Biology Program (award # NNA04CL13G), DOE SC Office of Basic Energy Sciences (award # FG02-05ER15668), and National Science Foundation Division of Molecular Biosciences (award #1158443), as well as an award to Kevin M. Culligan from the NH Agricultural Experiment Station (Grant NH00543). We gratefully acknowledge the assistance of the staff and faculty at Brookhaven National Labs/National Space Radiation Labs, including Dr. Adam Rusek, Richard Sautkaulis, and the late Dr. Betsy Sutherland.

SUPPLEMENTARY MATERIAL

The Supplementary Material for this article can be found online at: <http://www.frontiersin.org/journal/10.3389/fpls.2014.00364/abstract>

REFERENCES

- Adachi, S., Minamisawa, K., Okushima, Y., Inagaki, S., Yoshiyama, K., Kondou, Y., et al. (2011). Programmed induction of endoreduplication by DNA double-strand breaks in *Arabidopsis*. *Proc. Natl. Acad. Sci. U.S.A.* 108, 10004–10009. doi: 10.1073/pnas.1103584108
- Aklilu, B. B., Soderquist, R. S., and Culligan, K. M. (2014). Genetic analysis of the Replication Protein A large subunit family in *Arabidopsis* reveals unique and overlapping roles in DNA repair, meiosis and DNA replication. *Nucleic Acids Res.* 42, 3104–3118. doi: 10.1093/nar/gkt1292
- Amiard, S., Depeiges, A., Allain, E., White, C. I., and Gallego, M. E. (2011). *Arabidopsis* ATM and ATR kinases prevent propagation of genome damage caused by telomere dysfunction. *Plant Cell* 23, 4254–4265. doi: 10.1105/tpc.111.092387
- Ashburner, M., Ball, C. A., Blake, J. A., Botstein, D., Butler, H., Cherry, J. M., et al. (2000). Gene ontology: tool for the unification of biology. The Gene Ontology Consortium. *Nat. Genet.* 25, 25–29. doi: 10.1038/75556

- Baker, A., Graham, I. A., Holdsworth, M., Smith, S. M., and Theodoulou, F. L. (2006). Chewing the fat: beta-oxidation in signalling and development. *Trends Plant Sci.* 11, 124–132. doi: 10.1016/j.tplants.2006.01.005
- Benjamini, Y., and Hochberg, Y. (1995). Controlling the false discovery rate—a practical and powerful approach to multiple testing. *J. R. Statist. Soc. B Methodol.* 57, 289–300.
- Chen, I., Haehnel, U., Altschmied, L., Schubert, I., and Puchta, H. (2003). The transcriptional response of Arabidopsis to genotoxic stress— a high density colony array study (HDCA). *Plant J.* 35, 771–786. doi: 10.1046/j.1365-313X.2003.01847.x
- Choudhury, S., Panda, P., Sahoo, L., and Panda, S. K. (2013). Reactive oxygen species signaling in plants under abiotic stress. *Plant Signal. Behav.* 8, e23681-1–e23681-6. doi: 10.4161/psb.23681
- Cools, T., Iantcheva, A., Weimer, A. K., Boens, S., Takahashi, N., Maes, S., et al. (2011). The *Arabidopsis thaliana* checkpoint kinase WEE1 protects against premature vascular differentiation during replication stress. *Plant Cell* 23, 1435–1448. doi: 10.1105/tpc.110.082768
- Covington, M. E., and Harmer, S. L. (2007). The circadian clock regulates auxin signaling and responses in Arabidopsis. *PLoS Biol.* 5:e222. doi: 10.1371/journal.pbio.0050222
- Culligan, K. M., Robertson, C. E., Foreman, J., Doerner, P., and Britt, A. B. (2006). ATR and ATM play both distinct and additive roles in response to ionizing radiation. *Plant J.* 48, 947–961. doi: 10.1111/j.1365-313X.2006.02931.x
- Daly, M. J., Gaidamakova, E. K., Matrosova, V. Y., Vasilenko, A., Zhai, M., Leapman, R. D., et al. (2007). Protein oxidation implicated as the primary determinant of bacterial radioresistance. *PLoS Biol.* 5:e92. doi: 10.1371/journal.pbio.0050092
- De Coninck, B., Carron, D., Tavormina, P., Willem, L., Craik, D. J., Vos, C., et al. (2013). Mining the genome of *Arabidopsis thaliana* as a basis for the identification of novel bioactive peptides involved in oxidative stress tolerance. *J. Exp. Bot.* 64, 5297–5307. doi: 10.1093/jxb/ert295
- Delatte, T. L., Sedjiani, P., Kondou, Y., Matsui, M., de Jong, G. J., Somsen, G. W., et al. (2011). Growth arrest by trehalose-6-phosphate: an astonishing case of primary metabolite control over growth by way of the SnRK1 signaling pathway. *Plant Physiol.* 157, 160–174. doi: 10.1104/pp.111.180422
- De Schutter, K., Joubes, J., Cools, T., Verkest, A., Corellou, F., Babiyichuk, E., et al. (2007). Arabidopsis WEE1 kinase controls cell cycle arrest in response to activation of the DNA integrity checkpoint. *Plant Cell* 19, 211–225. doi: 10.1105/tpc.106.045047
- Ding, L. H., Park, S., Peyton, M., Girard, L., Xie, Y., Minna, J. D., et al. (2013). Distinct transcriptome profiles identified in normal human bronchial epithelial cells after exposure to gamma-rays and different elemental particles of high Z and energy. *BMC Genomics* 14:372. doi: 10.1186/1471-2164-14-372
- Eisen, M. B., Spellman, P. T., Brown, P. O., and Botstein, D. (1998). Cluster analysis and display of genome-wide expression patterns. *Proc. Natl. Acad. Sci. U.S.A.* 95, 14863–14868. doi: 10.1073/pnas.95.25.14863
- Friesner, J., and Britt, A. B. (2003). Ku80- and DNA ligase IV-deficient plants are sensitive to ionizing radiation and defective in T-DNA integration. *Plant J.* 34, 427–440. doi: 10.1046/j.1365-313X.2003.01738.x
- Friesner, J. D., Liu, B., Culligan, K., and Britt, A. B. (2005). Ionizing radiation-dependent gamma-H2AX focus formation requires ataxia telangiectasia mutated and ataxia telangiectasia mutated and Rad3-related. *Mol. Biol. Cell* 16, 2566–2576. doi: 10.1091/mbc.E04-10-0890
- Fulcher, N., and Sablowski, R. (2009). Hypersensitivity to DNA damage in plant stem cell niches. *Proc. Natl. Acad. Sci. U.S.A.* 106, 20984–20988. doi: 10.1073/pnas.0909218106
- Furukawa, T., Curtis, M. J., Tominey, C., Duong, Y., Wilcox, B. W., Aggoune, D., et al. (2010). A shared DNA-damage-response pathway for induction of stem-cell death by UV-B and by gamma irradiation. *DNA Repair (Amst)* 9, 940–948. doi: 10.1016/j.dnarep.2010.06.006
- Gaddameedhi, S., Reardon, J. T., Ye, R., Ozturk, N., and Sancar, A. (2012). Effect of circadian clock mutations on DNA damage response in mammalian cells. *Cell Cycle* 11, 3481–3491. doi: 10.4161/cc.21771
- Garcia, V., Bruchet, H., Camescasse, D., Fabienne, G., Bouchez, D. L., and Tissier, A. (2003). AtATM is essential for meiosis and the somatic response to DNA damage in plants. *Plant Cell* 15, 119–132. doi: 10.1105/tpc.006577
- Garm, C., Moreno-Villanueva, M., Burkle, A., Petersen, I., Bohr, V. A., Christensen, K., et al. (2013). Age and gender effects on DNA strand break repair in peripheral blood mononuclear cells. *Aging Cell* 12, 58–66. doi: 10.1111/acel.12019
- Goukassian, D., Gad, F., Yaar, M., Eller, M. S., Nehal, U. S., and Gilchrest, B. A. (2000). Mechanisms and implications of the age-associated decrease in DNA repair capacity. *FASEB J.* 14, 1325–1334. doi: 10.1096/fj.14.10.1325
- Gredilla, R., Garm, C., and Stevnsner, T. (2012). Nuclear and mitochondrial DNA repair in selected eukaryotic aging model systems. *Oxid. Med. Cell. Longev.* 2012:282438. doi: 10.1155/2012/282438
- Guo, Z., Kozlov, S., Lavin, M. F., Person, M. D., and Paull, T. T. (2010). ATM activation by oxidative stress. *Science* 330, 517–521. doi: 10.1126/science.1192912
- Heacock, M. L., Idol, R. A., Friesner, J. D., Britt, A. B., and Shippen, D. E. (2007). Telomere dynamics and fusion of critically shortened telomeres in plants lacking DNA ligase IV. *Nucleic Acids Res.* 35, 6490–6500. doi: 10.1093/nar/gkm472
- Hefner, E., Huefner, N., and Britt, A. B. (2006). Tissue-specific regulation of cell-cycle responses to DNA damage in Arabidopsis seedlings. *DNA Repair (Amst)* 5, 102–110. doi: 10.1016/j.dnarep.2005.08.013
- Hefner, E., Preuss, S. B., and Britt, A. B. (2003). Arabidopsis mutants sensitive to gamma radiation include the homologue of the human repair gene ERCC1. *J. Exp. Bot.* 54, 669–680. doi: 10.1093/jxb/erg069
- Huang da, W., Sherman, B. T., and Lempicki, R. A. (2009a). Bioinformatics enrichment tools: paths toward the comprehensive functional analysis of large gene lists. *Nucleic Acids Res.* 37, 1–13. doi: 10.1093/nar/gkn923
- Huang da, W., Sherman, B. T., and Lempicki, R. A. (2009b). Systematic and integrative analysis of large gene lists using DAVID bioinformatics resources. *Nat. Protoc.* 4, 44–57. doi: 10.1038/nprot.2008.211
- Irizarry, R. A., Hobbs, B., Collin, F., Beazer-Barclay, Y. D., Antonellis, K. J., Scherf, U., et al. (2003). Exploration, normalization, and summaries of high density oligonucleotide array probe level data. *Biostatistics* 4, 249–264. doi: 10.1093/biostatistics/4.2.249
- Jazayeri, A., Falck, J., Lukas, C., Bartek, J., Smith, G. C., Lukas, J., et al. (2006). ATM- and cell cycle-dependent regulation of ATR in response to DNA double-strand breaks. *Nat. Cell Biol.* 8, 37–45. doi: 10.1038/ncb1337
- Kaidi, A., and Jackson, S. P. (2013). KAT5 tyrosine phosphorylation couples chromatin sensing to ATM signalling. *Nature* 498, 70–74. doi: 10.1038/nature12201
- Kilian, J., Whitehead, D., Horak, J., Wanke, D., Weinl, S., Batistic, O., et al. (2007). The AtGenExpress global stress expression data set: protocols, evaluation and model data analysis of UV-B light, drought and cold stress responses. *Plant J.* 50, 347–363. doi: 10.1111/j.1365-313X.2007.03052.x
- Kim, H., and D’Andrea, A. D. (2012). Regulation of DNA cross-link repair by the Fanconi anemia/BRCA pathway. *Genes Dev.* 26, 1393–1408. doi: 10.1101/gad.195248.112
- Kim, Y. S. (2006). Analysis of gene expression upon DNA damage in Arabidopsis. *J. Plant Biol.* 49, 298–302. doi: 10.1007/BF03031159
- Kunz, H. H., Scharnewska, M., Feussner, K., Feussner, I., Flugge, U. I., Fulda, A., et al. (2009). The ABC transporter PXA1 and peroxisomal beta-oxidation are vital for metabolism in mature leaves of arabidopsis during extended darkness. *Plant Cell* 21, 2733–2749. doi: 10.1105/tpc.108.064857
- Lingard, M. J., Gidda, S. K., Bingham, S., Rothstein, S. J., Mullen, R. T., and Trelease, R. N. (2008). Arabidopsis PEROXIN11c-e, FISSION1b, and DYNAMIN-RELATED PROTEIN3A cooperate in cell cycle-associated replication of peroxisomes. *Plant Cell* 20, 1567–1585. doi: 10.1105/tpc.107.057679
- Lingard, M. J., and Trelease, R. N. (2006). Five Arabidopsis peroxin 11 homologs individually promote peroxisome elongation, duplication or aggregation. *J. Cell Sci.* 119, 1961–1972. doi: 10.1242/jcs.02904
- Lunn, J. E., Feil, R., Hendriks, J. H. M., Gibon, Y., Morcuende, R., Osuna, D., et al. (2006). Sugar-induced increases in trehalose 6-phosphate are correlated with redox activation of ADPglucose pyrophosphorylase and higher rates of starch synthesis in *Arabidopsis thaliana*. *Biochem. J.* 397, 139–148. doi: 10.1042/BJ20060083
- Magee, J. L., and Chatterjee, A. (1980). Radiation-chemistry of heavy-particle tracks.I. General-considerations. *J. Phys. Chem.* 84, 3529–3536. doi: 10.1021/j100463a008
- Mannuss, A., Trapp, O., and Puchta, H. (2012). Gene regulation in response to DNA damage. *Biochim. Biophys. Acta* 1819, 154–165. doi: 10.1016/j.bbaparm.2011.08.003
- Masterson, C., and Wood, C. (2000). Mitochondrial beta-oxidation of fatty acids in higher plants. *Physiol. Plant.* 109, 217–224. doi: 10.1034/j.1399-3054.2000.100301.x
- Menges, M., de Jager, S. M., Grussem, W., and Murray, J. A. (2005). Global analysis of the core cell cycle regulators of Arabidopsis identifies novel genes, reveals multiple and highly specific profiles of expression and provides a coherent

- model for plant cell cycle control. *Plant J.* 41, 546–566. doi: 10.1111/j.1365-313X.2004.02319.x
- Mentzen, W. I., Peng, J. L., Ransom, N., Nikolau, B. J., and Wurtele, E. S. (2008). Articulation of three core metabolic processes in Arabidopsis: fatty acid biosynthesis, leucine catabolism and starch metabolism. *BMC Plant Biol.* 8:76. doi: 10.1186/1471-2229-8-76
- Michael, T. P., Mockler, T. C., Breton, G., McEntee, C., Byer, A., Trout, J. D., et al. (2008). Network discovery pipeline elucidates conserved time-of-day-specific cis-regulatory modules. *PLoS Genet.* 4:e14. doi: 10.1371/journal.pgen.0040014
- Mole, R. H. (1984). The LD₅₀ for uniform low LET irradiation of man. *Br. J. Radiol.* 57, 355–369. doi: 10.1259/0007-1285-57-677-355
- Orth, T., Reumann, S., Zhang, X. C., Fan, J. L., Wenzel, D., Quan, S., et al. (2007). The PEROXIN11 protein family controls peroxisome proliferation in Arabidopsis. *Plant Cell* 19, 333–350. doi: 10.1105/tpc.106.045831
- Pastori, G. M., and Delrio, L. A. (1994). An activated-oxygen-mediated role for peroxisomes in the mechanism of senescence of *Pisum-Sativum* L Leaves. *Planta* 193, 385–391. doi: 10.1007/BF00201817
- Preuss, S. B., and Britt, A. B. (2003). A DNA-damage-induced cell cycle checkpoint in Arabidopsis. *Genetics* 164, 323–334.
- Ramsey, M. R., and Ellisen, L. W. (2011). Circadian function in cancer: regulating the DNA damage response. *Proc. Natl. Acad. Sci. U.S.A.* 108, 10379–10380. doi: 10.1073/pnas.1107319108
- Ricaud, L., Proux, C., Renou, J. P., Pichon, O., Fochesato, S., Ortet, P., et al. (2007). ATM-mediated transcriptional and developmental responses to gamma-rays in Arabidopsis. *PLoS ONE* 2:e430. doi: 10.1371/journal.pone.0000430
- Roa, H., Lang, J., Culligan, K. M., Keller, M., Holec, S., Cognat, V., et al. (2009). Ribonucleotide reductase regulation in response to genotoxic stress in Arabidopsis. *Plant Physiol.* 151, 461–471. doi: 10.1104/pp.109.140053
- Schluepmann, H., Berke, L., and Sanchez-Perez, G. F. (2012). Metabolism control over growth: a case for trehalose-6-phosphate in plants. *J. Exp. Bot.* 63, 3379–3390. doi: 10.1093/jxb/err311
- Shi, L., Kent, R., Bence, N., and Britt, A. B. (1997). Developmental expression of a DNA repair gene in Arabidopsis. *Mutat. Res.* 384, 145–156. doi: 10.1016/S0921-8777(97)00023-2
- Shiloh, Y., and Ziv, Y. (2013). The ATM protein kinase: regulating the cellular response to genotoxic stress, and more. *Nat. Rev. Mol. Cell Biol.* 14, 197–210. doi: 10.1038/nrm3546
- Shor, E., Fox, C. A., and Broach, J. R. (2013). The yeast environmental stress response regulates mutagenesis induced by proteotoxic stress. *PLoS Genet.* 9:e1003680. doi: 10.1371/journal.pgen.1003680
- Smyth, G. K. (2005). “Limma: linear models for microarray data,” In *Bioinformatics and Computational Biology Solutions Using R and Bioconductor*, eds R. Gentleman, V. Carey, S. Dudoit, R. Irizarry, and W. Huber (New York, NY: Springer), 397–420. doi: 10.1007/0-387-29362-0_23
- Sun, Y., Jiang, X., Chen, S., Fernandes, N., and Price, B. D. (2005). A role for the Tip60 histone acetyltransferase in the acetylation and activation of ATM. *Proc. Natl. Acad. Sci. U.S.A.* 102, 13182–13187. doi: 10.1073/pnas.0504211102
- Suzuki, N., Koussevitzky, S., Mittler, R., and Miller, G. (2012). ROS and redox signalling in the response of plants to abiotic stress. *Plant Cell Environ.* 35, 259–270. doi: 10.1111/j.1365-3040.2011.02336.x
- Tamura, K., Adachi, Y., Chiba, K., Oguchi, K., and Takahashi, H. (2002). Identification of Ku70 and Ku80 homologues in *Arabidopsis thaliana*: evidence for a role in the repair of DNA double-strand breaks. *Plant J.* 29, 771–781. doi: 10.1046/j.1365-313X.2002.01258.x
- Team, R. C. (2012). *R: A Language and Environment for Statistical Computing*. Vienna: R Foundation for Statistical Computing.
- Ulm, R., and Nagy, F. (2005). Signalling and gene regulation in response to ultraviolet light. *Curr. Opin. Plant Biol.* 8, 477–482. doi: 10.1016/j.pbi.2005.07.004
- Usadel, B., Blasing, O. E., Gibon, Y., Retzlaff, K., Hoehne, M., Gunther, M., et al. (2008). Global transcript levels respond to small changes of the carbon status during progressive exhaustion of carbohydrates in *Arabidopsis* rosettes. *Plant Physiol.* 146, 1834–1861. doi: 10.1104/pp.107.115592
- Vespa, L., Couvillion, M., Spangler, E., and Shippen, D. E. (2005). ATM and ATR make distinct contributions to chromosome end protection and the maintenance of telomeric DNA in Arabidopsis. *Genes Dev.* 19, 2111–2115. doi: 10.1101/gad.1333805
- Vespa, L., Warrington, R. T., Mokros, P., Siroky, J., and Shippen, D. E. (2007). ATM regulates the length of individual telomere tracts in Arabidopsis. *Proc. Natl. Acad. Sci. U.S.A.* 104, 18145–18150. doi: 10.1073/pnas.070466104
- Ward, J. (1998). “Nature of lesions formed by ionizing radiation,” in *DNA Damage and Repair*, Vol. 2, eds J. Nickoloff and M. Hoekstra (Totowa, NJ: Humana Press), 65–84. doi: 10.1385/0-89603-500-X:65
- Waterworth, W. M., Masnavi, G., Bhardwaj, R. M., Jiang, Q., Bray, C. M., and West, C. E. (2010). A plant DNA ligase is an important determinant of seed longevity. *Plant J.* 63, 848–860. doi: 10.1111/j.1365-313X.2010.04285.x
- West, C. E., Waterworth, W. M., Jiang, Q., and Bray, C. M. (2000). Arabidopsis DNA ligase IV is induced by gamma-irradiation and interacts with an Arabidopsis homologue of the double strand break repair protein XRCC4. *Plant J.* 24, 67–78. doi: 10.1046/j.1365-313X.2000.00856.x
- Yoshiyama, K., Conklin, P. A., Huefner, N. D., and Britt, A. B. (2009). Suppressor of gamma response 1 (SOG1) encodes a putative transcription factor governing multiple responses to DNA damage. *Proc. Natl. Acad. Sci. U.S.A.* 106, 12843–12848. doi: 10.1073/pnas.0810304106
- Zeeman, S. C., Smith, S. M., and Smith, A. M. (2007). The diurnal metabolism of leaf starch. *Biochem. J.* 401, 13–28. doi: 10.1042/BJ20061393
- Zheng, X. Y., Spivey, N. W., Zeng, W., Liu, P. P., Fu, Z. Q., Klessig, D. F., et al. (2012). Coronatine promotes *Pseudomonas syringae* virulence in plants by activating a signaling cascade that inhibits salicylic acid accumulation. *Cell Host Microbe* 11, 587–596. doi: 10.1016/j.chom.2012.04.014

Conflict of Interest Statement: The authors declare that the research was conducted in the absence of any commercial or financial relationships that could be construed as a potential conflict of interest.

Received: 09 February 2014; accepted: 08 July 2014; published online: 01 August 2014.

Citation: Missirian V, Conklin PA, Culligan KM, Huefner ND and Britt AB (2014) High atomic weight, high-energy radiation (HZE) induces transcriptional responses shared with conventional stresses in addition to a core “DSB” response specific to clastogenic treatments. *Front. Plant Sci.* 5:364. doi: 10.3389/fpls.2014.00364

This article was submitted to Plant Physiology, a section of the journal Frontiers in Plant Science.

Copyright © 2014 Missirian, Conklin, Culligan, Huefner and Britt. This is an open-access article distributed under the terms of the Creative Commons Attribution License (CC BY). The use, distribution or reproduction in other forums is permitted, provided the original author(s) or licensor are credited and that the original publication in this journal is cited, in accordance with accepted academic practice. No use, distribution or reproduction is permitted which does not comply with these terms.



Identification of “safe harbor” loci in indica rice genome by harnessing the property of zinc-finger nucleases to induce DNA damage and repair

Christian Cantos¹, Perigio Francisco¹, Kurniawan R. Trijatmiko², Inez Slamet-Loedin¹ and Prabhjit K. Chadha-Mohanty^{1*}

¹ Gene Transformation Lab, Plant Breeding, Genetics, and Biotechnology Division, International Rice Research Institute, Metro Manila, Philippines

² Indonesian Center for Agricultural Biotechnology and Genetic Resources Research and Development, Bogor, Indonesia

Edited by:

Alma Balestrazzi, University of Pavia, Italy

Reviewed by:

Alma Balestrazzi, University of Pavia, Italy

Mohan Achary, International Centre for Genetic Engineering and Biotechnology, India

***Correspondence:**

Prabhjit K. Chadha-Mohanty, International Rice Research Institute, DAPO Box 7777, Metro Manila 1301, Philippines

e-mail: p.chadha-mohanty@irri.org

Zinc-finger nucleases (ZFNs) have proved to be successful tools for targeted genome manipulation in several organisms. Their main property is the induction of double-strand breaks (DSBs) at specific sites, which are further repaired through homologous recombination (HR) or non-homologous end joining (NHEJ). However, for the appropriate integration of genes at specific chromosomal locations, proper sites for gene integration need to be identified. These regions, hereby named safe harbor loci, must be localized in non-coding regions and possess high gene expression. In the present study, three different ZFN constructs (pZFN1, pZFN2, pZFN3), harboring β -glucuronidase (GUS) as a reporter gene, were used to identify safe harbor loci on rice chromosomes. The constructs were delivered into IR64 rice by using an improved *Agrobacterium*-mediated transformation protocol, based on the use of immature embryos. Gene expression was measured by histochemical GUS activity and the flanking regions were determined through thermal-asymmetric interlaced polymerase chain reaction (TAIL PCR). Following sequencing, 28 regions were identified as putative sites for safe integration, but only one was localized in a non-coding region and also possessed high GUS expression. These findings have significant applicability to create crops with new and valuable traits, since the site can be subsequently used to stably introduce one or more genes in a targeted manner.

Keywords: zinc-finger nucleases (ZFNs), safe harbor loci, rice (*Oryza sativa* L.), homologous recombination (HR), double-strand breaks (DSBs)

INTRODUCTION

Rice (*Oryza sativa* L.) has emerged as a model cereal system for molecular studies as the complete genome has been sequenced, several tools for functional genomics are available, and the production of transgenic plants by efficient *Agrobacterium*-mediated transformation is easier than with other major cereals (Izawa and Shimamoto, 1996). In addition, rice is one of the leading food crops worldwide and increasing rice production is expected to play a significant role in reducing hunger and upgrading the economic status of developing countries.

Nowadays, due to recent advances in molecular biology, research focuses more and more on the ability to manipulate genomes at specific sites. Efficient methods for genome editing further promote gene discovery and functional gene analyses in model plants as well as the introduction of novel desired agricultural traits in important species. Genome editing technology enables efficient and precise genetic modification through the induction of a double-strand break (DSB) in a specific target sequence, followed by the generation of desired modifications during the subsequent DNA break repair (Puchta, 2002). Genome editing is achieved by integrating desired DNA

molecules into the target genome by employing mainly the homologous recombination (HR) pathway. However, in plants, these molecules are normally delivered by direct gene-transfer methods and often integrate into the target cell genome via non-homologous end joining (NHEJ) instead of HR (Britt and May, 2003). Currently, zinc-finger nucleases (ZFNs), transcription activator-like effector nucleases (TALENs), and clustered regulatory interspaced short palindromic repeats (CRISPR)/Cas-based RNA-guided DNA endonucleases are used as innovative techniques in genome editing (Gaj et al., 2013). These nucleases diverge in different aspects, starting from the composition, to specificity and mutation signatures (Kim and Kim, 2014). Knowledge of their specific features is essential for choosing the most appropriate tool for a range of applications.

ZFNs were among the first tools used for genome editing a decade ago, and are defined as artificial restriction enzymes composed of a fusion between the DNA-binding domain of a zinc-finger protein (ZFP) and the cleavage domain of the FokI endonuclease. The DNA-binding domain of ZFPs can be engineered to recognize a variety of DNA sequences, while the FokI endonuclease domain, which functions as a dimer, cleaves the

DNA and creates DSBs (Durai et al., 2005; Porteus and Carroll, 2005). Through directed co-localization and dimerization of two FokI nuclease monomers, ZFNs generate a functional site-specific endonuclease that creates a DSB at the targeted locus (Mani et al., 2005). Through the use of this methodology, the induced DNA sequence modifications can range from mutations to gene replacement, site-specific structural changes, or gene insertion, to name a few (Husaini et al., 2011).

DNA repair of DSBs is primarily carried out through HR and NHEJ. Depending on the desired modification, either pathway can be used in ZFN-mediated genomic engineering. Since HR relies on homologous DNA to repair the DSB, gene targeting can be achieved by supplying an exogenous template, termed a donor sequence, which is replicated and mostly used to introduce small mutations or large insertions. On the other hand, NHEJ is an error-prone repair process, ideal for generating mutations that can result in gene knockouts or knockdowns when the ZFN-mediated DSB is introduced into the protein coding sequence of a gene (Bibikova et al., 2003; Urnov et al., 2010). ZFNs have been successfully used for inducing DSBs in the genomes of various species, including plants (Lloyd et al., 2005; Wright et al., 2005). Successful HR-based gene replacement was observed at frequencies ranging from 0.2 to 4% in tobacco protoplasts, where acetolactase synthase genes *SurA* and *SurB* were mutated to confer resistance to herbicides (Townsend et al., 2009). In maize, Shukla et al. (2009) showed that insertional disruption of the *IPK1* gene, encoding the inositol-1,3,4,5,6-pentakisphosphate enzyme, resulted in both herbicide tolerance and alteration of the inositol phosphate profile in developing seeds. In addition, the trait/modification was stably transmitted to the next generation.

For the successful integration of genes at specific chromosomal locations, it is of utmost importance to identify proper sites for gene insertion. The results of Day et al. (2000) have shown that a transgene can be delivered into a specific chromosome position; this will allow the selection of a specific target site for a consistent and higher transgene expression. Therefore, the ability to achieve site-specific manipulation of the rice genome can improve the expression of transgenes as it is highly dependent on the locus of integration. These integration regions must possess high gene expression and preferably be localized in non-coding DNA regions (Curtin et al., 2012; Sadelain et al., 2012). In the present study, ZFNs were employed in order to identify such regions, hereby designated as safe harbor loci, on rice chromosomes. Three different ZFN constructs, containing β -glucuronidase (GUS) as a reporter gene, were used. The level of gene expression in different loci was measured through GUS assay, while the flanking regions were determined through thermal-asymmetric interlaced polymerase chain reaction (TAIL PCR). This represents the first report on the potential use of ZFNs for the identification of safe harbor loci in plants. A number of important agronomic traits to improve rice for higher yield, tolerance of environmental stresses, and metabolic engineering are polygenic in nature. A large number of genes are needed to modify the metabolic pathway; the safe harbor loci will allow pyramiding of transgenes in one locus. The results presented here can be of great practical applicability in generating crops with improved agronomic traits.

RESULTS

GENERATION OF TRANSGENIC RICE PLANTS USING ZFN CONSTRUCTS

Three different constructs, pZFN1, pZFN2, and pZFN3, were used to generate transgenic rice plants. The vector system is based on the assembly of ZFN expression cassettes, a plant selection expression cassette, and a GUS reporter cassette, onto the plant binary vector pRCS2. The constructs contain the *hpt* (hygromycin phosphotransferase) gene driven by the octopine synthase promoter (*OcsP*), while the GUS and ZFN expressions are driven by a heat-shock inducible promoter (*hspP*; GenBank Acc. No. NC_003076.8). The difference between pZFN1 and pZFN2 consists of the length of the *hpt* gene. Each construct was introduced into *A. tumefaciens* LBA4404 and subsequently co-cultivated with rice immature embryos. In the case of pZFN3, co-transformation of two binary vectors, one carrying the plant selection marker and the reporter repair plasmid and the other carrying only the constitutive ZFN expression cassette, was used (Figure 1). *Agrobacterium*-mediated transformation steps are summarized in Figure 2. Constructs pZFN1 and pZFN2 generated 171 (85.5%) and 133 (88.5%) calli resistant to hygromycin, while the pZFN3 construct showed the highest number of resistant calli (439, 146.3%). From the regenerable callus culture, 29 GUS-positive plants were obtained for pZFN1, 60 for pZFN2, and 188 for pZFN3 (Table 1). Based on the number of immature embryos used and the plants obtained, transformation efficiency was calculated for each construct. Results are shown in Table 1. The highest transformation efficiency (66.3%) was registered when the pZFN3 construct was used.

GUS EXPRESSION LEVELS IN RICE TRANSGENICS

Following *Agrobacterium*-mediated transformation, rice-positive transformants were identified based on histochemical GUS detection. Two-week-old plantlets were initially incubated at 42°C for 90–150 min in order to trigger expression of the GUS gene, which is driven by a *hspP*. Using the Image J software, pixel density is measured based on the blue color present in plant tissue. The numerical values obtained, were then categorized in three different levels of GUS intensity (high, medium, and low). Figure 3 shows the histochemical GUS analysis. The number of positive events categorized accordingly with the levels of GUS expression is presented in Table 2. Out of 29 positive events obtained using pZFN1, 8 showed high expression, while 21 events showed low GUS expression. In the case of pZNF2, out of 60 positive events, only 1 presented high GUS expression, 8 showed medium expression, and 51 showed low expression. The highest number of events with high GUS expression (113) was obtained when the pZFN3 construct was used.

IDENTIFICATION OF FLANKING SEQUENCES AND SAFE HARBOR LOCI REGIONS

Genomic DNA was extracted from all positive events and a two-step TAIL PCR was performed in order to identify the flanking sequences (Figure 4). All GUS-positive plants with different levels of expression gave specific TAIL-PCR products ranging from 500 to 1000 bp. Bands were subsequently purified from gel, cloned and sequenced. Following bioinformatic analysis, 28 sites for GUS insertion were identified (Supplementary Table 1).

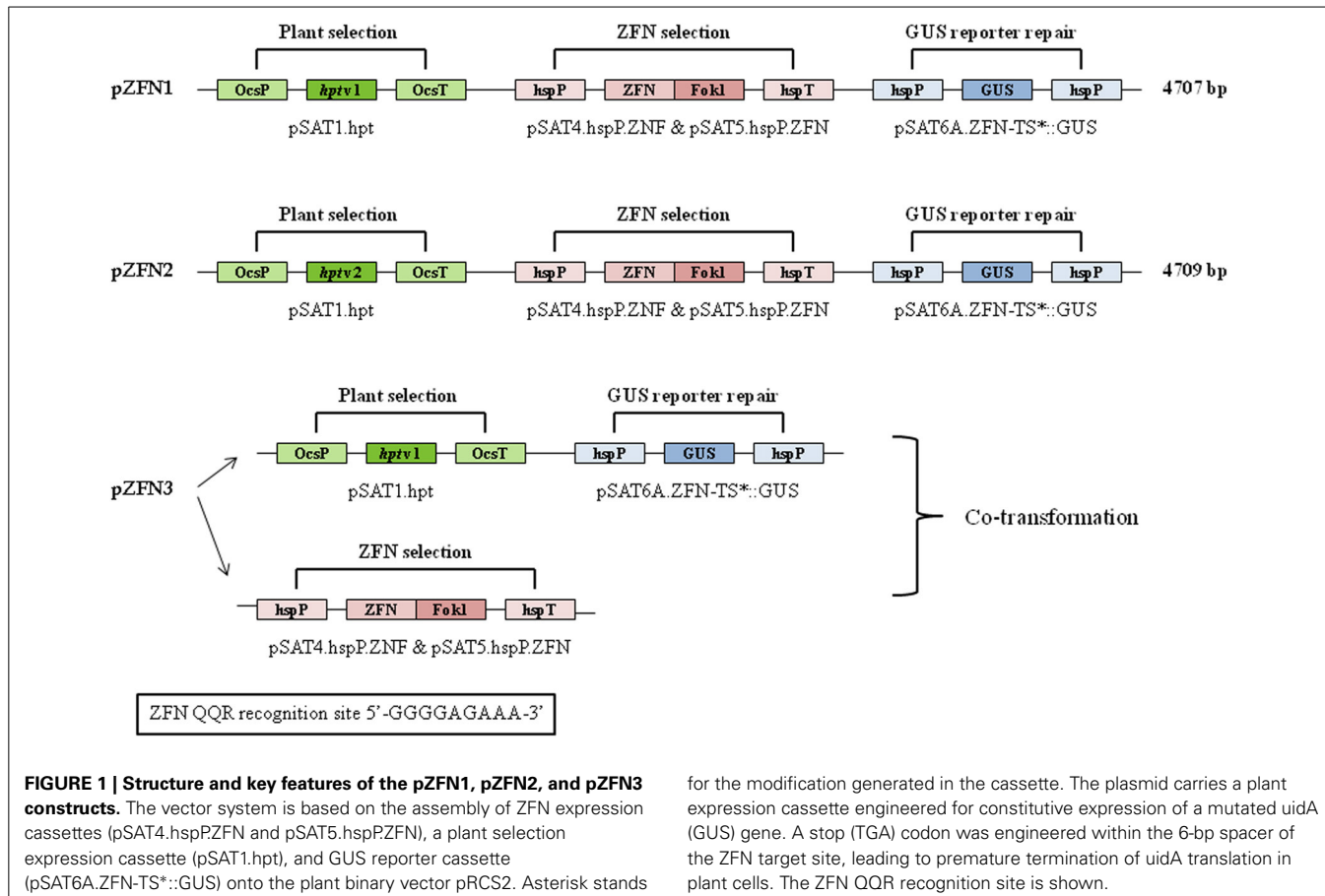


FIGURE 1 | Structure and key features of the pZFN1, pZFN2, and pZFN3 constructs. The vector system is based on the assembly of ZFN expression cassettes (pSAT4.hspP.ZNF and pSAT5.hspP.ZFN), a plant selection expression cassette (pSAT1.hpt), and GUS reporter cassette (pSAT6A.ZFN-TS*:GUS) onto the plant binary vector pRCS2. Asterisk stands

for the modification generated in the cassette. The plasmid carries a plant expression cassette engineered for constitutive expression of a mutated uidA (GUS) gene. A stop (TGA) codon was engineered within the 6-bp spacer of the ZFN target site, leading to premature termination of uidA translation in plant cells. The ZFN QQR recognition site is shown.

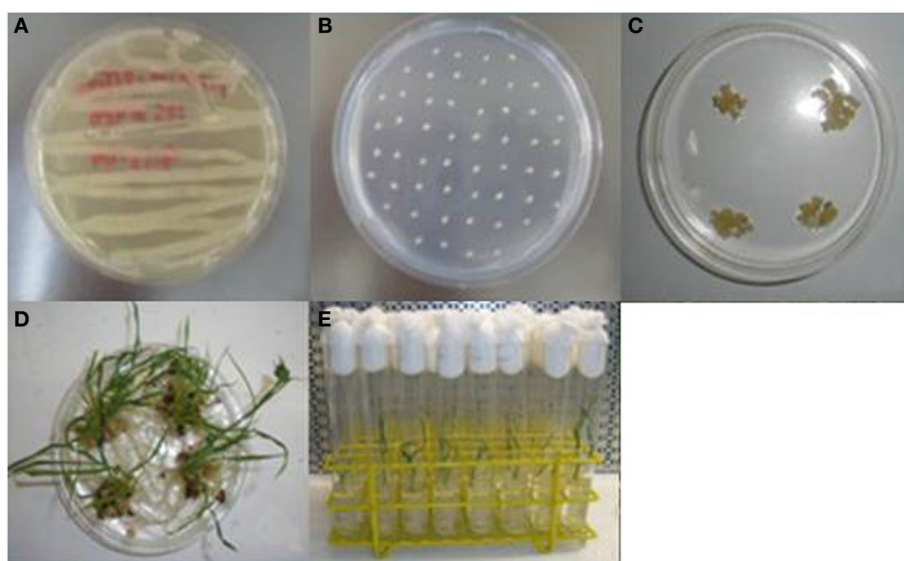


FIGURE 2 | Generation of transgenic rice plants by Agrobacterium-mediated transformation. (A) Growth of *A. tumefaciens* LBA4404 on AB medium; (B) co-cultivation of

immature embryos with *Agrobacterium* suspension; (C) selection of resistant calli; (D) regeneration of plantlets; (E) rice plantlets on MS0 rooting media.

Table 1 | Transformation efficiency of embryogenic calli derived from immature embryos of IR64 rice infected with *A. tumefaciens* LBA4404 containing ZFN constructs.

Constructs	Immature embryos	Resistant calli (%)	Regenerated calli (%)	GUS-positive plants	Transformation efficiency (%)
pZFN1	200	85.5	32.2	29	27.5
pZFN2	150	88.7	49.6	60	44.0
pZFN3	300	146.3	45.3	188	66.3

However, some of these regions were too short to be considered as safe harbor loci, while others presented low GUS expression. Out of the putative sites identified, three sequences chosen from plants exhibiting high GUS expression also presented a proper size (Table 3). One event showed integration on chromosome 1 (3404275–3405012), three independent events presented integration on chromosome 8 (5490900–5491654), and four independent events were integrated on chromosome 3 (8499895–8500138). When the sequences were verified for the presence/absence of coding genes, the BLAST results showed that the region on chromosome 1 is part of a gene (LOC_Os01g07212) encoding a putative staphylococcal nuclease homolog. Similarly, the region located on chromosome 8 is part of a gene (LOC_Os08g09480) coding for OsFBX268, an F-box domain-containing protein. Only the locus on chromosome 3 was shown to be localized in a non-coding DNA region (Table 3). Two putative genes, LOC_Os03g15470 and LOC_Os03g15480, are located near this region (Supplementary Figure 1), but the 243-bp sequence on chromosome 3 (8499895–8500138) is considered as non-coding. Since this region was identified from plants with high GUS expression, and no putative coding gene, it can be considered as a safe harbor locus for gene insertion. The nucleotide sequence was also converted to amino acid sequence, and no putative protein was shown to be encoded in this region.

DISCUSSION

In the present study, the ZFNs characteristic of inducing a DSB and subsequently trigger a response of proper DNA-repair pathways, was used to successfully insert the β -glucuronidase marker gene into the rice genome with the purpose of identifying safe regions for gene integration. The originality of this work derives from the use of ZFNs as an innovative technique for plant genome editing, associated with a newly standardized protocol for rice *Agrobacterium*-mediated transformation. Furthermore, the final result, identification of safe harbor loci for gene insertion, has a great impact related to practical applications in agriculture.

Several strategies can be used for ZFNs to modify the genome of plant species, depending on the presence and structure of the donor DNA and the plant DNA-repair machinery. Targeting a specific genomic sequence requires the delivery and expression of two ZFN monomers in the same cell, with the final goal of inducing site-specific mutagenesis, gene stacking, and/or gene replacement (Urnov et al., 2010).

Three constructs carrying the semi-palindromic target site of QQR ZFN were employed to generate transgenic rice plants.

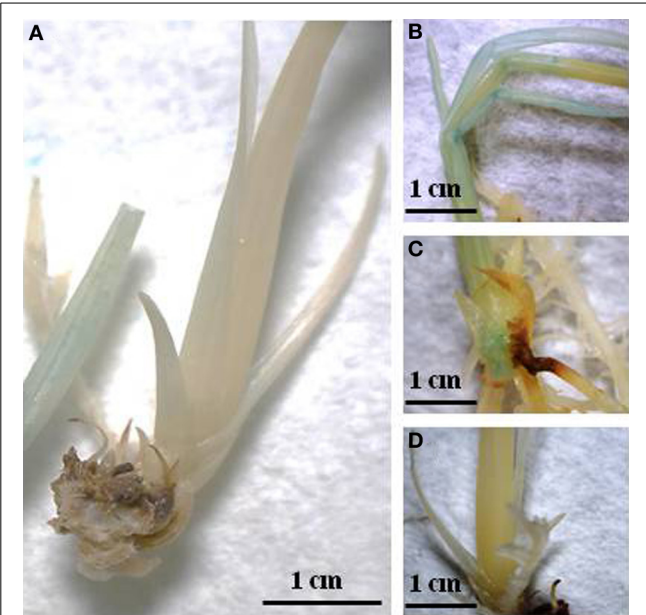


FIGURE 3 | Histochemical GUS staining; (A) Wild type; (B) Transgenic rice exhibiting high GUS expression; (C) Transgenic rice exhibiting medium GUS expression; (D) Transgenic rice exhibiting low GUS expression.

Table 2 | Events positive for GUS integration separated into groups (high, medium, and low) based on the intensity of GUS staining expression.

Constructs	Total events	High GUS expression	Medium GUS expression	Low GUS expression
pZFN1	29	8	0	21
pZFN2	60	1	8	51
pZFN3	188	113	40	30

QQR (Glutamine-Glutamine-Arginine) ZFN is a well-defined three-finger ZFN capable of recognizing and binding to 5'-GGGAAAGAA-3' nucleotide sequence. It was among the first chimera nucleases used and since then was successfully applied for genome engineering in both animals and plants (Smith et al., 2000; Weinthal et al., 2013). The vectors are based on the structure of a previously described pSAT plant expression vector system specifically designed to facilitate the assembly of multi-gene expression cassettes (Tzfira et al., 2005). The expression of the QQR coding sequence, as well as the expression of the GUS gene, is controlled by a hspP. This type of construct was successfully used in generating targeted mutations in *Arabidopsis* plants (Lloyd et al., 2005). The authors also estimated that QQR, when expressed under a heat-shock promoter, can induce mutations at a frequency as high as 0.2 mutations per gene, which is considerably higher than the previously reported HR-dependent frequencies (from 10^{-7} to 10^{-4}) for plant cells (Iida and Terada, 2005).

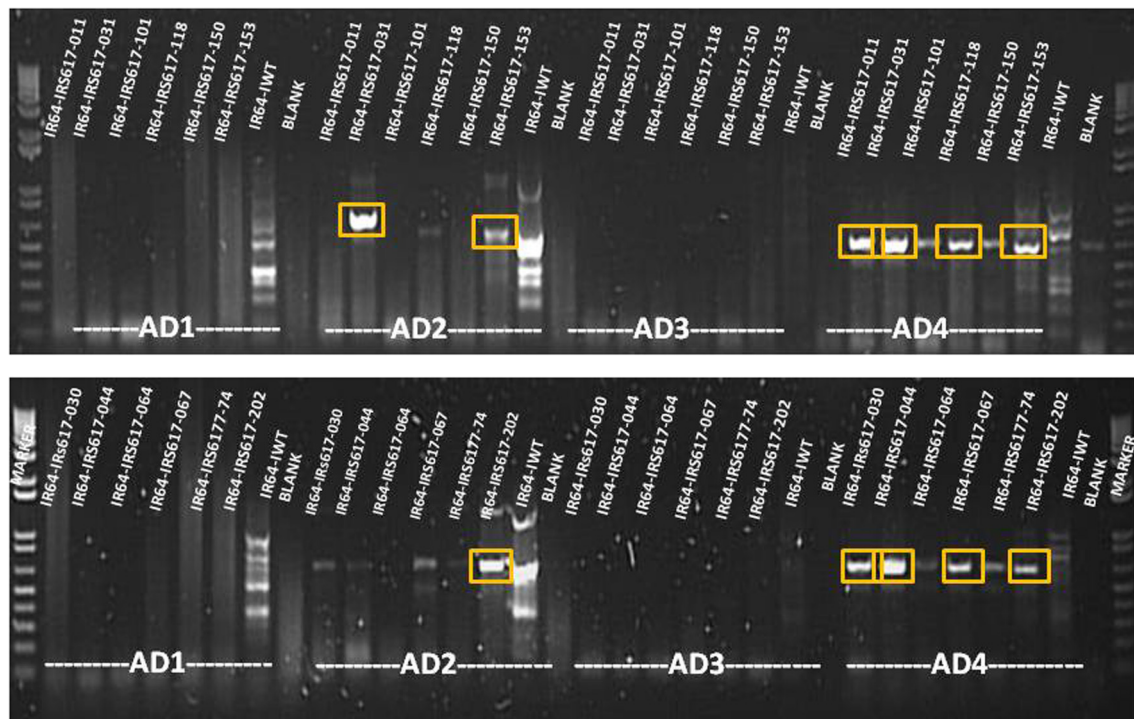


FIGURE 4 | Agarose gel analysis of TAIL PCR products amplified from GUS-positive insertion lines. Bands shown in boxes were cut and sequenced. AD1, AD2, AD3, and AD4 = non-specific primers.

Table 3 | Chromosomal localization and annotation of putative safe harbor loci identified in transgenic rice plants obtained by using ZFN constructs.

Sample ID	GUS expression	Chromosome region	Sequence length (bp)	Gene annotation	Protein
IR64-IRS617-176	High	Chr3:8499895–8500138	243	Non-coding	Non-coding
IR64-IRS617-177	High	Chr3:8499895–8500138	243	Non-coding	Non-coding
IR64-IRS617-190	High	Chr3:8499895–8500138	243	Non-coding	Non-coding
IR64-IRS617-202	High	Chr3:8499895–8500138	243	Non-coding	Non-coding
IR64-IRS617-201	High	Chr1:3404275–3405012	737	LOC_Os01g07212	Staphylococcal nuclease
IR64-IRS617-026	High	Chr8:5490900–5491654	754	LOC_Os08g09480	F-box domain
IR64-IRS617-030	High	Chr8:5490900–5491654	754	LOC_Os08g09480	F-box domain
IR64-IRS617-087	High	Chr8:5490900–5491654	754	LOC_Os08g09480	F-box domain

Among the three different constructs used for plant transformation, pZNF3 showed the highest transformation efficiency (66.3%) as well as the highest number of GUS-positive events (188 plants). This finding suggests that co-transformation of two separate vectors (one carrying the plant selection marker and the reporter repair plasmid, and the other carrying only the constitutive ZFN expression cassette) is more efficient than when the ZFNs and donors are delivered together in the same construct. In addition, the pZFN2 construct possessing a shorter variant of *hpt* gene showed higher transformation efficiency (44%) than pZFN1 (27.5%).

One of the main goals of genetic engineering is to attain stable transgenic events possessing predictable and reproducible levels of expression that can be characterized in terms of the effect

and implications of transgene insertion. In order to achieve this, it is important to gather detailed information about the transgene insertion site. The main attribute for safe regions to be used as gene integration sites is localization in non-coding DNA regions that permit high gene expression (Curtin et al., 2012; Sadelain et al., 2012). Techniques used for this purpose include detection of the physical position of transgenes by fluorescent *in situ* hybridization (FISH) (Salvo-Garrido et al., 2001; Choi et al., 2002) as well as genetic map position (Salvo-Garrido et al., 2004). Information on transgene insertions can also be obtained from the analysis of flanking regions (Sha et al., 2004). To identify the insertion site of the T-DNA flanking sequence, analyses were conducted using TAIL PCR. The method consists of the use of nested T-DNA border region-specific primers together

with shorter arbitrary degenerate primers for the unknown genomic DNA region flanking the insertion site (Liu et al., 1995). Such priming creates both specific and non-specific products, whose relative amplification efficiencies can be thermally controlled. In two serial PCRs, the unspecific products are gradually diluted out and in the final reaction the specific products are detectable on the gel by a slight shift in size due to the nested priming in the T-DNA region. In the present study, 28 flanking sequences for the GUS gene were identified following rice transformation with ZFN constructs. However, most of these sites possessed low expression and/or were localized in DNA coding regions. Only one region, located on chromosome 3 (8499895–8500138), retained both attributes and it can be considered as a safe harbor locus for gene insertion. This finding is highly important for future practical applications that could lead to the creation of crops with new valuable traits. In addition, ZFNs as part of new plant breeding technologies allow genome editing without the introduction of foreign DNA; thus, the resulting crops could be classified as non-GMO (Pauwels et al., 2014).

MATERIALS AND METHODS

VECTOR DESIGN

The constructs used in the present study were assembled and validated as per Tovkach et al. (2010). A schematic representation of plasmid maps is shown in **Figure 1**. The vector system is based on the assembly of ZFN expression cassettes (based on pSAT4.hspP.ZNF and pSAT5.hspP.ZNF plasmids), a plant selection expression cassette (based on pSAT1.hpt plasmid), and a GUS reporter cassette (based on pSAT6A.ZFN-TS*::GUS plasmid) onto the plant binary vector pRCs2. The nucleotide sequences of pSAT1.hpt, pSAT6A.ZFN-TS*::GUS, pSAT4.hspP.ZNF, and pSAT5.hspP.ZNF plasmids are available on the NCBI site. The plant selection cassette contains the *hpt* gene, which confers resistance to hygromycin and is driven by the OcsP. The GUS and ZFN expressions are driven by a hspP (GenBank Acc. No. NC_003076.8). The GUS reporter cassette contains a mutated GUS reporter gene, engineered to carry a TGA (stop) codon within the 6-bp spacer of the ZFN target site, constructed on a reporter repair plasmid. The QQR ZFN recognition site is 5'-GGGAAGAA-3'. Three different constructs were used and they were designated as pZFN1, pZFN2, and pZFN3 (**Figure 1**). The difference between pZFN1 and pZFN2 consists in the length of the *hpt* gene. As for pZNF3, it requires co-transformation of two binary vectors: one carrying the plant selection marker and the reporter repair plasmid and the other carrying only the constitutive ZFN expression cassette.

AGROBACTERIUM-MEDIATED TRANSFORMATION AND PLANT REGENERATION

Agrobacterium-mediated transformation of IR64 rice (*Oryza sativa L. indica*) was performed as described by Slamet-Loedin et al. (2014). Immature embryos (IE) harvested from rice panicles at 8–12 days after anthesis were dehulled and sterilized. IE were co-cultivated with *A. tumefaciens* LBA4404 for 7 days at 25°C under dark conditions in A201 medium. Following

co-cultivation, IE were transferred onto sterile Petri dishes containing A202 selection medium complemented with hygromycin and incubated under continuous light at 30°C for 5 days (first selection). Subsequently, IEs were placed on A203 medium and incubated under the same conditions for 10 days (second selection). After this period, the embryogenic calli were selected and placed on A203 medium under the same conditions and time period (third selection).

For plant regeneration, the resistant calli were incubated on pre-regeneration medium (A204) under continuous light at 30°C for 10 days. Proliferating calli were selected and transferred onto regeneration medium (A205). Subsequently, individual regenerated plantlets were placed in sterile glass tubes containing MS0 rooting medium and kept under continuous light at 25°C for 14 days. Plant material was then used for further analysis.

HISTOCHEMICAL GUS ASSAY

The location of GUS activity in plant tissues was determined histochemically as described by Jefferson et al. (1987). The GUS reaction mix consisted of the following: 50 mmol/L potassium ferrocyanide, 50 mmol/L potassium ferricyanide, 5 mL 0.2 mol/L sodium phosphate buffer, 0.5 mol/L sodium EDTA and 10% Triton X-100, and water. A separate solution of X-Gluc (5-Bromo-4-Chloro-3-Indolyl-Beta-D-Glucuronide) (Biosynth, Switzerland) at a concentration of 25 mg X-Gluc/mL of N-N dimethyl formamide was added to this reaction mix at a ratio of 352 μL of reaction mix to 48 μL of X-Gluc solution. In order to trigger the expression of the GUS gene, 2-week-old rice plantlets were incubated for 90–150 min at 42°C and subsequently recovered for an additional 24–72 h prior to GUS staining. Plantlets were then incubated in the GUS solution at 37°C for 16 h. The GUS solution was discarded and the plantlets were rinsed with water and bleached sequentially with 25, 50, and 75% ethyl alcohol and finally kept in 95% ethyl alcohol. Quantification of GUS activity was performed by using ImageJ (v. 1.45) software to identify the intensity of GUS gene expression and accordingly the transgenics were labeled as having high, medium, and low expression.

GENOMIC DNA EXTRACTION

Rice genomic DNA was extracted and purified following the protocol described by Dellaporta et al. (1983) with some modification in the extraction buffer as follows: 1 M Tris-HCl (pH = 8.0), 0.5 M EDTA, and 4 M NaCl and sodium bisulfate. Following extraction, genomic DNA was measured spectrophotometrically (NanoDrop ND-1000, NanoDrop, USA) by UV absorption at 260 nm, while DNA purity was evaluated on the basis of the UV absorption ratio at 260/280 nm and analyzed by 1% agarose gel electrophoresis in 1 × TAE SYBR SAFE® (Invitrogen, USA) staining.

THERMAL-ASYMMETRIC INTERLACED POLYMERASE CHAIN REACTION (TAIL PCR)

TAIL PCR was performed using the 5-Prime Taq DNA polymerase (5-Prime, USA) in a G-STORM® PCR System (Somerton Biotechnology Centre, UK) as per the supplier's recommendation. Genomic DNA isolated from plants with different levels

of GUS expression was subjected to two separate PCR runs. Primer sequences are shown in Supplementary Table 2. The reaction mix for the primary amplification was prepared in a total volume of 20 μ L and contained 1 \times 5-Prime Taq DNA polymerase buffer, 1 U 5-Prime Taq DNA polymerase, 0.2 mM dNTPs, 0.2 μ M specific left border primer (LB_pRCS2_F1), and 3 μ M of each arbitrary degenerate primer (AD1, AD2, AD3, and AD4). Each arbitrary degenerate primer was paired to the specific left border primer, resulting in four primer pair reactions for each sample. The PCR program for the primary TAIL PCR included 5 cycles at 94°C for 1 min, 55°C for 1 min, and 72°C for 2.3 min, 1 cycle at 94°C for 30 s, 44 °C for 1 min, and 72°C for 2.3 min, 15 cycles at 94°C for 30 s, 55°C for 1 min, and 72°C for 2.3 min, and the last cycle at 94°C for 30 s, 44°C for 1 min, and 72°C for 2.3 min, with a final elongation step at 72°C for 5 min. After the primary TAIL PCR, amplification products were diluted 10 \times for the secondary amplification. The reaction mixture contained the same components as the primary PCR, except for a different specific left border primer (LB_pRCS2_F2). The program included 20 cycles at 94°C for 30 s, 55°C for 1 min, 72°C for 2.3 min, 94°C for 30 s, 44°C for 1 min, and 72°C for 2.3 min, followed by a final elongation step at 72°C for 10 min.

All TAIL PCR products were visualized on a 1.5% agarose gel. PCR products were excised and purified using a QIAquick gel extraction kit (Qiagen, USA). The purified products were ligated in a pGEM T-easy vector system (Invitrogen, USA) and transformed in *E. coli* DH5a strain using the heat-shock method. Following bacterial transformation, the white/blue screening method was used to identify the positive colonies, which were then grown in LB liquid medium overnight at 37°C. Plasmid DNA was extracted using a Purelink® Quick Plasmid Miniprep kit (Invitrogen, USA) and digested using *EcoRI* restriction enzyme (Invitrogen, USA) to check for the presence of the ligated PCR product. Subsequently, plasmids were sequenced and analyzed with bioinformatic tools (Macrogen, Korea).

BIOINFORMATIC ANALYSIS

NCBI BLASTn (<http://blast.ncbi.nlm.nih.gov/Blast.cgi>) was used to locate the sequenced regions on the corresponding chromosomes. Sequences were checked using the rice annotation sites MSU (<http://rice.plantbiology.msu.edu>), RAP-DB (<http://rapdb.dna.affrc.go.jp/>), and Gramene (www.gramene.org/). Nucleotide sequences were transcribed to proteins using Expasy Tools (<http://web.expasy.org/translate/>) and the putative protein sequences were verified using the UniProt database (www.uniprot.org/uniprot/).

ACKNOWLEDGMENTS

We thank Dr. T. Tzfira for providing the ZFN constructs. We also acknowledge the contribution of Editha Abrigo for the rice plant transformation procedures.

SUPPLEMENTARY MATERIAL

The Supplementary Material for this article can be found online at: <http://www.frontiersin.org/journal/10.3389/fpls.2014.00302/abstract>

REFERENCES

- Bibikova, M., Beumer, K., Trautman, J. K., and Carroll, D. (2003). Enhancing gene targeting with designed zinc finger nucleases. *Science* 300, 764. doi: 10.1126/science.1079512
- Britt, A. B., and May, G. D. (2003). Re-engineering plant gene targeting. *Trends Plant Sci.* 8, 90–95. doi: 10.1016/S1360-1385(03)00002-5
- Choi, H. W., Lemieux, P. G., and Cho, M. J. (2002). Use of fluorescence *in situ* hybridization for gross mapping of transgenes and screening for homozygous plants in transgenic barley (*Hordeum vulgare* L.). *Theor. Appl. Genet.* 106, 92–100. doi: 10.1534/genetics.103.023747
- Curtin, S. J., Voytas, D. F., and Stupar, R. M. (2012). Genome engineering of crops with designer nucleases. *Plant Genome* 5, 42–50. doi: 10.3835/plantgenome2012.06.0008
- Day, C. D., Lee, E., Kobayashi, J., Holappa, L. D., Albert, H., and Ow, D. W. (2000). Transgene integration into the same chromosome location can produce alleles that express at predictable level, or alleles that are differently silenced. *Genes Dev.* 14, 2869–2880. doi: 10.1101/gad.849600
- Dellaporta, S. L., Wood, J., and Hicks, J. B. (1983). A plant DNA minipreparation: version II. *Plant Mol. Biol. Rep.* 1, 19–21.
- Durai, S., Mani, M., Kandavelou, K., Wu, J., Porteus, M. H., and Chandrasegaran, S. (2005). Zinc finger nucleases: custom-designed molecular scissors for genome engineering of plant and mammalian cells. *Nucleic Acids Res.* 33, 5978–5990. doi: 10.1093/nar/gki912
- Gaj, T., Gersbach, C. A., and Barbas, C. F. (2013). ZFN, TALEN, and CRISPR/Cas-based methods for genome engineering. *Trends Biotechnol.* 7, 397–405. doi: 10.1016/j.tibtech.2013.04.004
- Husaini, A. M., Rashid, Z., Mir, R. R., and Aquil, B. (2011). Approaches for gene targeting and targeted gene expression in plants. *GM Crops* 3, 150–162. doi: 10.4161/gmcr.2.3.18605
- Iida, S., and Terada, R. (2005). Modification of endogenous natural genes by gene targeting in rice and other higher plants. *Plant Mol. Biol.* 59, 205–219. doi: 10.1007/s11103-005-2162-x
- Izawa, T., and Shimamoto, K. (1996). Becoming a model plant: the importance of rice to plant science. *Trends Plant Sci.* 1, 95–99. doi: 10.1016/s1360-1385(96)80041-0
- Jefferson, R. A., Kavanagh, T. A., and Bevan, M. W. (1987). GUS fusions: β -glucuronidase as a sensitive and versatile gene fusion marker in higher plants. *EMBO J.* 6, 3901–3907.
- Kim, H., and Kim, S.-H. (2014). A guide to genome engineering with programmable nucleases. *Nature* 459, 442–445. doi: 10.1038/nature07845
- Liu, Y. G., Mitsukawa, N., Oosumi, T., and Whittier, R. F. (1995). Efficient isolation and mapping of *Arabidopsis thaliana* T-DNA insert junctions by thermal asymmetric interlaced PCR. *Plant J.* 8, 457–463. doi: 10.1046/j.1365-313X.1995.08030457.x
- Lloyd, A., Plaisier, C. L., Carroll, D., and Drews, G. N. (2005). Targeted mutagenesis using zinc-finger nucleases in *Arabidopsis*. *Proc. Natl. Acad. Sci. U.S.A.* 102, 2232–2237. doi: 10.1073/pnas.0409339102
- Mani, M., Smith, J., Kandavelou, K., Berg, J. M., and Chandrasegaran, S. (2005). Binding of two zinc finger nuclease monomers to two specific sites is required for effective double-strand DNA cleavage. *Biochem. Biophys. Res. Commun.* 334, 1191–1197. doi: 10.1016/j.bbrc.2005.07.021
- Pauwels, K., Podevin, N., Breyer, D., Carroll, D., and Herman, P. (2014). Engineering nucleases for gene targeting: safety and regulatory considerations. *Nat. Biotechnol.* 31, 18–27. doi: 10.1016/j.nbt.2013.07.001
- Porteus, M. H., and Carroll, D. (2005). Gene targeting using zinc finger nucleases. *Nat. Biotechnol.* 23, 967–973. doi: 10.1038/nbt1125
- Puchta, H. (2002). Gene replacement by homologous recombination in plants. *Plant Mol. Biol.* 48, 173–182. doi: 10.1007/978-94-010-0448-0_12
- Sadelain, M., Papapetrou, E. P., and Bushman, F. D. (2012). Safe harbours for the integration of new DNA in the human genome. *Nat. Rev. Cancer* 12, 51–58. doi: 10.1038/nrc3179
- Salvo-Garrido, H., Travella, S., Bilham, L. J., Harwood, W. A., and Snape, J. W. (2004). The distribution of transgene insertion sites in barley determined by physical and genetic mapping. *Genetics* 167, 1371–1379. doi: 10.1534/genetics.103.023747
- Salvo-Garrido, H. G., Travella, S., Schwarzbacher, T., Harwood, W. A., and Snape, J. W. (2001). An efficient method for the physical mapping of transgenes in barley using *in situ* hybridization. *Genome* 44, 104–110. doi: 10.1534/genetics.103.023747

- Sha, Y., Li, S., Pei, Z., Luo, L., Tian, Y., and He, C. (2004). Generation and flanking sequence analysis of a rice T-DNA tagged population. *Theor. Appl. Genet.* 108, 306–314. doi: 10.1007/s00122-003-1423-9
- Shukla, V. K., Doyon, Y., Miller, J. C., DeKelver, R. C., Moehle, E. A., Worden, S. E., et al. (2009). Precise genome modification in the crop species *Zea mays* using zinc-finger nucleases. *Nature* 459, 437–441. doi: 10.1038/nature07992
- Slamet-Loedin, I., Chadha-Mohanty, P., and Torrizo, L. (2014). Agrobacterium-mediated transformation: rice transformation. *Methods Mol. Biol.* 1099, 261–271. doi: 10.1007/978-1-62703-715-0_21
- Smith, J., Bibikova, M., Whitby, F. G., Reddy, A. R., Chandrasegaran, S., and Carroll, D. (2000). Requirements for double-strand cleavage by chimeric restriction enzymes with zinc finger DNA-recognition domains. *Nucleic Acid Res.* 28, 3361–3369. doi: 10.1093/nar/28.17.3361
- Tovkach, A., Zeevi, V., and Tzfira, T. (2010). “Validation and expression of zinc finger nucleases in plant cells,” in *Engineered Zinc Finger Proteins, Methods in Molecular Biology*, Vol. 649, eds J. P. Mackay and D. J. Segal (New York, NY: Humana Press), 315–336.
- Townsend, J. A., Wright, D. A., Winfrey, R. J., Fu, F., Mauder, M. L., Joung, J. K., et al. (2009). High-frequency modification of plant genes using engineered zinc-finger nucleases. *Nature* 459, 442–445. doi: 10.1038/nature07845
- Tzfira, T., Tian, G. W., Lacroix, B., Vyas, S., Li, J., Leitner-Dagan, Y., et al. (2005). pSAT vectors: a modular series of plasmids for autofluorescent protein tagging and expression of multiple genes in plants. *Plant Mol. Biol.* 57, 503–516. doi: 10.1007/s11103-005-0340-5
- Urnov, F. D., Rebar, E. J., Holmes, M. C., Zhang, H. S., and Gregory, P. D. (2010). Genome editing with engineered zinc finger nucleases. *Nat. Rev. Genet.* 11, 636–646. doi: 10.1038/nrg2842
- Weinthal, D. M., Taylor, R. A., and Tzfira, T. (2013). Non-homologous end-joining-mediated gene replacement in plant cells. *Plant Physiol.* 162, 390–400. doi: 10.1104/pp.112.212910
- Wright, D. A., Townsend, J. A., Winfrey, R. J., Irwin, P. A., Rajagopal, J., Lonosky, P. M., et al. (2005). High-frequency homologous recombination in plants mediated by zinc finger nucleases. *Plant J.* 44, 693–705. doi: 10.1111/j.1365-313X.2005.02551.x

Conflict of Interest Statement: The authors declare that the research was conducted in the absence of any commercial or financial relationships that could be construed as a potential conflict of interest.

Received: 03 March 2014; paper pending published: 22 May 2014; accepted: 09 June 2014; published online: 26 June 2014.

Citation: Cantos C, Francisco P, Triyatmiko KR, Slamet-Loedin I and Chadha-Mohanty PK (2014) Identification of “safe harbor” loci in indica rice genome by harnessing the property of zinc-finger nucleases to induce DNA damage and repair. *Front. Plant Sci.* 5:302. doi: 10.3389/fpls.2014.00302

This article was submitted to Plant Physiology, a section of the journal *Frontiers in Plant Science*.

Copyright © 2014 Cantos, Francisco, Triyatmiko, Slamet-Loedin and Chadha-Mohanty. This is an open-access article distributed under the terms of the Creative Commons Attribution License (CC BY). The use, distribution or reproduction in other forums is permitted, provided the original author(s) or licensor are credited and that the original publication in this journal is cited, in accordance with accepted academic practice. No use, distribution or reproduction is permitted which does not comply with these terms.

Advantages of publishing in Frontiers



OPEN ACCESS

Articles are free to read,
for greatest visibility



COLLABORATIVE PEER-REVIEW

Designed to be rigorous
– yet also collaborative,
fair and constructive



FAST PUBLICATION

Average 85 days from
submission to publication
(across all journals)



COPYRIGHT TO AUTHORS

No limit to article
distribution and re-use



TRANSPARENT

Editors and reviewers
acknowledged by name
on published articles



SUPPORT

By our Swiss-based
editorial team



IMPACT METRICS

Advanced metrics
track your article's impact



GLOBAL SPREAD

5'100'000+ monthly
article views
and downloads



LOOP RESEARCH NETWORK

Our network
increases readership
for your article

Frontiers

EPFL Innovation Park, Building I • 1015 Lausanne • Switzerland
Tel +41 21 510 17 00 • Fax +41 21 510 17 01 • info@frontiersin.org
www.frontiersin.org

Find us on

